Imperial College of Science, Technology and Medicine

Royal School of Mines

Department of Earth Science and Engineering

Assessment of the atmospheric fate and environmental impact of amine emissions from post combustion CO_2 capture

by

Saba Manzoor

A thesis submitted for the degree of

Doctor of Philosophy of Imperial College London

September 2015

Abstract

Emissions from post combustion CO_2 capture plants using amine solvents are of concern due to their adverse impacts on the human health and environment. Potent carcinogens such as nitrosamines and nitramines resulting from the degradation of the amine emissions in the atmosphere have not been fully investigated. It is, therefore, imperative to determine the atmospheric fate of these amine emissions, such as their chemical transformation, deposition and transport pathways away from the emitting facility to perform essential human health and environmental risk assessments.

In this study an in-depth analysis of the complex atmospheric chemistry mechanisms of monoethanolamine, methylamine and dimethylamine are considered. Rate constants describing the atmospheric chemistry reactions of the amines are obtained within experimental accuracy using theoretical quantum chemistry methods and kinetic modelling. Their dispersion away from the emitting PCCC facility in the atmosphere is quantified using an atmospheric dispersion model, ADMS 5. The cancer incident probability for humans living in vicinity of the plant is also predicted. The implementation of the developed methodology is illustrated by conducting worst-case scenarios on three emitting facilities at different geographical locations.

In conclusion, the established method is independent from experimental parameters which can assess the fate of any generic amine emission and its environmental impact regardless of the size and geographical location of the CO_2 capture facility. Since PCCC technology is yet to be widely implemented at a commercial scale in operation; the developed method can ensure if a proposed facility complies with the air quality regulatory limits, essential for its chemical discharge permit. The technique can be used to propose ideal plant parameters with respect to its design and recommend ideal geographical locations for industrial installations such that the CO_2 capture advantage of using amines can outweigh the risk associated with solvent discharge issues.

DEDICATED TO MY PARENTS,

ABAJAN & AMEDEDE

Affirmation

The scientific findings presented in the thesis are solely mine and have not been presented for any other degree previously. Publication and conference proceedings resulting from this research are listed below:

Manzoor, S., Simperler, A. and Korre, A., 2015. A theoretical study of the atmospheric chemistry mechanisms of amines emissions from post combustion CO_2 capture technology. International Journal of Greenhouse Gas Control 41, 219 – 228.

Manzoor, S., Korre, A., Durucan, S. and Simperler, A., 2014. Atmospheric Chemistry Modelling of Amine Emissions from Post Combustion CO_2 Capture Technology. Energy Procedia 63, 822-829.

A list of conferences presentations is also given below:

Manzoor, S., Korre, A., Durucan, S. and Simperler, A. A theoretical assessment of the atmospheric fate of amine emissions from post combustion technology and their impacts on human health. Platform Presentation at the 8th Trondheim Conference on CO_2 Capture, Transport and Storage TCCS-8, 2015, June 16-18, Norway.

Manzoor, S., Korre, A and Simperler, A. Human health risk assessment of amine emissions from post combustion plant technology. Platform Presentation at the Society of Environmental Toxicology and Chemistry (SETAC) Europe 25th Annual Meeting, 2015 May3-7; Barcelona, Spain.

Manzoor, S., Korre, A and Simperler, A. Exposure and human health risk assessment of the impacts from amine emissions from post combustion CO_2 capture technology. Platform Presentation at the 3rd UK and Ireland Exposure Science Meeting, 2015 April 24; Imperial College London, UK.

Manzoor, S., Korre, A and Simperler, A. A methodology of the assessment of environmental and human health risks from amine emissions from post combustion CO_2 capture technology. Platform Presentation at the European Geosciences Union General Assembly, 2015 April 12-17; Vienna, Austria.

Manzoor, S., Korre, A and Simperler, A. Environmental and Human health risk assessment of amine emissions from post combustion power plants. Platform Presentation at the 248th American Chemical Society National Meeting and Exposition, 2015 March 22-26; Denver, US.

Manzoor, S., Simperler, A, Korre, A. and Durucan, S., 2014. A theoretical study of the atmospheric chemistry mechanisms of amines emissions from post combustion CO_2 capture technology. Poster presentation at the Atmospheric Chemical Mechanisms conference, 2014 December, UC Davies, US.

Manzoor, S., Korre, A., Durucan, S., Simperler, A. 2014. Atmospheric chemistry modelling of amine emissions from post combustion CO_2 capture plants. (Platform presentation at the Greenhouse Gas Control Technologies Conference GHGT-12, Austin, Texas in October 2014.

Manzoor, S., Simperler, A., Korre, A. Atmospheric chemistry modelling of amine emissions from post combustion CO_2 capture plants. Poster presented at: UKCCSRC Biannual Meeting; 2014 Sept 10-11; Cardiff University, UK.

Manzoor, S., Korre, A., Durucan, S. Study of emission from the Ferrybridge CCPilot100+ capture plant. Platform Presentation at: CCPilot100+ Conference, 2014 April 23; University of Leeds, UK.

Manzoor, S., Simperler, A., Korre, A. Atmospheric chemistry modelling of amine emissions from post combustion CO_2 capture plants. Poster presented at: NSCCS User Meeting; 2013 Dec 11; Imperial College London, UK.

Copyright Declaration

‘The copyright of this thesis rests with the author and is made available under a Creative Commons Attribution Non-Commercial No Derivatives licence. Researchers are free to copy, distribute or transmit the thesis on the condition that they attribute it, that they do not use it for commercial purposes and that they do not alter, transform or build upon it. For any reuse or redistribution, researchers must make clear to others the licence terms of this work’

Acknowledgements

This research is funded by the Scottish Power Academic Alliance as part of the SOLVfate project carried out in collaboration with SINTEF Materials and Chemistry and supported by the CLIMIT program of the Research Council of Norway, Mitsubishi Heavy Industries and ENEL. The authors are grateful for the support of the EPSRC UK National Service for Computational Chemistry Software and the Imperial College High Performance Computing Service who supplied the computational resources. The authors also thank the Cambridge Environmental Research Consultants (CERC) for making available ADMS 5 and a specially compiled version of their Amine Chemistry module for this research. Many thanks to John Dyke, Ed Lee and Theo Goncalves (University of Southampton), Gabriel da Silva (University of Melbourne), Claus Nielsen (University of Oslo), Dominik Weiss, Daniela Fecht, Jennifer Le Blond and Susan Hodgson (Imperial College London) Vladimir Mokrushin (National Institute of Standards and Technology) as well as Matthias Karl (Norwegian Institute for Air Research) for helpful discussions.

On a personal note, I thank my supervisors Professor Anna Korre and Professor Sevket Durucan for giving me the opportunity to purse this degree. For the constant help and support and the push for an extra mile in achieving the targets I am grateful to Dr. Alexandra Simperler.

To have had such a pleasant working environment and for always been there for me, I am indebted to my group members. I thank Dr. Amer Syed for making me see the brighter side of life, Guangyao Si for the immense moral support and encouragement, Dr. Ji-Quan Shi for always been there to listen to me and guide me, Dr Rajesh Govindan and Dr Julio Castro Molinare for always being there to help unconditionally, Indranil Pan for teaching me how to be patient and persistent, Dr. Jorge de La Torre Guzman, Dr. Zhenggang Nie and Wenzhuo Cao for providing a very friendly working environment.

To all my PhD course mates, Dr. Ting Zhang, Dr. Rebbca Hihinashvili, Durr-e-Shawar Malik, Dr. Ali Qaseminejad Raeini, Karwan Mustafa, Deni Zenteno, Xue Wan, Tony Luong, Renato, Miriam Wright, James Lewis, Dr. Biyami Jolly, and

Qinghua Lei. Very special thanks to Dr. Gaurav Singh to have found this opportunity for me and for the constant encouragement and motivation.

Finally my parents, Manzoor ul-haq and Nighat Manzoor and my siblings, Shireen Manzoor and Khyber Manzoor and my very close family friends, Mohib Asad, Nigar Asad, Muhammed Saleem, Farah Khan and Zainab Khalon, who have shown faith in all the important decisions I have made in life.

Table of Contents

ABSTRACT I

AFFIRMATION III

COPYRIGHT DECLARATION V

ACKNOWLEDGEMENTS VI

TABLE OF CONTENTS VIII

LIST OF FIGURES XIV

LIST OF TABLES XVIII

CHAPTER 1 INTRODUCTION AND OBJECTIVES 1

1.1 MOTIVATION 1

1.2 RESEARCH OBJECTIVES 4

1.3 THESIS STRUCTURE 6

CHAPTER 2 OVERVIEW OF AMINES USED IN POST-COMBUSTION CO_2 CAPTURE AND THEIR CHEMICAL DEGRADATION PATHWAYS 9

2.1 AMINE SOLVENTS 9

2.2 POST-COMBUSTION CO_2 CAPTURE PROCESS 10

2.3 AMINE DEGRADATION MECHANISMS 11

2.3.1 Thermal degradation 12

2.3.2 Oxidative degradation *14*

2.3.2.1 Comparison of MEA degradation in real PCCC plants with laboratory based experiments 18

2.3.3 Atmospheric degradation *18*

2.3.3.1 Nitrosamine and nitramine emissions 23

2.4 SUMMARY 23

2.5 CONCLUSIONS 24

CHAPTER 3 OVERVIEW OF ATMOSPHERIC DISPERSION MODELLING OF AMINE EMISSIONS FROM CO_2 CAPTURE 26

3.1 INTRODUCTION 26

3.2 AMINE ATMOSPHERIC CHEMISTRY 28

3.3 AIR POLLUTION DISPERSION MODELS 29

3.3.1 Gaussian Plume Models *30*

3.3.1.1 AERMOD (Beychok 2005) 33

3.3.2 Advanced Gaussian Dispersion Models *34*

3.3.2.1 ADMS 5 34

3.3.2.2 CALPUFF 36

3.3.3 Lagrangian *36*

3.3.3.1 Particle Dispersion Model 37

3.3.4 Eulerian model *37*

3.3.4.1 CSIRO and WRF-Chem 37

3.3.4.2 TAMP 38

3.4 SUMMARY 38

3.5 CONCLUSIONS 39

CHAPTER 4 HUMAN HEALTH AND ENVIRONMENTAL RISK ASSESSMENT 40

4.1 INTRODUCTION 40

4.2 RISK ANALYSIS 42

4.3 HUMAN HEALTH RISK ASSESSMENT 44

4.3.1 Hazard Identification (USEPA 1998b) *44*

4.3.2 Hazard Characterisation (Rovira et al. 2013). *44*

4.3.3 Exposure Assessment *45*

4.3.3.1 Exposure pathways 45

4.3.4 Risk Characterisation *46*

4.3.4.1 Non-carcinogenic Risk 46

4.3.4.2 Carcinogenic Risk 47

4.4 ENVIRONMENTAL RISK ASSESSMENT (ROVIRA *ET AL.* 2013) 51

4.4.1 Hazards and Characterisation of NDMA in drinking water *52*

4.4.2 Derivation of the Guideline PNEC value of NDMA in drinking water by WHO *54*

4.4.3 Derivation of the Guideline PNEC value of NDMA in drinking water by Cal-EPA *54*

4.4.4 Other Guideline PNEC values of NDMA in drinking water *55*

4.5 SUMMARY OF SAFETY LIMITS IN AIR AND WATER 55

4.6 CONCLUSIONS 56

CHAPTER 5 A THEORETICAL STUDY OF THE REACTION KINETICS OF AMINES RELEASED INTO THE ATMOSPHERE FROM CO_2 CAPTURE 58

5.1 INTRODUCTION 58

5.2 ATMOSPHERIC CHEMISTRY COMPUTATIONAL DETAILS 62

5.2.1 Atmospheric chemistry model *62*

5.2.2 Reactions described with Transition State Theory *64*

5.2.3 Reactions described with RRKM theory *65*

5.2.4 Photolysis *68*

5.3 RESULTS AND DISCUSSION 70

5.3.1 Calculated rate constants of the three amines of interest *70*

5.3.2 Amine + OH reactions (k_{OH} pathway) *74*

5.3.2.1 Tropospheric amine lifetime 77

5.3.3 Alkyl amino radical reaction + NO reactions (k_3 NO pathway) *78*

5.3.4 Alkyl amino radical + NO_2 reactions ($k_{4a,b}$ NO_2 pathways) *82*

5.3.5 Amino alkyl + O_2 reactions (k_2 O_2 pathway)....87

5.3.6 Nitrosamine Photolysis: vertical excitation energies of the nitrosamines (J_5 hν pathway)....91

5.4 CONCLUSIONS 95

CHAPTER 6 ATMOSPHERIC CHEMISTRY AND DISPERSION MODELLING....97

6.1 INTRODUCTION....97

6.2 STUDY SITES 99

6.2.1 Ferrybridge CCPilot 100+....99

6.2.2 Peterhead Power Plant 99

6.2.3 Technology Centre Mongstad....99

6.3 SAFETY LIMITS....99

6.4 SCENARIO RISK ANALYSIS 101

6.5 ATMOSPHERIC CHEMISTRY AND DISPERSION MODELLING....102

6.5.1 ADMS 5 with its amine chemistry module (CERC 2010, CERC 2012b, CERC 2012a, CERC 2012d, CERC 2012c) 102

6.5.2 Atmospheric chemistry schemes....103

6.5.3 Capture plants....105

6.5.4 Amine emissions 110

6.5.5 Worst-case scenario approach to calculate tolerable amine emissions, as given by Karl et al. (2011) (with certain modifications)....110

6.5.5.1 Maximum tolerable amine emissions 112

6.5.5.2 IDM and IDM-FFY modelling 114

6.5.6 Wet and dry deposition....114

6.5.7 Deterministic Risk assessment....115

6.6 RESULTS AND DISCUSSION....116

6.6.1 Atmospheric amine chemical transformation and dispersion calculations 116

6.6.1.1 Long term average concentrations....116

6.6.1.2 Short term average MEA concentration for the worst-case scenario on Ferrybridge 130

6.6.1.3 Monthly MEA concentration for the worst-case on Ferrybridge 131

6.6.2 Deposition to soil and water 134

6.7 PARAMETRIC SENSITIVITY ANALYSIS ON WORST-CASE SCENARIO FOR FERRYBRIDGE . 137

6.7.1 Rate constants describing the atmospheric chemistry 141

6.7.2 Stack and exit flue parameters 143

6.7.3 Background gas concentrations 145

6.7.1 Different meteorological years 146

6.7.2 With and without terrain 148

6.7.3 Different emission scenario 148

6.8 COMPARISON TO CERC RESULTS 148

6.8.1 Mongstad 148

6.8.2 Ferrybridge 149

6.1 VERIFICATION AND VALIDATION OF MODELLED RESULTS 151

6.2 CONCLUSIONS 152

CHAPTER 7 RISK ASSESSMENT ON HUMAN HEALTH AND ENVIRONMENT 155

7.1 INTRODUCTION 155

7.2 CANCER RISK ASSESSMENT 156

7.2.1 Hazard identification and characterisation 156

7.2.2 Derived Minimal Effect Level (DMEL) 157

7.2.2.1 T25 dose descriptor estimation 157

7.2.2.2 DMEL estimation via extrapolation from high to low dose 158

7.2.2.3 Adjustment of DMEL for route to route extrapolation 159

7.2.3 Exposure pathway 159

7.2.4 Carcinogenic Risk characterisation 160

7.2.5 Uncertainty analysis 161

7.3 RESULTS AND DISCUSSION 162

7.3.1 Determination of DMEL 162

7.3.2 Exposure assessment 164

7.3.3 Human health risk assessment *166*

7.3.4 Probabilistic risk assessment *170*

7.4 ENVIRONMENTAL RISK ANALYSIS 173

7.5 CONCLUSIONS 174

CHAPTER 8 CONCLUSIONS AND RECOMMENDATIONS FOR FUTURE RESEARCH 176

8.1 ACHIEVEMENTS AND CONCLUSIONS FROM THE RESEARCH 176

8.2 LIMITATIONS AND UNANSWERED QUESTIONS 180

8.3 RECOMMENDATION FOR FUTURE RESEARCH 181

REFERENCES 183

List of Figures

Figure 1.1: There are three vital pathways for large scale CO_2 capture from coal-fired power generation (modified from Jordal *et al.* (2004). 2

Figure 1.2: Protocol overview for the determination of atmospheric fate of atmospheric amines and amine degradation products and carrying out environmental and human health risks assessments. 6

Figure 1.3: An overview of the thesis structure. 6

Figure 2.1: The most common amine solvents used for capture CO_2 in post combustion technology. 10

Figure 2.2: Amine-based post combustion CO_2 capture technology illustration of the Ferrybridge Carbon Capture Plant 100+ operated by Scottish and Southern Energy, SSE (credit SSE). 11

Figure 2.3: Plausible MEA thermal degradation reaction pathway (Strazisar *et al.* 2003, Davis and Rochelle 2009, da Silva *et al.* 2012). 14

Figure 2.4: Possible MEA oxidative degradation pathways in the presence and absence of oxygen (modified from Bello and Idem (2005)). 16

Figure 2.5: Reaction between MEA and the organic acids such as acetic, glycolic, oxalic and formic acids (modified from Lepaumier *et al.* (2011)). 17

Figure 2.6: The most likely mechanistic pathway for the formation of HEPO (modified from Strazisar *et al.* (2003)). 18

Figure 2.7: Conventional chemical structures of the atmospheric degradation products of amines such as aldehydes, amides, nitrosamines and nitramines. 19

Figure 2.8: The proposed atmospheric degradation pathways for MEA following H-abstraction from either the (a) NH_2 (b) CH_2 or (c) CH_2OH groups (adapted from Shao and Stangeland (2009)). 22

Figure 3.1: An outline of the air dispersion modelling procedure (adapted from Bluett *et al.* (2004)) 27

Figure 3.2: A pictorial depiction of plume rise and dispersion from an industrial stack (Beychok 2005). 31

Figure 3.3: A pictorial illustration of ADMS model features (from (CERC)). 35

Figure 4.1: Source-pathway-receptor paradigm. 40

Figure 4.2: A risk analysis paradigm (modified from (Fazil 2005)). 43

Figure 4.3: Exposure route and its effect (adapted from (USETox^{TM})). 46

Figure 4.4: Pathways for NDMA metabolism (adapted from Cal-EPA (2006) and IPSC (2002)). 53

Figure 5.1: A simple atmospheric chemistry scheme of a generic amine (A) undergoing reaction with OH to form the radical (A*) which can react with NO to form NS, with NO_2 to form NA and with O_2 to form imine. The reaction kinetics of each of the reaction step describing the scheme is represented by its corresponding rate constant, k. 59

Figure 5.2: TD-DFT (B3LYP/ aug-ccpTVZ) predictions of the total molar extinction coefficient (cm^2 $molecule^{-1}$) versus wavelength for the three nitrosamines of interest in the spectral region for tropospheric photolysis. 69

Figure 5.3: The overlap region of the simulated UV-VIS absorption spectrum of N-nitroso dimethylamine (TD-DFT / B3LYP/aug-ccpVTZ) and the solar actinic flux curve for mid-day 21st June 2012. 70

Figure 5.4: Energy level diagram for (a) CH_3NH_2 + OH (b) $(CH_3)_2NH$ + OH and (c) $HOCH_2CH_2NH_2$ + OH reactions (N-Branch) using M062X/6-31G(2d,p) level of theory (relative 298K Gibbs free energy in kJ/mol). 77

Figure 5.5: A M062X study of the potential energy surface of the association of (a) CH_3N + NO and the dissociation of the resulting nitrosamine, CH_3NH-NO (b) $(CH_3)_2N$ + NO and the dissociation of the resulting nitrosamine, $(CH_3)_2N$-NO (c) $HOCH_2CH_2NH$ + NO and the dissociation of the resulting nitrosamine, $HOCH_2CH_2NH$-NO. 79

Figure 5.6: Energy diagram for (a) CH_3NH + NO (b) $(CH_3)_2N$ + NO and (c) $HOCH_2CH_2NH$ + NO reactions using M062X/6-31G(2d,p) level of theory (relative 298K Gibbs free energy in kJ/mol). 82

Figure 5.7: A M062X study of the potential energy surface of the association of (a) CH_3NH + NO_2 and the dissociation of the resulting nitrosamine, CH_3NH-NO_2 (b) $(CH_3)_2N$ + NO_2 and the dissociation of the resulting nitrosamine, $(CH_3)_2N$-NO_2 (c) $HOCH_2CH_2NH$ + NO_2 to form the nitrosamine, $HOCH_2CH_2NH$-NO_2. 84

Figure 5.8: Energy level diagram for (a) CH_3NH + NO_2 (b) $(CH_3)_2N$ + NO_2 and (c) $HOCH_2CH_2NH$+ NO_2 reactions, at the M062X/ 6-31G (2d, p) level of theory (relative 298K Gibbs free energy in kJ/mol). 86

Figure 5.9: A M062X study of the potential energy surface of the association of (a) CH_3NH + O_2 (b) $(CH_3)_2N$ + O_2 and the dissociation of the resulting nitrosamine, $(CH_3)_2N$-O_2 (c) $HOCH_2CH_2NH$ + O_2. 89

Figure 5.10: Energy level diagram for (a) CH_3NH + O_2 (b) $(CH_3)_2N$ + O_2 and (c) $HOCH_2CH_2NH$ + O_2 reactions, at the M062X/ 6-31G (2d, p) level of theory (relative 298K Gibbs free energy in kJ/mol). 91

Figure 6.1: Atmospheric chemistry schemes with rate constants, k, describing the kinetics of each of the reaction and the corresponding ordinary differential equations describing the atmospheric chemistry scheme for (a) MA (b) DMA and (c) MEA. 104

Figure 6.2: Wind rose plot for depicting the flow vector (direction towards which the wind was blowing) in m/s for (a) Ferrybridge (2012) (b) Peterhead (2008) and (c) Mongstad (2012). 106

Figure 6.3: Terrain elevation centered on (a) Ferrybridge CCPilot 100+ (b) Peterhead (SSE) (c) Mongstad on a 30 km by 30 km domain and along with the (d) geographical location of each of these sites. 109

Figure 6.4: Flow scheme for the worst case study (adapted from Karl *et al.* (2011)). 112

Figure 6.5: Contoured distributions of maximum annual concentration of amines in air for the worst case scenario in 2012: (a) MA (b) DMA (c) MEA and (d) the total NS and NA (ng/m^3) resulting from MA, DMA and MEA emissions for Ferrybridge. 119

Figure 6.6: Contoured distributions of maximum annual concentration of amines in air for the worst case scenario in 2008: (a) MA (b) DMA (c) MEA and (d) the total NS and NA (ng/m^3) resulting from MA, DMA and MEA emissions for Peterhead. 121

Figure 6.7: Contoured distributions of maximum annual concentration of amines in air for the worst case scenario in 2012: (a) MA (b) DMA (c) MEA and (d) the total NS and NA (ng/m^3) resulting from MA, DMA and MEA emissions for Mongstad. 123

Figure 6.8: Pie charts showing the maximum contribution to NS and NA from the three amines MA, DMA and MEA for the worst case scenario modelled at Ferrybridge. 125

Figure 6.9: Pie charts showing the maximum contribution to NS and NA from the three amines MA, DMA and MEA for the worst case scenario modelled at Peterhead..... 126

Figure 6.10: Pie charts showing the maximum contribution to NS and NA from the three amines MA, DMA and MEA for the worst case scenario modelled at Mongstad..... 127

Figure 6.11: Bar chart showing the maximum annual concentration of NS and NA (ng/m^3) from all the three amines in air for the worst case scenario both from the chemical transport modelling and IDM-FFY approach for (a) Ferrybridge for 2012 (b) Peterhead for 2008 and (c) Mongstad for 2012. 129

Figure 6.12: Short term average concentrations (ng/m^3) against distance from source (m) for (a) MEA (b) resulting Nitrosamine (c) Nitramine, for MEA in year 2012 at Ferrybridge. ... 131

Figure 6.13: Monthly maximum average concentrations (ng/m^3) against months for (a) MEA and a box and whiskers plot showing the (a) lowest (37 ng/m^3), lower quartile (52.2 ng/m^3), median (72.3 ng/m^3), upper quartile (89.3 ng/m^3) and highest value (134 ng/m^3) of the MEA concentration for every month of the year 2012 and (b) resulting NS and NA, in year 2012, with their respective box and whisker plot showing lowest (0.02ng/m^3), lower quartile (0.04 ng/m^3), median (0.12 ng/m^3), upper quartile (0.14 ng/m^3) and highest value (0.22 ng/m^3) of the sum of NS and NA concentrations resulting from MEA for the sensitivity testing on the worst case scenario on Ferrybridge. The outlier for MEA concentration is 134 ng/m^3, whereas, 0.22 ng/m^3 for NS and NA. 133

Figure 6.14: A graphical representation of the sensitivity analysis on the most uncertain parameters with a box and whiskers plot showing the lowest (0.1 ng/m^3), lower quartile (0.23 ng/m^3), median (0.29 ng/m^3), upper quartile (0.31 ng/m^3) and highest value (0.77 ng/m^3) of the sum of NS and NA concentrations resulting from the three amines for the sensitivity testing on the worst case scenario on Ferrybridge. Six outliers were also obtained at values 0.10, 0.46, 0.52, 0.53 and 0.77 ng/m^3. 141

Figure 6.15: Plots showing an exponential dependency of the NS and NA concentrations with (a) Stack height and (b) Stack diameter. 144

Figure 6.16: Plot showing a linear dependency of the NS and NA concentrations with [O_3] / $\mu g\ m^{-3}$. 146

Figure 6.17: A graphical representation of the sensitivity analysis on the meteorological years from 2004 to 2013 with a box and whiskers plot showing the lowest (0.26 ng/m^3), lower quartile (0.27 ng/m^3), median (0.29 ng/m^3), upper quartile (0.30 ng/m^3) and highest value (0.37 ng/m^3) of the sum of NS and NA concentrations resulting from the three amines for the sensitivity testing on the worst case scenario on Ferrybridge. One outlier was also obtained at a value 0.37 ng/m^3 The red straight line corresponds to the safety limit of 0.3 ng m^{-3}. 147

Figure 7.1: Rescaled annual average concentration of [NS+NA] ng m^{-3} to Census Output Areas for exposure assessment for the worst case estimates from the three amines over a 30 km by 30 km domain centered on (a) Ferrybridge for the meteorological year of 2012 (b) Peterhead for 2008 and (c) Mongstad for 2012. 166

Figure 7.2: Census area output showing the total (adult + child + infant) carcinogenic risk to the population in the study domain centered on (a) Ferrybridge (b) Peterhead and (c) Mongstad..... 168

Figure 7.3: (a) Highlighted census area exposed to concentrations above 0.3 ng/ m^3 (b) total cancer risk for Ferrybridge for the sensitivity scenario of maximum concentration of O_3. 170

Figure 7.4: Probability density function of Monte Carlo simulations result for the (a) infant health risk (b) child health risk (c) adult health risk and (d) comparison of the distributions for infant, child and adult with the reference risk level of 10^{-6}..... 172

Figure 8.1: A pictorial representation of some of the operational or under construction PCCC plants worldwide. 180

List of Tables

Table 3.1: Comparisons of dispersion models with respect to their features for the purposes of this study. 38

Table 4.1: Regulatory standards set for the tolerable carcinogenic risk levels in human in air for nitrosamines and nitramines (modified from Låg *et al.* (2011)). 48

Table 4.2: Summary of regulatory standards set for the tolerable carcinogenic risk levels for human in water for nitrosamines and nitramines (modified from Låg *et al.* (2011)). 55

Table 4.3: Summary of safety limits stated by various studies for MEA, nitrosamines and nitramines in air, drinking water and the aquatic environment (reproduced from Karl *et al.* (2011)) 56

Table 5.1: Reaction scheme and the corresponding rate constants of methylamine (MA), dimethylamine (DMA) and monoethanolamine (MEA). 61

Table 5.2: The differential equations describing the amine atmospheric chemistry scheme (after CERC (2012a)) 62

Table 5.3: The calculated k_{OH} constant for CH_3NH + OH reaction using various computational levels of theory. 64

Table 5.4: The calculated enthalpy of formation for the structures for consideration in the ChemRate program. 67

Table 5.5: Vertical electronic excitation wavelength and corresponding oscillator strength for the relevant n -> π^* transition for the three target nitrosamines predicted by TD-DFT (B3LYP/ aug-ccpTVZ) level of theory 68

Table 5.6: A summary of the rate constants (cm^3 molecule $^{-1}$ s^{-1}) describing the atmospheric chemistry scheme for each of the amines studied using quantum chemistry theoretical methods and kinetic modelling. The nitrosamine photolysis rate constant is given relative to that of NO_2, (J / $J(NO_2)$, for Ferrybridge Peterhead and Mongstad; $\boldsymbol{k_{OH}}$ is given as a sum of the rate of attack of the OH on the amino group, $\boldsymbol{k_1}$, and the attack on the alkyl group ($\boldsymbol{k_{1b}}$) and therefore the branching ratio for the OH attack is reported as $\boldsymbol{k_1}$/ $\boldsymbol{k_{OH}}$. 72

Table 5.7: A summary of the activation energies (E_a) evaluated at 298K for each of the reaction pathway in the atmospheric chemistry schemes for each of the amines studied. 73

Table 5.8: Calculated branching ratios for H abstraction of the amines by OH 75

Table 5.9: Tropospheric lifetime of the amine in the atmosphere determined form k_{OH} calculated in this work as well as from literature. 78

Table 5.10: Vertical electronic excitation wavelength, corresponding oscillator strength, photolysis rate, J, and the corresponding mean life times for the relevant n -> π* transition for the three target nitrosamines predicted at TD-DFT (B3LYP/ aug-ccpTVZ) level of theory and solar actinic flux for Ferrybridge at mid-day for different times of the year and at 198m stack height. 93

Table 5.11: Vertical electronic excitation wavelength, corresponding oscillator strength, photolysis rate, J, and the corresponding mean life times for the relevant n -> π* transition for the three target nitrosamines predicted at TD-DFT (B3LYP/ aug-ccpTVZ) level of theory and solar actinic flux for Peterhead at mid-day for different times of the year and at 170m stack height. 94

Table 5.12: Vertical electronic excitation wavelength, corresponding oscillator strength, photolysis rate, J, and the corresponding mean life times for the relevant n -> π* transition for the three target nitrosamines predicted at TD-DFT (B3LYP/ aug-ccpTVZ) level of theory and solar actinic flux for Mongstad at mid-day for different times of the year and at 65m of stack height. 94

Table 6.1: Safety limits stated by various studies for MEA, nitrosamines and nitramines in air, drinking water and the aquatic environment. (Reproduced from Karl *et al.* (2011)). 100

Table 6.2: Source parameters for each of the emitting facility. 106

Table 6.3: Background concentrations of pollutant gases around the capture plant for the particular meteorological year studied. 107

Table 6.4: Calculated emission rates for the individual amine species from the TCM emission data (CERC 2012d, CERC 2012c) 110

Table 6.5: Maximum amine concentrations ($Cmax$), maximum sum NS and NA concentrations and the amine concentration, percentage transformation of the parent amine to NS and NA at the unity emissions for Ferrybridge and Peterhead but at likely emissions at Mongstad and their corresponding maximum tolerable amine emission rate estimates ($Emax$) 114

Table 6.6: Maximum long-term average air concentrations of amines, nitrosamines and nitramines for the worst case scenario modelled for each site and compared against those calculated using FFYs, where A represents Amine, NS is nitrosamine and NA is nitramine. 116

Table 6.7: Monthly maximum long term average concentrations of MEA, NS and NA (ng/m^3) for the worst case emissions scenario for the meteorological year 2012. 132

Table 6.8: The wet and dry deposition flux calculated for the amines, total nitrosamines and total nitramines for the worst case scenario modelled for each site. 135

Table 6.9: The concentrations of amines, nitrosamines and nitramines for the worst case scenario modelled for each site in water estimated from wet deposition fluxes and compared against safety limits. 135

Table 6.10: The values of the uncertain model parameters increased and decreased by a factor of 2 of its true value for consideration in sensitivity analysis conducted on the baseline worst-case scenario on Ferrybridge. 139

Table 6.11: Sensitivity analysis for different model parameters: maximum long term average concentrations of the total NS and NA from the three amines at the maximum tolerable emissions from Ferrybridge. 140

Table 6.12: Sensitivity analysis for different meteorological years: maximum long term average concentrations of the total NS and NA from the three amines at the maximum tolerable emissions and the percentage change (%Δ) from the baseline value of 0.29 ng m^{-3} in 2012..... 147

Table 6.13: Maximum long term average concentrations of NS+NA (ng/m^3) for the alternate emissions scenario for the meteorological year 2012..... 148

Table 6.14: A summary of the rate constants (cm^3 molecule $^{-1}$ s^{-1}) describing the atmospheric chemistry scheme for each of the amines studied using quantum chemistry theoretical methods and kinetic modelling established in this work and those considered by CERC (2012c) and CERC (2012d) as well as those form experimental studies. 150

Table 7.1: Summary of parameters defined in the risk model for the different age groups of the population (USEPA 1998b). 160

Table 7.2: Probability distribution functions for the uncertain parameters defined in the risk model (TR = triangular [min, mode, max], LN= lognormal [geometric mean, geometric standard deviation])..... 161

Table 7.3: Estimation of DMEL for NDMA using the obtained T25 from raw data collected by Peto *et al.* (1991b) for bile duct tumours in male rats. 162

Table 7.4: Maximum amine emission rates, total NS and NA concentratrions calcuated for Ferrybridge, Peterhead and Mongstad for the worst case scenario. 164

Table 7.5: The number of infants, children and adults living around Ferrybridge, Peterhead and Mongstad as par their respective census data..... 166

Table 7.6: Environmental risk analysis for each of the capture plant with their corresponding PEC/PNEC values..... 174

Chapter 1 Introduction and Objectives

1.1 Motivation

Global warming and climate change are the consequences of the rapidly escalating emissions of greenhouse gases (GHG), in particular CO_2, into the atmosphere. Over the last decade, the major contributing sources of CO_2 emissions have been industries such as power plants, cement factories, refineries etc. (Martin *et al.* 2012). According to the Intergovernmental Panel on Climate Change (IPCC 2007b, IPCC 2007a), the average global temperature during the 21st century is anticipated to rise by 2°C. This will most likely cause extreme weather conditions, floods, droughts, accelerating sea level rise and heat waves. Food production will be affected and pressure on scarce water resources for the growing world population will increase; hence, threatening the ecosystems (Wiliams 2002, Stern 2006, IPCC 2007b, IPCC 2007a, Shao and Stangeland 2009). In order to overcome such consequences, it would be beneficial to deploy CO_2 capture and storage (CCS) technology as one of the means to reduce GHG emissions by 50-85 % from 2000 to 2050 (IPCC 2007b, IPCC 2007a).

The three leading and most suitable options for commercial deployment on coal-fired power generation in specific as illustrated in Figure 1.1 are:

- Pre-combustion capture which involves the gasification of coal to remove CO_2 from the fuel prior to combustion.
- Post combustion CO_2 capture (PCCC) which uses amines as solvents for separating CO_2 from the flue gas stream after combustion.

- Oxyfuel combustion which is the combustion of the fuel with oxygen and recycled flue gas to yield a high CO_2 concentration product stream requiring minimal treatment prior to beneficial use or disposal.

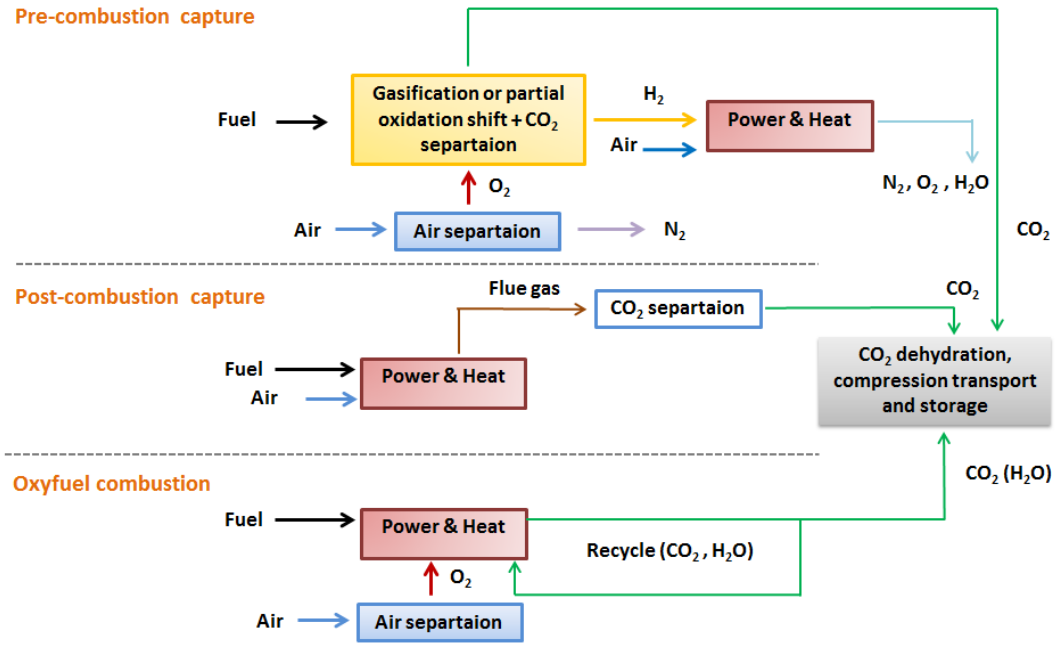


Figure 1.1: There are three vital pathways for large scale CO_2 capture from coal-fired power generation (modified from Jordal *et al.* (2004).

The most progressive and widely accepted mitigation technology for coal power plants has been the PCCC for large scale CO_2 capture (IEA 2004, IPCC 2007a). An amine-based monoethanolamine (MEA) solvent is considered as the reference solvent for post combustion CO_2 capture, due to its fine properties towards CO_2 (Bråten *et al.* 2009). It is assumed to remove up to 85-95% CO_2 from gaseous effluents (Lepaumier *et al.* 2011).

However, during the CO_2 capture by the amine solvent, small amounts of the amine and the amine degradation products formed during the capture process, get entrained in the flue gas emissions into the atmosphere, despite efforts to clean the flue gas (Eide-Haugmo *et al.* 2009, Booth *et al.* 2012a, Booth *et al.* 2012b). The fate of the released amines is now governed by atmospheric processes such as their transport pathways away from the emitting facility, chemical transformation reactions, expected dispersion and deposition to soil and water (Booth *et al.* 2012a, Booth *et al.* 2012b).

In the atmosphere, the photo-oxidation of selective amines results in the production of degradation products such as, nitrosamines and nitramines which undergo deposition to soil and water. Consequently, these chemicals find their way into the food chain to accumulate in animals, vegetables and fruits, and get ingested by humans. Theoretical studies have shown that nitrosamines and nitramines are suspected carcinogens in mammals even at extremely low concentrations (Reh *et al.* 2000, Karl *et al.* 2008, Låg *et al.* 2011). The toxicological literature data suggests that many of the photo-chemically unstable nitrosamines are extremely carcinogenic as compared to the photo-chemically stable nitramines (Tuazon *et al.* 1984, Brown 1999, Låg *et al.* 2011, Nielsen *et al.* 2011a, Selin 2011). It is speculated that nitramines will add to the human health risk even when released in small concentrations (Brakstad *et al.* 2010). For this reason, the PCCC process and the risks associated with it are of particular interest in this work.

Since the fate of the amines used for PCCC technology is undetermined, there is a lack of awareness with respect to the atmospheric processes. They are poorly comprehended due to their complexity, which unavoidably increases the uncertainty in the emissions from the amine capture technology. There are obviously challenges encountered in quantifying these processes. The atmospheric chemistry of the amines is highly complex and due to their high vapour pressures at atmospheric conditions, performing experimental investigations resembling realistic conditions is challenging.

Very few pilot plant studies have been conducted to characterise the amine degradation products (Strazisar *et al.* 2003, Lepaumier *et al.* 2011). There are also a limited number of experimental investigations on amine degradation which have been carried out in the laboratory (Nielsen *et al.* 2011a, Nielsen *et al.* 2011b, Karl *et al.* 2012, Angove *et al.* 2013). As the experimental investigations are sparse, theoretical methods such as quantum chemical methods and kinetic modelling may be an option to fill the gaps present in the literature. They can determine the kinetics of the atmospheric reactions of interest within experimental accuracy (Galano and Alvarez-Idaboy 2008, Bråten *et al.* 2009, Tian *et al.* 2009, Nielsen *et al.* 2010, Nielsen *et al.* 2011b, Onel *et al.* 2012, Borduas *et al.* 2013, Onel *et al.* 2013, Xie *et al.* 2014).

On the other hand, determining the concentrations of the released compounds into the air, their expected dispersion, deposition and transport pathways away from the emitting PCCC plant have also not been extensively experimentally investigated. Some studies have attempted at determining these concentrations either experimentally, theoretically or using a combination of both. (Karl *et al.* 2011, Tønnesen 2011, CERC 2012d, Fowler and Vernon 2012, de Koeijer *et al.* 2013, Azzi *et al.* 2014, Karl *et al.* 2014, Karl *et al.* 2015).

Henceforth, it is crucial to enhance the existing knowledge with regards to the atmospheric fate of the amine emissions from PCCC process by quantifying the atmospheric processes to determine their associated human health (Booth *et al.* 2012a, Booth *et al.* 2012b) and environmental risks.

1.2 Research Objectives

It is imperative to address the key knowledge gaps that exist for identifying the risks posed by emissions from amine-based PCCC technology. Therefore, the aim of this research is to determine the atmospheric fate of a suite of nitrosamines and nitramines emitted from an amine-based solvent PCCC plant in order to assess their impact on the human health and the environment. The objectives are to:

1. Assess the atmospheric fate of the components from post-combustion amine based CO_2 capture, such as a suite of nitrosamines and nitramines representing degradation products of generic amines such as MEA, methylamine (MA) and dimethylamine (DMA) from post-combustion CO_2 capture plants by:

(i) Considering a detailed chemistry scheme that takes into account degradation of the most commonly used amines and the formation and subsequent degradation of substantial by-products. This can be achieved by carrying out quantum chemical calculations based on quantum chemistry and kinetic modelling for the determination of the rate constants of the reaction of amines with OH radicals and of the resulting alkyl amino radicals with NO, NO_2 and O_2

(ii) Performing atmospheric chemistry, dispersion and deposition calculations using an air pollution dispersion model to take into account chemical transformation along with dispersion and deposition, in order to estimate

the air and ground concentration levels (dry and wet deposition) in time and space with respect to the emitting facility.

2. Determine the risk associated with the nitrosamines and nitramines of interest on the human health and the natural environment.

(i) For the human health risk assessment, the calculated exposure concentrations from the atmospheric chemistry and dispersion modelling needs to be compared against the tolerant nitrosamine and nitramine concentration in air, which is known as the derived minimal effect level (DMEL). The DMEL in this study will be derived from considering the cancer oral slope factor of the substances of interest and employing extrapolation modelling techniques from high-dose animal exposures conducted on rats to low-dose human exposures. The obtained DMEL will be used in calculating the cancer risk through inhalation, according to the USEPA (1998b) approach.

(ii) Additionally, a Monte Carlo approach will be used to account for uncertainty in performing the risk assessment modelling and in estimating the probability of cancer risk caused by exposure to these pollutants. By doing so, the cancer incident probability for humans can be predicted and an assessment of it spatial distribution in the study area can also be achieved.

(iii) For the environmental risk assessment, calculations will be based on the determination of PEC/PNEC, i.e. the ratio between environmental concentrations (PEC) and the concentration resulting in potential harm (PNEC). A high risk is associated with areas where PEC > PNEC.

Overall, the intention is to develop a methodology to consider amine chemistry and atmospheric dispersion in order to perform risk assessments. Below is an outline of the protocol (Figure 1.2) developed for the determination of the environmental fate of atmospheric amines emissions and performing environmental and human health risks assessments.

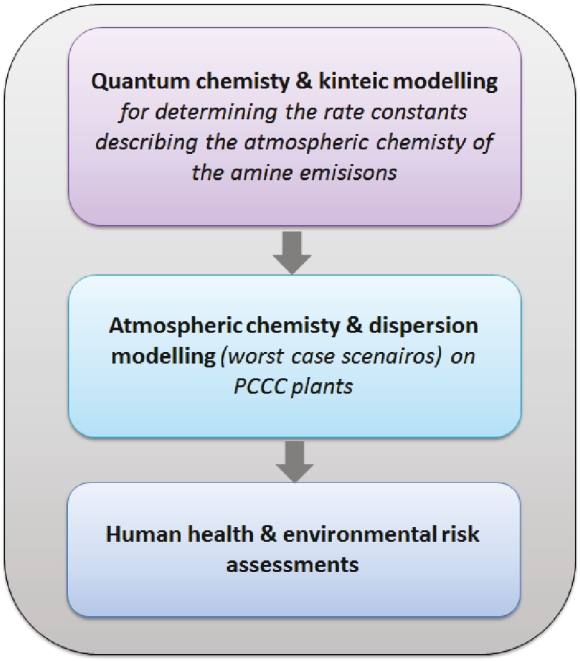


Figure 1.2: Protocol overview for the determination of atmospheric fate of atmospheric amines and amine degradation products and carrying out environmental and human health risks assessments.

1.3 Thesis Structure

The structure of the thesis is depicted in Figure 1.3, where chapter 1 introduces and highlights the objectives of this research study.

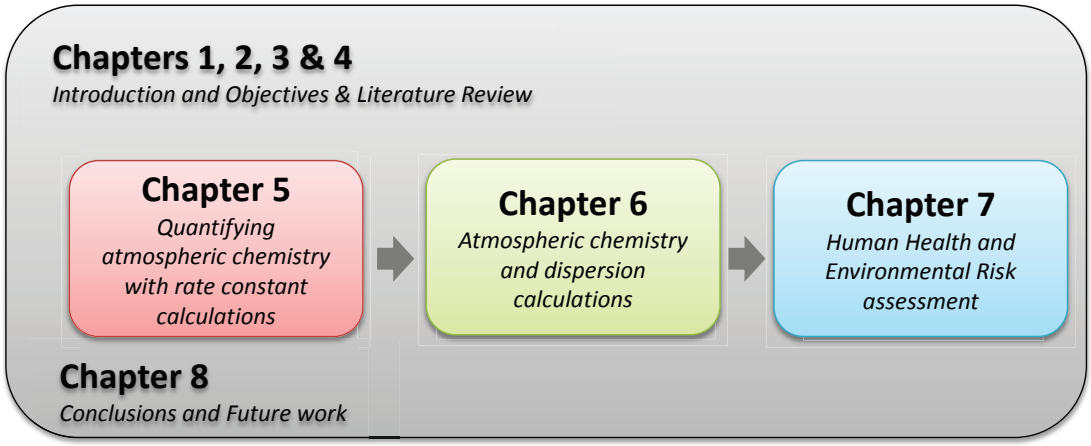


Figure 1.3: An overview of the thesis structure.

Chapter 2 gives an overview of the PCCC process using amines for CO_2 capture and describes the three most common amine degradation pathways of oxidative, thermal and atmospheric degradation pathways that occur to produce the harmful amine

degradation products. It also compares MEA degradation in real PCCC plant to laboratory based experiments.

Chapter 3 explains the basic concepts of air dispersion and describes the most common atmospheric dispersion models used for air quality purposes. After evaluating the existing models, the dispersion model most suitable for this work is proposed. Recent atmospheric chemistry dispersion studies performed in the literature are also discussed.

Chapter 4 reviews the human health and environmental impacts of amine and amine degradation products associated with CO_2 capture. It gives an impression of the relevant steps to consider in performing risk assessments of these chemical discharges.

Chapter 5 describes in detail the derivation of the rate constants describing the kinetics of the atmospheric chemistry reaction pathways for MA, DMA and MEA using quantum chemistry and kinetic modelling. It demonstrates that the developed theoretical method is applicable to any generic amine for the purposes of determining the rate kinetics of each of the pathways in the atmospheric chemistry scheme.

Chapter 6 presents the results from performing atmospheric, dispersion and deposition modelling of MA, DMA and MEA emissions for three PCCC plants. For each case, the total nitrosamines and nitramines concentrations are calculated for a worst case scenario and compared against safety guideline values in order to perform a simple deterministic human health and environmental risk assessment. A sensitivity test on a base line case study on Ferrybridge power plant was performed to determine the parameters that most influenced the fate of the total nitrosamine and nitramine from the three amines considered in this work.

Chapter 7 amalgamates the results from the atmospheric chemistry and dispersion calculations to human health and environmental risk assessments from amine degradation products. Human health risk assessment is performed according to the USEPA (1998b) method to quantify the risk of developing cancer through inhalation for children and adults living within the vicinity of the emitting facility. On the other hand, environmental risk assessment is based on the calculations of PEC/PNEC, i.e.

the ratio between environmental concentrations (PEC) and the concentration resulting in potential harm (PNEC).

Chapter 8 presents the main findings, conclusions drawn from this work along with suggestions for future work.

Chapter 2 Overview of amines used in post-combustion CO_2 capture and their chemical degradation pathways

This review addresses the solvent degradation mechanisms pertinent to possible emissions from amine-based PCCC technology of which the atmospheric degradation mechanism is of particular interest. The focus is on MEA and its corresponding nitrosamines and nitramines.

2.1 Amine solvents

Amines are organic chemicals derived from ammonia by substitution of one or more hydrogen atoms by an alkyl or an aryl (R) organic group. They can take conventional structures of primary (RNH_2), secondary (R_2NH) or tertiary (R_3N) amines (McNaught and Wilkinson 1997). Amine solvents have been extensively used for CO_2 capture. Some of the most commonly used polar amines have an alcoholic (OH) functional group and belong to the generic group of alkanolamines. Such a group consists of monoethanolamine (MEA), diethanolamine (DEA), methyldiethanolamine (MDEA), di-isopropanolamine (DIPA) and monomethylethanolamine (MMEA), with their corresponding structures as illustrated in Figure 2.1. Alkanolamines are basic in nature, miscible in water, corrosive and have an odour of a rotten fish typical for the amine family of compounds.

Over the years, MEA has been considered the bench mark solvent for PCCC due to its fine properties towards CO_2, such as being non-volatile, having a fast absorption rate, high water solubility and being cheap (Lepaumier *et al.* 2011, Martin *et al.* 2012). As the PCCC technology is improving, there is on-going research to develop other solvent systems such as the cyclic and glycol amines (Figure 2.1) comprising of 2-amino-2-methylproponol (AMP), piperazine (PIPA) and di-glycolamine (DGA). Various forms of substituted alkanolamines, polyamines and blends of more than one amine solvents have also been used for CO_2 capture. The details of the exact amine solvent or the composition of the mix blends used by a particular PCCC facility are usually kept confidential. This is due to issues of solvent degradation and corrosivity associated with their use in this technology and their implications on the immediate surrounding environment.

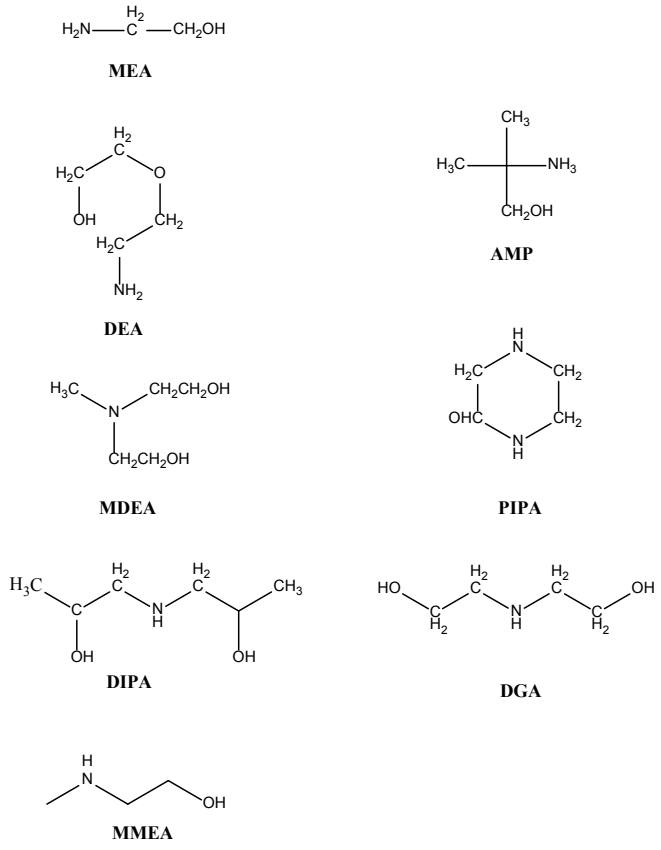


Figure 2.1: The most common amine solvents used for capture CO_2 in post combustion technology.

2.2 Post-combustion CO_2 capture process

The general PCCC process is depicted in Figure 2.2, where it can be seen that the flue gas from the power plant is cooled before it enters the absorption column (1). As

the flue gas rises through the column, it comes into contact with a mixture of water and amine solvent (from the top absorber inlet (2)). Here the CO_2 from the flue gas stream is chemically absorbed by an aqueous amine solvent to form a carbonate salt (3) (Lepaumier *et al.* 2011). The remaining (cleaned) flue gas is vented at the top of the absorber, which has only trace amounts of CO_2 by then (4). The carbonate salt leaves the absorber at the bottom (5) to be transferred to the top of the stripper (6). The hot amine solvent from the reboiler (7) is transferred to the stripper where it heats the carbonate salt, causing it to release the absorbed CO_2 (8). The resulting pure amine is transferred from the stripper to the reboiler to be heated and then transferred back to the stripper (8) or sent to the absorber to be used again i.e. recycled (9). The pure CO_2 (10) is dried and compressed and transported for secure storage offshore (11).

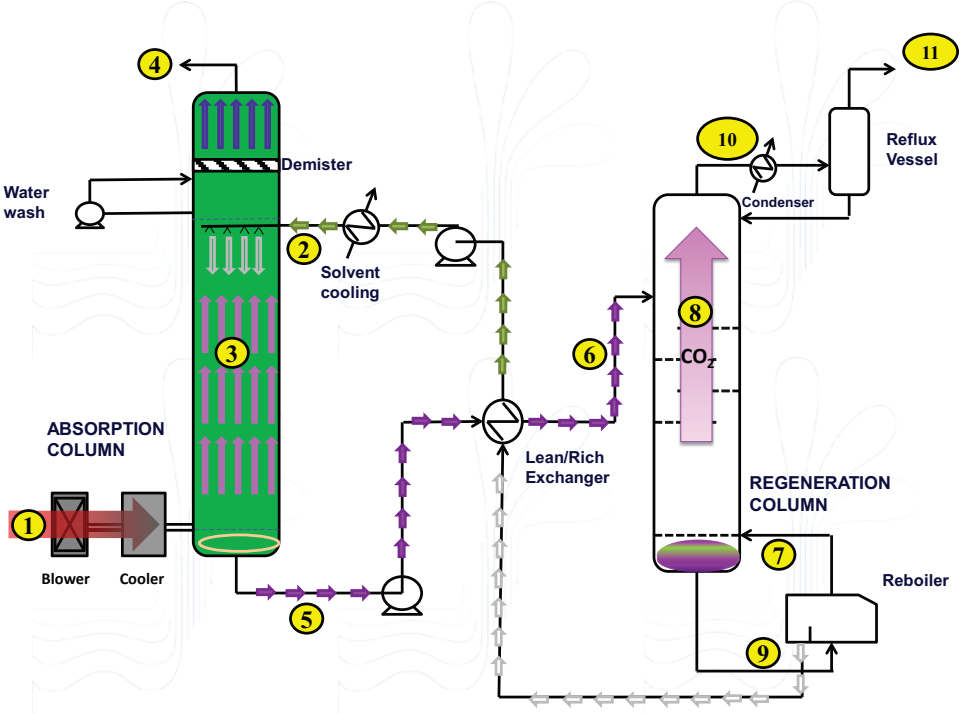


Figure 2.2: Amine-based post combustion CO_2 capture technology illustration of the Ferrybridge Carbon Capture Plant 100+ operated by Scottish and Southern Energy, SSE (credit SSE).

2.3 Amine degradation mechanisms

Regulating the emissions of amine solvent and amine degradation products from PCCC plants has recently been the centre of attention due the inevitable production of harmful substances in the process. Understanding the complex chemistry of

solvent degradation both within and outside the plant as well as recognising the resulting degradation products is a prerequisite for this. By doing so, improved solvent systems could be developed. However, there are challenges to comprehending the amine degradation mechanisms occurring during the capture process. This is due to the amine solvent being exposed to varying operation conditions of temperature, pressure, oxygen etc. during the PCCC process which results in the formation of various types of degradation products in different parts of the capture plant. Studies have revealed that amine degradation in the PCCC process can occur via three different mechanisms:

1. Oxidative degradation which is influenced by O_2 concentration in the flue gas and it is most likely to occur in the absorber where the highest O_2 concentrations occur (da Silva *et al.* 2012).
2. Thermal degradation which is influenced by temperature and it is most likely to occur in the stripper where the topmost temperatures of up to 120 °C are confronted.
3. Atmospheric degradation which is influenced by light ($h\upsilon$) and OH radicals, O_2, NO_2, NO in the atmosphere.

The kind of degradation products that may form depend on the type of amine solvent used, the specific mechanism occurring and the length of the CO_2 capture process by the amine. Amine solvents such as, DEA, MDEA, MEA etc. (Figure 2.1) have been extensively studied in the literature for the kind of degradation products they form due to their extensive application in natural gas treatment using PCCC technology (Meisen and Kennard 1982, Kennard and Meisen 1983, Hsu and Kim 1985, Kennard and Meisen 1985, Chakma and Meisen 1988).

2.3.1 Thermal degradation

The influence of temperature on amine degradation when CO_2 is present has been under examination since the mid-20th century (Polderman *et al.* 1955, Chakma and Meisen 1997, Kohl and Nielsen 1997, Lepaumier *et al.* 2009). It has been postulated that thermal degradation is more likely to occur in the stripper and the reboiler of the capture plant, where high temperature and high CO_2 concentrations are encountered (Lepaumier *et al.* 2011). CO_2 concentration has been discovered to have a first order effect on the rate of amine degradation, whereas, the concentration of amine has even a more pronounced effect than first order. As a result of high temperature and partial

pressures of CO_2, successive formation of thermal degradation products of amines are more likely to occur (Davis and Rochelle 2009, Lepaumier *et al.* 2011).

Generally, amines upon reaction with CO_2 form carbonate salts. Though the reaction is reversible, if the amine solvent is heated, the carbonate salt reacts further with the amine to form thermal degradation products. Further degradation products are formed by the amine undergoing hydrolysis reactions.

The thermal degradation mechanism of MEA has been under some debate due to different explanations suggested with respect to the order of the occurrence of the thermal degradation products identified for MEA such as, the 2-oxazolidinone (OZD), N-(2-hydroxyethyl)ethylenediamine (HEEDA) and N-(2-hydroxyethyl)imidazolidinone (HEIA). However, an agreed reaction mechanism for MEA thermal degradation based on the findings of Davis and Rochelle (2009) is illustrated in Figure 2.3 and an outline given below:

1. MEA and CO_2 react in the absorber to form a carbonate salt.
2. The ring closure of the carbonate produces 2-oxazolidone (OZD).
3. The opening of the OZD with another molecule of MEA forms the dimer N-(2-hydroxyethyl)-ethylenediamine (HEEDA).
4. HEEDA and CO_2 react again to generate another molecule of carbonate and then intermolecular cyclisation occurs to give N-(2-hydroxyethyl) imidazolidinone (HEIA), which is not very reactive and remains in the solution. HEIA is very stable and is considered as the major degradation product, whereas, HEEDA is unstable in the presence of CO_2.
5. HEEDA reacts with another molecule of OZD to form a trimer, which in the presence of CO_2 forms N-(2-aminoethyl)-N'-(2-hydroxyethyl) imidazolidinone (AEHEIA).

Thermal degradation is responsible for approximately 20-30 % of the total MEA loss (Strazisar *et al.* 2003, Bello and Idem 2005).

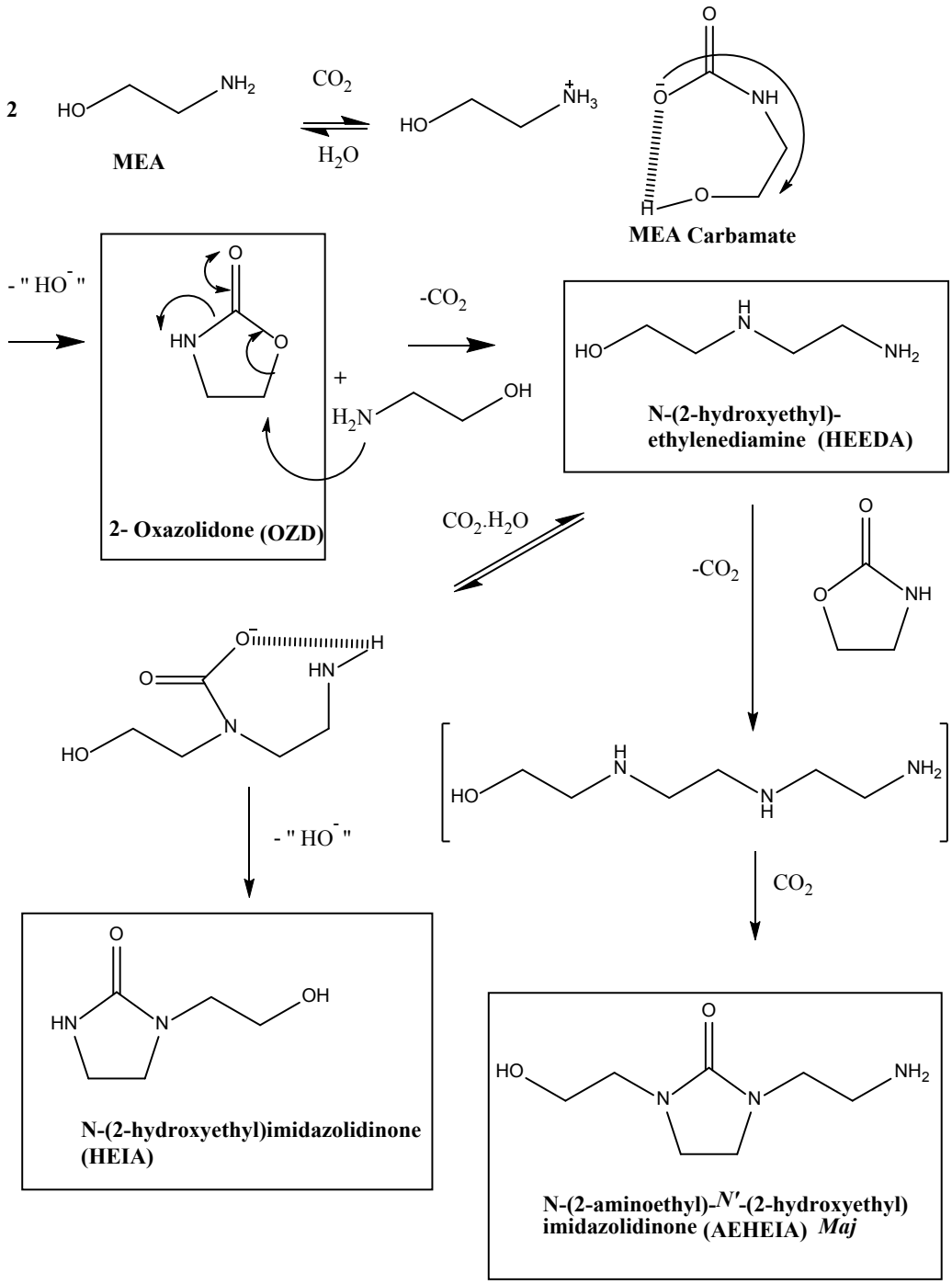


Figure 2.3: Plausible MEA thermal degradation reaction pathway (Strazisar *et al.* 2003, Davis and Rochelle 2009, da Silva *et al.* 2012).

2.3.2 Oxidative degradation

Even though there is a sound understanding of thermal degradation, there is a lack of awareness regarding oxidative degradation of amine solvents used in the PCCC process. In the capture plant, this type of degradation most likely occurs in the absorber due to the high O_2 concentration in the flue gas or in the presence of

metallic ions in solution (due to corrosion or via anticorrosion metallic salts such as $CuCO_3$) that act as catalysts for the degradation. Organic carboxylic acids (such as formic, acetic, glycolic and oxalic acids), ammonia methylamine, formaldehyde, acetaldehyde, *N*-(2-hydroxyethyl)formamide (HEF) and *N*-(2-hydroxyethyl)imidazole (HEI) constitute the identified degradation products. However, such degradation processes lead to an unavoidable loss of amine and reduce the CO_2 capture efficiency of the plant.

The mechanism of the oxidative chemical degradation is complicated and still not clear. A suggested reaction mechanism for MEA is illustrated in Figure 2.4 and Figure 2.5. A brief outline of the process is given below (Strazisar *et al.* , Chi and Rochelle 2002, Strazisar *et al.* 2003, Goff and Rochelle 2004, Bello and Idem 2005, Bedell 2009, da Silva *et al.* 2012, Gouedard *et al.* 2012):

1. Amines such as MEA react with the metal cations like Fe^{2+}, Fe^{3+} or Cu^{+} to form the single electron oxidants known as oxide radicals.
2. In the absence of dissolved O_2, the oxide radical reacts with metal cations or other oxidants to form imines.
3. In the presence of dissolved O_2, the oxide radical forms peroxide radical upon further reaction with O_2.
4. The peroxide radicals undergo further reaction with amine to form imines and hydrogen peroxides.
5. Degradation products such as, ammonia and organic acids for MEA are formed when the imines undergo oxidative fragmentation and hydrolysis.
6. Few intermediate products (formaldehyde and acetaldehyde) and some oxalic acids (acetic, glycolic, oxalic and formic acids) are produced as well.
7. It is anticipated that the resulting organic acids can undergo further reactions with the parent solvent, MEA, to form various other products such as HEF, *N*-(2-hydroxyethyl) acetamide (HEA), 2-hydroxy-*N*-(2-hydroxyethyl) acetamide (HHEA) and *N*-*N'*-bis(2-hydroxyethyl) oxalamide (BHEOX).

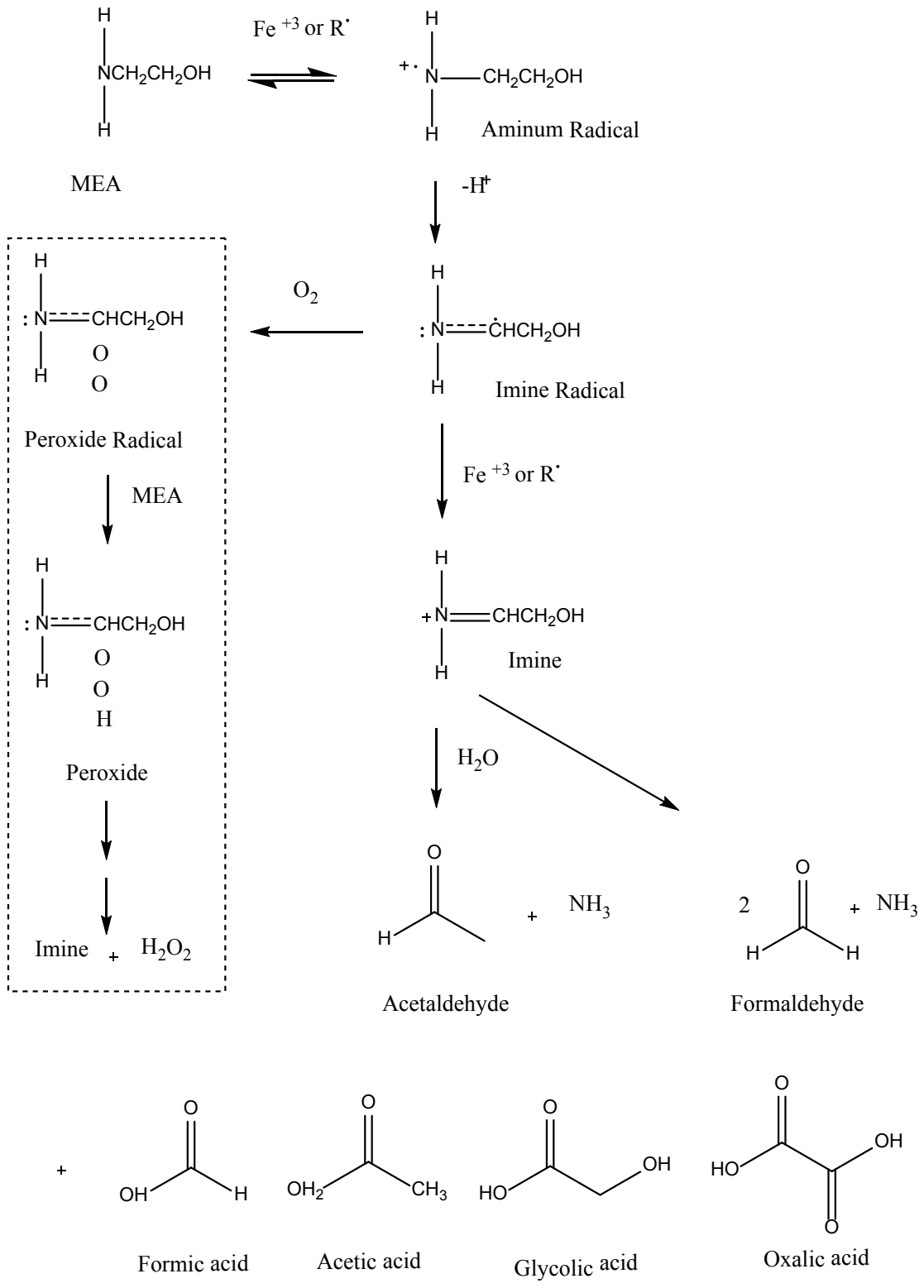


Figure 2.4: Possible MEA oxidative degradation pathways in the presence and absence of oxygen (modified from Bello and Idem (2005)).

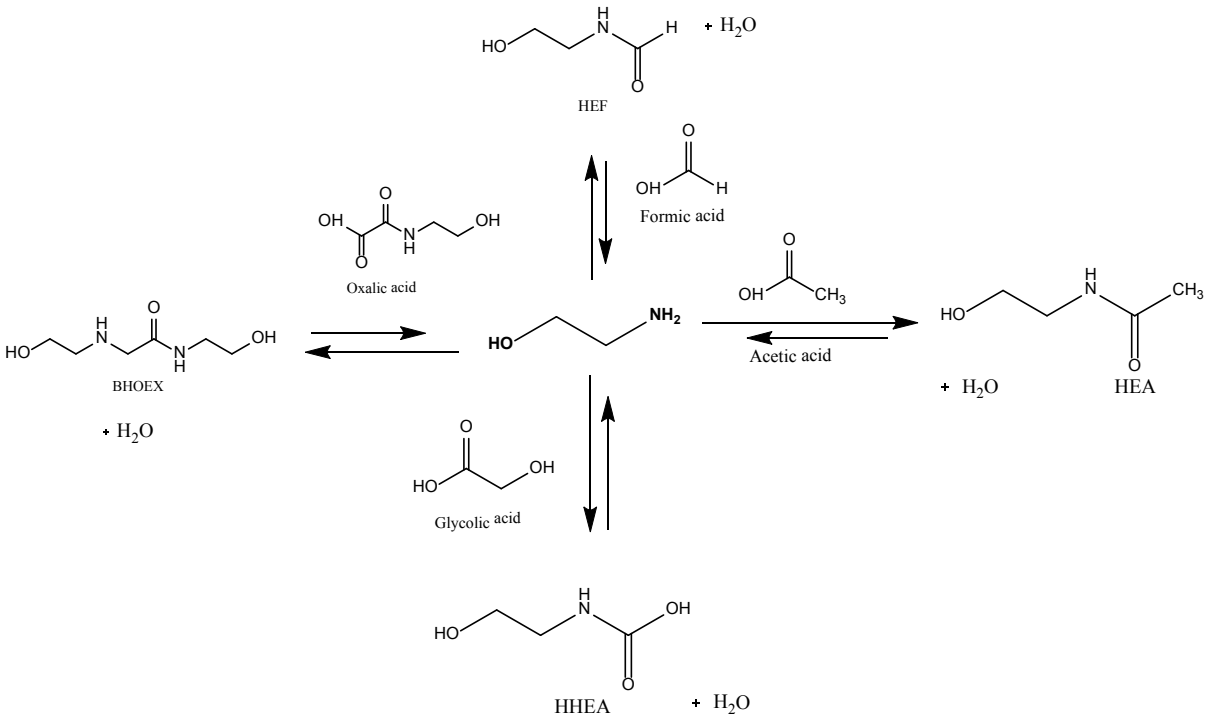


Figure 2.5: Reaction between MEA and the organic acids such as acetic, glycolic, oxalic and formic acids (modified from Lepaumier *et al.* (2011)).

Furthermore, there is a likelyhood of forming 4-(2-hydroxyethyl) piperazin-2-one (HEPO) upon the reaction of a degradation product, *N-(*2-hydroxyethyl) glycine, formed in the first stage of oxidation with MEA as illustrated in Figure 2.6.

Very little HEPO is formed from oxidative degradation; however, if very high temperatures are encountered then its concentration rises. It is deduced that the production of HEPO is an interplay between the two degradation processes (thermal and oxidative).

Oxidation degradation can be reduced from occurring within the capture plant by regulating the concentrations of CO_2, metal ions and O_2. Using oxidative inhibitors like chelating ligands such as, ethylenediaminetetraacetic acid (EDTA), which can bind strongly to the metal ions and as a result reduce the degradation process (Stern 2006).

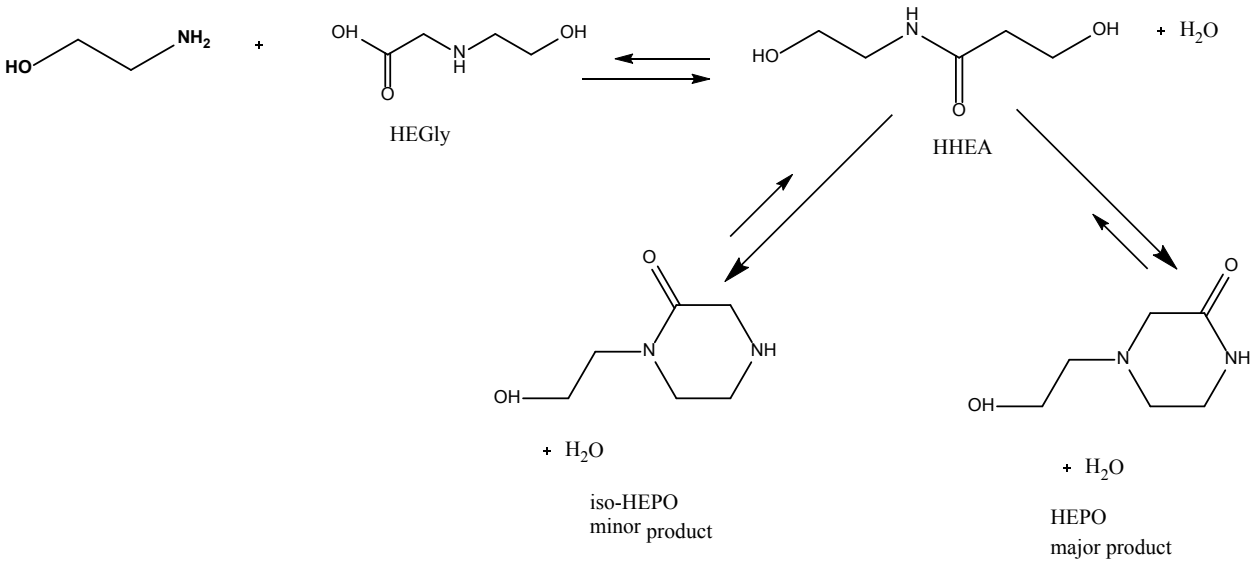


Figure 2.6: The most likely mechanistic pathway for the formation of HEPO (modified from Strazisar *et al.* (2003)).

2.3.2.1 Comparison of MEA degradation in real PCCC plants with laboratory based experiments

To comprehend which part of the PCCC amine-based system governs the amine degradation, degradation products of MEA under real PCCC conditions and laboratory based experiments (where the absorber conditions were depicted by the oxidative degradation experimental studies and the stripper conditions by thermal degradation) have been compared (Lepaumier *et al.* 2011, da Silva *et al.* 2012). From the degradation products characterised it is discovered that oxidative degradation is dominant over thermal degradation of MEA in a real PCCC plant. Also the degradation products such as, carboxylic acids are responsible for further degradation of the MEA solvent. In consequence of the varying conditions of temperature, pressure, O_2, CO_2 etc. encountered by the solvent in pilot plant, diverse range of degradation products are formed as opposed to stable conditions in laboratories.

2.3.3 Atmospheric degradation

During the PCCC process, small amounts of the amine solvent are either degraded (as part of the recycling process) or escape into the atmosphere in the flue gas that is vented out from the capture plant. Following the emissions into the atmosphere, the released amine compounds undergo even more complex atmospheric degradation

pathways in comparison to the other two degradation mechanisms, producing a wider array of products. A screening study has shown that there is an inevitable production of malevolent chemical substances, such as aldehydes, nitrosamines, nitramines and nitramides (Figure 2.7) upon the photo-oxidation of the emitted amines. All have undesirable impacts on the human health and natural environment (Låg *et al.* 2011).

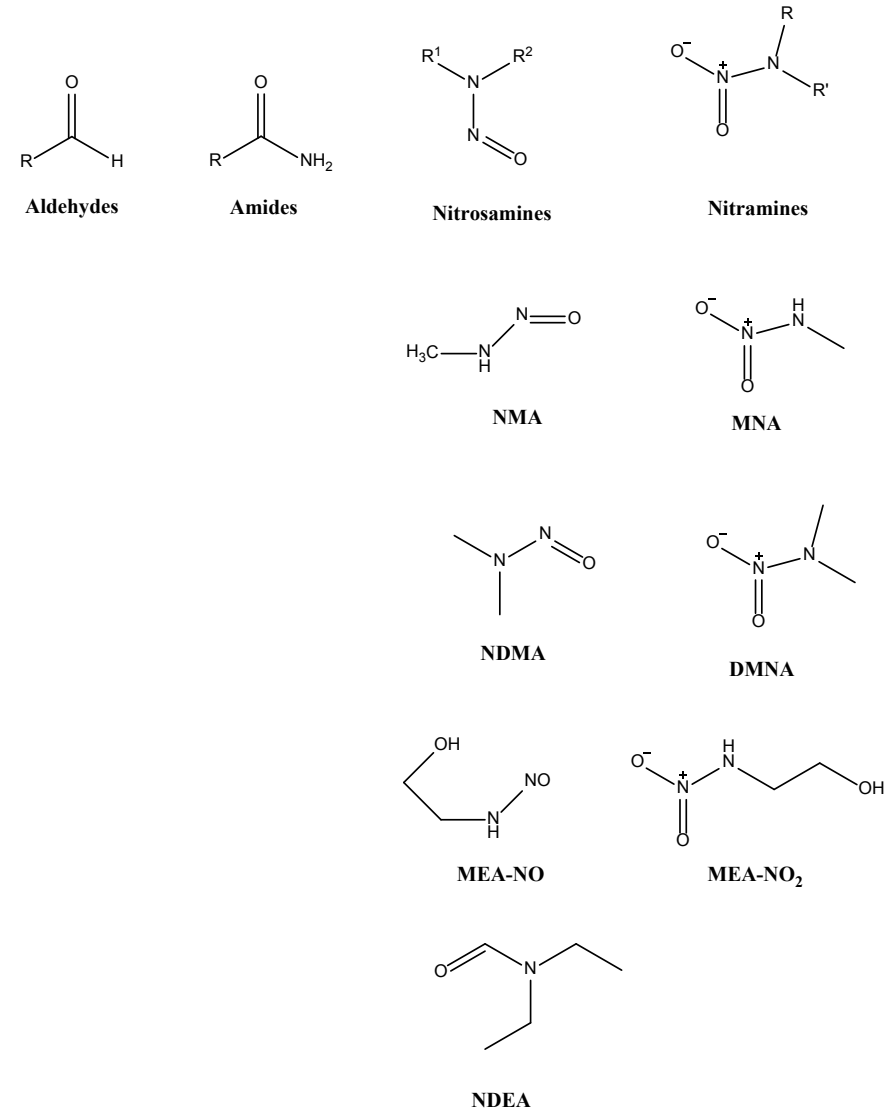


Figure 2.7: Conventional chemical structures of the atmospheric degradation products of amines such as aldehydes, amides, nitrosamines and nitramines.

Nitrosamines have the chemical structure of R^1 R^2 N-N=O, with an amine bonded to a nitroso moiety. The most commonly studied nitrosamine is N-nitrosodimethylamine (NDMA) owing to its toxic nature and detrimental environmental impacts. NDMA has been recognised as a Group 2A carcinogen. Recently it has been discovered that *N*-ethyl-*N*-nitroso-ethanamine (NDEA) has even

more adverse impacts than NDMA due to its pronounced toxicity. Such a class of compounds is soluble in water.

Nitramines on the other hand are organic molecules of the generic structure, R^1 R^2 N-NO_2, with a NO_2 moiety bonded to an amine. Dimethylnitramine (DMNA), methylnitramine (MNA) and ethanolnitramine (MEA-NO_2) are potential amine reaction products.

Generally, OH radicals initiate the atmospheric degradation by reacting with amines. Various radicals are formed following the initiation reactions, which undergo further reactions with other chemicals and radicals to form a wide range of degradation products.

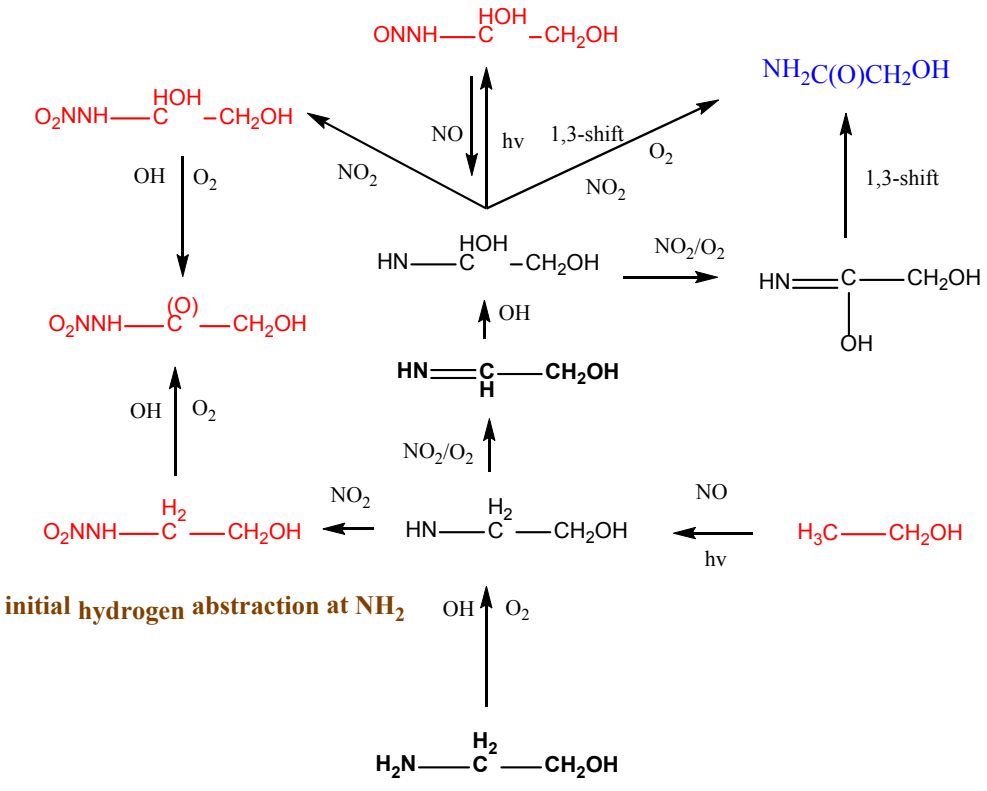
Studies postulate that the atmospheric degradation of MEA generates two distinct set of degradation products (Bråten *et al.* 2009, Knudsen *et al.* 2009). Abstraction of the hydrogen by OH at the $–CH_2$ and $–CH_2OH$ generates 2-hydroxy-acetamide and formamide (NH_2CHO). Additional amides and a few peroxyacetyl-nitrates are produced as well. In contrast, abstraction of the hydrogen from the NH_2- group generates different amides along with nitramines and nitrosamines. In the night, the degradation is further encouraged by reactions with NO_3 and O_3.

Experimental investigations at the European Photochemical Reactor, EUPHORE, in Valencia (Spain) studied the atmospheric photo-oxidation of MEA. Results demonstrated that over 80% of the MEA and OH radical reactions occur at $–CH_2$, whereas less than 10% occurs at $–CH_2OH$ and $–NH_2$. Formamide and formaldehyde (CH_2O) are formed as the major products (>80%) whereas amino acetaldehyde (NH_2CH_2CHO) and 2-oxo acetamide ($NH_2C(O)CHO$) detected as minor products (<10%). 2-nitroamino ethanol ($O_2NNHCH_2CH_2OH$) has also been detected to be the product in both cases, with its yield dependent on the atmospherically relevant NO_x conditions considered in the experiments (Nielsen *et al.* 2011a).

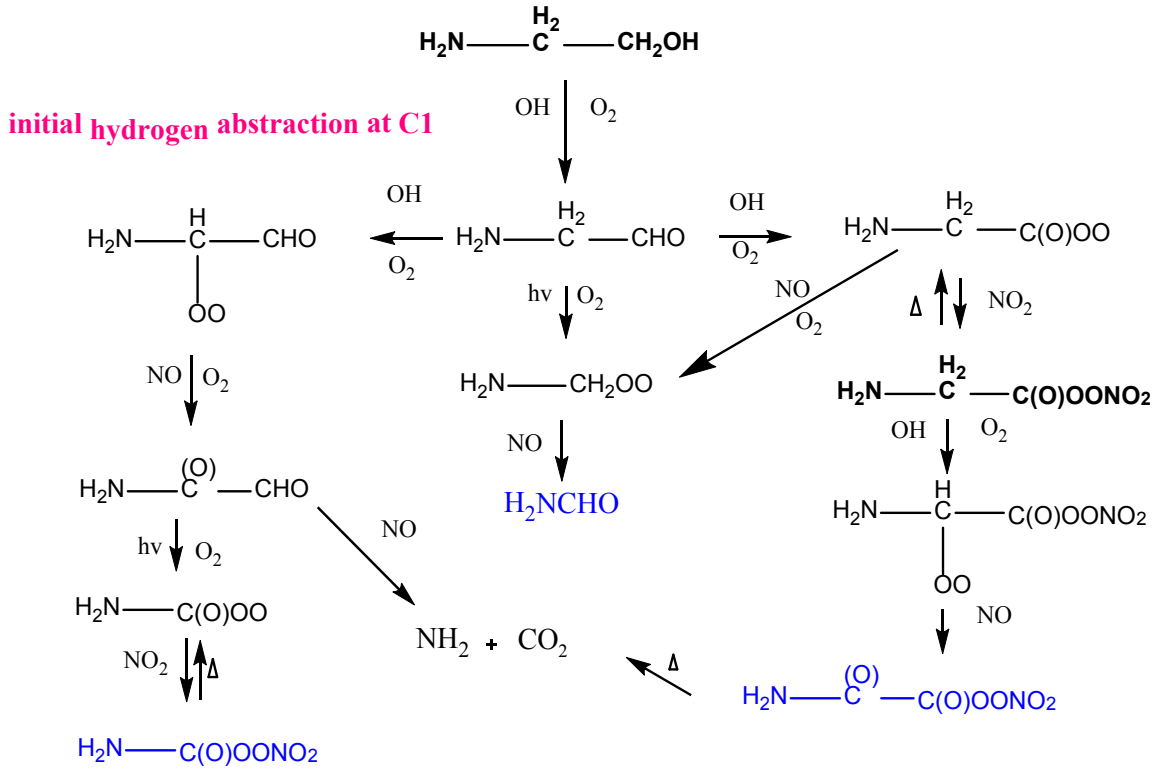
The proposed chemical reactions occurring in atmospheric degradation of MEA forming the mentioned degradation product are illustrated in Figure 2.8 (Bråten *et al.* 2009, Nielsen *et al.* 2011a, Nielsen *et al.* 2011b). The likely nitrosamines and nitramines produced as a consequence of atmospheric degradation are highlighted in red colour. Final products with a lifetime against atmospheric oxidation by the OH

radical (τ OH) of greater than 3 days are highlighted in blue, whereas, intermediate products with lifetime (τ OH) less than 3 days are highlighted in bold.

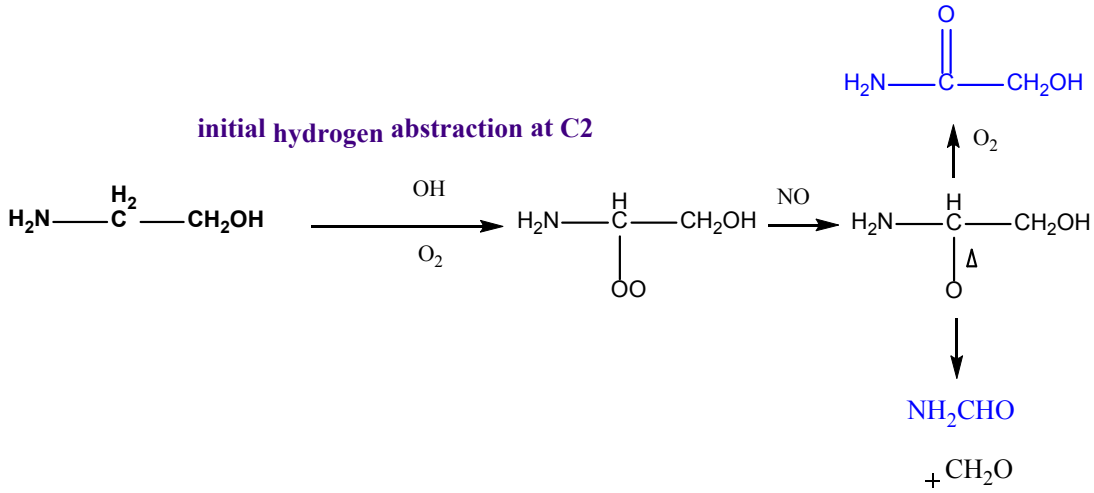
It is discovered that the atmospheric degradation pathway for MEA differs from the pathways followed by other amines such as MDEA, AMP and PIPA which have been explained in detail by Bråten *et al.* (2009). Nevertheless, it is inferred from the chemical reactions for atmospheric degradation of the amine solvents, that nitrosamines and nitramines are formed in sunlight owing to the existence of OH radicals. However, their formation in the atmosphere is limited by the photo-catalytic degradation. Therefore, nitrosamines are photo-chemically unstable as opposed to nitramines which are stable. For this reason, there is a higher potential to form the nitramines instead (Booth *et al.* 2012a, Booth *et al.* 2012b).



(a)



(b)



(c)

Figure 2.8: The proposed atmospheric degradation pathways for MEA following H-abstraction from either the (a) NH_2 (b) CH_2 or (c) CH_2OH groups (adapted from Shao and Stangeland (2009)).

2.3.3.1 Nitrosamine and nitramine emissions

Usually, solvent emissions are governed by the process design and plant operating conditions. The emissions from a PCCC plant mainly contain the solvent and ammonia with small amounts of nitrosamines and nitramines and low concentrations of various other degradation products (as identified in the previous sections).

A study in Maasvlakete (in Netherlands) on an MEA running PCCC plant recorded small amounts of nitrosamines (5 to 47 ng/Nm^3) and similar concentrations of MEA-nitramine to nitrosamines (Kolderup 2012). The measurements were taken at five different locations along the stack that included sampling points between absorber and the water wash (WW) unit, between the WW and demister, above the demister at the highest point, the inlet Brownian Demister Unit (installed on the pilot plant BDU) and at the outlet BDU. Other studies have also agreed with the obtained results (Aas and da Silva 2010, Graff 2010). There is barely any emission data reported for other solvents, but nevertheless, it is anticipated that the emission levels will coincide with those of MEA. Higher nitrosamine concentrations will be observed for secondary and/or tertiary amine solvents as they have a higher potential of forming them which will certainly be of higher concern (Booth *et al.* 2012b).

There is also a lack of experimental measurements of ambient air concentrations of nitrosamines and nitramines around the vicinity of an emitting plant. Reported values of MEA collected weekly around the emitting facility, Mongstad, are below 0.01 ng m^{-3} (Tønnesen 2011). de Koeijer *et al.* (2013) could not detect any nitrosamine and nitramine despite making measurements eleven times over a period of four days at three different locations around the emitting facility, Mongstad. They concluded that there is a need for extensive field experiments to be performed to assist with the understanding of the impacts of amine based PCCC technology on the environment (Karl *et al.* 2011).

2.4 Summary

The potential impact of amine degradation products on the environment makes its essential to study the amine degradation mechanisms to enable us to see if employing PCCC technology is safe to the human health and the environment. MEA being the reference solvent for the CO_2 capture has been widely studied; however, other solvents such as DEA, MDEA, AMP, PZ and amine blends have also been under

attention. Nevertheless, there is still lack of information regarding their degradation chemistry.

The types of degradation mechanisms that amines such as, MEA undergo in the capture plant and then in the atmosphere have been described. The influence of temperature, O_2, CO_2, metal ions etc. on the degradation products are also highlighted. The key products characterised from MEA degradation in capture plants constitute of ammonia, HEHEAA and HEPO. While, the main degradation products identified in laboratory experiments depicting atmospheric conditions have been OZD, HEEDA, and HEIA from thermal degradation and ammonia, HEA, HEI and HEF from oxidative degradation.

With regards to degradation products formed outside of the plant i.e. after the amines are emitted to the atmosphere, aldehyde and imines have been confirmed to be the major products. However, the products of major concern are nitrosamines and nitramines due their cariogenic nature. A wide range of products have been discovered and numerous others remain unidentified. Various suggestions made with respect to the degradation mechanisms still lack in evidence.

2.5 Conclusions

It is concluded that despite various studies comprehending amine degradation, the degradation processes still remain poorly specified. There are yet to be methods developed for the evaluation of nitrosamines and nitramines concentrations formed through atmospheric degradation especially (Nielsen *et al.* 2011a, Nielsen *et al.* 2011b). It is for this reason prudent to carry out more investigations to enhance the understanding of the amine degradation chemistry occurring both within the plant and in the environment as well as to characterise the amine degradation products formed. By identifying and determining the quantitative estimates of these chemical discharges produced, the potential harm they pose due to their carcinogenic nature can be assessed.

The objective of this work is to assess the atmospheric fate of the amine emissions in particular. Therefore, the focus is on investigating and comprehending the atmospheric degradation mechanisms of the reference solvent, MEA and its degradation products. Due to the challenges faced in performing experimental investigations to measure these chemical discharges, theoretical methods need to be

employed to produce results within experimental accuracy. By doing so, the understanding of the mechanisms and kinetics of the reaction pathways in the atmospheric schemes of interest can be enhanced (discussed in chapter 5).

Chapter 3 Overview of atmospheric dispersion modelling of amine emissions from CO_2 capture

3.1 Introduction

A quantitative understanding of the atmospheric fate of amines from amine based CO_2 capture process is essential for human health and environmental assessment. In order to do so, it is a perquisite to consider atmospheric chemistry along with the expected dispersion processes to determine concentration time profiles with spatial distribution of the amines and their degradation products. By doing so, it is possible to account for the complex interactions of the atmospheric processes involved in influencing the amine atmospheric fate. The information gained forms the foundation for the risk assessment associated with amine emissions.

The amines and amine degradation products emitted from the PCCC plant, when released into the atmosphere are transported over large distances by large-scale air flows and dispersed by small-scale air flows and turbulence, mixing them with ambient air. The process of dispersion by wind is complex due to the existence of various sized eddies in the atmospheric flow (Bluett *et al.* 2004). There are challenges in the collection of experimental data of the discharged pollutants in time and space with respect to the emitting facility. To be able to characterise and quantify this by describing the behaviour of emitted pollutants from an industrial plant to the atmosphere, mathematical simulations of the chemistry and physics

controlling the transformation, transportation, and dispersion of chemical pollutants in the air can be performed by computer programs.

Programs such as air quality dispersion models can estimate the atmospheric concentration levels, dry and wet deposition fluxes of the emitted chemical pollutants over distance and time from the source. In order to do this, these programs require information on emission rates of the different chemicals from the source, characteristics of the emission source, local topography, meteorology (such as wind speed and direction, ground surface temperature and cloud cover) of the site and background concentration of the chemical pollutants. The use of such information in a computer-based air dispersion model is illustrated in Figure 3.1. It shows that a dispersion model primarily consists of four stages; the data input, concentration and dispersion calculations and analysis (Bluett *et al.* 2004).

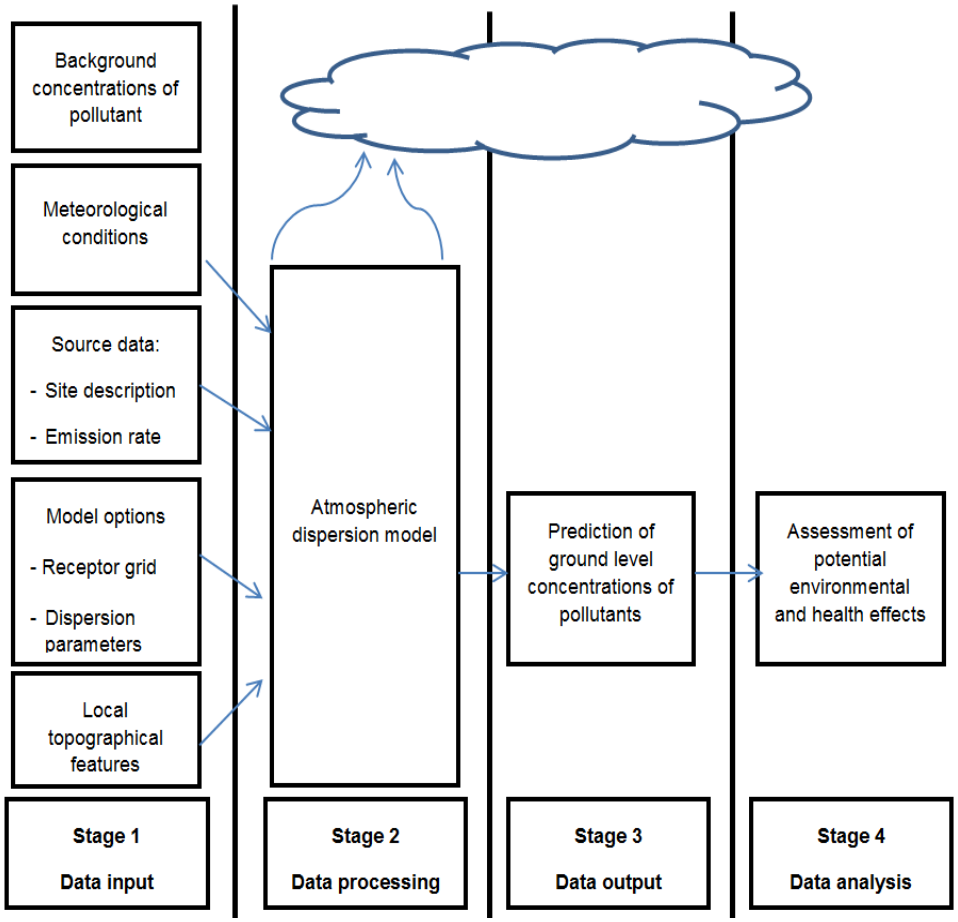


Figure 3.1: An outline of the air dispersion modelling procedure (adapted from Bluett *et al.* (2004)).

Conducting air dispersion modelling studies assist in understanding the behaviour of the chemical discharges from such industrial processes. It is essential that both amine chemistry studies and theoretical atmospheric dispersion studies are considered together in order to understand their fate in the atmosphere as much as possible. In the previous chapter, an insight into the chemical degradation pathways of the amines in the atmosphere was given. To build upon it, the following sections describe and discuss the fundamentals of atmospheric dispersion. The types of air quality models used in literature to quantify the atmospheric processes are explained. The dispersion model most appropriate for this study is evaluated based on the available options. Recent studies on the atmospheric dispersion of amines and their degradation products are also highlighted.

3.2 Amine atmospheric chemistry

To be able to predict the fate of the amine degradation products in the atmosphere, there is a need to incorporate the atmospheric degradation chemistry of nitrosamines and nitramines into air dispersion models. However, the development of the chemistry model relies on enhanced understanding of the chemistry of the amine and amine degradation products in gaseous phase (and aqueous phase), which apparently is very complex, owing to the various chemical substances involved and the reactions they undergo in gaseous. As the amine chemistry is very complex, it poses a challenge for the dispersion modelling and it is a necessary to carry out considerable research before detailed chemistry schemes can be implemented into dispersion models.

So far studies have established that with regards to the atmospheric amine chemistry, the OH radical-initiated gaseous chemistry is the most important process, where the amine and their products both react with the OH forming complex and branched chemical pathways. The proposed degradation reaction schemes of amine degradation in CO_2 capture (described in section 2), suggest that the PCCC emissions and the amine degradation products formed in the atmosphere are mainly of NH_3, NO_x (NO and NO_2), CO_2, amines, aldehydes, amides, alkyl amines, nitrosamines and nitramines. Out of these, nitrosamines and nitramines have been known to be malevolent to human health and natural environment. Research is on-

going to investigate the time scales of chemical reactions of the OH radicals with nitrosamines, nitramines etc., to develop a detailed chemistry scheme.

Key factors to assist with determining the exact concentrations of the emitted amines and the resulting products are (Fowler and Vernon 2012):

(i) Emission rates of the various chemicals emitted from the source i.e. the amount of amine, nitrosamine and nitramine released from PCCC plant,
(ii) Rate of chemical transformations of the amine into nitrosamine and/or nitramine in the atmosphere
(iii) Nitrosamine and/or nitramine decay rate in the atmosphere
(iv) Rate of atmospheric dispersion of the emitted chemicals
(v) Wind speed and direction
(vi) Specific features of the turbulence between source and receptor
(vii) Likely concentrations of the emitted and newly formed chemicals in the atmosphere and
(viii) Wet and dry deposition of these chemical substances.

All these factors can be determined if a model performs both complex chemical transformation reactions and complex gas dispersion calculations simultaneously. It will help achieve precise and realistic estimates of the concentration of amines and their degradation products, along with their deposition flux distributions in the immediate environment surrounding a PCCC plant.

In view of the above factors, different types of air quality models are evaluated in terms of their capabilities for the purposes of this work, where reactive chemical pollutants are considered for which vital chemical and physical processes need to be accounted for and that too for long term dispersion modelling. The key feature in deciding their suitability is the ability to consider chemistry along with advection and dispersion calculations.

3.3 Air pollution dispersion models

Dispersion modelling can be used for (Bluett *et al.* 2004) :

- Determining compliance of emissions with air quality guidelines and managing real emissions,
- Assessing the risk of released harmful substances and

- Running 'numerical laboratories' for the purposes of scientific investigations, including experiments which are costly in real world.

The essential chemical and physical processes considered in air pollution models consist of the following (Fatehifar *et al.* 2006):

1. Advection (horizontal transport)
2. Horizontal diffusion
3. Dry and wet deposition processes
4. Vertical diffusion and transport
5. Emissions and chemical reactions

These processes can be described mathematically by the following system of partial differential equations as shown below:

$$\frac{\partial C}{\partial t} = -\frac{\partial (U_x C)}{\partial x} - \frac{\partial (U_y C)}{\partial y} - \frac{\partial (U_z C)}{\partial z} - \frac{\partial}{\partial x}\left(D_x \frac{\partial C}{\partial x}\right) + \frac{\partial}{\partial y}\left(D_y \frac{\partial C}{\partial y}\right) + \frac{\partial}{\partial z}\left(D_z \frac{\partial C}{\partial z}\right) + E - (K_1 + K_2)C + Q(C) \quad (3.1)$$

Where C represents the concentration of the chemical pollutant (such as the amines and the degradation products), U is the wind velocity, D is the diffusion coefficient in each direction, E is the emission source, K_1 and K_2 are the wet and dry deposition coefficients and $Q(C)$ signifies chemical reactions.

It is, however, important to note that atmospheric dispersion models cannot be used to predict the magnitude, location and timings of the ground concentrations with 100% accuracy. The accuracy and quality of the results are influenced by the appropriate model for the task, accurate information of the source and meteorological data (Bluett *et al.* 2004).

3.3.1 Gaussian Plume Models

Gaussian plume models are the oldest (Bosanquet and Pearson 1936) and the most widely used model type e.g. AERMOD. Such models base their underlying assumption for the dispersion of continuous and buoyant air plumes initiating from ground level or raised sources such as, industrial stacks to follow a Gaussian distribution. This means that they predict the plume distribution to follow a normal distribution. The characteristics of the mean turbulence and flow are assumed to be

uniform in time. A pictorial illustration of a Gaussian distribution of pollutant concentrations is given in Figure 3.2.

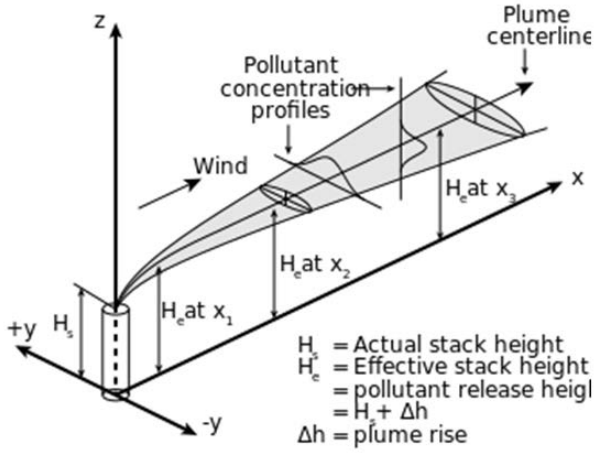


Figure 3.2: A pictorial depiction of plume rise and dispersion from an industrial stack (Beychok 2005).

To solve E.q 3.1, some assumptions are made (Fatehifar *et al.* 2006):

(i) Steady-state conditions are assumed i.e. $\partial C/\partial t = 0$
(ii) Wind velocity only in the x- direction, U_x , is considered and those in the y and z are assumed to be 0, since wind is assumed to be invariant and consistent with height, therefore, a steady flow.
(iii) Constant eddy diffusivities are assumed i.e K = constant.
(iv) No deposition to the ground i.e. $K_1 + K_2 = 0$.
(v) Mass is conserved and therefore $Q = \int_{-\infty}^{\infty}\int_{0}^{\infty} UC(x,y,z)dzdy \;\; when\; x > 0$
(vi) Conservative transport is considered, i.e. no chemical reactions which give $Q = 0$.
(vii) Transport in the x-direction i.e. advection surpasses longitudinal diffusion in the x-direction i.e. $\frac{\partial}{\partial x}\left(D_x \frac{\partial C^s}{\partial x}\right) = 0$

By applying the above made assumptions the system of partial differential reduces to:

$$\frac{\partial (U_x C)}{\partial x} = \frac{\partial}{\partial y}\left(D_y \frac{\partial C}{\partial y}\right) + \frac{\partial}{\partial z}\left(D_z \frac{\partial C}{\partial z}\right) + E \qquad (3.2)$$

When the above equation is solved, the solution is as shown (Dacunto and Hendricks 2007):

$$C(x,y,z) = \frac{Q}{4\pi x\sqrt{D_y D_z}} exp\left(\frac{-y^2}{4D_y\left(\frac{x}{U}\right)}\right) exp\left(\frac{-z^2}{4D_z\left(\frac{x}{U}\right)}\right) \tag{3.3}$$

It should be noted that E.q 3.3, is for a domain with no boundary conditions considered. Therefore, typical deviation parameters (such as σ_y and σ_z which describe the width of the concentration distribution i.e. Eq 3.4 and 3.5) are considered. An additional assumption with regards to the most of the dispersion occurring in the downwind x direction is made. Upward dispersion i.e. reflection of the plume from the ground is also accounted for and as result the final solution takes the following form (Dacunto and Hendricks 2007) as shown in E.q 3.6:

$$\sigma_y{}^2 = 2\, D_y(\frac{x}{U}) \tag{3.4}$$

and

$$\sigma_z{}^2 = 2\, D_z(\frac{x}{U}) \tag{3.5}$$

i.e.

$$C(x,y,z,H) = \frac{Q}{2\pi\sigma_y\sigma_z U} exp\left(-\frac{y^2}{2\sigma_y{}^2}\right)\left\{exp\left(-\frac{(z-H)^2}{2\sigma_z{}^2}\right) + exp\left(-\frac{(z+H)^2}{2\sigma_z{}^2}\right)\right\} \tag{3.6}$$

where $C(x,y,z,H)$ is the pollutant concentration as a function of downwind position (x,y,z); Q is the mass emissions rate; σ corresponds to the disk area in a simple model (values depend upon downwind distance, x); $H = h_s + \Delta h$ and is the effective stack height including the rise of the hot plume near the source.

The first exponential term of E.q 3.6 is the distribution of the mass in cross-wind dimension (y) at a given downwind distance x and the last two exponential terms are the distribution of mass in vertical dimension (z) at a given downwind distance x (includes the effect of surface reflection).

Along with the reflection from the ground there are also reflections from inversions at the top of the atmospheric boundary layer, which can considerably influence concentration. Therefore, equation 3.6 is expanded to account for it; here the height, H, is considered as $2H_i - H$ (Škraba *et al.* 2012) and H_i is the inversion height or atmospheric boundary layer height:

$$C = \frac{Q}{2\pi\sigma_y\sigma_z U} exp\left(-\frac{y^2}{2{\sigma_y}^2}\right)\left\{exp\left(-\frac{(z-H)^2}{2{\sigma_z}^2}\right) + exp\left(-\frac{(z+H)^2}{2{\sigma_z}^2}\right) + exp\left(-\frac{(z-2H_i-H)^2}{2{\sigma_z}^2}\right) + exp\left(-\frac{(z+2H_i-H)^2}{2{\sigma_z}^2}\right) + exp\left(-\frac{(z-2H_i-H)^2}{2{\sigma_z}^2}\right)\right\} \quad (3.7)$$

Hence, the above equation is representative of the Gaussian plume model. Additionally, such models consider the dispersion of the pollutant as approximately related to a stability class which is classified as being one of 'A' which represents very unstable cases through to 'F' or 'G' the most stable cases.

On the whole, the plume model stimulates hourly average concentration from the emission rate and uniform meteorological conditions across the modelling domain. These models are generally applicable when the chemical pollutants are considered inert (i.e. no chemical transformation reactions), the terrain not complex and meteorological conditions uniform across the modelling domain.

3.3.1.1 AERMOD (Beychok 2005)

AERMOD is a steady-state Gaussian plume dispersion model capable of simulating dispersion and deposition of air pollutant emissions up to 50 km from industrial sources. It has a terrain pre-processor which can evaluate the impact of complex terrain on the dispersion of the plume. However, AERMOD is limited in the consideration of complex chemical reactions occurring in the plume and their deposition to soil and water. Thus, it would not be helpful for the purposes of this study.

3.3.2 Advanced Gaussian Dispersion Models

Unlike the Gaussian plume model, advanced Gaussian dispersion models (e.g. ADMS 5), consider an advanced approach where the spread of the plume is precisely linked to the characteristics of the atmospheric turbulence. Two distinct parameters are used to express the boundary layer;

(a) The boundary layer height which is the height above the ground at which the air stops being turbulent and

(b) The Monin-Obukhov length which is a parameter linked to turbulence creation in the boundary layer.

These parameters are determined from the meteorological data and surface properties such as, surface roughness, surface wetness and surface albedo (the fraction of solar radiation reflected from the surface of the earth into space) (CERC 2010).

Advanced dispersion models like the Gaussian puff models (e.g. CALPUFF) consider pollutant releases as a series of puffs that are transported by winds. Distinct amounts of pollutant emissions are represented as puffs that increase in volume as a consequence of turbulent mixing. Such models account for complex atmospheric dispersion and deposition conditions over a longer distance unlike the simple Gaussian models (Thielen *et al.* 2007).

Advanced Gaussian models consider time dependent emissions that vary horizontally and time dependent meteorological conditions. They are applicable when the chemical pollutants are not inert but undergoing chemical transformations, the meteorological conditions varying across the modelling domain (i.e. incompatible with a steady-state Gaussian model), sources or receptors located in complex terrain (which impact the meteorological and plume-dispersion properties) and if the chemical pollutants accumulate in calm conditions or re-circulate with wind direction (Bluett *et al.* 2004).

3.3.2.1 ADMS 5

Atmospheric Dispersion Modelling System ADMS 5 (Cambridge Environmental Research Consultants, Cambridge, UK) is a dispersion model employed for modelling air quality impact of pollutants from industrial sources (Figure 3.3).

ADMS 5 is a new generation Gaussian plume air dispersion model, with its atmospheric boundary layer properties characterised by the boundary layer depth and the Monin-Obukhov length L_{MO}, in contrast to using the single parameter Pasquill-Gifford class (used by other Gaussian model). Under stable conditions, L_{MO}, is positive, whereas, it is negative under unstable or convection conditions. Its integrated plume rise model uses a Runge-Kutta method to solve conservation equations to determine plume rise. It also accounts for the effect of plume buoyancy, momentum and penetration of boundary layer inversion.

The model is applicable up to 60 km from the source and it possesses various advance features which makes it a suitable candidate for accessing the fate of pollutants from industrial installations. ADMS 5 has a complex terrain model to calculate the 3D flow and turbulence field over the study domain for studying the effects of terrain elevation and surface roughness on the dispersion. In order to investigate the chemical transformation of amines emitted from a capture plant together with their dispersion and transport, it has a specially designed Amine Chemistry Module (adapted from Nielsen *et al.* (2011a)) in the ADMS 5 atmospheric dispersion model(CERC 2012a). Within ADMS 5, it is possible to describe the entire atmospheric fate of the involved amines, including their growth and decay as previously reported by CERC (2012d, CERC 2012c). ADMS 5 with its amine chemistry module is commercially available to use. Additionally, its dry and wet deposition model estimates the rate of dry and wet deposition of the modelled species to the ground.

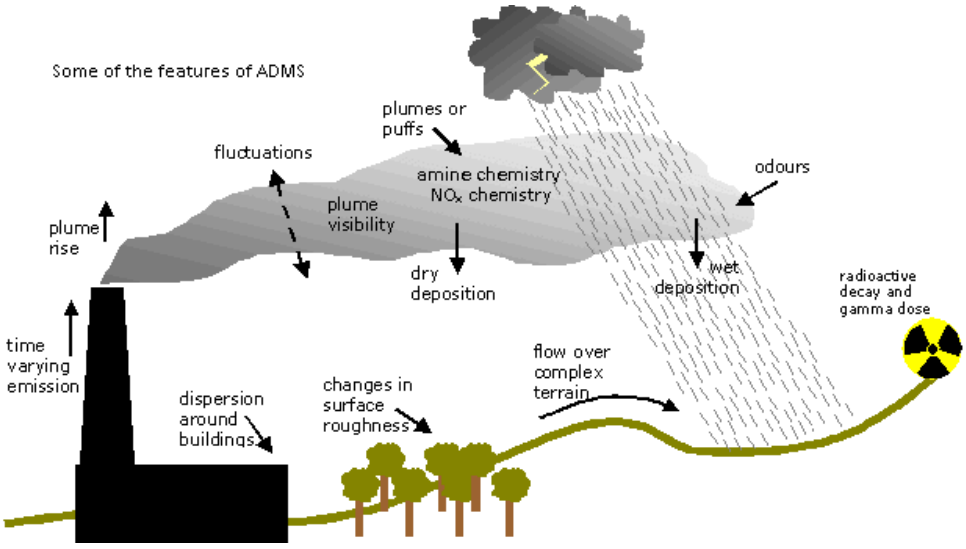


Figure 3.3: A pictorial illustration of ADMS model features (from (CERC)).

3.3.2.2 CALPUFF

CALPUFF is a non-steady state puff model capable of simulating the influence of temporal and spatial variation of meteorological conditions on air pollution transformation, dispersion, transport and deposition. The model can be considered for long range dispersion modelling such as 100 km from the sources, as well as for complex terrain. Although, CALPUFF can consider NO_x chemistry, it can be extended to amine chemistry. US Environmental Policy Agency declared CALPUFF as the guideline model which is considered as reference for regulatory purposes for long range pollutant transport of greater than 50km (Scire *et al.* 2000).

As part of a study on behalf of Gassnova (Fowler and Vernon 2012), DNV implemented a simplified amine gas-phase chemistry consisting of radical gas-phase reactions, photochemistry, gas-liquid equilibrium processes and location dependent variables, such as NO_x emitted from the process, into a non-steady state Gaussian puff atmospheric dispersion model CALPUFF. Since, the key factor in simulating amine transformation processes is the time parameter, it is considered in CALPUFF. This makes it possible to model chemical pollutant transport step-by-step from the source to the receptor, since it is a time-varying dispersion model.

It should be noted that both the developers of CALPUFF, Fowler and Vernon (2012) and ADMS 5, CERC (2012d) described the chemistry using rate constants from literature and in the absence of experimental rates, assumptions were used. Such an approach has some uncertainties associated with it. Nevertheless, these models can still be used with more accurate rates to make reliable estimates of the chemical pollutants of interest.

However, in the open source code of the CALPUFF model, amine chemistry is yet to be included. Therefore, this model is omitted since consideration of amine chemistry is essential for this study.

3.3.3 Lagrangian

A Lagrangian model mathematically tracks the plume particles as they disperse in the atmosphere and models their motion as a random walk process (Lamb 1932, Batchelor 2000). It then evaluates the dispersion by performing statistical calculations of the trajectories of a large number of plumes particles. The model

considers a moving frame of reference to follow the plume particles as they disperse from their initial position.

3.3.3.1 Particle Dispersion Model

This NILU's Lagrangian Praticle Dispersion Model (Stohl *et al.* 2005) is very complex and computationally expensive. As this study aims for a practicable approach, this type of model is omitted. Furthermore, it is not commercially available to use.

3.3.4 Eulerian model

Eulerian model evaluates dispersion in the same manner as the Lagrangian model. The only difference is that Eulerian model uses a stationary 3D Cartesian grid as a frame of reference (Lamb 1932, Batchelor 2000). However, Eulerian models have a minimum grid size of 1 km which prohibits it from resolving the minute details of the plume processes such as, dispersion that take place close to the source.

Both the Lagrangian and Eulerian models are appropriate for really complex terrain and for climatic environments where fine details are essential. In general, both mode types require very long run times and are limited in accounting for vital chemical and physical process. They are, therefore, used for short term dispersion modelling. Examples of these include The Air Pollution Model developed (TAMP), Lagrangian probability density function (PDF), the USEPA-model WRF/CMAQ and the Computation Fluid Dynamics (CFD) models.

3.3.4.1 CSIRO and WRF-Chem

Emmerson *et al.* (2013) for CSIRO integrated degradation of MEA scheme into an Eulerian 3D chemical transport model.

Very recently Karl *et al.* (2015) and Karl *et al.* (2014) incorporated the amine chemistry into a mesoscale numerical weather prediction system, Weather Research and Forecasting (WRF) Eulerian model coupled with Chemistry (WRF-Chem).

The limitation of CSIRO and WRF-Chem models is that the schemes considered are specific to MEA degradation chemistry and these models are also not commercially available to use.

3.3.4.2 TAMP

The Air Pollution model (TAMP) developed by CSIRO (Hurley *et al.* 2005, TAMP 2010) comprises of a Lagrangian and an Eulerian model. This integrated model includes prognostic meteorological processor and air quality modules to evaluate the dispersion of air pollution plumes. The Lagrangian model is employed in the inner most grid domain, where it considers the chemical and microphysical processes occurring in the plume estimated from the Eulerian model employed for the outer domain.

Karl *et al.* (2011) and de Koeijer *et al.* (2013) have used TAMP to perform inert dispersion of amine emissions from a PCCC capture plant and then used experimentally determined formation yields of nitrosamines and nitramines from literature to consider chemistry with dispersion calculations. However, this is a very conservative approach and therefore cannot be used in this work. Also, this model is not commercially available to use.

3.4 Summary

From the Table 3.1, the different dispersion models are compared with detail to their features such their ability to consider amine chemistry along with dispersion, deposition calculations as well as their computational cost and commercial availability.

Table 3.1: Comparisons of dispersion models with respect to their features for the purposes of this study.

	Rigorous Validation by developers	Amine chemistry module	Wet and dry deposition	Range	Computationally expensive	Commercially available
AERMOD	Yes	No	Yes	50km	No	Yes
CALPUFF	Yes	No	Yes	>50km	No	Yes
ADMS 5	Yes	Yes	Yes	~60km	No	Yes
TAMP	No	No	Yes	>50km	No	No
WRF-Chem	~	Yes	Yes	>50km	Yes	No

3.5 Conclusions

An overview of the dispersion modelling with their scientific approach was explained. Different models were explained in terms of their modelling methodology, scientific concepts, and essential features relevant to this work. Upon evaluating existing models for the purposes of this PhD research, the advanced air dispersion model ADMS 5 with its amine chemistry module, was considered to be the best suitable choice for atmospheric chemistry, dispersion and deposition of amines from PCCC technology for the purposes of this study, with respect to its commercial availability and computational cost. It has been rigorously validated by its developers as well.

Chapter 4 Human health and environmental risk assessment

4.1 Introduction

It has already been well established by now that post combustion technology has the potential to emit toxic organic compounds which can impact the natural environmental and human health. The emitted chemicals can enter into different environmental borders such as water, soil and vegetation, affecting the human population through both direct and indirect pathways, which comprise of inhalation, ingestion, dermal contact etc. as illustrated in Figure 4.1 (Suciu *et al.* 2013). Therefore, concerns associated with amine-based PCCC technology need to be addressed prior to regulatory approval and before its introduction at a commercial scale.

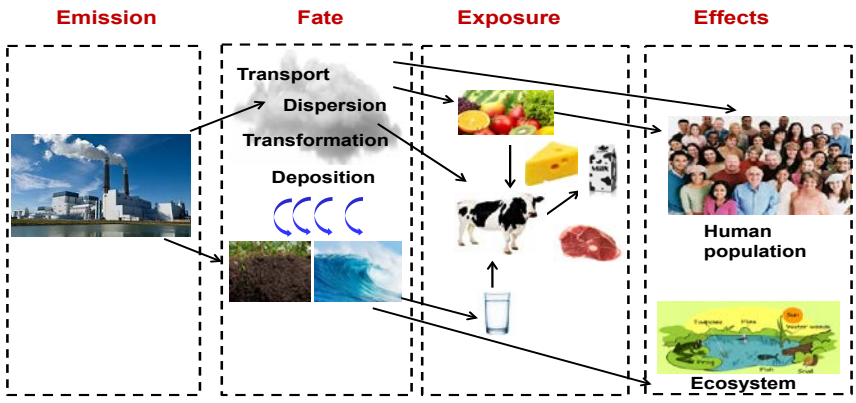


Figure 4.1: Source-pathway-receptor paradigm.

Recent investigations have discovered that amines in general, are skin irritants and can be toxic to animals at significant concentrations. Studies on MEA for instance, have revealed that it is a skin irritant and long term exposure of it to the skin causes skin burns and necrosis (Lessmann *et al.* 2009). This is the most significant effect of MEA. It is irritating to the eye and respiratory tract as well. Some preliminary guidelines have been established for critical levels of atmospheric concentrations of inhalation exposure risk for amines such as MEA, above which humans should not be exposed to over time. The critical MEA air concentration MEA is set to 10 $\mu g/m^3$ (Låg *et al.* 2011). In general, MEA along with other amines such as MDEA, AMP and PIPA are not known to be carcinogens.

However, about 90% of 300 nitrosamines tested in animal, human and bioassay studies have well established that this class of compounds possess carcinogenic properties (Fritz 1975, Låg *et al.* 2009, Låg *et al.* 2011). The effect on humans from exposure to nitrosamine in tobacco smoke has been documented since a long time. One of the very first studied performed by Magee and Barnes (1956), revealed that NDMA causes liver damage in animals. These investigations propose that nitrosamines undergo DNA alkylation, causing permanent genetic mutations in the DNA of the cells, consequently, making them cancerous.

On the other hand, experimental studies conducted in vivo and in vitro have revealed that nitramines promote tumour by undergoing deamination to form formaldehyde and ammonia. Nitramines such as, dimethyl nitramine (DMNA) and monoethanol nitramine (MEA-NO_2) have shown carcinogenic effects on laboratory animals but they are less lethal than their corresponding nitrosamines (Selin 2011).

The types of tumours caused by exposure to these harmful chemicals consist of lung, skin, stomach, skin, kidney, nasal cavities, liver, brain, oesophagus, oral cavity, pancreases, hematopoietic system, gut, urinary bladder, nervous system etc. (Olajos and Coulston 1978, Verna *et al.* 1996). Experimental investigations have established that the covalent binding of these carcinogenic compounds show a linear dose-response relationship in the low dose region. This suggests that there is no threshold dose for the genotoxic effect on humans. So although the present data on these substances is scant, there is enough evidence to infer that these classes of compounds pose risk to the humans even at the lowest exposure concentration.

In conjunction with studying the impacts on humans, there are environmental impacts associated with the amines when they undergo deposition to the soil and water, where they are subject to natural processes, such as biodegradation into nitrogen components, which are essential for plant growth. If increased amine deposition occurs then there is an increase in nitrogen content in the soil and water which leads to eutrophication. Consequently, enhancing biomass production and reducing plant biodiversity.

Chronic impacts on algae, bacteria and fish in the aquatic environment from long term exposure to nitrosamines and nitramines in the aquatic environment have also been discovered (Brooks and Wright 2008).

Although, there is no internationally agreed methodology for performing human health and environmental risk assessment of genotoxic substance, it is nevertheless crucial to consider a reliable and most commonly used approach for human health and environmental risk assessment.

In this work, human health and environmental risk assessment is explained as a process for focusing on the effects as a result of coming in contact with risk agents, to establish risk management controls (Crawford-Brown 1999, USEPA 1999).

4.2 Risk Analysis

Risk analysis involves the observation of circumstances in which a target receptor is at a risk of being exposed to a hazard (OECD 2003). Such a process is comprised of three parts as illustrated in Figure 4.2 and explained according to Rovira *et al.* (2013):

- Risk communication is the information transfer between general population, policy makers and managers.
- Risk management is the consideration of socio-economic and political aspects whilst making decisions with relevance to risk assessment knowledge.
- Risk assessment is the method of calculating the kind and likelihood of unfavourable effects on human and environment as consequence of being exposed to a stressor in polluted environmental channels (OECD 2003). By doing so, the characteristic features of both the target receptor and risk agent

are cogitated. The risk assessment paradigm constitutes of four stages (EPA 2015):

- Hazard identification which examines the potential of a stressor to cause adverse effects on a target (human or ecological systems) along with detecting the nature of the effect.
- Hazard characterisation also known as dose-response assessment which investigates the mathematical correlation between the effects and the exposure i.e. the harm caused to the receptor at varying exposure levels.
- Exposure assessment takes into account the amount, frequency, and duration of the exposure to the substance.
- Finally, risk characterisation evaluates the increased risk caused by such exposure to the exposed population.

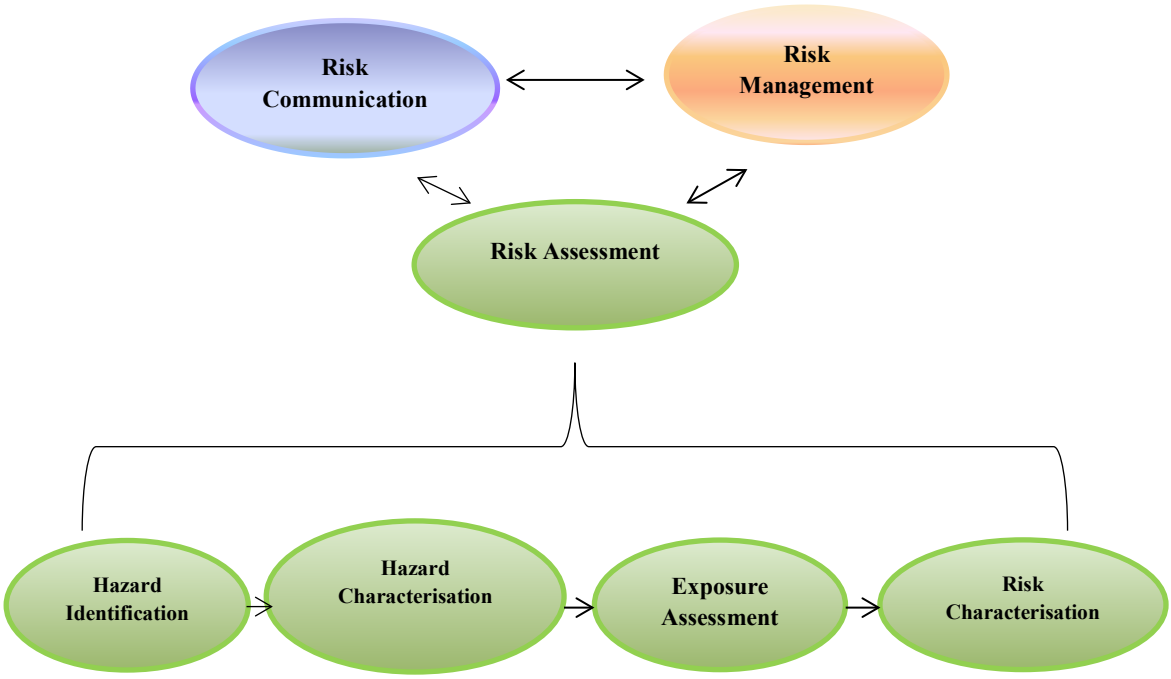


Figure 4.2: A risk analysis paradigm (modified from (Fazil 2005)).

The human health risk assessment assists policy makers to comprehend the potential risk posed through various environmental channels. By gathering all this information as part of risk analysis, it is then possible to establish protective health guideline limits under which the chemicals of interest would not adversely affect the human health.

In the subsequent sections, human health and environmental risk assessment is explained in detail.

4.3 Human Health Risk Assessment

4.3.1 Hazard Identification (USEPA 1998b)

Hazard identification involves ascertaining the probability of a stressor to trigger a rise in the occurrence of a particular hostile health problem such as cancer etc. in the target receptor. If the stressor is a chemical, the hazard identification involves the investigation of its literature data to acquire the evidence to identify the association of the chemical stressor to its adverse effects. If the target receptor is human and the stressor is a chemical then exposure to it, may consequently lead to negative effects such as, cancer, skin irritation, disease, defects in reproductive system, corrosiveness, acute and long term toxicity death etc.

The sources of data for hazard identification come from clinical investigations involving humans. Such data makes it possible to determine the connection between the specific stressor and its subsequent influence on the target. However, such studies are sparse owing to the ethical concerns associated with the testing of human for environmental hazards. An alternative to human testing is to perform tests on animals such as, mice, rats, dogs, etc. which can provide information that can be used to infer the prospective hazard to humans. By doing so, gaps in knowledge can be addressed. However, extrapolating the outcomes from animal to human is inevitably associated with uncertainties.

Investigations that assist with the hazard identification consist of:

(a) Toxicokinetics studies which look into the processes of absorption of the chemical stressor by the target (if human then by the human body), metabolism and secretion.

(b) Toxicodynamics studies which analyse the various mechanisms a chemical stressor can negatively affect the human health.

4.3.2 Hazard Characterisation (Rovira *et al.* 2013).

Hazard characterisation investigates the association of the stressor dose to its consequential effects on the receptor. Epidemiological studies with direct studies on

humans assist in the evaluation of a dose-stressor relationship. Such investigations also help to identify the dose level at which the adverse effect of the stressor on the human begins. Since the toxic effects are determined directly on humans and not on animals, therefore, such an approach avoids the need to perform any type of animal to human extrapolation. The only one thing that might affect the study results is the variation in conditions of the study environment.

On the other hand, studies on animals and those that are in vitro studies have controlled environments. However, there is a pre-requisite of considering extrapolation methods. Due to lack of experimental studies, use of regressions and classification theoretical methods are also made.

4.3.3 Exposure Assessment

Exposure is defined as the contact between the stressor and the noticeable surface of the target receptor. An exposure assessment considers the pathway and route of exposure, the stressor concentration in a specific media, the exposure frequency and duration, the exposed population accounting for their age and gender and the interaction rate. The exposure dose is determined as follows (Rovira *et al.* 2013):

$$Dose = \frac{[Stressor]x\ Frequency\ \ x\ Contact\ Rate}{Body\ Weight} \tag{4.1}$$

4.3.3.1 Exposure pathways

The chemical stressor can enter the receptor e.g. human, through various direct and indirect pathways. These comprise of inhalation, dermal contact or skin direct absorption, ingestion of food, drinking water, soil and dust, through a skin wound or intravenous injection into the blood (Figure 4.3). The appropriate exposure pathway is considered for a particular stressor and emission scenario. In the case of gaseous amines in the atmosphere, the inhalation exposure route is a relevant pathway to consider (Rovira *et al.* 2013) .

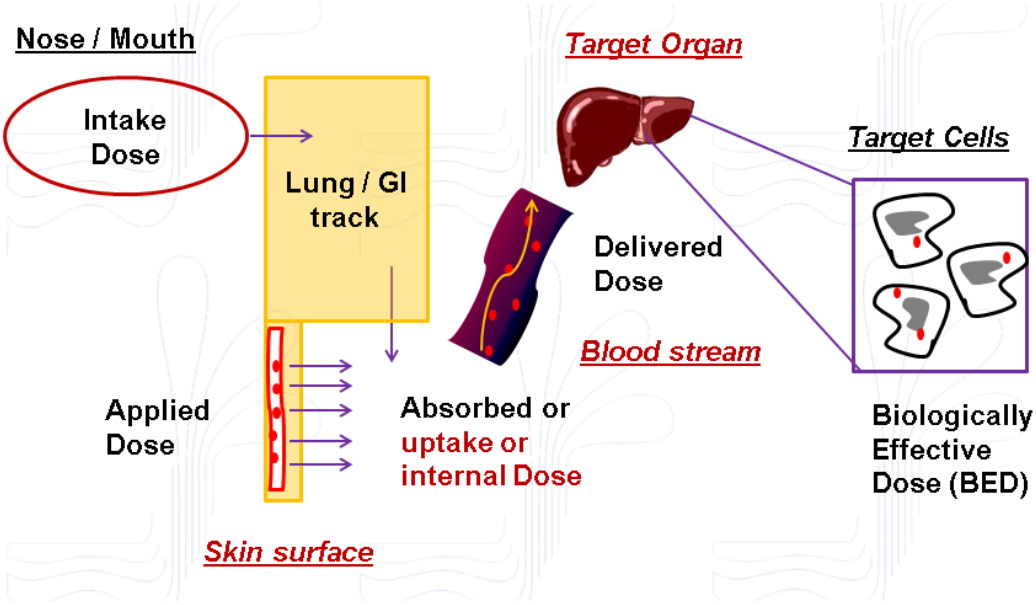


Figure 4.3: Exposure route and its effect (adapted from (USETox^{TM})).

4.3.4 Risk Characterisation

Risk characterisation is the final stage in risk assessment, which reviews and amalgamates the knowledge gathered from the previous stages to conclude concerning risks. Here the likelihood and the extent of the negative effects on human health of the population exposed are evaluated to convey the main outcomes with any uncertainties. On the whole, the evaluated risk can either be non-carcinogenic or carcinogenic.

4.3.4.1 Non-carcinogenic Risk

When the chemical stressor is not carcinogenic then there is a reference dose (RfD) below which no harmful effects can occur on humans for a lifetime daily exposure to the stressor. The RfD is a ratio of the no observed effect level (NOEL) derived from studies on animals, to the uncertainty factors associated with interspecies extrapolation and subchronic to chronic extrapolation as well as the consideration of subtle individual groups such as children and elderly people (USEPA 1998b, Rovira *et al.* 2013):

$$RfD = \frac{NOEL}{Uncertainty\ factors} \tag{4.2}$$

In the absence of NOEL, the lowest observed effect level (LOEL) is considered, which again adds to the uncertainly factors used in the calculation of RfD. The RfD is used in the determination of the non-carcinogenic risk which is a ratio of the exposed dose to the RfD:

$$Risk_{non-cancer} = \frac{Dose}{RfD} \tag{4.3}$$

If the $Risk_{non-cancer}$ exceeds 1 then the exposed population is at a risk of developing deleterious effects from exposure to the specific stressor under inspection (USEPA 1990).

4.3.4.2 Carcinogenic Risk

For carcinogenic stressors, it is assumed that harmful effects on humans from exposure can occur at any dose levels (USEPA 2005). Therefore, no reference dose and no-threshold approach is considered. Various techniques are employed for the assessment of dose-responses for such a case. These range from non-linear to linear to multiple extrapolation methods. The carcinogenic risk is then defined from the low-dose region by considering the slope factor which is the value of toxicity at which an individual is likely to develop cancer from exposure over a life time to the specific chemical under study (USEPA 1998b):

$$Risk_{cancer} = Exposure\ x\ Slope\ Factor \tag{4.4}$$

Tolerable Carcinogenic Risk Levels In Humans for Nitrosamines and Nitramines

Stressors such as, nitrosamines and nitramines have been established to be potent carcinogens. Therefore, the amount of these chemical discharges made into the environment by industries etc. for instance; need to be under the regulatory standards set by local and international authorities. As a result, the establishment of tolerable risk estimates of these carcinogenic compounds both in air and water are vital for policies relating to public health. A range of 10^{-5} to 10^{-6} has been calculated for lifetime cancer risk by different organisations using experimental data, as shown in Table 4.1 (USEPA 1986, USEPA 1990, Cal-EPA 2006, WHO 2008, HealthCanada 2011, Låg *et al.* 2011, Ravnum *et al.* 2014). This means that from a lifetime exposure

to these carcinogens, either 10 or 1 in a million people might acquire cancer. Ten in a million is assumed to be a minimal risk whereas as 1 in a million is an insignificant risk.

Various regulatory authorities have derived the minimal effect level (DMEL) which is the minimum amount of nitrosamines and nitramines in air to be emitted from power plants etc. to avoid the risk of developing cancer through inhalation from lifetime exposure to these pollutants (Table 4.1).

Table 4.1: Regulatory standards set for the tolerable carcinogenic risk levels in human in air for nitrosamines and nitramines (modified from Låg *et al.* (2011)).

	Risk level	WHO	Health Canada	US EPA	CalEPA	Låg *et al.* (2011)	Ravnum *et al.*, 2014
Air concentration (ng/m^3)	10^{-5}	3.13	3.13	0.7	2.78	0.4, 5.20	
	10^{-6}	0.313	0.313	0.07	0.278	0.520	0.86

Derivation of DMEL for NDMA air concentrations

The calculation of some of the values reported for DMEL in Table 4.1, is shown below to gain an understanding of how DMEL has been calculated in this work (explained in chapter 7).

Since NDMA is recognised as the most potent carcinogenic nitrosamine, for this reason it has been the most extensively studied nitrosamine. As a consequence, all the DMEL calculations are based on it. Due to the sparse toxicity data for other nitrosamines, the data for NDMA can be generalised to the rest nitrosamine class of compounds.

No risk estimates for nitramines have been made as well due to scant toxicity data on them (Låg *et al.* 2011). Yet, they are assumed to be potent carcinogens according to Goodall and Kennedy (1976). Therefore, the cancer risk estimates calculated for NDMA can be used for nitramines due to its greater potency in comparison to nitramines (Låg *et al.* 2011).

- ***DMEL from inhalation studies***

The atmospheric concentrations of NDMA stated in Table 4.1 for Norwegian Institute of Public Health, NIPH (Låg *et al.* 2011) have been calculated from the

most sensitive inhalation study by Klein *et al.* (1991). In this study, thirty-six rats classified into four groups were exposed to 0, 120, 600 and 3000 µg/m^3 of NDMA for two hundred and seven days for four to five hours per day and up to four times per week. Two years was the median sacrifice rat age but for the highest exposure rat group this age was very small. Significant rise in nasal tumours was noted, with tumour incidences of 0%, 36% and 86 % occurring for the first three NDMA concentrations. T25 which is the chronic dose rate resulting in 25% of animals in developing tumours at a certain tissue location within its lifetime was obtained from a linear dose-response curve, with the extrapolation of the lowest dose (giving marked rise in tumour) to a 25% tumour incidence. Therefore, the lowest dose in the study was 120 µg/m^3, at which 13 out of 36 rats (i.e. 36%) developed nasal tumours. None were reported for the control experiment. Usually a human daily exposure is defined as 24 hours per week for up to adult lifetime of 75 years. So the exposure duration in the study was corrected from 2 years for rats to that of the human chronic lifetime using a correction factor of 0.03 as follows:

$$\begin{aligned} Corrected\ exposure\ concentration &= 120\ \mu g/\ m^3 x\ 0.03 \\ &= 3.6\ \mu g/\ m^3 \end{aligned} \tag{4.5}$$

At the dose of 3.6 µg/m^3 about 36% tumour incidences were observed. The determined concentration was then extrapolated to the concentration at which 25% tumour incidence occurred i.e. the T25:

$$T25 = 3.6\ \mu g/m^3\ * \left(\frac{25/100}{36/100}\right) = 2.5\ \mu g/m^3/day \tag{4.6}$$

The evaluated T25 was used in the determination of DMEL of the chemical species of interest by applying a very large assessment factor of 6250 (REACH 2010):

$$DMEL = \frac{T25}{Assessment\ factor} = \frac{2.5}{6250} = \mathbf{0.4\ ng/m^3} \tag{4.7}$$

The assessment factor accounts for interspecies/ intraspecies extrapolations as well as the carcinogenic nature of NDMA and various other extrapolations. The obtained DMEL communicates to a lifetime cancer risk of 10^{-5}.

❖ ***DMEL from studies by Peto et al. (1991a), Peto et al. (1991b) according to REACH guidelines***

NIPH (Låg *et al.* 2011) also determined tolerable cancer risk levels from T25 calculated using REACH (2010) procedures. The data used was the data processed by WHO from studies conducted by Peto *et al.* (1991a) and Peto *et al.* (1991b) in which sixteen dose groups of 60 rats per sex were exposed to NDMA ranging from 0 – 1.224 mg/kg bw/day in drinking water, from the sixth week till death. The control consisted of 240 rats. Results showed linear dose-response relationship in the low dose region, whereas, in the higher dose range the relationship changed to cubic. Tumours occurred in the bile duct region with female rats being the most sensitive to it.

NIPH (Låg *et al.* 2011) estimated the T25 at highest dose of 0.076 mg/kg bw/day at which 7 incidence of tumours were noted out of a group of 48 rats with 4 out of 192 rats in the control developing tumour. After adjusting for background liver tumours cases (Dybing *et al.* 1997), about 13% of the tumour incidence in female rats occurred when exposed to a dose of 0.076 mg/ kg bw/ day. The T25 was then obtained as follows:

$$T25 = 0.076 * \left(\frac{25/100}{13/100}\right) = 0.15\ mg/kg\ bw/day \tag{4.8}$$

Extrapolation from oral to inhalation route was achieved as presented (REACH 2010):

$$\begin{aligned} &Corrected\ inhalatory\ dose \\ &= Oral\ dose * \frac{1}{Standard\ respiratory\ volume\ of\ rat\ (1.15 m^3/kg/day)} \\ &* \frac{Oral\ rat}{Inhalation\ human} \end{aligned} \tag{4.9}$$

Where, the oral dose was determined from the T25 which was extrapolated to a risk of 10^{-5} and 10^{-6} as shown:

$$Oral\ dose = 0.15 * \left(\frac{10^{-5}}{25/100}\right) = 0.006\ \mu g/kg\ bw/day \tag{4.10}$$

and

$$Oral\ dose = 0.15 * \left(\frac{10^{-6}}{25/100}\right) = 0.0006\ \mu g/kg\ bw/day \quad (4.11)$$

Hence, high to low dose extrapolation was conducted as shown:

$$Corrected\ air\ levels = 0.006\ \mu g/kg\ bw/day * \frac{1}{1.15 m^3/kg/day} * 1 \quad (4.12)$$

$$= 0.0052\ \mu g/m^3 for\ 10^{-5}\ risk$$

and

$$Corrected\ air\ levels = 0.0006\ \mu g/kg\ bw/day * \frac{1}{1.15 m^3/kg/day} * 1 \quad (4.13)$$

$$= 0.00052\ \mu g/m^3\ = \mathbf{0.52 ng/m^3} for\ 10^{-6}\ risk$$

Results showed the NDMA is more carcinogenic via inhalation route as opposed to the oral route. It was inferred that for any nitrosamine with T25 less than 1 mg/kg bw/ day was associated with high carcinogenic potency.

This experimental data has also been used by Cal-EPA (2006), HealthCanada (2011), USEPA (1986) and WHO (2008) to carry out cancer risk estimations from NDMA exposure in drinking water using different assessment factors. USEPA (1986) also calculated the risk form inhalation exposure.

4.4 Environmental Risk Assessment (Rovira *et al.* 2013)

For an environmental risk assessment the hazard identification and characterisation steps are grouped as one step, known as the effect assessment. It evaluates the predicted no effect concentration (PNEC) below which no adverse effects occurs in the environmental compartment considered. PNEC is determined from the ratio of lowest level of toxicity short term testing on species (LE_{50}) or no observed effect concentration (NOEC) for long term, to an assessment factor associated with

uncertainties with interspecies/intraspecies extrapolation, short to long term extrapolation etc.:

$$PNEC = \frac{LE_{50}\ or\ NOEC}{Assessment\ factor} \tag{4.14}$$

Exposure assessments employing chemical fate and transport model evaluate the predicted environmental concentration (PEC) in the environmental compartment under study (Suciu *et al.* 2013). They do so by estimating wet deposition of the chemical pollutants of interest to aquatic environments such as, lakes which not only affects aquatic life but also humans via drinking water. Both PEC and PNEC are used in evaluating the risk to the environmental from chemical stressor:

$$Risk_{environment} = \frac{PEC}{PNEC} \tag{4.15}$$

If the $Risk_{environment}$ ratio is below 1 then no risk is posed by the stressor to the environment (USEPA 1998a, IHCP 2003).

4.4.1 Hazards and Characterisation of NDMA in drinking water

NDMA can find its way into the environment such as lakes where the water can be used by humans for drinking etc. Then considering the NDMA Henry's law constant value of 1.82×10^{-6} atm m^3/mole at 37°C (Mirvish *et al.* 1976), which suggests that there will be no partitioning of NDMA from water into the air when an individual is exposed to NDMA in water. Also taking into account the very low value of the NDMA skin permeability constant, Kp, of 0.000265 cm/hr (CICADS 2002) suggests that from dermal exposure to it there won't be a significant contribution to the full exposure (Cal-EPA 2006).

Studies by Fussgaenger and Ditschuneit (1980) and Pedal *et al.* (1982) have reported two deaths from acute ingestion of NDMA from liver failure. Epidemiological studies by Risch *et al.* (1985), Gonzalez *et al.* (1994), La Vecchia *et al.* (1995), Pobel *et al.* (1995) have reported stomach cancer incidences and Rogers *et al.* (1995) upper digestive tract. Some have reported lung cancers too (Goodman *et al.* 1992, De Stefani *et al.* 1996). Therefore, there is enough evidence to support the fact that

nitrosamines such as, NDMA are potent carcinogens to human by various routes of exposure such as drinking water etc.

The mechanism by which NDMA leads to cancer includes bioconversion to form methyldiazonium ions by liver enzymes, producing carcinogenic DNA adduct such as O^6-methylguanine is illustrated in Figure 4.4 (Haggerty and Holsapple 1990, Lee *et al.* 1996).

Consequently, it is prudent to establish guideline values of NDMA in drinking water. However, despite the various investigations into the effects of NDMA on humans, the quantification of the associated carcinogenic risk still remains a knowledge gap.

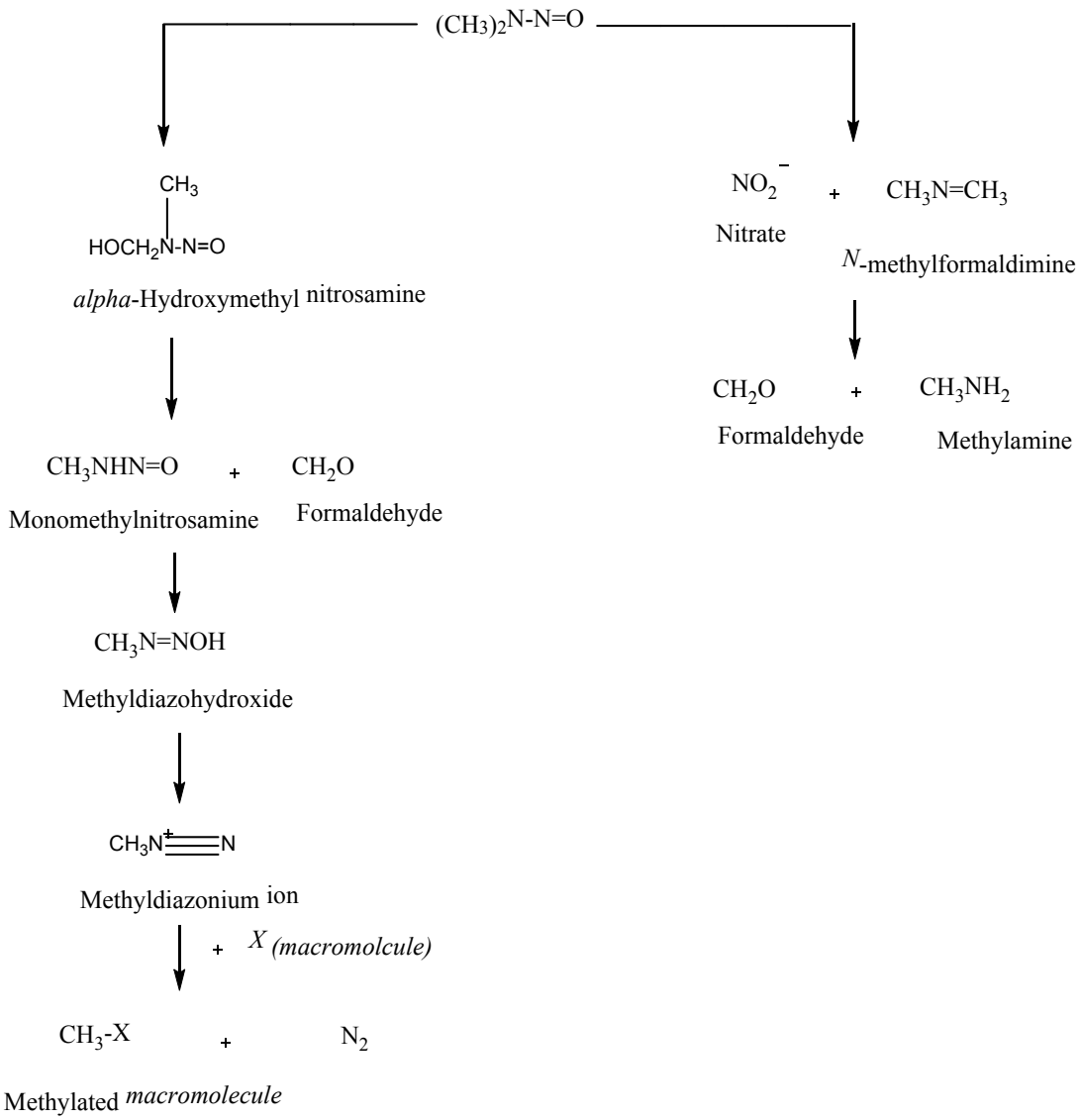


Figure 4.4: Pathways for NDMA metabolism (adapted from Cal-EPA (2006) and IPSC (2002)).

4.4.2 Derivation of the Guideline PNEC value of NDMA in drinking water by WHO

WHO (2008) calculated the NDMA dose at which there is a 5% increase in risk, TD_{05}. This was achieved from considering the studies conducted by Brantom (1983), Peto *et al.* (1991a) and Peto *et al.* (1991b) for quantitative risk assessment of hepatic cancers in male and female rats. The value for TD_{05} calculated was 18 µg/kg bw/day which resulted in a unit risk (the rise in risk per unit rise in dose) of 2.77 $x10^{-3}$ per µg/kg bw/day (HealthCanada 2005). This suggests that the rise of cancer is 1 in 360 for every µg of NDMA per kg of bw per day of exposure for a lifetime. No animal to human extrapolation was implied. Hence the guideline value calculated by WHO (2008) for NDMA in drinking water for a cancer risk of 10^{-5} is as shown:

$$\begin{aligned} &Guideline\ [NDMA]_{drinking\ water} \\ &= \frac{Body\ weight\ \ x\ 10^{-5}}{unit\ risk\ x\ [water\ consumed\ by\ day]} \\ &= \frac{60\ kg\ x\ 10^{-5}}{2.77\ x\ 10^{-3} per\ \mu g/kg bw/day\ x \frac{2L}{day}} = 0.1\ \mu g/L\ =\ \mathbf{100\ ng/L} \end{aligned} \tag{4.16}$$

4.4.3 Derivation of the Guideline PNEC value of NDMA in drinking water by Cal-EPA

California Public Health Goal (Cal-EPA 2006) used data from Peto *et al.* (1991a) and Peto *et al.* (1991b) to establish a safety guideline value for NDMA exposure to keep the cancer risk of 10^{-6} to be negligible as follows:

1. Extrapolating from rat to human dose consists of taking the ratio of rat to human body weight and raising it to a power of 1/4:

$$\begin{aligned} dose_{human} &= dose_{rat}\ (0.032mg/kg/day) x\ (\frac{0.25\ kg}{70kg})^{\frac{1}{4}} \\ &= 0.0078mg/kg/day \end{aligned} \tag{4.17}$$

   where 0.032mg/kg/day is the dose at which 10 % incidence of bile duct tumours in rats was observed (Cal-EPA 2006).

2. Evaluating the slope of a linear dose-response relationship with 10% incidence tumours and no tumour incidence in the absence of exposure gives the oral cancer potency:

$$Oral\ potency = \frac{(0.1-0)}{(0.0078 mg/kg/day - 0)} = 12.8\ (mg/kg/day)^{-1} \quad (4.18)$$

3. The obtained oral potency is used in evaluating the health protective NDMA concentration according to the following relationship:

$$Health\ protective\ [NDMA] = \frac{10^{-6}\ x\ Body\ weight\ (kg)}{Oral\ cancer\ potency\ (mg/kg/day) x\ daily\ amount\ of\ water\ ingested\ (\frac{L}{day})} \quad (4.19)$$

Hence,

$$[NDMA] = \frac{10^{-6}\ x\ 70kg}{12.8\ (mg/kg/day) x\ 2\ \left(\frac{L}{day}\right)} = 3x10^{-6}\frac{mg}{L} = \mathbf{3\ ng/L} \quad (4.20)$$

Thus, the protective health guideline value established is 3 ng /L associated with a negligible lifetime cancer risk of 1 in a million.

4.4.4 Other Guideline PNEC values of NDMA in drinking water

Various other PNEC values for NDMA in drinking water are shown in Table 4.2, calculated by various regulatory authorities worldwide.

Table 4.2: Summary of regulatory standards set for the tolerable carcinogenic risk levels for human in water for nitrosamines and nitramines (modified from Låg *et al.* (2011)).

	Risk level	WHO	Health Canada	US EPA	CalEPA	NIPH (Låg *et al.* 2011)
Drinking water (ng/L)	10^{-5}	100	40	7		
	10^{-6}		4	0.7	3	4

4.5 Summary of safety limits in air and water

There are various thresholds established by different studies, some of which are highlighted in the Table 4.3. It gives the safety limit of 10 µg/m^3 (monthly average)

for MEA in air via the inhalation exposure pathway which could affect the human health at a subchronic level.

The safety limit for nitrosamines in air of 0.02 ng/m^3 (monthly average) is also listed which can be carcinogenic to humans from long term exposure. The aquatic and drinking water limits of 25 ng/L and 7 ng/L are also shown for nitrosamines, which if exceeded can be carcinogenic to humans and also adversely impact the algae and bacteria in the aquatic environments.

For nitramines the aquatic and drinking water limits of 200 ng/L and 1000 ng/L should not be exceeded so as not to harm human health and fish in the aquatic environments.

Hence, these thresholds should be adhered to in order to circumvent the dire consequences on humans and aquatic species as a consequence of having higher concentrations of these chemicals in water.

Table 4.3: Summary of safety limits stated by various studies for MEA, nitrosamines and nitramines in air, drinking water and the aquatic environment (reproduced from Karl *et al.* (2011)).

Chemical species	Exposure pathway	Toxicity	Safety limit	Reference
MEA	Inhalation	Human health, subchronic	10 µg/m^3 (monthly average)	Låg *et al.* (2009)
	Aquatic	Algae/bacteria, chronic	7500 ng/L	Brooks and Wright (2008)
Nitrosamines	Inhalation	Human health, carcinogenic	0.02 ng/m^3 (monthly average)	(USEPA)
	Drinking water	Human health, carcinogenic	7, 4 ng/L	Richardson *et al.* (2007), Cal-EPA (2006) Låg *et al.* (2011)
	Aquatic	Algae/bacteria, chronic	25 ng/L	Brooks and Wright (2008)
Nitramines	Drinking water	Human health, carcinogenic	1000 ng/L	Wollin and Dieter (2005)
	Aquatic	fish, chronic	200 ng/l	Brooks and Wright (2008)

4.6 Conclusions

This chapter explained the various stages of human health risk assessment and environmental risk assessments from the exposure of harmful chemicals such as, nitrosamines and nitramines. In conclusion, MEA is considered to be non-mutagenic in nature; therefore, it presents no significant risk to the human health. The main

health risk is associated with the degradation products formed such as, nitrosamine and nitramine from MEA. These classes of compounds have been discovered to be carcinogenic in nature from experimental studies. It is, therefore, a prerequisite to establish safety limits above which the human population should not be exposed. By doing so, the risk of developing cancer from lifetime exposure to these chemicals is avoided. The government and environmental regulation authorities have as a result set regulatory limits both in air and water for nitrosamines and nitramines to which industries using amine for CO_2 capture should comply with.

The Norwegian Climate and Pollution Agency (Climate 2011) had issued a discharge permit of 0.3 ng/m^3 for total nitrosamines and nitramines released in the flue gas in the air and 4 ng/L in water during the operation of Mongstad PCCC plant (Låg *et al.* 2011). Conversely, in the UK or EU in general there are no environmental assessment levels or environmental quality standards set for the nitrosamines and nitramines. Therefore, the thresholds for Mongstad are considered instead as useful benchmarks since they have been calculated with regards to the methods used under the EU regulations on registration, evaluation, authorisation and restriction of chemicals (REACH). Equally, there are several other thresholds as mentioned in Table 4.3, established by various investigations especially with regards to drinking water and aquatic environment which need to be taken into account during risk assessments.

On the whole, as part of the literature review an insight into the amine degradation mechanisms involved in PCCC technology was made along with the scientific approach considered for studying these emissions by quantifying the dispersion processes using dispersion models. Finally, the risk paradigm was explained for establishing human and environmental risk assessment. So now in the next chapter, a quantitative understanding atmospheric chemistry of the amines of interest will be attained by establishing reaction kinetics describing the reaction pathways.

Chapter 5 A theoretical study of the reaction kinetics of amines released into the atmosphere from CO_2 capture

5.1 Introduction

The amine emissions into the atmosphere are subject to various chemical transformation reactions (Figure 5.1). OH radicals are abundant in the atmosphere as they are naturally produced from the photolysis of O_3. They can abstract a hydrogen atom from the NH_2 group of an amine to form an amino radical. This highly unstable radical species undergoes additional reactions with NO and NO_2 to form nitrosamines (or alkyldiazohydroxides in the case of primary nitrosamines) and nitramines, which are harmful to both humans and the natural environment (Låg *et al.* 2011). The amino radical also reacts with O_2 to form the corresponding imine, which is non-toxic.

In sunlight, the nitrosamine undergoes photolysis reactions to form an amino radical, which can once again react with NO, NO_2 and O_2 to repeat the whole cycle of reactions. On the other hand, nitramines are comparatively stable and do not undergo photolysis but rather dissociate to their corresponding imines.

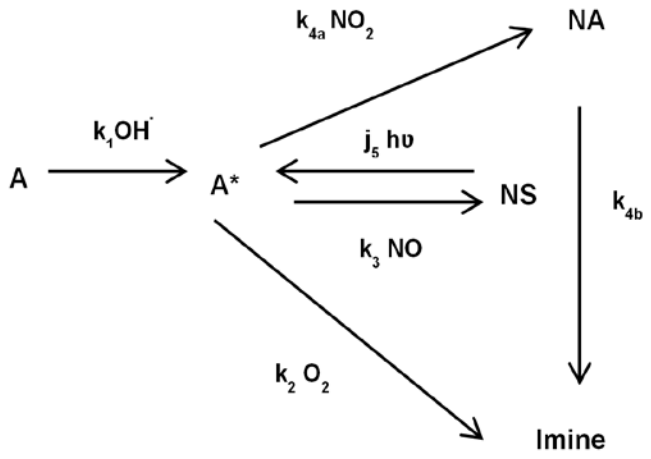


Figure 5.1: A simple atmospheric chemistry scheme of a generic amine (A) undergoing reaction with OH to form the radical (A*) which can react with NO to form NS, with NO_2 to form NA and with O_2 to form imine. The reaction kinetics of each of the reaction step describing the scheme is represented by its corresponding rate constant, *k*.

The atmospheric chemistry of the amines is complex and due to their high vapour pressures at atmospheric conditions, performing experimental investigations resembling realistic conditions is challenging. Their polarity and hygroscopic nature and great affinity to surface, additionally augments the problems in performing experimentations. As a consequence limited experimental investigations on amine degradation have been carried out in the laboratory.

Some of these studies have attained quantitative understanding of the atmospheric chemistry of amine emissions by evaluating kinetics describing the degradation mechanistic pathways governing the consumption and production of the chemical species of interest. Their specific focus was on the determination of rate constants for the reactions of amines with OH radicals (Atkinson *et al.* 1977, GORSE *et al.* 1977, Atkinson *et al.* 1978, Pitts *et al.* 1978, Harris and Pitts 1983, Anderson and Stephens 1988, Koch *et al.* 1996, Carl and Crowley 1998, Karl *et al.* 2012, Nielsen *et al.* 2012, Onel *et al.* 2012, Xie *et al.* 2014). A few others have investigated the gas phase reactions of alkyl amino radicals with NO, NO_2 and O_2 (Lindley *et al.* 1979, Tuazon *et al.* 1984, Lazarou *et al.* 1994, Tuazon *et al.* 1994, Nielsen *et al.* 2011a). Some pilot plant studies have also been conducted to characterise the amine degradation products (Strazisar *et al.* 2003, Lepaumier *et al.* 2011).

As the experimental investigations are sparse, quantum chemical methods may be an option to fill the gaps in available literature. Some have been performed to determine the rate of reaction of alkylamine with OH radicals (Galano and Alvarez-Idaboy 2008, Bråten *et al.* 2009, Tian *et al.* 2009, Onel *et al.* 2013). Recently, scientists have determined rates for MEA and OH reactions (Nielsen *et al.* 2010, Nielsen *et al.* 2011b, Onel *et al.* 2012, Borduas *et al.* 2013, Xie *et al.* 2014). However, due to the limited number of studies performed both at experimental and theoretical levels; the atmospheric chemistry of the amines has not been fully explored. This is in particular for the amines (MA, DMA and MEA) considered in this study which form as a consequence of volatilization of the emissions from PCCC process.

The chemical reactions describing the atmospheric chemistry for each of the amines studied in this work are shown in Table 5.1. The atmospheric chemistry scheme (Figure 5.1 and Table 5.1) can be represented by ordinary differential equations, ODEs in

Table **5.2**. This system of ODEs is solved to estimate the change in concentration of the species considered in time if the initial concentration is known. In order to do this, it is imperative to determine the kinetics of the reaction steps making up the scheme, represented by various rate constants (Table 5.1 and

Table **5.2**) such as the k_1 which is the rate constant for formation of amino radical by OH reaction, k_{1b} the rate constant for the formation of alkyl radical by OH reaction, k_2 the rate constant for the formation of imine by the reaction of amino radical with O_2, k_3 is the rate constant for the formation of nitrosamine by the reaction of amino radical with NO, k_{4a} is the rate constant for the formation of nitramine by the reaction of amino radical with NO_2 reaction, k_{4b} is the rate constant for the nitramine dissociation to imine and $J_5 h\upsilon$ is the rate constant for nitrosamine photolysis.

In this study, the rate constants describing the atmospheric chemistry scheme for each of the amines considered are evaluated theoretically using quantum chemistry and Rice–Ramsperger–Kassel–Marcus (RRKM) theory/ master equation based kinetic modelling (Table 5.1). Quantum chemistry and kinetic modelling provide assistance and guidance for experimental research (Goodsite *et al.* 2011). Gas-phase reaction kinetics have been studied using quantum theoretical methods (Galano *et al.* 2006) and RRKM theory (Andersen and Carter 2008). The estimation of the rate

constant using RRKM theory requires vibrational frequencies of the reactants and transition states. Reliable choices of quantum theoretical method cater to these requirements by providing barrier heights estimations and vibrational frequencies of the reactants and the transition states, so as to calculate rate constants within experimental agreement. Thereof deduced rate constants may serve as input variables for advection-diffusion-reaction equations to determine accurately the levels of these chemical discharges species over time and space. The obtained concentration estimates of individual species can be used to assess the human health and environmental risk they pose. As the calculations are independent from experimental parameters, the methodology developed here may prove universal in comprehending the atmospheric chemistry of amine emissions from PCCC.

Table 5.1: Reaction scheme and the corresponding rate constants of methylamine (MA), dimethylamine (DMA) and monoethanolamine (MEA).

MA				
CH_3NH_2 +OH	→	$CH_3NH + H_2O$		k_1
	→	$CH_2NH_2 + H_2O$		k_{1b}
$CH_3NH + O_2$	→	$CH_2{=}NH_2 + O_2H$		k_2
$CH_3NH + NO$	→	$CH_3NH\text{-}NO$ hυ		k_3
		→	$CH_3NH + NO$	J_5
$CH_3NH + NO_2$	→	$CH_3NH\text{-}NO_2$		k_{4a}
		→	$CH_2{=}NH_2 + HONO$	k_{4b}
DMA				
$(CH_3)_2NH + OH$	→	$(CH_3)_2N + H_2O$		k_1
	→	$(CH_3)NHCH_2 + H_2O$		k_{1b}
$(CH_3)_2N + O_2$	→	$CH_2{=}N\text{-}CH_3 + O_2H$		k_2
$(CH_3)_2N + NO$	→	$(CH_3)_2N\text{-}NO$ hυ		k_3
		→	$(CH_3)_2N + NO$	J_5
$(CH_3)_2N + NO_2$	→	$(CH_3)_2N\text{-}NO_2$		k_{4a}
		→	$CH_2{=}N\text{-}CH_3 + HONO$	k_{4b}
MEA				
$OH(CH_2)_2NH_2$+OH	→	$OH(CH_2)_2NH + H_2O$		k_1
	→	$OHCH_2CHNH_2 + H_2O$		k_{1b}
	→	$OHCHCH_2NH_2 + H_2O$		k_{1c}
	→	$O\text{-}(CH_2)_2NH_2 + H_2O$		k_{1d}

$OH(CH_2)_2NH + O_2$	→	$OHCH_2CH=NH + O_2H$		k_2
$OH(CH_2)_2NH + NO$	→	$OH(CH_2)_2NH\text{-}NO$	hυ	k_3
			→$OH(CH_2)_2NH + NO$	J_5
$OH(CH_2)_2NH+NO_2$	→	$OH(CH_2)_2NH\text{-}NO_2$		k_{4a}
		→	$HOCH_2CH=NH + HONO$	k_{4b}

Table 5.2: The differential equations describing the amine atmospheric chemistry scheme (after CERC (2012a)).

Loss of the amine	$\frac{d[Amine]}{dt} = -k_{1+1b}[OH]\,[Amine]$
Production of the amino radical	$\frac{d[Radical]}{dt} = k_1\,[OH]\,[Amine] + J_5\,h\upsilon\,[Nitrosamine] - k_2\,[Radical][O_2] - k_3\,[Radical][NO] - k_{4a}[Radical][NO_2]$
Production of nitrosamine	$\frac{d[Nitrosamine]}{dt} = k_3\,[Radical][NO] - J_5\,h\upsilon\,[Nitrosamine]$
Production of nitramine	$\frac{d[Nitramine]}{dt} = k_{4a}\,[Radical][NO_2] - k_{4b}\,[Nitramine]$

5.2 Atmospheric chemistry computational details

5.2.1 Atmospheric chemistry model

All quantum chemical calculations have been performed with Gaussian 09 (Frisch *et al.* 2009). In order to estimate the barrier height of the reaction from reactants to products via a transition state, only an error of 1 kcal / mol is permitted. Estimation of accurate barrier heights is a prerequisite for modelling kinetics. Truhlar group has extensively shown that the hybrid meta-density M06-2X (Fernandez-Ramos *et al.* 2006, Zhao and Truhlar 2008, Zheng *et al.* 2009) functional of the density function theory (DFT) is considered to be one of the best functionals for determining barrier heights (Zhao and Truhlar 2008). The developers have found M06-2X to have better performance than the second-order Møller-Plesset-type perturbation theory (MP2) (Møller and Plesset 1934) functional. It also performs better than B3LYP (Becke 1988, Lee *et al.* 1988, Becke 1993, Stephens *et al.* 1994) functional, which underestimates barrier heights (Zhao *et al.* 2005). On the contrary, M062X agrees best with coupled cluster theory CCSD(T) (Raghavachari *et al.* 1989) results (Zhao and Truhlar 2008). However, evaluating the M062X performance in depth is beyond the scope of this work.

The developers state that it is reliable in the determination of main group thermochemistry and kinetics. M06-2X is one of the best functions for studying

reactions involving radicals (Zhao and Truhlar 2008, Zhou *et al.* 2011, So *et al.* 2014, Xiao *et al.* 2014). Studies have employed M06-2X for investigating mechanisms and determining kinetics of their reactions of interest (Zhou *et al.* 2011, So *et al.* 2014). Robinson and Lindstedt showed that M06-2X functional estimated reaction barriers for hydrogen exchange reactions involving n-propoyl within good agreement to coupled cluster based methods (Robinson and Lindstedt 2013). In particular, (Jackson and Attalla 2010) and Xie *et al.* (2014) have used it for the determination of the kinetics of the degradation pathways of MEA after the H-abstraction of MEA with OH.

Since, the main focus in this work is on the H-transfer, bond dissociation and association processes, therefore, after testing a range of functional and basis sets (Table 5.3) the M06-2X functional and the 6-31G (2d, p) basis set (Pople *et al.* 1987) produced reaction rates closest to experiment (i.e. k_{OH} for MA). There M06-2X/ 6-31G (2d,p) is considered sufficiently reliable for investigating the mechanisms and estimating the kinetics of the reactions of the amines with OH and the resulting amino radicals with NO, NO_2 and O_2. Other than being highly reliable in predicting barrier heights and vibrational frequencies of transition states for the rate constant calculations closest to experimental values, M06-2X/6-31G(2d,p) method is chosen over M06-2X/ aug-ccpTVZ due to computational cost.

The geometry optimisations of all the stationary points on the potential energy surface (PES) of the target amines and their reaction partners were calculated using the above level of theory. All structures of interest were fully optimised without any constraints. An 'ultrafine' grid was used in the calculations and the SCF convergence criterion set to 10^{-9}. Stationary points such as minima and transitions states on the minimum energy path of these PESs were characterised by harmonic vibrational frequency analysis. Transition state structures were verified by the presence of one imaginary frequency and a zero for a minimum. The connection between all the transition state structures and their expected reactants and products were confirmed by performing intrinsic reaction coordinate (IRC) calculations also at the same computational level.

Three distinct types of reactions were considered: (i) reactions with a barrier, (ii) reactions without a barrier and (iii) a photolysis reaction. Transition state theory (TST) and RRKM theory were applied to determine the rate constants of interest.

Table 5.3: The calculated k_{OH} constant for CH_3NH + OH reaction using various computational levels of theory.

Computational level of theory	k_{OH} (cm^3/molecule.s)	Experimental k
HF/ 6-31 G d,p	6.17×10^{-19}	2.22×10^{-11}[a]
UMP2/ ccpVTZ	1.39×10^{-14}	
UMP2/ aug-ccpVTZ	3.36×10^{-14}	
CCSDT/ aug-ccptvz//UMP2/aug-ccptvz	1.13×10^{-9}	
M062X/ 631 G 2d, p	2.05×10^{-11}	1.97×10^{-11}[b]
M062X/ ccpVTZ	7.96×10^{-12}	
M062X/ aug-ccpVTZ	2.09×10^{-11}	
CCSDT/aug-ccpVTZ//M062X/aug-ccpVTZ	4.40×10^{-12}	

[a] Atkinson *et al.* (1977), [b]Onel *et al.* (2013)

In Table 5.3, rates were calculated using geometries optimised at each of the computation level of theory shown in the table by treating them all in the same fashion as discussed. Except for two instances where (a) geometries were optimised using the UMP2/ aug-ccpVTZ and single point energies performed at the CCSDT/aug-ccpVTZ based on the optimised geometries at the UMP2/ aug-ccpVTZ and (b) geometries optimised using the M06-2X/aug-ccpVTZ and single point energies performed at the CCSDT/aug-ccpVTZ based on the optimised geometries at the M06-2X/aug-ccpVTZ. Generally, Coupled Cluster (CC) calculations are used to combat the incorrect treatment of instantaneous electro-electron repulsions. They employ an excitation operator which produces a linear combination of Slater determinants. This calculations are computationally very costly, so there are often attempts to use single point CC calculations atop a geometry achieved with a different functional or theory. In this work,, the capability of CCSDT (coupled cluster singlet, doublets and triplets) was studied atop of an M06-2X and UMP2 calculation. As can be seen in Table 5.1., there is no improvement. This may be due to forcing CC theory upon potential energy surfaces created by single reference methods such as MP2 and DFT. Thus, it is not advisable to mix these methods in such fashion, but rather use CC for a full optimization when computer time is not an issue.

5.2.2 Reactions described with Transition State Theory

Transition states were located with the Quadratic Synchronous Transit (QST2) method (Peng and Bernhard Schlegel 1993, Peng *et al.* 1996) by starting from the reactant and product geometries. For the radical reactions, the starting point chosen was a geometry that was a maximum energy in a PES scan along the reaction

coordinate. This estimated transition state was then optimised towards a saddle point of the first order. Then intrinsic reaction coordinate (IRC) calculations were performed to find the corresponding reactants and products.

To calculate the rate for the reaction between the amine and the OH radical, ΔG was determined as the difference between the free energy of the reactant and the transition state. ΔG was then used in Eyring-Polanyi's equation (E.q 5.1) (Eyring 1935) to calculate the rate constant, k_1, which accounts for the rate of formation of the alkyl amino radical and H_2O. The Wigner tunnelling correction factor (Γ) (E.q 5.2) (Wigner 1932) was used for correcting the rate constant.

$$k(T) = \Gamma(T)\frac{k_B T}{h}\, e^{\left(-\frac{\Delta G^{\neq}}{RT}\right)} \tag{5.1}$$

$$\Gamma(T) = 1 + \left(\frac{1}{24}\right)\left(\frac{|\upsilon^{\neq}|}{k_B T}\right)^2 \tag{5.2}$$

Where $\Delta G^{\neq}$ is the Gibbs energy of activation, k_B is Boltzmann's constant, h is Planck's constant, T is absolute temperature and $\upsilon^{\neq}$ is the imaginary frequency of the asymmetric stretch along the reaction coordinate.

k_{OH} values for the amines + OH reactions were also determined by using EPI-Suite (Atkinson *et al.* 1977) which is a structure-activity-relationship (SAR) programme developed by the EPA's Office of Pollution Prevention Toxics and Syracuse Research Corporation (SRC).

5.2.3 Reactions described with RRKM theory

For the alkyl amino radicals and NO and NO_2 barrierless radical recombination reactions (k_3 and k_{4a} in Table 5.1), the calculations of high-pressure rate constants and thermal functions were performed with ChemRate 1.5.8 (Mokrushin *et al.* 2011) at 298.15 K and 1 atm. ChemRate contains a master equation solver that determines the rate constants for the reactions in the energy transfer region under non-steady state conditions using RRKM theory (Barker and Golden 2003). It can estimate the rate of reactions involving little or no barrier heights. The model performs the calculations by initially locating a transition state even for barrier less reactions, taking into account geometrical and vibrational data for the reactants and products determined from Gaussian 09 calculations.

However, Chemrate is unable to take into account of the fact that the determination of transition states in barrier less reactions is achieved by means of a subtle balance between entropic and enthalpic effects (Klippenstein 1992). The accuracy of these effects is dependent on the level of quantum chemical method considered. Extended versions of RRKM theory consider variational theory and therefore are capable of determining the right transition states for accurate predictions of rate calculations. Variational treatments are found be implemented in codes such as VariChem (Klippenstein *et al.* 1999) and PolyRate (Lu *et al.* 1992). However, evaluating the accuracy of RRKM theory is beyond the scope of this work. It was intend to employ a computationally cheap method for the barrier less reaction rate estimations. As a consequence, RRKM theory implemented in ChemRate became the choice of method for the rate calculation of the barrier less radical recombination reactions of the alkyl amino radicals and NO and NO_2. The necessary thermo-chemistry data was be extracted from the quantum chemical calculations, which are produced as additional outputs during frequency calculations. Such data was based on density and sum of states for the M062X optimised geometries. Argon was used as bath gas considered for the calculations. The collisional energy transfer was described using an exponential-down model.

The Lennard Jones parameters for the active species are needed to describe the collision, and they have been obtained using their experimental critical temperature and the critical pressure (Thermopedia) of their non-radical species. This approach is even valid in case of a radical, as the electronic structure does not matter.

Enthalpies of formation for alkyl amino radicals and the resulting nitrosamines, nitramines and imines were calculated (Table 5.4) using the real time predictor Mol-Instincts tool (CHEMESSEN). It takes into account quantum mechanics, Quantitative Structure-Property Relationships (QSPR), artificial neural networking to predict thermochemical properties. The model calculations are benched marked with experimental data. However, in the absence of experimental measurements, the estimated parameters are inspected using chemical analysis to verify the quality of the predicted thermochemical properties.

Table 5.4: The calculated enthalpy of formation for the structures for consideration in the ChemRate program.

Species	*Enthalpy of formation / kJ mole^{-1} at 298 K	Exp	Entropy of formation (S) / J mole $^{-1}$ K^{-1} at 298 K	Exp
Methylamino radical	-15.0		244.2	
Dimethylamino radical	-16.1		284.3	
Monoethanolamino radical	-168.6		298.1	
N-nitrosomonomethyl amine	-56.0		290.4	
N-nitrosodimethyl amine	-54.7	-44.8[a]	315.6	
N-nitrosomonoethanol amine	-197.0		342.4	
Methylnitramine	-25.5	-74.4[b]	299.6	
Dimethylnitramine	-10.6	-5.0[c]	331.5	
Ethanolnitramine	-252.9		348.9	
NO2	33.2	34.2[d]	226.9	240.2[d]
Methanimine	106.1	149.0[e]	259.4	
N-methylmethanimine	55.9	44.0[b]	284.9	
Imine 2-iminoethanol	-131.0		297.1	
HONO	-71.1	-78.5[d]	322.1	254.07[d]
Methyl peroxy	42.6	51.9[f]	351.1	
Dimethyl peroxy	-85.4		228.4	
Monoethanol peroxy	-179.9		246.6	
HOO	17.0	13.8[d]	239.4	229.1[d]

[a]Korsunskii *et al.* (1967); [b] Linstrom and Mallard (1998); [c] Computational Chemistry Comparison and Benchmark DataBase (http://cccbdb.nist.gov/exp1x.asp) ; [d] Gurvich *et al.* (1991); [e] McMillen and Golden (1982); [f]Meloni *et al.* (2006).

In Table 5.4, the enthalpy of formations for the species are in close agreement to the sparse experimental measurements available in literature. However, there is a poor agreement in the case of methylnitramine and methanimine, for reasons associated to the low level of accuracy of this estimation program for these particular chemical species. Since, both methylamine and methanimine are products of the reactions considered, it was assumed that despite their enthalpies of formation not being in close agreement to literature, the rate calculations would not be significantly influenced due to the reaction barrier height dependent on the energies of the reactant and transition state. For the purposes of the work, it was intended to use one enthalphy of formation estimation tool for all the species

The respective entropies of formation of the alkyl amino radicals and the resulting nitrosamines, nitramines and imines were calculated using the energies obtained from the M062X optimised geometries for consideration in ChemRate. The ChemRate model was also used for calculation k_2 and k_{4b} for every amine considered, as shown in Table 5.1.

5.2.4 Photolysis

To determine the rate of the nitrosamine photolysis (J_5 hυ pathway in Table 5.1), time-dependent density functional theory, TD-DFT, (Kootstra *et al.* 2000, Romaniello and de Boeij 2005), using the B3LYP (Becke 1988, Stephens *et al.* 1994) hybrid functional and the aug-ccpVTZ basis set (Dunning 1989) was employed to calculate the UV-Vis spectra (Figure 5.2) of the nitrosamines. Prior to the TD-DFT calculations, geometries of the studied nitrosamines were optimised using the same level of theory. TD-DFT (B3LYP/aug-ccpTVZ) gave a more accurate determination of the vertical excitation wavelength and oscillator strength (Table 5.5) than M062X/6-31G (2d,p) and is very useful in estimating accurate UV-Vis absorption spectra for medium sized organic substances (Silva-Junior *et al.* 2008).

Table 5.5: Vertical electronic excitation wavelength and corresponding oscillator strength for the relevant n -> π* transition for the three target nitrosamines predicted by TD-DFT (B3LYP/ aug-ccpTVZ) level of theory

Nitrosamine	Vertical excitation wavelength	Oscillator Strength
N-nitrosomethylamine	363.78	0.0013
N-nitrosodimethylamine	357.92	0.0014
N-nitrosomonoethanolamine	364.34	0.0005
Experimental (NDMA)	368.4	0.00065

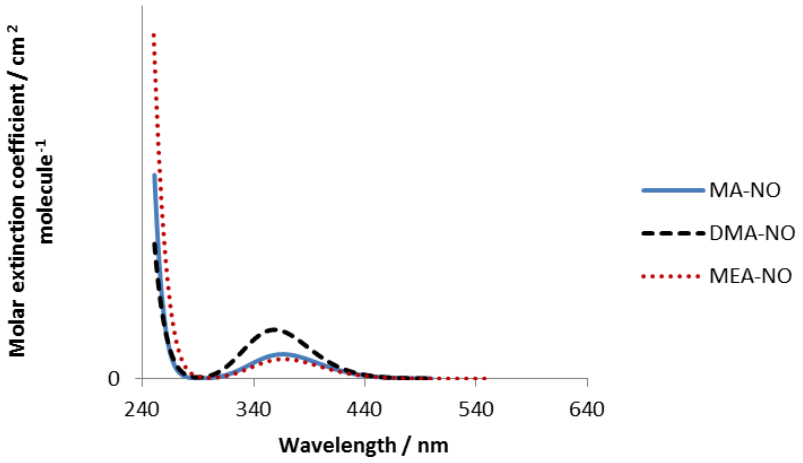


Figure 5.2: TD-DFT (B3LYP/ aug-ccpTVZ) predictions of the total molar extinction coefficient (cm^2 $molecule^{-1}$) versus wavelength for the three nitrosamines of interest in the spectral region for tropospheric photolysis.

Lifetimes (τ) are estimated by calculating the photolysis rate constant (J_5 hυ). This is determined by numerically integrating the intersection area between the simulated UV spectrum and solar actinic flux at a particular geographical location and time of the year in the region of the n -> π* electronic transition centred around 365 nm, as follows:

$$J = \int F(\lambda)\sigma(\lambda,T)\phi(\lambda,T)d\lambda \tag{5.3}$$

$$\tau_{\text{Photolysis}} = \frac{1}{J} \tag{5.4}$$

where J is the photolysis rate (J_5 hυ) which is a function of $F(\lambda)$, the solar actinic flux at a specified latitude, longitude and time of the year (photons s^{-1} nm^{-1} cm^{-2}), $\sigma(\lambda,T)$ is the molar extinction coefficient (cm^2 $molecule^{-1}$) at the wavelength and temperature of the chemical substance and $\phi(\lambda,T)$ is the quantum yield of the photolysis reaction (value of 1). The photolysis frequency, τ, expresses the rate of photolysis as a first-order decay process and, therefore, the reciprocal of this value gives the nitrosamine photolysis lifetime.

Figure 5.3 illustrates the overlap region of the simulated UV-Vis absorption spectrum of N-nitroso dimethylamine and the solar actinic flux curve generated using the Tropospheric Ultraviolet and Visible (TUV) Radiation Model from the National Centre for Atmospheric Research (NCAR) for the Ferrybridge latitude and longitude on 21st June 2012 and at 198 m stack height.

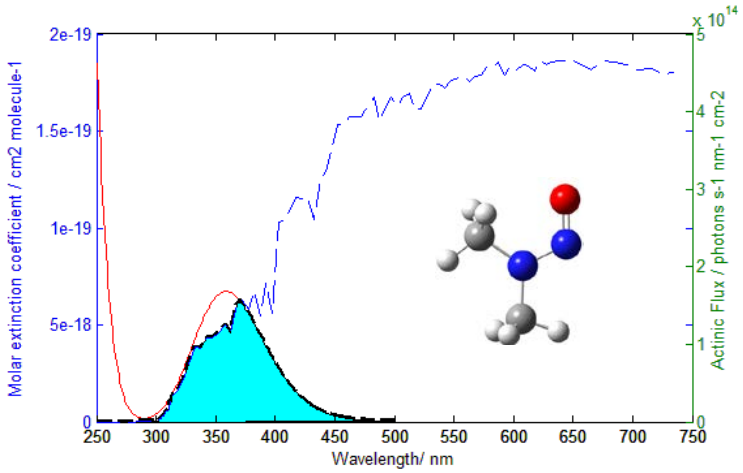


Figure 5.3: The overlap region of the simulated UV-VIS absorption spectrum of N-nitroso dimethylamine (TD-DFT / B3LYP/aug-ccpVTZ) and the solar actinic flux curve for mid-day 21st June 2012.

Photolysis constant for the nitrosamines under study was calculated in the same way for the different capture facilities considering their geographical location (latitude and longitude) and the exact stack height.

5.3 Results and discussion

5.3.1 Calculated rate constants of the three amines of interest

As already discussed, most of the previous work determined the rate constant for the reactions of amines with OH radicals (Atkinson *et al.* 1977, GORSE *et al.* 1977, Atkinson *et al.* 1978, Pitts *et al.* 1978, Harris and Pitts 1983, Anderson and Stephens 1988, Koch *et al.* 1996, Carl and Crowley 1998, Karl *et al.* 2012, Nielsen *et al.* 2012, Onel *et al.* 2012, Xie *et al.* 2014). Only a few scientists have investigated the gas phase reactions of alkyl amino radicals with NO, NO_2, O_2 or the reactions of dimethyl amino radicals (Lindley *et al.* 1979, Lazarou *et al.* 1994). Lindley experimentally determined the relative rates of $k_2 / k_3 = (1.48 + 0.07) \times 10^{-6}$, $k_2 / k_{4a} = (3.90 + 0.28) \times 10^{-7}$, and $k_{4b} / k_{4a} = 0.22 + 0.06$.

A summary of the rate constants (cm^3 $molecule^{-1}$ s^{-1}) describing the atmospheric chemistry scheme for each of the amines studied using quantum chemistry theoretical methods and kinetic modelling is given in Table 5.6. The corresponding activation energies and the pre-exponential factors evaluated at 298K for each of the reaction pathway in the atmospheric chemistry schemes for each of the amines studied are given in Table 5.7. As shown in Table 5.6, the calculated rate coefficients

for DMA are in very good agreement i.e. they are within the same order of magnitude to those determined experimentally. It is, therefore, assumed that the level of theory used for DMA is appropriate for MA and MEA. The k_1 rate closely agrees to those calculated using EPI-Suite except for MEA. The SAR model used by the EPI-Suite is unable to consider the most stable configurations of the amine and the OH radical when estimating the exact barrier height of the reaction and hence cannot predict the exact OH branching ratio (Nielsen *et al.* 2012). The SAR model does not function well for amines comprising OH groups or bulky amines (Nielsen *et al.* 2012) and cannot perform an accurate prediction of the rate of reaction of the OH radical with the MEA.

The magnitude of the rate constants suggests that the fastest reaction is the reaction of the amine with the OH radical, k_{OH}. The reaction of the amino radical with the O_2 is the slowest. The rate coefficients, k_2, for the amino radicals with O_2 are several orders of magnitude smaller than for the corresponding reactions with NO (k_3) and NO_2 (k_{4a} and k_{4b}) (Tang and Nielsen 2012). The k_2 values determined using both theories show similar trends and they closely agree to the experimental value for DMA. However, the value determined using TST is an order of magnitude lower and that from RRKM is higher than the experimental value. TST theory considers only thermal equilibrium, whereas RRKM also accounts for pressure which can affect the reaction. Therefore, the values obtained through RRKM are used in this study as they are more reliable.

Table 5.6: A summary of the rate constants (cm^3 molecule $^{-1}$ s^{-1}) describing the atmospheric chemistry scheme for each of the amines studied using quantum chemistry theoretical methods and kinetic modelling. The nitrosamine photolysis rate constant is given relative to that of NO_2, (J / $J(NO_2)$, for Ferrybridge Peterhead and Mongstad; k_{OH} is given as a sum of the rate of attack of the OH on the amino group, k_1, and the attack on the alkyl group (k_{1b}) and therefore the branching ratio for the OH attack is reported as k_1/ k_{OH}.

	k_{OH}	Branching ratio, k_1/ k_{OH}	k_2		k_3	k_{4a}	k_{4b}	J / $J(NO_2)$
			RRKM	*TST*				
MA	2.18×10^{-11}	0.35	3.64×10^{-18}	1.89×10^{-20}	1.70×10^{-12}	9.7×10^{-13}	2.02×10^{-13}	0.53, 0.74, 0.53
Exp	2.22×10^{-11}[a]	0.25[b]						
	1.97×10^{-11}[c]							
	1.73×10^{-11}[d]							
EPI-Suite	2.22×10^{-11}							
DMA	6.26×10^{-11}	0.38	3.64×10^{-18}	3.68×10^{-20}	8.37×10^{-14}	3.15×10^{-13}	1.10×10^{-14}	1.24, 1.26, 1.24
Exp	6.49×10^{-11}[d]	0.37[e]	1.24×10^{-19}[e]		8.53×10^{-14}[f]	3.18×10^{-13}[f]	1.0×10^{-14}[e]	0.53[e]
	6.27×10^{-11}[c]							
	6.54×10^{-11}[g]							
	7.1×10^{-11}[b]							
EPI-Suite	6.55×10^{-11}							
MEA	9.20×10^{-11}	0.05	2.49×10^{-16}	3.86×10^{-18}	5.62×10^{-14}	8.40×10^{-15}	4.14×10^{-15}	0.58, 0.59, 0.58
Exp	9.20×10^{-11}[h]	0.08[b]						
	7.61×10^{-11}[c]							
	7.27×10^{-11}[i]							
	7.02×10^{-11}[j]							
EPI-Suite	3.58×10^{-11}							

N.B The *experimental* k_2 and k_{4b} for DMA are calculated from the ratios reported by Lindley *et al.* (1979).

[a] Atkinson *et al.* (1977), [b] Nielsen *et al.* (2011a), [c] Onel *et al.* (2012), [d] Carl and Crowley (1998), [e] Lindley *et al.* (1979), [f] Lazarou *et al.* (1994), [g] Atkinson *et al.* (1978), [h] Karl *et al.* (2012), [i] Xie *et al.* (2014), [j] Borduas *et al.* (2013).

Table 5.7: A summary of the activation energies (E_a) evaluated at 298K for each of the reaction pathway in the atmospheric chemistry schemes for each of the amines studied.

Rate constants	E_a (kJ/mol)		
	MA	DMA	MEA
k_1	24.0 (25.5) [a]	23.5	26.9
k_{1b}	33.2 (39.6)[a]	24.9	21.3
$k_{1b'}$		32.3	21.4
k_{1c}			30.9
k_2	46.4	57.9	46.1
k_3	16.7	24.3	25.5
k_{4a}	17.9	20.1	28.1
k_{4b}	25.2	26.7	28.8

[a]Tian *et al.* (2009)

*Where $k_{OH} = k_1+k_{1b}$ for MA; $k_1+k_{1b}+k_{1b'}$ for DMA and $k_1+k_{1b}+k_{1b'}+k_{1c}$ for MEA

The activation energies at 298K for the H-abstraction from the amino and the alkyl groups of MA by OH were in good agreement to those determined by Tian *et al.* (2009). Atkinson *et al.* (1977) determined the overall rate constant, k_{OH}, by flash photolysis resonance fluorescence over a temperature range of 299-426 K and reported a relationship of $k_{OH+MA}= 1.02x10^{-11}exp(1.9\pm1.26$ kJ $mol^{-1})/RT$. Galano and Alvarez-Idaboy (2008), used computational methods and determined the overall rate constant, kOH, over a temperature range of 290 – 310 K, reporting $k_{OH+MA} = 5.89x10^{-11}exp(-5.98$ kJ $mol^{-1})/RT$. For DMA, Atkinson *et al.* (1978) reported $kOH+DMA= 2.89x10^{-11}$ $exp(2.05\pm1.25$ kJ $mol^{-1})/RT$ and Galano and Alvarez-Idaboy 2008, reported $k_{OH+DMA}= 2.72x10^{-11}$ $exp(1.59$ kJ $mol^{-1})/RT$. For MEA, Onel *et al.* (2012) measured the overall rate constant, k_{OH}, by laser induced fluorescence over temperature range of 296-510 K and reporting $k_{OH+MEA} = 2.88x10^{-11}exp(2.43$ kJ $mol^{-1}/RT)$.

The activation energies, E_a, for the total k_{OH} rate constant for the amines determined over a range of temperatures by these studies are in close agreement to one another. In this work, the rates for each H-abstraction pathway were determined separately for the amines of interest. To determine the total rate, k_{OH}, the rate constants from all the

H-abstraction pathways are added. However, activation energies are not additive, like the rates for the individual H-abstraction pathways; therefore, total Ea from all the H-abstraction pathways is not determined in this work and compared to literature.

In the following sections the reaction paths that are essential to obtaining the rate coefficients are discussed in detail using MA, DMA and MEA.

5.3.2 Amine + OH reactions (k_{OH} pathway)

When the amine emissions are released into the atmosphere from the PCCC plant they are confronted with abundant OH radicals. The reaction with the OH is considered to be the main amine gaseous phase loss route with a typical atmospheric removal time of six hours. These OH radicals can abstract a H atom from either the N of the amino group or the C of the alkyl group, resulting in different proportions of the alkyl amino and alkyl radicals. The alkyl amino radical is of interest as it undergoes further reactions with NO, NO_2 and O_2 forming in particular the harmful nitrosamine and nitramines, as opposed to the alkyl radicals which form aldehydes (Nielsen *et al.* 2011a). The reactions of the alkyl amino radicals differ from those of the C-centred radicals owing to the difference in their electro-negativities (Tang and Nielsen 2012).

Before the reaction, the oxygen of the OH radical aligns collinear to the amino N-H and the OH radical forming a H-bond to the N lone pair. During the reaction, the hydrogen leaves the nitrogen atom and joins the OH radical to form the alkyl amino radical and H_2O as the products. The OH group can also align to the C-H of the alkyl group, abstract a hydrogen atom and then form imine and H_2O.

Figure 5.4 a-c illustrate the reaction starting from a pre-reaction complex and finishing in a post-reaction complex for all the three amines under study. The transition state structures found are qualitatively geometrically similar to those by Onel *et al.* (2012).

As the calculated k_{OH} is supposed to be the sum of rates for H abstraction from an amine group (k_1) and from the non-amine group (k_{1b}) it is essential to consider the following branching ratio:

$$k_{OH} = k_1 + k_{1b} \quad (5.5)$$

$$\text{OH branching ratio (289 K)} = \frac{k_1}{(k_1 + k_{1b})} = \frac{k_1}{k_{OH}} \quad (5.6)$$

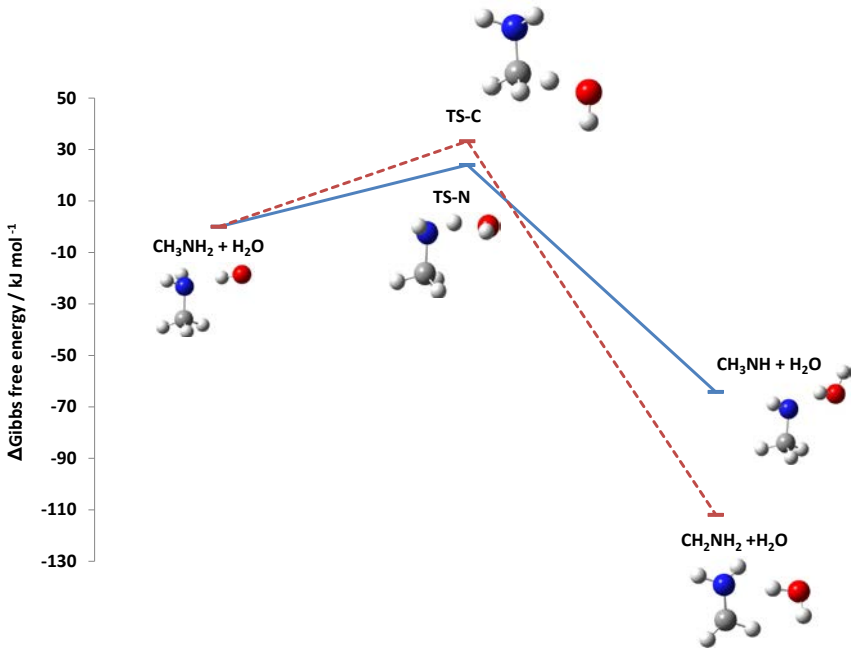
The branching ratio represents the balance between the initial attack on the amino group compared to an attack at the non-amine group. A low branching ratio means fewer amounts of nitrosamine and nitramine are formed.

The calculated branching ratios are given in Table 5.8. The calculated branching ratio for MA + OH is 65C:35N, whereas the experimental branching ratio is found to be 75C:25N (Nielsen *et al.* 2011a). For DMA + OH, the calculated value is 62C:38N which is very close to the experimental value of 63C:37N. Finally, with MEA + OH, only 5% of the H abstraction occurs at the N, whereas the remaining 95 % occurs at both the C and O. The calculated value is lower than the 8 % determined by Nielsen *et al.* (2011a), most likely owing to the variability in the experimental conditions whilst performing the rate determination.

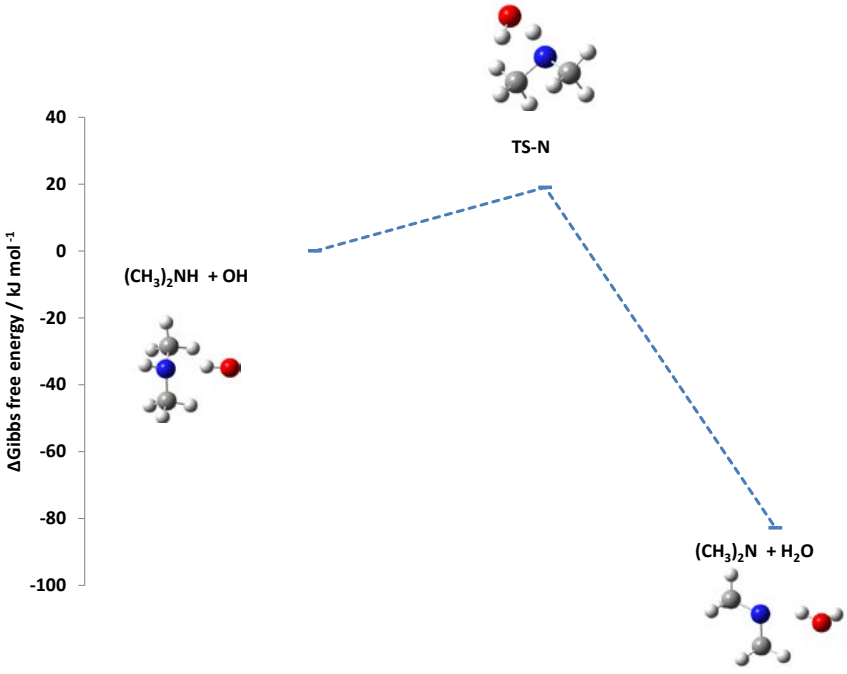
Table 5.8: Calculated branching ratios for H abstraction of the amines by OH

	Branching ratio	Literature
MA	65C:35N	75C: 25N [a]
		47C: 53N [b]
DMA	62C: 38N	63C: 37N [c]
		58C: 42N [a]
		22C: 78N [b]
MEA	95 C:5 N:1 O	80 C: 10N :10 O [a]
		82C:17N:1 O [d]

[a]Nielsen *et al.* (2011a); [b] Onel *et al.* (2012); [c]Lindley *et al.* (1979);[d]Xiao *et al.* (2014)


50
30
10
-10
-30
-50
-70
-90
-110
-130
ΔGibbs free energy / kJ mol-1
TS-C
TS-N
CH3NH2 + H2O
CH3NH + H2O
CH2NH2 +H2O

(a)


40
20
0
-20
-40
-60
-80
-100
ΔGibbs free energy / kJ mol-1
TS-N
(CH3)2NH + OH
(CH3)2N + H2O

(b)

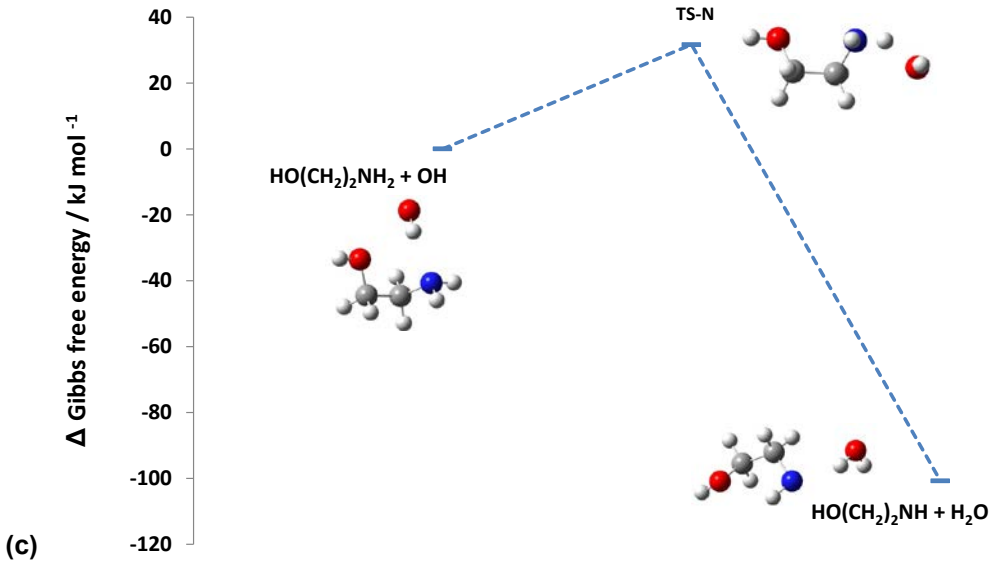


Figure 5.4: Energy level diagram for (a) CH_3NH_2 + OH (b) $(CH_3)_2NH$ + OH and (c) $HOCH_2CH_2NH_2$ + OH reactions (N-Branch) using M062X/6-31G(2d,p) level of theory (relative 298K Gibbs free energy in kJ/mol).

5.3.2.1 Tropospheric amine lifetime

The function of amines and its carcinogenic degradation products in the Earth's atmosphere is matter of concern. For this reason, it is imperative to determine their life times in the atmosphere. In the case of amines, the reaction of the amine with OH is the dominant removal pathway for the amine, i.e. the rate of this reaction influences the lifetime of the amine. Therefore, the tropospheric lifetime of amines in the atmosphere which is the time taken for the amine concentration to fall to 1/e of its initial concentration (Finlayson-Pitts and Pitts Jr 1999) can be determined according to the second order reaction relationship between the OH radical and amine:

$$\tau_{OH} = \frac{1}{[OH]\, k_{OH}} \tag{5.7}$$

Where [OH] = 1.5 x 10^6 radical cm^{-3} for a typical 12 hr daytime (Seinfeld and Pandis 2006).

The calculated lifetimes of the amines of interest are shown in Table 5.9 and they are found to be in agreement with the findings in the literature. It is apparent from the lifetimes that MA has the longest lifetime since it has the smallest rate constant in comparison to the other two amines, whereas, MEA has the shortest lifetime.

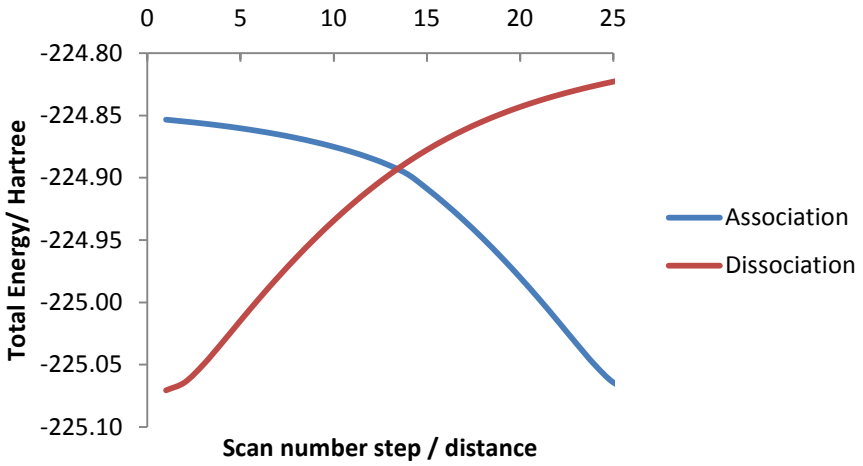
Table 5.9: Tropospheric lifetime of the amine in the atmosphere determined form k_{OH} calculated in this work as well as from literature.

Amine	k_{OH} (cm^3 $molecule^{-1}$ s^{-1})	τ_{OH} (hr)	Literature
MA	2.18×10^{-11}	8.5	8.3[a], 9.4[b], 10.7[c]
DMA	6.26×10^{-11}	3.0	2.9[c], 3.0[b], 2.8[d], 2.6[e]
MEA	9.20×10^{-11}	2.0	2.0[f], 2.4[b], 2.5[i], 2.6[j]

[a] Atkinson *et al.* (1977), [b]Onel *et al.* (2012),[c] Carl and Crowley (1998),[d]Atkinson *et al.* (1978), [e] Nielsen *et al.* (2011a), [f] Karl *et al.* (2012), [i] Xie *et al.* (2014),[j] Borduas *et al.* (2013).

5.3.3 Alkyl amino radical reaction + NO reactions (k_3 NO pathway)

The reactions of alkyl amines with NO have been the centre of attention due to the production of carcinogenic nitrosamines in the atmosphere (Magee and Barnes 1956). The addition reaction of the amino radical and NO radical is barrierless, proven by a scan of the N-NO bond breaking process (Figure 5.5) at the level of theory used in the present study.



(a)

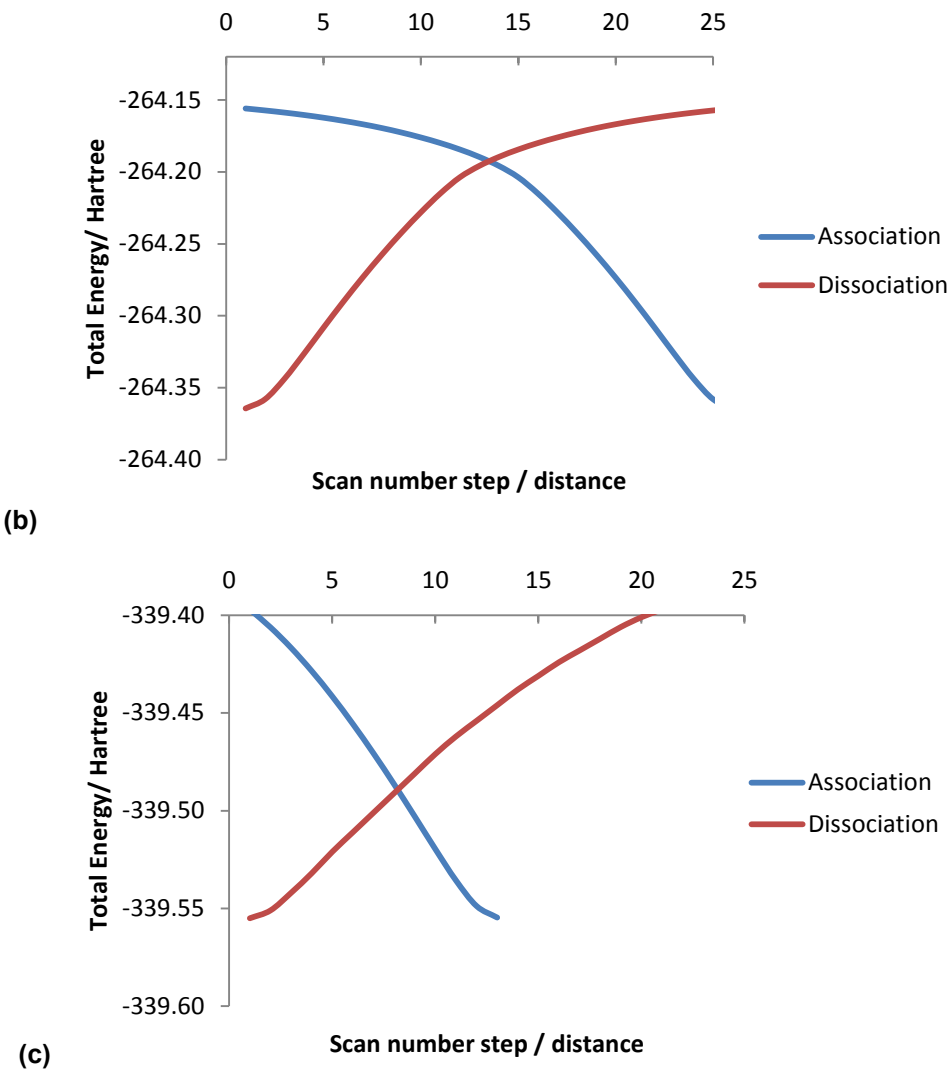


Figure 5.5: A M062X study of the potential energy surface of the association of (a) CH_3N + NO and the dissociation of the resulting nitrosamine, CH_3NH-NO (b) $(CH_3)_2N$ + NO and the dissociation of the resulting nitrosamine, $(CH_3)_2N$-NO (c) $HOCH_2CH_2NH$ + NO and the dissociation of the resulting nitrosamine, $HOCH_2CH_2NH$-NO.

In this study, the reaction of amino radical and NO (for all the amines) is investigated considering all the pathways for the proposed products (Figure 5.6) and then the rate is determined for the most likely pathway.

Researchers (Tang and Nielsen, 2012) have studied reactions of methyl amino and NO forming methyl nitrosamine that dissociates to form the imine, CH_2NH and HON through one route. Their alternative route suggests the formation of CH_2NHNOH (with a relatively lower barrier height than the former route), which upon reaction with O_2 forms CH_2NH + NO + HO_2. However, the latter pathway is refuted by the recent theoretical studies performed by da Silva (2013), who instead

proposed that diazomethane CH_2NN and water are the most stable products of this radical-radical recombination reaction.

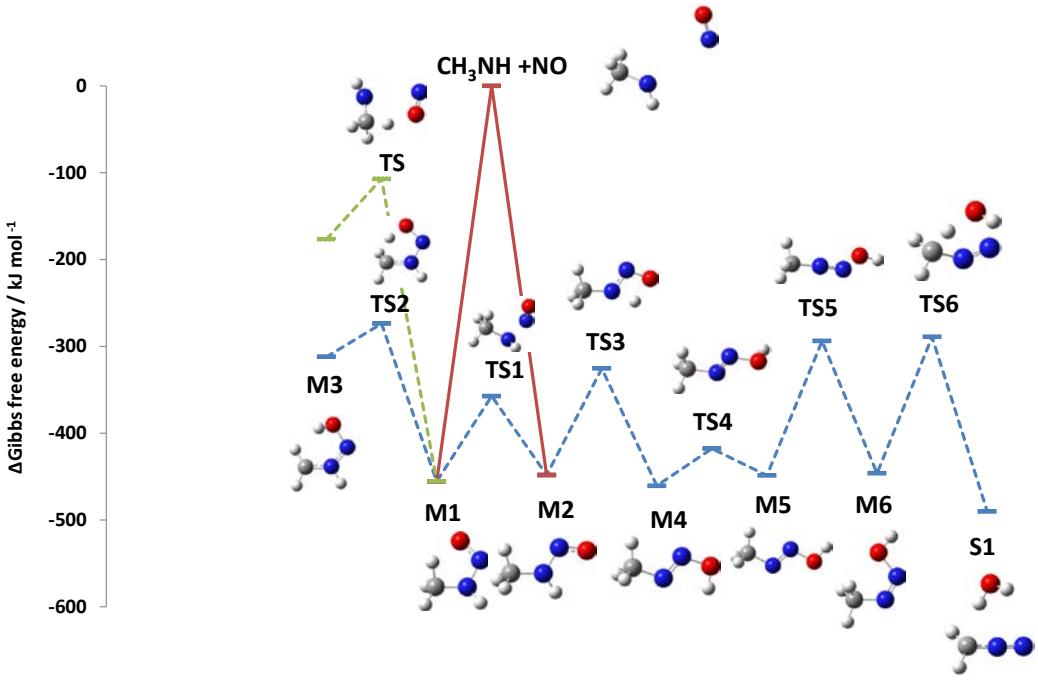
As can be seen from Figure 5.6 (a), this barrierless reaction results in the formation of two conformers (M1 and M2) of the primary nitrosamine (CH_3NHNO). M1 with a syn-conformation is thermodynamically more stable than its anti-conformer, M2. M1 interconverts to M2 via a transition state, TS1. M1 can undergo a sigmatropic 1,4- H-shift from the adjacent methyl group to the O in the N-NO group via a five-membered-ring transition state, TS2, forming CH_2NHNOH (M3). The later can react with O_2 and form CH_2NH + NO+ HO_2. Alternatively, CH_2NH and HO_2 are also formed from the direct hydrogen abstraction from M1. As this route has a high barrier height of 167 kJ/mol which is higher than the TS2 one, it can therefore be considered less viable at atmospheric conditions.

The dissociated pathway for the anti-conformer M2 undergoes is described in the same manner as by da Silva (2013). M2 undergoes a sigmatropic 1,3- H-shift from the adjacent -NH group to the O atom and proceeds via a four-membered-ring transition state, TS3, to form a trans-CH_3NNOH (M4) in which the H of the hydroxyl group is cis to the N=N bond. M4 goes through an internal rotation of 180° of the OH-group via TS4 to form M5 with the H trans to the N=N group. Following this, cis-CH_3NNOH (M5) is formed via transition state, TS5 from the cis-trans isomerisation of M5 about the unsaturated N=N bond. The TS5 was discovered in this study at the computation level of theory employed, and has not been reported elsewhere in literature. Finally the most stable products, diazomethane and H_2O (S1) form as the M6 undergoes dehydration reaction via TS6. This proposed route is more plausible since it proceeds via transition states lower in energy than TS2 (51.6 kJ/mol) and it is irreversible. However, there have been no experimental investigations reported to support the likelihood of diazomethane forming as a product of these reactions. Therefore, the rate for this pathway is not calculated and the pathway proceeding via the TS2 as the imines which has been reported experimentally Nielsen *et al.* (2011a), is considered.

For the secondary alkyl amine radicals, such as the DMA radical, they form stable nitrosamines in an exothermic barrierless reaction, which do not undergo further dissociation (Figure 5.6b). Also, MEA forms a stable nitrosamine via a barrierless reaction (confirmed by a scan of the bond breaking process, Figure 5.5 that does not

undergo further dissociation (Figure 5.6). This is not the case for MA as observed (Figure 5.6a), where the primary nitrosamines formed are unstable and follow different dissociation pathways to form stable products such as diazomethane (da Silva, 2013). As the likelihood of diazomethane forming is experimentally not supported, the pathway forming the imines, which has been reported experimentally Nielsen *et al.* (2011a), is considered.

RRKM theory has been used for treating reactions with 'barrierless' transition states (Andersen and Carter 2008). Therefore, for the purposes of this study, the rate coefficients for the alkyl amino and NO radical-radical combination reactions are calculated using the RRKM theory in ChemRate and are shown in Table 5.6 and the enthalpy of formation for each of the species required for calculating the rate are listed in Table 5.4. The rate constant calculated for the dimethyl amino radical and NO radical is found to be in excellent agreement to that determined experimentally. There are no reported experimental rate constants for the reaction of methyl amino and monoethanol amino radicals with NO. It is, therefore, assumed that applying the same level of computational theory and RRKM theory as for DMA case, the rate constants obtained for the MA and MEA cases will be reliable. The pathway proceeding via the TS2 is only considered in the case of MA as it forms an unstable nitrosamine.



(a)

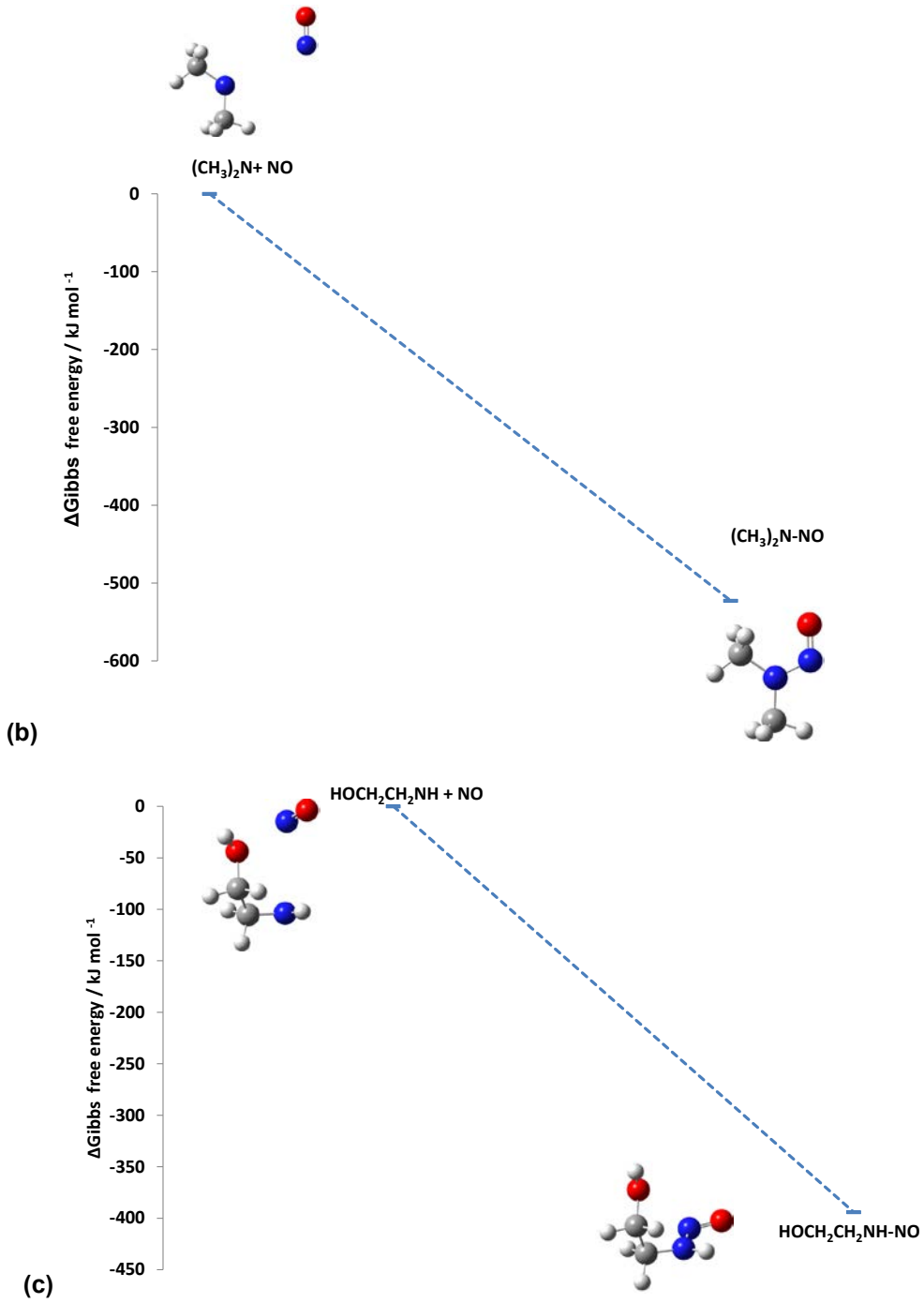
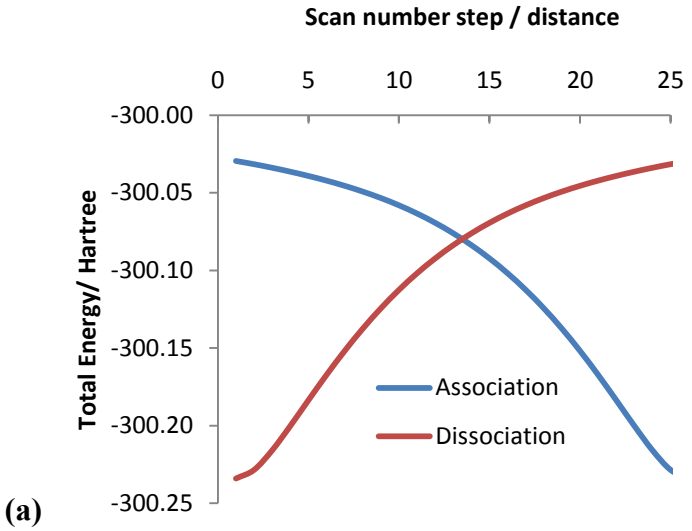


Figure 5.6: Energy diagram for (a) CH_3NH + NO (b) $(CH_3)_2N$ + NO and (c) $HOCH_2CH_2NH$ + NO reactions using M062X/6-31G(2d,p) level of theory (relative 298K Gibbs free energy in kJ/mol).

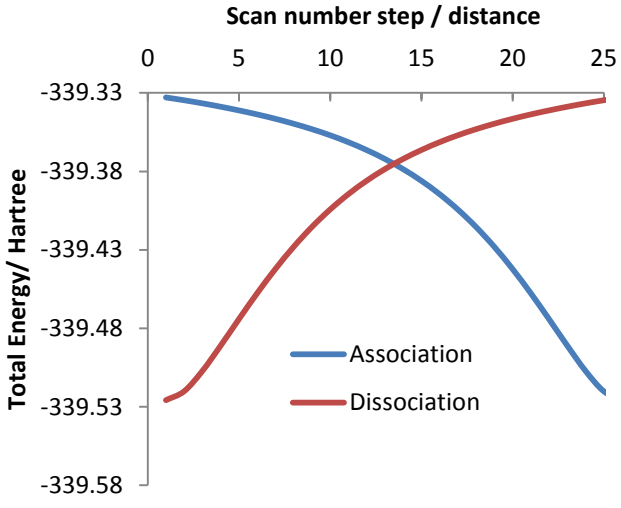
5.3.4 Alkyl amino radical + NO_2 reactions ($k_{4a,b}$ NO_2 pathways)

The alkyl amino radicals are susceptible to attack by NO_2 and can undergo an addition reaction. These reactions are not only exothermic but barrierless too. A scan

of the PES following the reaction coordinate of the N-NO_2 bond cleavage process confirmed this (Figure 5.7).



(a)



(b)

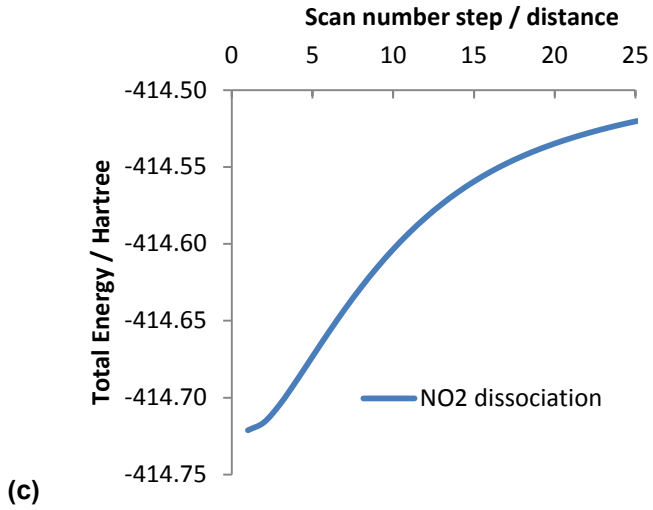


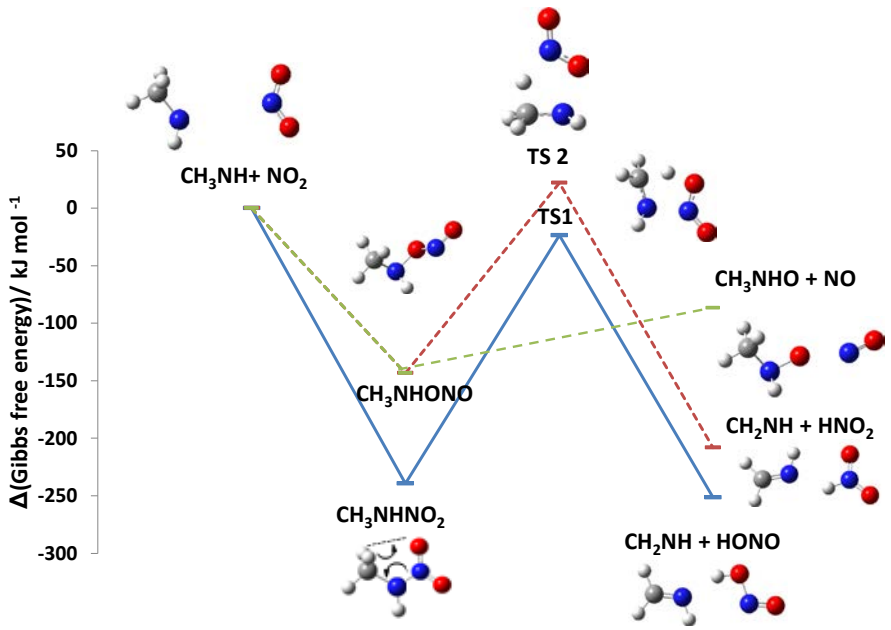
Figure 5.7: A M062X study of the potential energy surface of the association of (a) CH_3NH + NO_2 and the dissociation of the resulting nitrosamine, CH_3NH-NO_2 (b) $(CH_3)_2N$ + NO_2 and the dissociation of the resulting nitrosamine, $(CH_3)_2N$-NO_2 (c) $HOCH_2CH_2NH$ + NO_2 to form the nitrosamine, $HOCH_2CH_2NH$-NO_2.

In this study, the reactions of the three alkyl amino radicals and NO_2 are investigated considering all the pathways for the proposed products (Figure 5.8). This reaction step produces intermediates such as nitramines (CH_3NH-NO_2, $(CH_3)_2N$-NO_2 and $HOCH_2CH_2NH$-NO_2) and nitrosoxy amines (CH_3NH-ONO, $(CH_3)_2N$-ONO and $HOCH_2CH_2NH$-ONO). Quantum chemistry calculations have elucidated three dissociation routes for the resulting intermediates which agree to the findings reported by Tang and Nielsen (2012). The N-nitramine dissociates by undergoing a sigmatropic 1,4- H-shift from the adjacent methyl group to the O in the N-NO_2 via a five-membered-ring transition state, TS1 (Figure 5.8). Simultaneously, the N-N bond breaks to form an imine and nitrous acid, HONO. Lindley *et al.* (1979) have experimentally determined the nitramine/imine branching ratio (0.22 ± 0.06) in the DMA and NO_2 reaction.

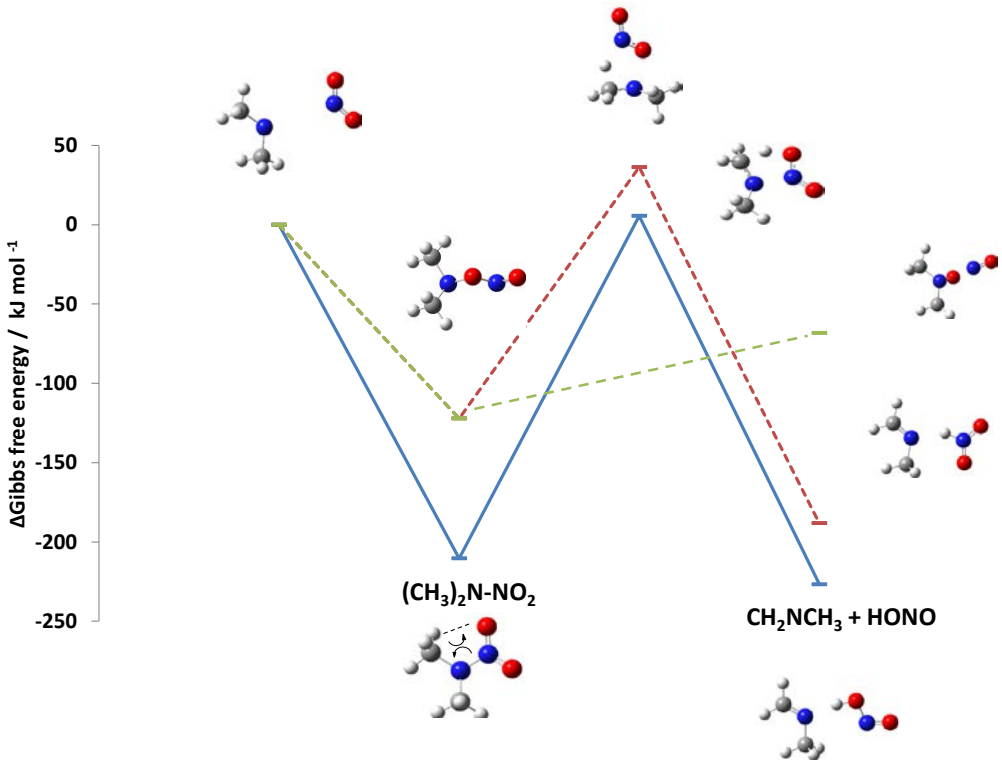
The nitrosoxy amine adduct dissociates via two possible routes: (a) a barrierless and an exothermic O-NO bond cleavage process to form an alkyl nitroxide and NO radical (established by performing a bond-fission scan) or (b) a sigmatropic 1,4 H-shift from the adjacent methyl group to the N in the O-NO via a five-membered-ring transition state, TS2, forming an imine and nitryl hydride (HNO_2). The later route is likely insignificant in the atmosphere given the high energy of the TS2 relative to TS1 (45.3, 30.8 and 42.4 kJ/mol, respectively for the MA, DMA and MEA).

The determined reaction mechanisms for DMA using quantum theoretical calculations agree well with those from the experiments carried out at atmospheric conditions (Lindley *et al.* 1979, Tuazon *et al.* 1984, Tuazon *et al.* 1994, Nielsen *et al.* 2011a) in which the production of thermally stable nitramines, N-nitrosoxy amine, imines and HONO or nitroxide and NO were discovered. Theoretical calculations performed by Tang and Nielsen (2012) support the mechanisms established here for MA and DMA as well.

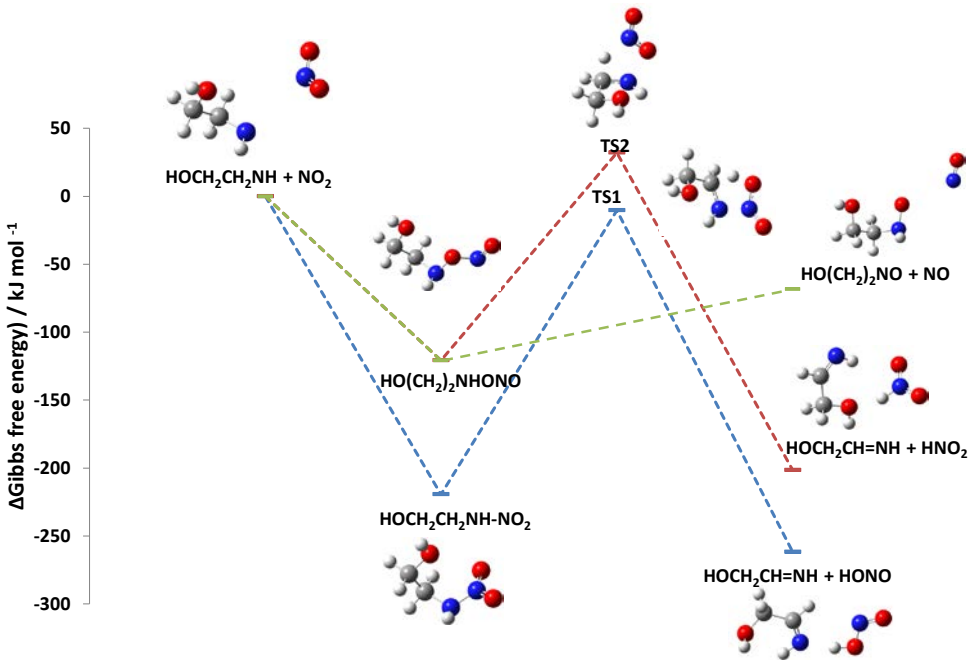
For the rate constant calculations the rate of reaction of the amino radical with the NO_2 to form nitramine (k_{4a}) via a barrierless reaction is determined using ChemRate. After the collision between the NO_2 and amino radical to form the nitramine, the thermally excited nitramine can then either be quenched by collision or dissociate via TS1 into an imine. The ratio of the imine to the nitramine is pressure dependent despite a high barrier height (216, 216 and 209.1 kJ/mol, respectively for the MA, DMA and MEA). The energies of the resulting imine and the nitramine are comparable (difference of 12.0, 16.2 and 42.3 kJ/mol, respectively for the MA, DMA and MEA) which means that the reaction is not in equilibrium. Since TST assumes thermal equilibrium RRKM is chosen to calculate k_{4b}.



(a)



(b)



(c)

Figure 5.8: Energy level diagram for (a) $CH_3NH + NO_2$ (b) $(CH_3)_2N + NO_2$ and (c) $HOCH_2CH_2NH+ NO_2$ reactions, at the M062X/ 6-31G (2d, p) level of theory (relative 298K Gibbs free energy in kJ/mol).

5.3.5 Amino alkyl + O_2 reactions (k_2 O_2 pathway)

Alkyl amino radicals can also undergo H-abstraction reactions with O_2 resulting in imine formation. According to the level of theory employed, the addition of the O_2 to the alkyl amino radical is an exothermic process which proceeds via a transition state to form the peroxy adduct (two conformers of the peroxy exist for MA with a negligible rotational barrier) suggesting that this PES possesses a transition state (established by a scan of the bond breaking process, Figure 5.9) as shown in Figure 5.10.

These findings are not in agreement to those from Tang and Nielsen (2012), where it was suggested that such a reaction is barrierless. However, the three dissociation routes for the resulting intermediates calculated, agree to the findings reported by these authors (Tang and Nielsen 2012). The peroxy adduct dissociates via two possible pathways to give a H-bonded imine and hydroperoxyl (HO_2) product complex **(**Figure 5.10**)**. The first occurs via a sigmatropic 1,4 H-shift from the adjacent methyl group to the O atom in the OON plane via a five-membered-ring transition state, TS2, breaking the N-O bond and forming the C=N bond simultaneously. The second one occurs via a sigmatropic 1,4 H-shift from the adjacent methyl group to the O atom via a four-membered-ring transition state, TS4 (with an O-H bond). The barrier height of TS2 is lower (by 119.0, 113.1 and 118.4 kJ/mol, respectively for the MA, DMA and MEA) than TS4 owing to differences in their geometries.

The imine and HO_2 product complex is also formed by abstracting a H atom directly from the alkyl amino radical proceeding via transition state, TS3. However, owing to the relatively higher barrier heights of TS3 and TS4 (26.4, 22.3 and 15.1 respectively for the MA, DMA and MEA; and 119.0, 113.1 and 118.4 kJ/mol respectively for the MA, DMA and MEA, relative to TS2), the pathway that governs the formation of the imine and HO_2 is via the five-membered-ring transition state, TS2, at atmospheric conditions.

Since the pathway proceeding via TS and TS2 is more likely at ambient conditions, the rate coefficient for this particular pathway is sensible as input for dispersion modelling. From the calculations it was apparent that the formation of TS2 is the rate determining step (r.d.s). Therefore, the rate that was calculated for the r.d.s was k_2. Since the imine is (78.3, 77.6 and 107.9 kJ/mol, respectively for the MA, DMA and

MEA) more stable than the peroxy adduct, therefore, this is an exothermic reaction in equilibrium.

By using TST and RRKM, the values obtained for k_2 show a similar trend, however, the values determined using TST are an order of magnitude lower and those from RRKM are higher than the experimental value for DMA (Table 5.6). TST theory considers only thermal equilibrium, whereas, RRKM can also account for pressure that can affect the reaction. The reason for the substantial difference for k_2 between the two theories is not clear. A possible explanation for the difference in the values can be attributed to the fact that both the theories estimate the rate differently as they are based on different assumptions. TST theory is based on the local-equilibrium and no-recrossing assumptions (Truhlar and Garrett 1984). On the other hand, RRKM theory considers the total number of states of the transition structure and the reaction path degeneracy. The density and sum of states are calculated using Whiten-Rabinovitch algorithms (Whitten and Rabinovitch 1963) with vibrational frequencies and moments of inertia (Mokrushin *et al.* 2011).

The different assumptions and approaches considered by the two theories can certainly contribute to the difference in the rate constant values. The k_2 reaction pathway is a dissociation reaction that involves a peroxy adduct dissociating to form the resulting products where the rate is influenced by pressure. TST theory considers only thermal equilibrium, whereas, RRKM can also account for pressure that can affect the reaction (personal conversation with C J Nielsen, University of Oslo). TST might therefore be an incomplete model for calculating the rate constant. Since, RRKM theory has been used for modelling the kinetics of unimolecular dissociation reactions; therefore, for this study the values obtained through RRKM are used as they are more reliable.

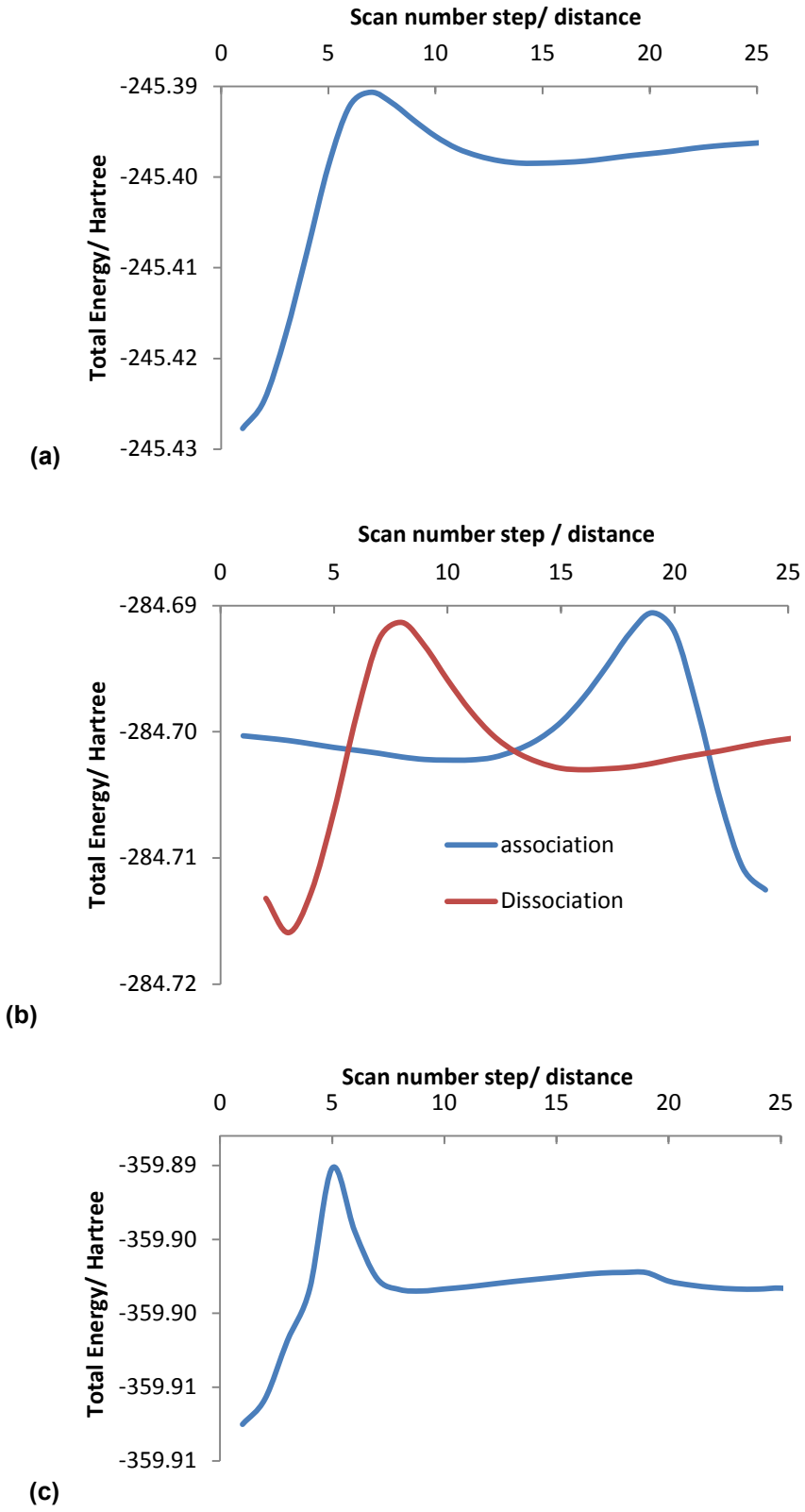
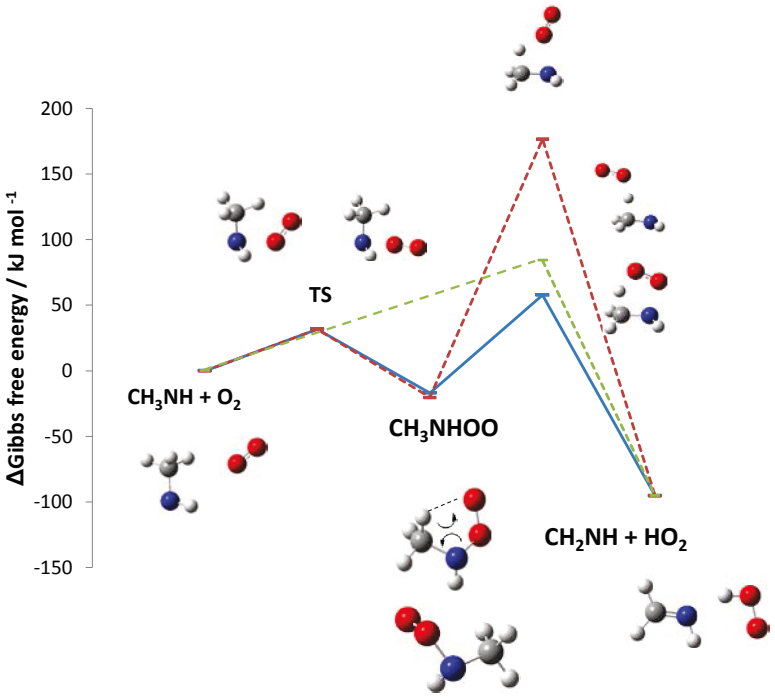
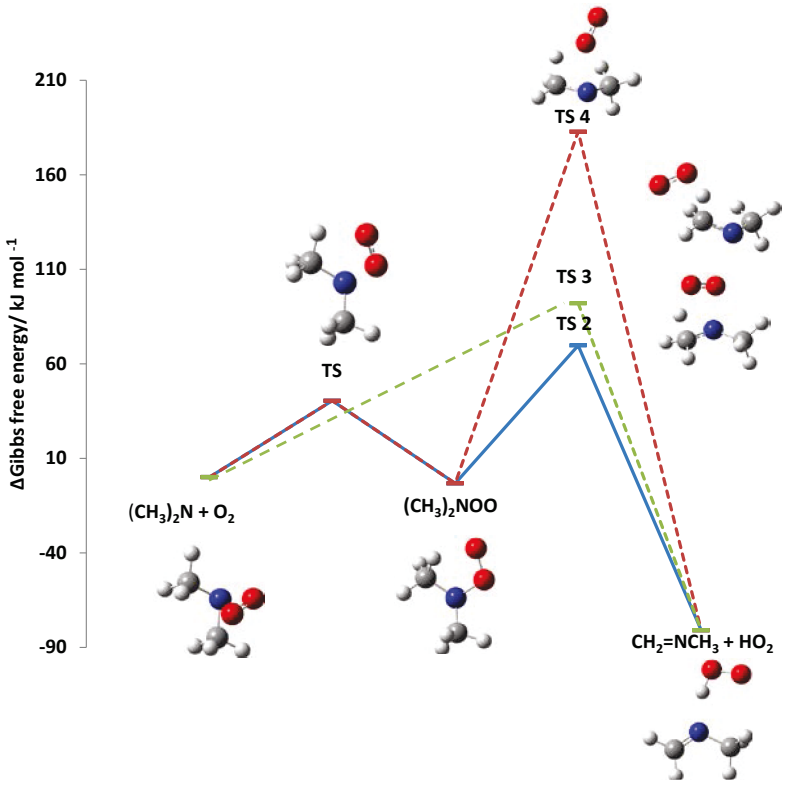


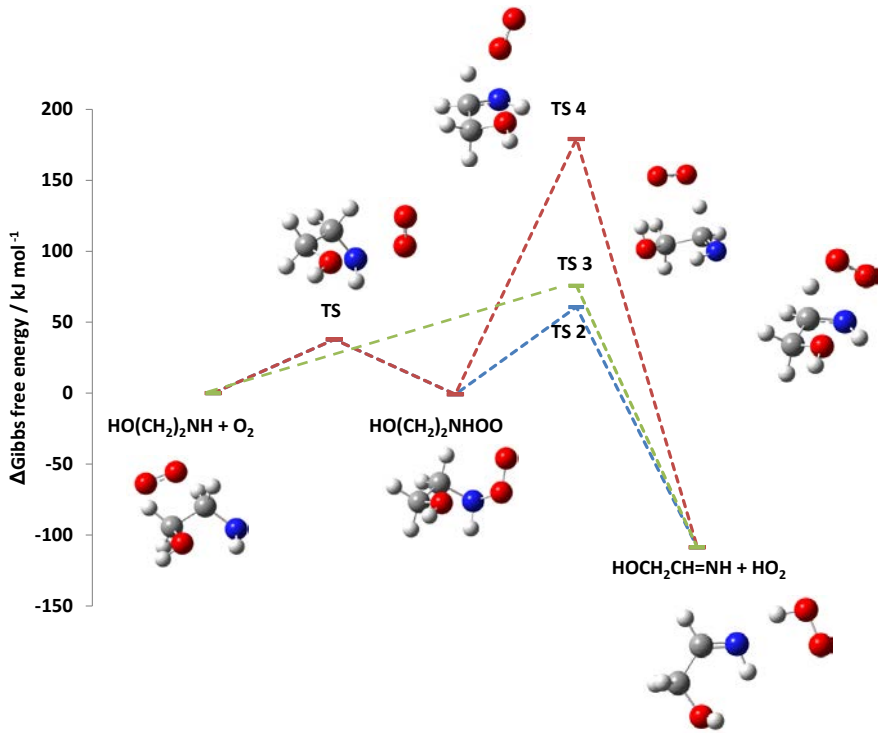
Figure 5.9: A M062X study of the potential energy surface of the association of (a) $CH_3NH + O_2$ (b) $(CH_3)_2N + O_2$ and the dissociation of the resulting nitrosamine, $(CH_3)_2N\text{-}O_2$ (c) $HOCH_2CH_2NH + O_2$.


200
150
100
50
0
-50
-100
-150
ΔGibbs free energy / kJ mol -1
TS
CH3NH + O2
CH3NHOO
CH2NH + HO2

(a)


210
160
110
60
10
-40
-90
ΔGibbs free energy/ kJ mol -1
TS 4
TS 3
TS 2
TS
(CH3)2N + O2
(CH3)2NOO
CH2=NCH3 + HO2

(b)



(c)

Figure 5.10: Energy level diagram for (a) $CH_3NH + O_2$ (b) $(CH_3)_2N + O_2$ and (c) $HOCH_2CH_2NH + O_2$ reactions, at the M062X/ 6-31G (2d, p) level of theory (relative 298K Gibbs free energy in kJ/mol).

5.3.6 Nitrosamine Photolysis: vertical excitation energies of the nitrosamines (J_5 hυ pathway)

Nitrosamines undergo photochemical degradation in the atmosphere in the presence of solar radiation with life time of less than half hour, depending on the surroundings. This is due to the organic chromophore N-N=O which absorbs ultraviolet radiation around a wavelength of 365 nm and electronic excitations of n electrons to the π* excited state resulting in N-NO bond cleavage.

The photolysis of NDMA was investigated in the gas phase by Lindley *et al.* (1979), Geiger and Huber (1981). Tuazon *et al.* (1984) also determined the nitrosamine photolysis frequency relative to that of NO_2 ($J_{NDMA}/ J_{NO2} = 0.53 \pm 0.03$), correlating to a quantum yield of 1 at 290 nm, which is in agreement to the very first measurements of 1.03 + 0.10 value at 363.5 nm calculated by Geiger and Huber (1981). Nielsen *et al.* (2011a) also reported a value for 0.34 ± 0.03 for J_{NDMA}/ J_{NO2}. However, owing to the very low vapour pressures of nitrosamines at atmospheric conditions, it remains challenging to perform experimental investigations. The calculated vertical excitation wavelength and oscillator strengths (0.0006 - 0.0011, shown in

Table 5.10, Table 5.11 and Table 5.12) in this work are in agreement with the experimental findings.

The photolysis rate of nitrosamines is dependent on their spectral properties and the intensity of the solar ultraviolet radiation available. In the northern hemisphere, at a given latitude and longitude, the levels of solar radiation are at their maximum in the summer (~21st June), their lowest in winter (~21st December) and equal at the equinox (21st March and 21st September). Hence, photolysis is the dominant gas phase removal pathway for nitrosamine during summer time.

The tropospheric ultraviolet and visible radiation model from the National Centre for Atmospheric Research (NCAR) was employed to generate solar spectral actinic flux for the latitude and longitude at which the particular capture plant (Ferrybridge, Peterhead and Mongstad) is situated, at specified times of the year and at stack height (Table **5**.10, Table 5.11 and Table 5.12).

The overlap of the simulated UV-Vis spectra for the target nitrosamines and the solar actinic flux for different conditions at around 365 nm was considered. Table 5.10, Table 5.11 and Table 5.12, show the calculated photolysis frequencies and life times at the different conditions considered. The photolysis frequency is reported relative to NO_2 ($J/J(NO_2)$) using the NO_2 photolysis rate constant for the given site.

Results show that the photolysis rate constants are within the same order of magnitude for all the given nitrosamines as they all share the same organic chromophore, N-N=O. The simulated UV spectra for the three nitrosamines show a strong overlap with the solar actinic flux curves (for all the different conditions considered) around 363.5 nm, resulting in very fast photolysis rate, J, and consequently very short atmospheric photolysis lifetimes.

Since J is a function of the solar actinic flux, the obtained photolysis rate for any given nitrosamine is relatively slow in winter, therefore, they exist for longer in the atmosphere in winter. These nitrosamines have their shortest life times in the summer at the maximum available solar flux. At the two equinox conditions, the photolysis rates (and consequently the life times) are almost identical.

The primary nitrosamines (MA-NO and MEA-NO) have similar photolysis rate constants, whereas the secondary nitrosamine has a rate constant almost twice as high. Hence, DMA-NO photolysis is comparatively faster resulting in a shorter lifetime.

The photolysis frequency increases with altitude (Table 5.10, Table 5.11 and Table 5.12). As a consequence, the nitrosamine lifetime becomes shorter with increasing photolysis rate, as expected.

Generally, the photolysis ratio shows negligible change for any given nitrosamines, with the secondary nitrosamine having almost twice larger ratio than the two primary nitrosamines with similar values.

Contrary to nitrosamines, nitramines show no absorption at wavelengths greater than 300 nm. Therefore, nitramines possess mean life times of several orders of magnitude higher than nitrosamines.

Finally the mean photolysis life times of the nitrosamines between the three different sites are compared. It is seen that due to the higher altitude of Mongstad and lower solar radiation flux in comparison to Ferrybridge and Peterhead, the nitrosamines have a comparatively lower photolysis frequency and consequently a longer lifetime.

Table 5.10: Vertical electronic excitation wavelength, corresponding oscillator strength, photolysis rate, J, and the corresponding mean life times for the relevant n -> π* transition for the three target nitrosamines predicted at TD-DFT (B3LYP/ aug-ccpTVZ) level of theory and solar actinic flux for Ferrybridge at mid-day for different times of the year and at 198m stack height.

Nitrosamines	Time/ Altitude (km)	Vertical excitation wavelength (nm)	Oscillator strength	Photolysis frequency J (s^{-1})	J / J (NO_2)	Mean photolysis lifetime (τ / hr)
N-nitroso methylamine	21st March	366.06	0.0005	4.79×10^{-3}	0.72	0.058
	21st June			6.23×10^{-3}	0.76	0.045
	21st Sept			4.73×10^{-3}	0.72	0.059
	21st Dec			1.60×10^{-3}	0.75	0.170
N-nitroso dimethyl amine	21st March	358.7 (363.5)[a]	0.001	8.28×10^{-3}	1.24	0.034
	21st June			1.09×10^{-2}	1.23	0.025
	21st Sept			8.16×10^{-3}	1.24	0.034
	21st Dec			2.69×10^{-3}	1.26	0.103
N-nitroso monoethanolamine	21st March	367.05	0.0004	3.85×10^{-3}	0.58	0.072
	21st June			4.97×10^{-3}	0.56	0.056
	21st Sept			3.79×10^{-3}	0.58	0.073
	21st Dec			1.30×10^{-3}	0.61	0.213
	/0.5 km			1.38×10^{-3}	0.62	0.201
	/ 1 km			1.61×10^{-3}	0.62	0.172
	/ 2 km			1.71×10^{-3}	0.62	0.163

[a] Geiger and Huber (1981)

Table 5.11: Vertical electronic excitation wavelength, corresponding oscillator strength, photolysis rate, *J*, and the corresponding mean life times for the relevant n -> π* transition for the three target nitrosamines predicted at TD-DFT (B3LYP/ aug-ccpTVZ) level of theory and solar actinic flux for Peterhead at mid-day for different times of the year and at 170m stack height.

Nitrosamines	Time/ Altitude (km)	Vertical excitation wavelength (nm)	Oscillator strength	Photolysis frequency J (s^{-1})	J / J (NO_2)	Mean photolysis lifetime (τ / hr)
N-nitroso methylamine	21st March	366.06	0.0005	4.39×10^{-3}	0.72	0.063
	21st June			6.03×10^{-3}	0.71	0.046
	21st Sept			4.61×10^{-3}	0.77	0.060
	21st Dec			1.02×10^{-3}	0.75	0.274
N-nitroso dimethyl amine	21st March	358.7 (363.5)[a]	0.001	7.56×10^{-3}	1.24	0.037
	21st June			1.05×10^{-2}	1.23	0.026
	21st Sept			7.96×10^{-3}	1.33	0.035
	21st Dec			1.71×10^{-3}	1.27	0.163
N-nitroso monoethanolamine	21st March	367.05	0.0004	3.52×10^{-3}	0.58	0.079
	21st June			4.81×10^{-3}	0.56	0.058
	21st Sept			3.67×10^{-3}	0.61	0.076
	21st Dec			8.25×10^{-4}	0.61	0.337
	/0.5 km			8.91×10^{-4}	0.62	0.312
	/1 km			1.01×10^{-3}	0.62	0.274
	/2 km			1.22×10^{-3}	0.63	0.228

[a] Geiger and Huber (1981)

Table 5.12: Vertical electronic excitation wavelength, corresponding oscillator strength, photolysis rate, *J*, and the corresponding mean life times for the relevant n -> π* transition for the three target nitrosamines predicted at TD-DFT (B3LYP/ aug-ccpTVZ) level of theory and solar actinic flux for Mongstad at mid-day for different times of the year and at 65m of stack height.

Nitrosamines	Time/ Altitude (km)	Vertical excitation wavelength (nm)	Oscillator strength	Photolysis frequency J (s^{-1})	J / J (NO_2)	Mean photolysis lifetime (τ / hr)
N-nitroso methylamine	21st March	366.06	0.0005	2.91×10^{-3}	0.53	0.095
	21st June			4.34×10^{-3}	0.53	0.064
	21st Sept			2.85×10^{-3}	0.53	0.098
	21st Dec			4.14×10^{-4}	0.54	0.672
N-nitroso dimethyl amine	21st March	358.7 (363.5)[a]	0.001	6.81×10^{-3}	1.24	0.041
	21st June			1.02×10^{-2}	1.24	0.027
	21st Sept			6.66×10^{-3}	1.24	0.042
	21st Dec			9.64×10^{-4}	1.26	0.288
N-nitroso monoethanolamine	21st March	367.05	0.0004	3.25×10^{-3}	0.59	0.085
	21st June			4.76×10^{-3}	0.58	0.058
	21st Sept			3.18×10^{-3}	0.59	0.087
	21st Dec			4.67×10^{-4}	0.61	0.594
	/0.5 km			5.06×10^{-4}	0.66	0.549
	/1 km			5.63×10^{-4}	0.73	0.493
	/2 km			6.64×10^{-4}	0.33	0.418

5.4 Conclusions

The atmospheric chemistry reactions of the amines (MA, DMA and MEA) with OH and the resulting alkyl amino radicals with NO, NO_2 and O_2 were studied employing theoretical methods to elucidate reliable estimates of the rate constants describing each reaction step in the scheme. Other possible removal mechanisms such as reactions of with NO_3 or Cl radicals or deposition are not considered as they are not within the scope of this work.

As can be seen from Table 5.6, the calculated rate constants for DMA are in very good agreement with those determined experimentally as they are within the same order of magnitude. It is, therefore, assumed that in the absence of experimentally reported rate constants, the method used for evaluating the kinetics describing the atmospheric chemistry of DMA is appropriate for MA and MEA as well as any generic amine.

As the rates are independent from experimental parameters, the developed novel method may prove universal in comprehending the atmospheric chemistry of any generic amine used in the PCCC process. The main advantage of this technique is that one standard method can be employed to investigate the mechanisms and evaluate kinetics for each reaction pathway of the entire atmosphere scheme within experimental accuracy.

Upon comparison of the estimated rate constants, it is apparent that the fastest reaction is the reactions of the amine with the OH radical, $k_{1\ OH}$. The reaction of amino radical with O_2, k_2, is the slowest step. This proposes that imines would be more stable and as a result prevail in the atmosphere. It is, therefore, to no surprise that methylene imine has been detected in interstellar cloud dust (Godfrey *et al.* 1973, Dickens *et al.* 1997).

The function of amines and its carcinogenic degradation products such as, nitrosamines and nitramines in the Earth's atmosphere is matter of concern. For this reason, it is imperative to determine their life times in the atmosphere. From the estimated tropospheric lifetimes of the emitted amine in the atmosphere, it is apparent that MA has the longest lifetime, whereas, MEA has the shortest. It is also observed that although primary amines form primary nitrosamines, these have very short lifetimes unlike those formed from secondary amines which are stable. While

nitrosamines undergo photolysis, nitramines are comparatively stable and they can undergo dissociation to form their corresponding imines.

Hence, a quantitative understanding of the atmospheric chemistry of amine emissions is attained by evaluating kinetics describing the considered degradation mechanistic pathways governing the consumption and production of the chemical species of interest. The deduced rate constants now serve as input variables for advection-diffusion-reaction equations to determine accurately the levels of these chemical discharges in the air as demonstrated in the next chapter. The obtained concentration estimates of individual species can be used to assess the human health and environmental risk they pose.

Chapter 6 Atmospheric chemistry and dispersion modelling

6.1 Introduction

Amine emissions from a PCCC facility into the atmosphere undergo chemical transformation, dispersion and deposition processes with their concentration as a function of time from emitting facility. Atmospheric chemistry combined with dispersion and deposition calculations assist in quantifying the change in concentration in time and space from the source. Initial studies that attempted to determine the fate of the amine emissions did not consider chemistry with dispersion calculations simultaneously. This implies that dispersion calculations were performed assuming that the emitted amine was inert and did not undergo any reactions in the atmosphere. To account for the degradation products such as nitrosamines and nitramines, their instantaneous formation from the parent amine at the stack is assumed. The respective concentrations of the by-products is then determined as a fraction of the parent amine concentration, where this certain fraction is acquired from experimentally determined fixed formation yields (FFY) (Karl *et al.* 2011, de Koeijer *et al.* 2013). Such an approach only considers the amine emission without taking into account the detailed atmospheric degradation of the amine. Therefore, the spatial distribution of the concentrations of the reaction products has the same dispersion pattern as the parent amine. As a consequence, the highest impact of air concentrations is always near the plant. This does not realistically represent the change in their concentration with increasing distance from

the plant. Hence, the estimated concentration of the resulting nitrosamines and nitramines are not evaluated accurately. Therefore, it is indeed vital to obtain reliable concentrations of the resulting nitrosamines and nitramines within the area affected by the amine emissions around a facility to establish a realistic understanding of their associated risks.

To overcome this short coming some recent studies in the literature have considered amine atmospheric chemistry reactions with dispersion and deposition studies (CERC 2012d, Fowler and Vernon 2012, Emmerson *et al.* 2013, Karl *et al.* 2014, Wu and Nelson 2014, Karl *et al.* 2015). However, except for studies by Karl *et al.* (2014) and Karl *et al.* (2015), they have all considered rate constants from literature and assumed values in the absence of experimental rate constants. It is, therefore, suggested that it would be more appropriate to develop a theoretical method capable of calculating the rate constants describing all the reaction pathways in the amine atmospheric chemistry scheme (benched marked with existing experiment data as illustrated in chapter 5) in the absence of experimental data as opposed to making subjective assumptions. By doing so, the error in calculations can be reduced. Hence, it is important to build up on the existing knowledge and gain a better understanding of the atmospheric processes involved such as the atmospheric chemistry of the amines of interest, their expected dispersion and deposition to soil and water.

In this work to investigate the chemical transformation of amines emitted from a capture plant together with their dispersion and transport, the specially designed Amine Chemistry Module in the ADMS 5 atmospheric dispersion model was employed (CERC 2012a, CERC 2012b). Within ADMS 5, it is possible to describe the entire atmospheric fate of the involved amines including their growth and decay as previously reported by CERC (CERC 2012d, CERC 2012c). In Europe, this model is a regulatory standard; it has been widely employed for air quality modelling for the assessments of impacts from emissions produced by industries for instance. The rate coefficients obtained from quantum chemistry and kinetic modelling (in the previous chapter), were used in the model's parameterisation of the chemistry mechanism of amines.

6.2 Study Sites

To demonstrate the application of the developed methodology, case studies on three important post combustion capture plants were conducted to quantify the change in concentration of the amine discharges in time and space with respect to the emitting facility.

6.2.1 Ferrybridge CCPilot 100+

The first emitting facility is the UK's largest CO_2 capture pilot plant in Ferrybridge, CCPilot 100+. It was functional in 2012 and 2013 capturing 100 tonne of CO_2 per day with a 90 % capture rate (Fitzgerald *et al.* 2014).

6.2.2 Peterhead Power Plant

The second facility considered is the 'to be' world's first industrial-scale application of the CO_2 capture and storage technology at a gas-fired power station in Peterhead in UK. The Peterhead project is expected to capture 1 million tonnes of CO_2 per year with a 90 % CO_2 capture rate (Shell 2015).

6.2.3 Technology Centre Mongstad

The final emitting facility considered is the CO_2 Technology Centre Mongstad (TCM) in Norway. It is the world's largest amine testing facility that operated since 2012 with a capacity of capturing 100, 000 tonnes of CO_2 per year with a CO_2 capture rate of 85% (de Koeijer *et al.* 2009, TCM 2012, de Koeijer *et al.* 2013).

6.3 Safety limits

The resulting concentrations of nitrosamines and nitramines from a PCCC process should be within the safety limits proposed by various scientists and regulatory authorities, to keep the risk negligible to human health and the environment. For the TCM, the Norwegian Climate and Pollution Agency had issued a discharge permit of 0.3 ng/m^3 for total nitrosamines and nitramines released in the flue gas in the air and 4 ng/L in water during its operation (Låg *et al.* 2011). However, in the UK or EU in general there are no environmental assessment levels or environmental quality standards set for the nitrosamines and nitramines. Therefore, the safety thresholds for TCM are considered instead in this study, as they are useful benchmarks since they have been calculated with regards to the methods used under the EU regulations on

registration, evaluation, authorisation and restriction of chemicals (REACH). Nevertheless, there are several other thresholds that have been established by various research studies and international regulatory authorities that should also be considered when performing risk assessments.

Some of the safety limits are summarised in Table 6.1. It shows the monthly safety limit for MEA in air via the inhalation exposure pathway which if exceeded could affect the human health at a subchronic level. The safety limits for nitrosamines in air are also listed which can be carcinogenic to humans from long term exposure. The aquatic and drinking water limits for both nitrosamines and nitramines are also shown which if exceeded can be carcinogenic to humans and also adversely impact the algae, bacteria and fish in the aquatic environments. Hence, these thresholds should be adhered to in order to circumvent the dire consequences of having higher concentrations of these chemicals in air and water both on humans and aquatic species.

Table 6.1: Safety limits stated by various studies for MEA, nitrosamines and nitramines in air, drinking water and the aquatic environment. (Reproduced from Karl *et al.* (2011)).

Chemical species	Exposure pathway	Toxicity	Safety limit	Reference
MEA	Inhalation	Human health, subchronic	10 μg/m^3 (monthly average)	Låg *et al.* (2009)
	Aquatic	Algae/bacteria, chronic	7500 ng/L	Brooks and Wright (2008)
Nitrosamines	Inhalation	Human health, carcinogenic	0.02 ng/m^3 (monthly average)	(USEPA)
	Drinking water	Human health, carcinogenic	7, 4 ng/L	Richardson *et al.* (2007), Cal-EPA (2006), Knudsen *et al.* (2009)
	Aquatic	Algae/bacteria, chronic	25 ng/L	Brooks and Wright (2008)
Nitramines	Drinking water	Human health, carcinogenic	1000 ng/L	Wollin and Dieter (2005)
	Aquatic	fish, chronic	200 ng/l	Brooks and Wright (2008)

6.4 Scenario risk analysis

For emitting facilities to obtain an emission permit for an amine solvent based PCCC unit, it is essential to conduct a risk analysis. A scenario risk analysis can be used as a tool to reveal the impact of the most uncertain parameters and assumptions made (de Koeijer *et al.* 2013). This is due to the high uncertainties associated with the environmental concentrations of the compounds of interest and their toxic effects.

Usually a hypothetical worst-case scenario is considered for the plants. It is highly unlikely to be realistic but nevertheless it is only useful when safety limits for air and water are not surpassed (de Koeijer *et al.* 2013). The worst-case scenario follows the precautionary principle to avoid risks for the environment and public health in a situation where the data basis (emission totals, chemical kinetics and branching ratios, meteorological variables, etc.) is relatively weak. Since the worst-case scenario neglects chemistry, only atmospheric processes that act linearly on the concentration are considered. As a result, air concentrations have a linear dependency on emissions of amines.

With such a worst-case scenario study the maximum tolerable emissions of amines from CO_2 capture resulting in concentrations of the nitrosamines and nitramines not exceeding pre-defined safety limits (established in literature as well as in this work), can be determined. The maximum tolerable emission can be used as guideline value for the plant operators. Subsequently, the worst-case scenario can be refined as soon as more accurate information on the formation yields becomes available. If emission data for a likely case is available for a particular emitting facility, then it could be used for estimating the influence of the boundaries presented in the worst case (de Koeijer *et al.* 2013).

As part of this study, worst case scenarios (that considers chemistry) on the three capture plants are conducted. Sensitivity analysis is also performed on the uncertain parameters considered in the modelling studies in order to determine the parameters that most influence the fate of the nitrosamines and nitramines.

6.5 Atmospheric chemistry and dispersion modelling

6.5.1 ADMS 5 with its amine chemistry module (CERC 2010, CERC 2012b, CERC 2012a, CERC 2012d, CERC 2012c)

The atmospheric dispersion calculations were performed using the ADMS 5 Gaussian plume air dispersion model and its integrated Amine Chemistry Module (CERC 2012a) A generic amine chemistry scheme (Figure 5.1) based on experimentally evaluated chemistry scheme for MEA by Nielsen *et al.* (2011a) (discussed in chapter 5) has been integrated in ADMS 5 with its dispersion algorithms by its developers. The amine atmospheric chemistry scheme can be described by a set of ordinary differential equations as shown in

Table **5.2**. The system of ordinary differential equation is then solved by providing rate constants as input parameters for each of the reaction steps within the amine chemistry scheme. The amine chemistry module can also take into account if the resulting nitrosamine formed from an emitted amine is photochemically unstable due to fast photolysis in the atmosphere. Such is the case for primary amines that form primary nitrosamines which readily isomerise to their corresponding imine.

NO_x (i.e. NO and NO_2) emissions and background concentrations along with ozone, O_3 background concentrations are also essential model input parameters. ADMS meteorological pre-processor data are used to determine photolysis rates on an hourly basis. The OH radical concentration is determined from the ambient hourly O_3 concentration and the photolysis rate constant for nitrogen dioxide, J_{NO2}, from Eq.6.1. The emission rate of species at source is provided as input together with the amine specific rate constants and the characteristics of the emission source i.e. stack height and diameter, exhaust gas emission temperature and velocity at stack exit, geographic location and meteorology. The user must also specify the parameter, c which is used in calculating the hourly change in the OH radical concentrations and is determined using the following relationship (Eq.6.1) (CERC 2012a):

$$[OH] = c\ x\ [O_3]\ x\ J_{NO2} \tag{6.1}$$

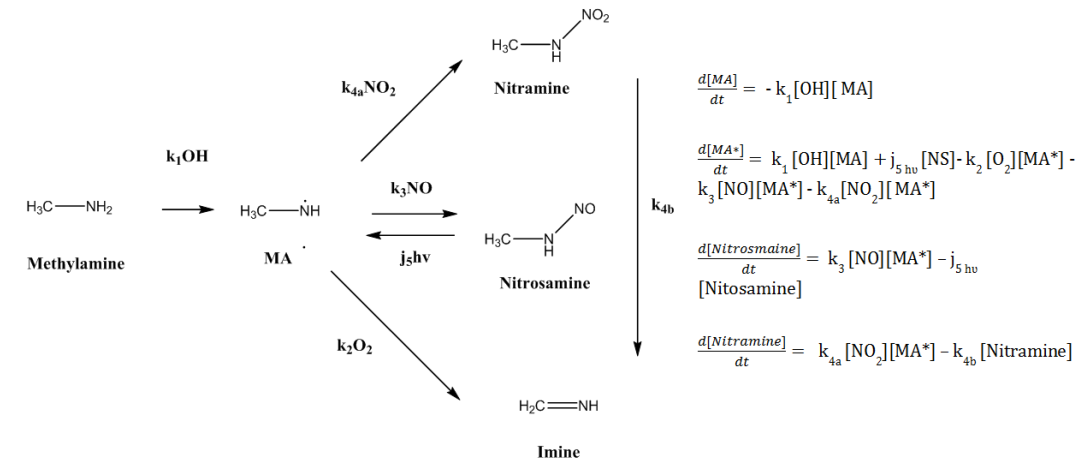
$$\text{where } J_{NO2} = 8x10^{-4} \exp\left(-\frac{10}{K}\right) + 7.4x10^{-6}K \tag{6.2}$$

Here, J_{NO_2} is the annual average photolysis rate of NO_2 (dependent on the solar radiation and latitude), O_3 background concentration and OH radical concentration.

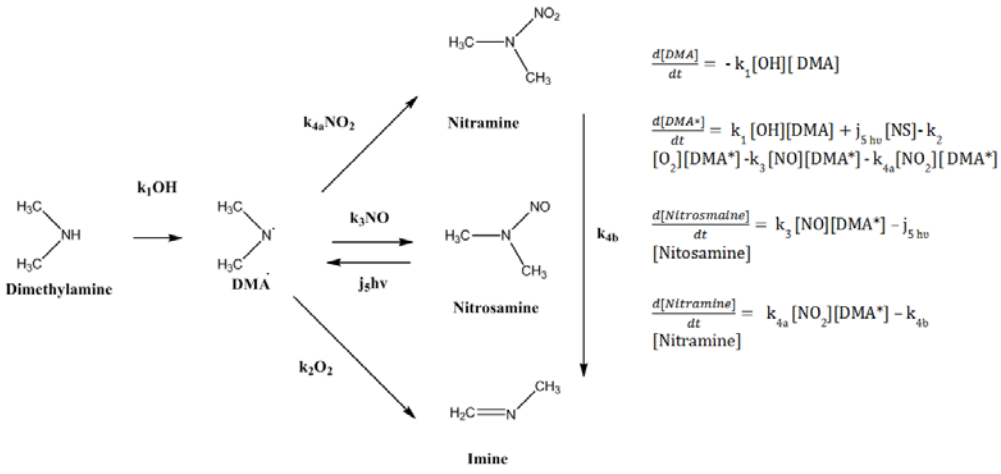
The input rate parameters along with all the other mentioned parameters are then used by the ADMS 5 model in the differential equations. An adaptive time-stepping method is employed for integrating the differential equations (CERC 2012e). However, before that, the standard ADMS dispersion algorithms (as were stated in E.q 3.7 chapter 3) are solved to determine the concentrations of the species of interest as well as the age of the primary pollutants (such as amines) at each receptor point. The process of calculating the dispersion and then the chemistry is carried out for every hour. After each hourly dispersion calculation, the 'age' of the pollutants is calculated by considering the plume travel time. For the chemistry calculations, there needs to be the consideration of timescales. The reaction equations are applied over time, dt, to the background and then to the pollutants from the source. In addition, the dilution and entrainment calculations account for the fact that the pollutants in the plume are diluted as they travel. These last two steps are reiterated for every time step, *t*, until time equals to the pollutant age.

6.5.2 Atmospheric chemistry schemes

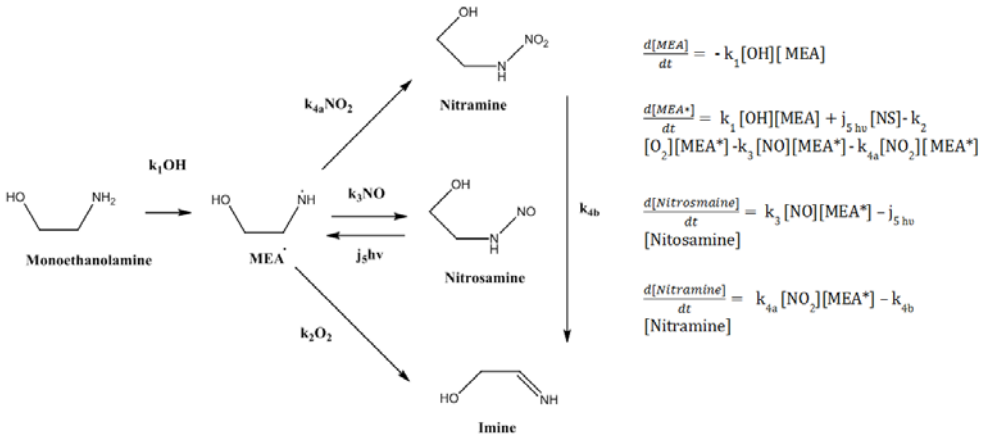
In the last chapter the atmospheric chemistry schemes for MA, DMA and MEA were studied employing quantum chemistry theoretical methods and kinetic modelling to establish the kinetics of the reactions involved (Table 5.6). Below are the schemes represented for MA, DMA and MEA and their corresponding system of ordinary differential equations in Figure 6.1. The established rates are used in solving these ODEs along with the standard ADMS 5 dispersion algorithms.



(a)



(b)

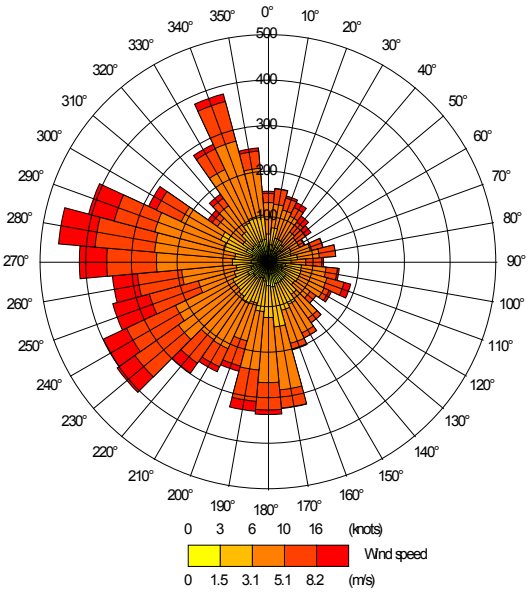


(c)

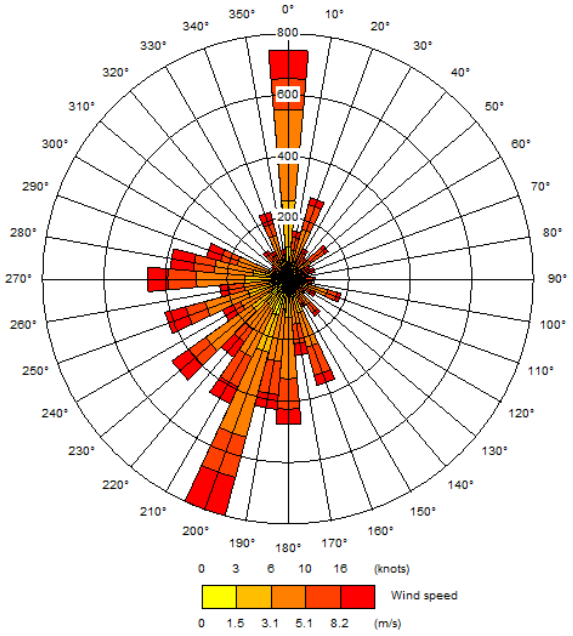
Figure 6.1: Atmospheric chemistry schemes with rate constants, k, describing the kinetics of each of the reaction and the corresponding ordinary differential equations describing the atmospheric chemistry scheme for (a) MA (b) DMA and (c) MEA.

6.5.3 Capture plants

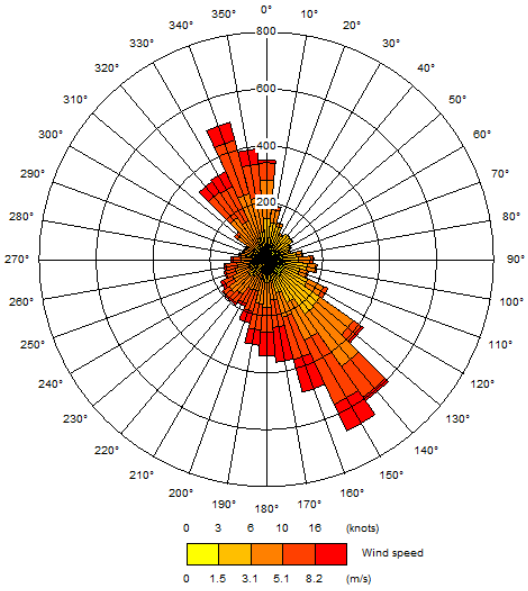
It is assumed that the absorber stack is the emission source of amines since they mainly leak into the atmosphere from here (CERC 2012d, CERC 2012c). Atmospheric chemistry and dispersion modelling for each of the amines mentioned is performed for a particular meteorological year. Meteorological data is taken from the UK Met office and National Oceanic and Atmospheric Administration (NOAA) for the UK sites whereas Norwegian Meteorological Institute (met.no eKlima service) was used for the Mongstad site. The meteorological year modelled for Ferrybridge is 2012, which is the year it started to operate, and the relevant data was obtained from Castleford weather station. The wind rose for Ferrybridge is illustrated in Figure 6.2a. Since Peterhead is yet not functional therefore a test study is performed on the meteorological year 2008 (Figure 6.2b). Data from the Fesland-Bergen weather station for the year 2012 was considered for Mongstad, as it was operational in the year 2012 (Figure 6.2c). The summary of parameters used in the each site is presented in Table 6.2.



(a)



(b)



(c)

Figure 6.2: Wind rose plot for depicting the flow vector (direction towards which the wind was blowing) in m/s for (a) Ferrybridge (2012) (b) Peterhead (2008) and (c) Mongstad (2012).

Table 6.2: Source parameters for each of the emitting facility.

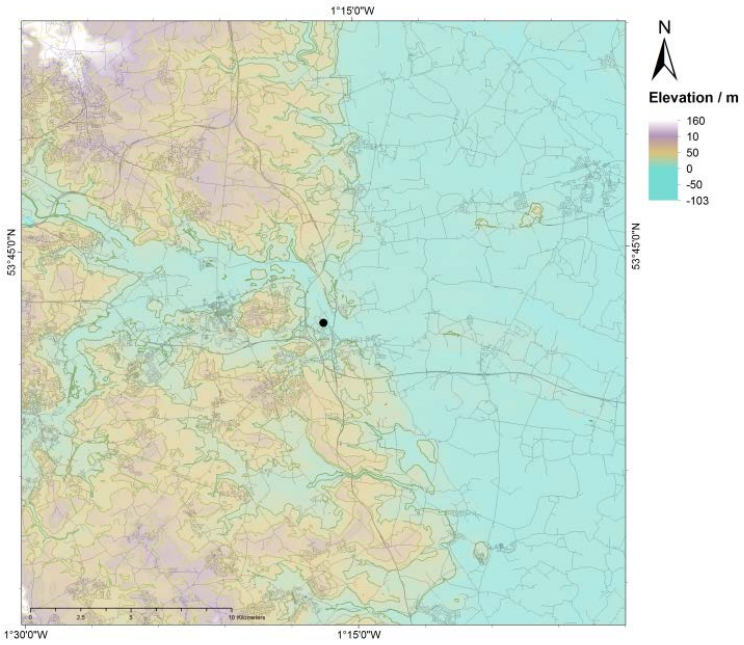
	Stack height (m)	Stack diameter (m)	Stack exit velocity (m/s)	Exhaust as emissions temperature at stack exit (°C)	Volume flow rate (m^3/s) at emission temperature
Ferrybridge	198	9.74	20	90	1490
Peterhead	170	9	26.2	70	1667
Mongstad	65	6.53	20	30	670

The background concentrations of pollutant gases in the vicinity of the plant were used to represent ambient concentrations of pollutants in the atmosphere in the meteorological year of interest. These were obtained from the Department of Environment Food and Rural Affairs (DEFRA) and Norwegian Meteorological Institute met.no (eKlima) shown in Table 6.3.

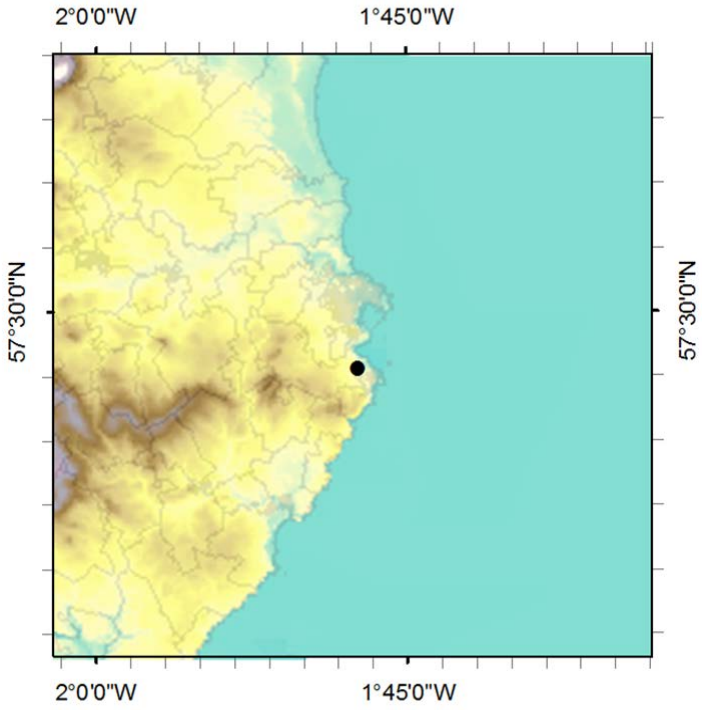
Table 6.3: Background concentrations of pollutant gases around the capture plant for the particular meteorological year studied.

		Ferrybridge 2012	Peterhead 2008	Mongstad 2012
NO_x	µg / m^3	25.1	11.0	20.0
NO_2	µg / m^3	16.2	6.47	15.0
NO	ppb	4.61	2.37	2.60
O_3	µg / m^3	65.0	33.0	63.3
PM10	µg / m^3	16.9	10.5	-
PM2.5	µg / m^3	10.9	7.68	-

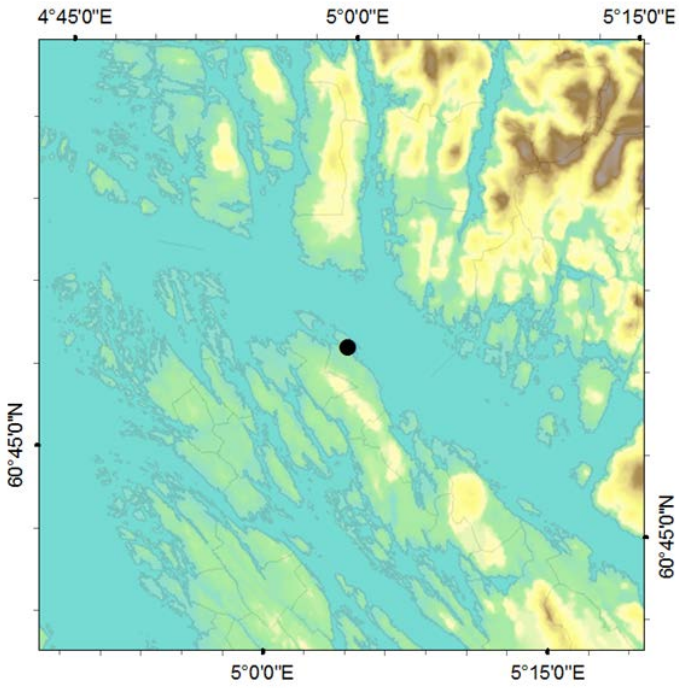
Terrain elevation data for Ferrybride and Peterhead is obtained from the UK OS Profile DTM dataset and from European Statistics (Eurostat) for Mongstad. The terrain features for each of the site are shown in Figure 6.3 along with their geographic location.


1°15'0"W
N
Elevation / m
160
10
50
0
-50
-103
53°45'0"N
53°45'0"N
1°30'0"W
1°15'0"W

(a)


2°0'0"W
1°45'0"W
57°30'0"N
57°30'0"N
2°0'0"W
1°45'0"W

(b)



(c)



(d)

Figure 6.3: Terrain elevation centered on (a) Ferrybridge CCPilot 100+ (b) Peterhead (SSE) (c) Mongstad on a 30 km by 30 km domain and along with the (d) geographical location of each of these sites.

6.5.4 Amine emissions

Emissions of amine and other by-products from the capture facility are in most cases confidential. There are no amine emissions rates reported for Ferrybridge CCPilot100+ due to confidentiality reasons and simply because of the lack of experimental measurements conducted on site. Since Peterhead is yet to function there are no amine emission rates for it as well. Therefore, both for Ferrybridge and Peterhead, the dispersion model simulatons for the amines of interest were performed assuming that 1 g/s of amine was emitted for one meterological year.

However, likely emission rates of amines have been reported from Mongstad (de Koeijer *et al.* 2009, CERC 2012d, CERC 2012c). The emission rates stated by de Koeijer *et al.* (2013) are reported for the generic class of amines such as as primary, secondary and tertairy amines. Only the emissions for MEA are specified. On the other hand, the emission rates conveyed by CERC (2012c) and CERC (2012d) are explicity defined for the specific amine as shown in Table 6.4. Therefore, these are used in its atmospheric chemistry dispersion modelling for one meterological year.

However, one assumption made in this work is that no nitrosamines are emitted from the stack and so the emission rate reported for nitrosamines by CERC (2012c) and CERC (2012d) is not considered in the calculations.

Table 6.4: Calculated emission rates for the individual amine species from the TCM emission data (CERC 2012d, CERC 2012c).

Emitted species	Composition	Emission rate (g/s)
Methylamine	0.1 ppmv	0.082
Dimethylamine	0.05 ppmv	0.060
Monoethanolamine	1.0 ppmv	1.623
Nitroso monoethanolamine	0.25 ppbv	4.92×10^{-4}
Nitramine	0 ppmb	
NO_x		1.79

6.5.5 Worst-case scenario approach to calculate tolerable amine emissions, as given by Karl *et al.* (2011) (with certain modifications)

The results acquired for unity emission, E_{unit}, are used to estimate the maximum tolerable emission of amines, E_{max} (in g/s) (Karl *et al.* 2011). It is assumed that the emissions are constant throughout each day and throughout the year i.e. no time varying factors are applied to the emission rates. The maximum concentration output, $C_{max,out}$, at unity emission is scaled until the critical concentration of the

amine in air (or deposition), C_{crit}, is reached. By doing so, the exceedance factor, e, of the emission source strength is acquired:

$$\mathrm{e} = \left(C_{max,out}/C_{crit}\right) \tag{6.3}$$

If the unity emission (1 g/s) is divided by e, then the amine maximum tolerable emission, E_{max}, from the PCCC facility with respect to the C_{crit} in air, can be obtained:

$$E_{max} = E_{unit} * \frac{C_{crit}}{C_{max,out}} \tag{6.4}$$

The E_{max} for the worst case scenario is calculated, as follows:

- C_{crit} in air for nitrosamines and nitramines is around 0.3 ng/m^3 (Låg *et al.* 2011).

-The percentage transformation of the amine to the corresponding nitrosamine and nitramine is calculated at a specific point as follows:

$$\%\ \text{transformation of amine to NA + NS} = \frac{[NS]+[NA]}{[Amine]} * 100 \tag{6.5}$$

Where [NS]+[NA] is the maximum total concentration of NS and NA in the study domain and [Amine] is the amine concentration at the particular point in the domain where the maximum sum of NS and NA occurs.

-The C_{crit} in air for the emitted amine is determined as shown:

$$C_{crit} = \left(\frac{C_{crit}\ NS + NA}{\%\ Transformation} * 100\right) \tag{6.6}$$

- C_{crit} determined and C_{max} of amine at unity emission can then be used to calculate the maximum tolerable emission of the amine, E_{max}, for the worst case scenario as follows:

$$E_{max} = E_{unit} * \frac{C_{crit}}{C_{max,out}} = E_{unit} * \frac{\left(\frac{C_{crit}\ NS+NA}{\%\ Transformation} * 100\right)}{C_{max} Amine} \tag{6.7}$$

Since the above approach considered unity emissions of amines, therefore, to consider likely amine emissions, the E_{unit} is substituted by the likely amine emission rate and the $C_{max,out}$ is for the likely emission amine rate.

A flow scheme of the worst case study is illustrated in Figure 6.4 to show the how the tolerable emission of amine is determined. The process involves five stages similar to those used by Karl *et al.* (2011):

1. Local meteorological and emission inputs.
2. Specification of critical levels of amine (deduced from the critical levels of nitrosamines in air) in air.
3. Atmospheric dispersion calculations.
4. Maximum atmospheric concentration along with deposition fluxes in every grid cell.
5. Determination of the tolerable emission of amine.

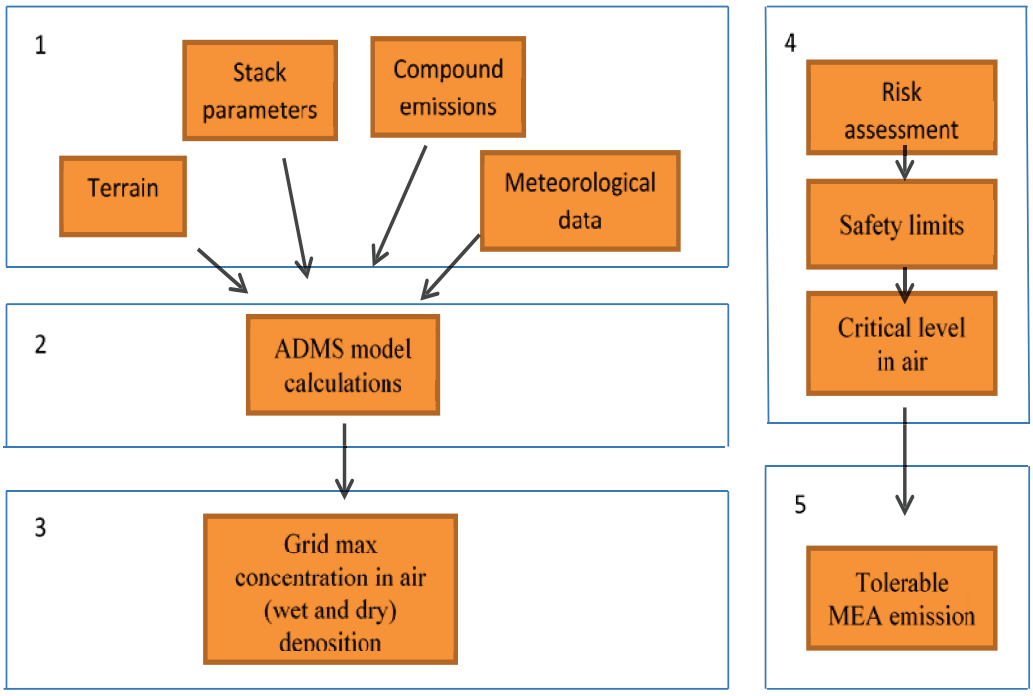


Figure 6.4: Flow scheme for the worst case study (adapted from Karl *et al.* (2011)).

6.5.5.1 Maximum tolerable amine emissions

The results are shown in Table 6.5, both from the likely emission case and the unity emission cases which are used to calculate the maximum tolerable emission rates for a worst case scenairo such that the resulting nitrosamine and nitramines

concentration from all the three amines are below the thershold limit and giving an acceptable risk.

NO_x emissions from the stack were also considered since the formation of the nitrosamines and nitramines depends on the reactions with NO and NO_2. NO_x emission rate for Ferrybridge was provided by the pilot plant operators and in the absence of data the same value was assumed for Peterhead. For Mongstad the value reported by CERC (2012c) and CERC (2012d) was considered. The NO_x emissions rate for the coal fired Ferrybridge plant is very large in comparison to that reported for the gas-fired Mongstad. Genereally, NO_X emissions are dependent on the type of fuel used, however, in the absence of detailed information, it can only be speculated that the large value for the Ferrybridge provided might have corresponded to a certain pilot study conducted on the plant where high NO_x emissions were considered. A value of 0.49 % of NO_2 in NO_x emissions is considered in all the calculation for Ferrybridge and Peterhead, whereas, 10 % for Mongstad based on CERC (2012c) and CERC (2012d) reported value (Table 6.5).

Table 6.5 lists the maximum of the long term averaged concentration of the emitted amine (C_{max},) at unity emission in the Ferrybridge and Peterhead study domain whereas at likely emission at Mongstad. The maximum sum of the nitrosamines and nitramines from each of the amine and the amine concentration at that particular point in the grid are shown. The percentage tranformation of the amine into its corresponding nitrosamine and nitramine is calculated as well. These results are used in establishing the maximum tolerable amine emission rates (E_{max}) for the worst case study for each of the three sites, Ferrybridge, Peterhead and Mongstad. The same method as Karl *et al.* (2011) is followed in evaluating the maximum tolerable emissions, however, instead of using fixed formation yields (FFYs), the determined percentage transformations of the parent amine into its corresponding NS and NA, obtained from the model results (Table 6.5) is considered.

Table 6.5: Maximum amine concentrations (C_{max}), maximum sum NS and NA concentrations and the amine concentration, percentage transformation of the parent amine to NS and NA at the unity emissions for Ferrybridge and Peterhead but at likely emissions at Mongstad and their corresponding maximum tolerable amine emission rate estimates (E_{max}).

	Emitted species	[Amine] (ng m^{-3})	Sum of NS + NA (ng m^{-3})	Transformation of amine to NS+NA (%)	C_{max} (ng m^{-3})	E_{max} (g s^{-1})
Ferrybridge	MA	0.84	7.82×10^{-4}	0.09	2.58	125
	DMA	0.91	7.82×10^{-4}	0.09	2.52	138
	MEA	1.36	4.85×10^{-3}	0.36	4.03	20.8
	NO_x					5.96×10^{2}
Peterhead	MA	1.51	1.50×10^{-2}	0.99	5.52	5.49
	DMA	2.15	5.69×10^{-3}	0.26	5.55	20.5
	MEA	1.66	3.45×10^{-3}	0.21	5.39	26.8
	NO_x					5.96×10^{2}
Mongstad	MA	3.58	7.76×10^{-4}	0.02	5.05	22.5
	DMA	2.85	2.73×10^{-1}	9.58	3.58	2.88
	MEA	78.0	5.12×10^{-2}	0.07	97.1	7.67
	NO_x					1.79

6.5.5.2 IDM and IDM-FFY modelling

In addition to the chemical transport modelling study, an Inert Dispersion Model (IDM) calculation was also performed in ADMS 5 for comparison purposes for each of the sites. FFYs from experimental studies (Nielsen *et al.* 2011a) have been applied to the IDM results to calculate the nitrosamines and nitramines concentrations. This modelling is referred to as the Inert Dispersion Model - Fixed Formation Yields (IDM-FFY) in this work.

6.5.6 Wet and dry deposition

The released amines emissions from the PCCC plant into the atmosphere and the resulting degradation products undergo wet and dry deposition into aquatic environments and soil. ADMS 5 has a dry deposition model which accounts for spatially varying deposition velocity by assuming that dry deposition is proportional to near-surface concentration as shown:

$$F_{dry} = v_d C(x, y, 0) \tag{6.8}$$

Where (F_{dry}) is the rate of dry deposition per unit area per unit time, v_d is the deposition velocity and C represents the atmospheric concentration at ground level. On the other hand, the wet deposition model uses washout coefficient (Λ) method where irreversible uptake is assumed. The total rate of wet deposition per unit plane area per interval of time (F_{wet}) is determined by employing integration over a vertical column of air as shown:

$$F_{wet} = \int_0^{\infty} \Lambda C \, dz \tag{6.9}$$

Hence, the strength of the plume decreases following wet deposition with downwind distance.

In order to be able to compare to the safety limits proposed by various scientists and regulatory authorities, the estimated wet deposition flux (F_{Wet}) by the model is converted to concentration estimates in water (C_{wet}) for comparison with the safety limit for drinking water and aquatic species (in ng/L for each of the chemical species of interest for which the values were stated in Table 6.1) according to the following relationship by Karl *et al.* (2011):

$$C_{wet} = \frac{F_{wet}}{P \, x \, 10^{-6}} \tag{6.10}$$

Where F_{Wet} is the deposition flux calculated by the model in µg/m^2/s, 10^{-6} is the conversion factor from µg to ng, P is the the average precipitation amount, for Ferrybridge, Peterhead and Mongstad (809, 1597 and 1990 mm/year) for their respective meteorological years (2012, 2008 and 2012) considered in this study.

6.5.7 Deterministic Risk assessment

The resulting concentrations of nitrosamines and nitramines from all the three amines from the maximum tolerable emissions scenario modelled at each site are then compared against the safety limits (the maximum concentration of these chemicals in air and in wet and dry deposition which won't be harmful) to access the

risk they pose. If the concentrations exceed the critical levels, then the compound is expected to have an adverse impact on the human health and environment.

6.6 Results and discussion

6.6.1 Atmospheric amine chemical transformation and dispersion calculations

6.6.1.1 Long term average concentrations

In this work, the atmospheric chemistry of MA, DMA and MEA is introduced in ADMS 5 by the rate constants determined in this study (Table 5.6). The model is used to simulate the yearly average concentrations for the amines of interest at the emission rates calculated (Table 6.5). The maximum long term average concentrations of the target amines and their corresponding nitrosamine and nitramine are listed in Table 6.6. Results are in annual average values which are used to compare with the guideline values.

Table 6.6: Maximum long-term average air concentrations of amines, nitrosamines and nitramines for the worst case scenario modelled for each site and compared against those calculated using FFYs, where A represents Amine, NS is nitrosamine and NA is nitramine.

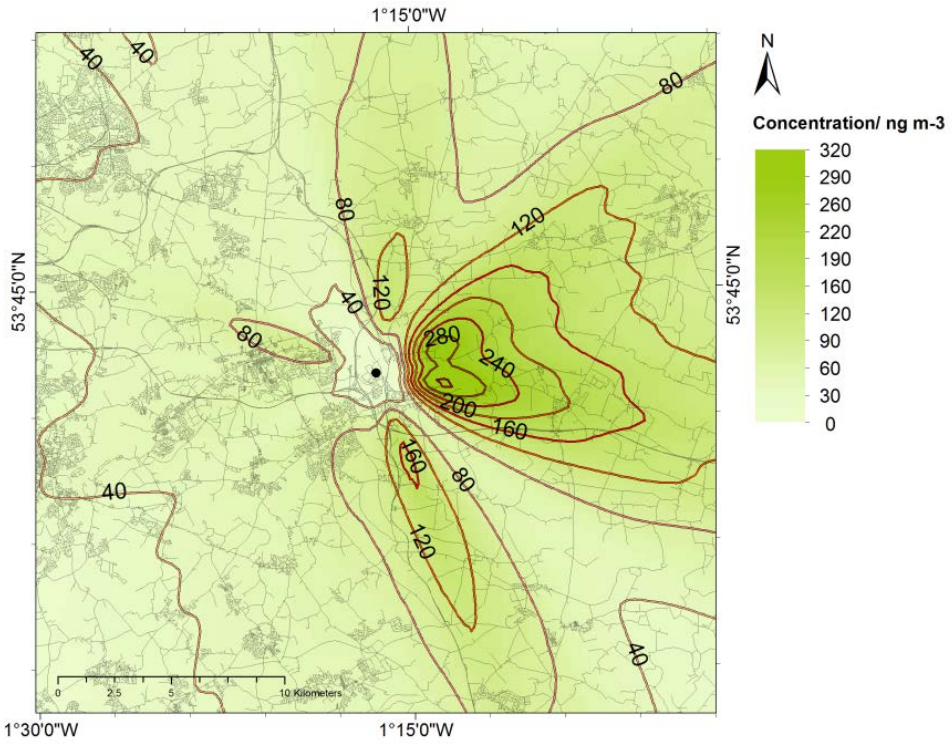
Atmospheric concentrations		[A] / ng m^{-3}		[NS] / ng m^{-3}	[NA] / ng m^{-3}	[NS+NA] (ng/m^3)	Using FFYs (ng/m^3
Ferrybridge	MA	323	(327)	0	9.77×10^{-2}		
	DMA	348	(361)	2.38×10^{-2}	1.05×10^{-1}		
	MEA	51.6	(54.4)	9.87×10^{-3}	5.87×10^{-2}	0.29	17.4
Peterhead	MA	17.8	(18.0)	0	6.53×10^{-2}		
	DMA	67.0	(67.3)	6.62×10^{-2}	5.54×10^{-2}	0.28	3.68
	MEA	83.5	(88.1)	2.95×10^{-2}	6.54×10^{-2}		
Mongstad	MA	1.64×10^{3}	(1.67×10^{3})	0	1.46×10^{-1}		
	DMA	20.6	(21.4)	4.83×10^{-3}	1.92×10^{-2}	0.34	31.6
	MEA	547	(571)	3.28×10^{-2}	1.31×10^{-1}		

N.B Concentrations shown in brackets from Inert Dispersion modelling (IDM) where chemistry is not considered.

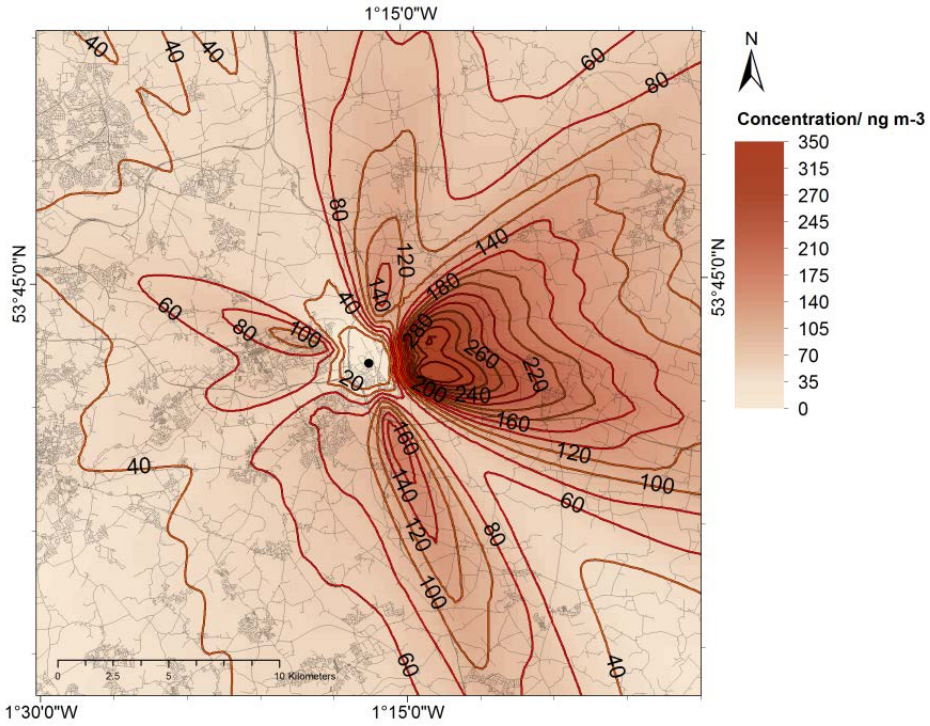
Contour maps illustrating the annual average concentrations of the amine emissions and the total NS and NA from all the three amines (MA, DMA and MEA) for the modelled meteorological year specific to each site, over an area of 900 km^2 centred on the emitting source for a grid resolution of 300 m × 300 m are shown in Figure

6.5, Figure 6.6 and Figure 6.7. For all amines, results show that the highest concentrations of the emitted species are found within 2-3 km of the emission source owing to the applied Gaussian dispersion. This also causes the concentrations to decrease with increasing distance from the PCCC facility. However, the opposite is observed for the total NS and NA concentrations, since they form as the amine reacts with the OH radicals to form the alkyl amino radical to react with NO and NO_2 in the atmosphere (Figure 6.5d, Figure 6.6d and Figure 6.7d). Terrain and the meteorological conditions modelled influence the pattern of dispersion of these species in the atmosphere from the emitting source.

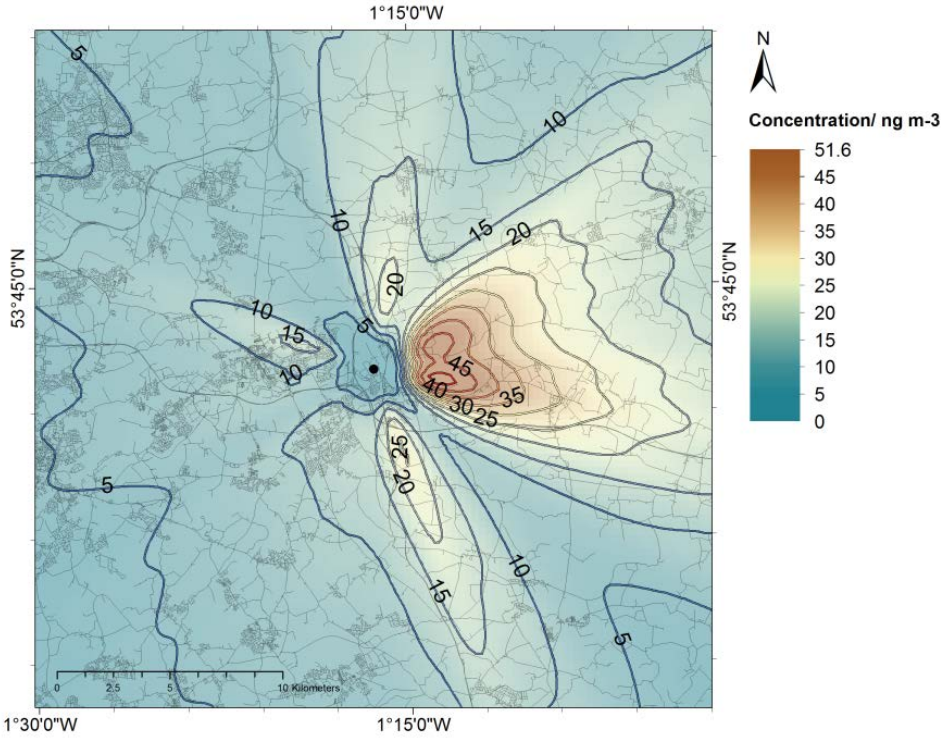
From Table 6.6, it can be seen that the calculated maximum long term calculated average concentrations for the sum of nitrosamine and nitramine for the worst case modelled on Ferrybridge for 2012 is 0.29 ng m^{-3}, which is lower than the critical concentration of 0.3 ng/m^3 by 3 %. For Peterhead it is 6 % lower whereas for Mongstad it exceeds by 13 %. Hence, it is suggested that the risk posed by the resulting degradation products is acceptable for Ferrybridge and Peterhead but not so much for Mongstad.



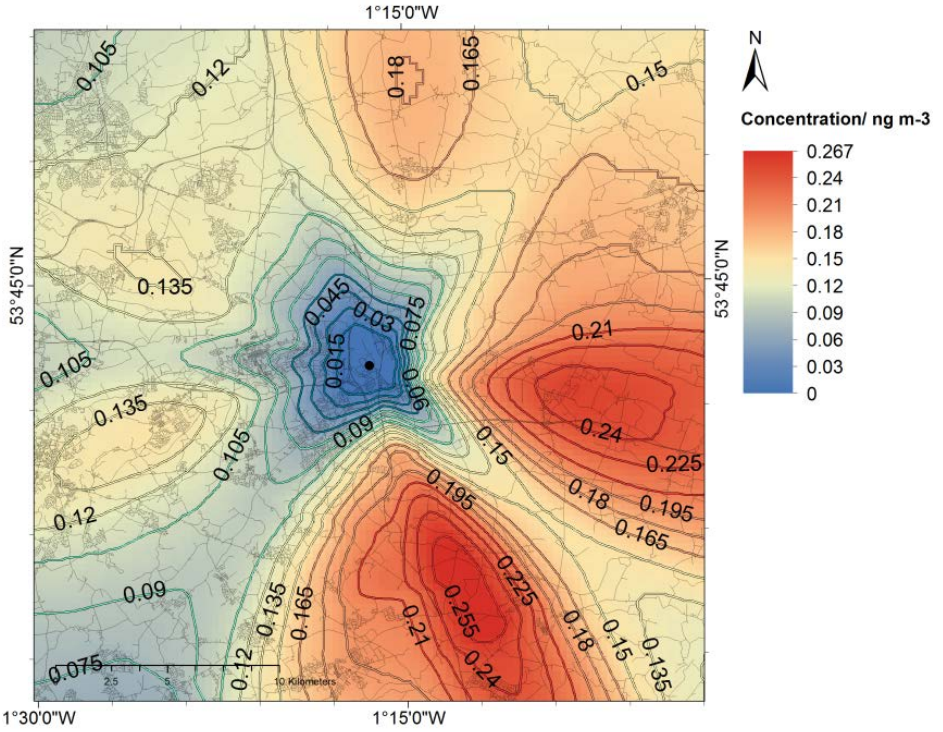
(a)


1°15'0"W
53°45'0"N
1°30'0"W
1°15'0"W
N
Concentration/ ng m-3
350
315
270
245
210
175
140
105
70
35
0
0
2.5
5
10 Kilometers

(b)

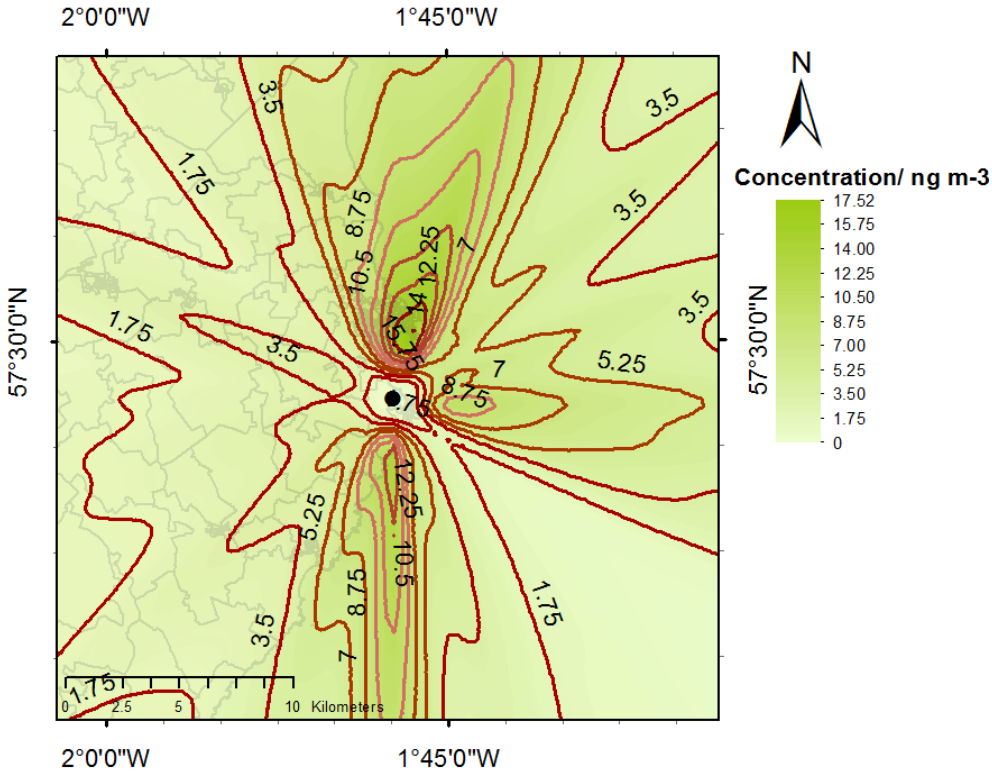

1°15'0"W
53°45'0"N
1°30'0"W
1°15'0"W
N
Concentration/ ng m-3
51.6
45
40
35
30
25
20
15
10
5
0
0
2.5
5
10 Kilometers

(c)

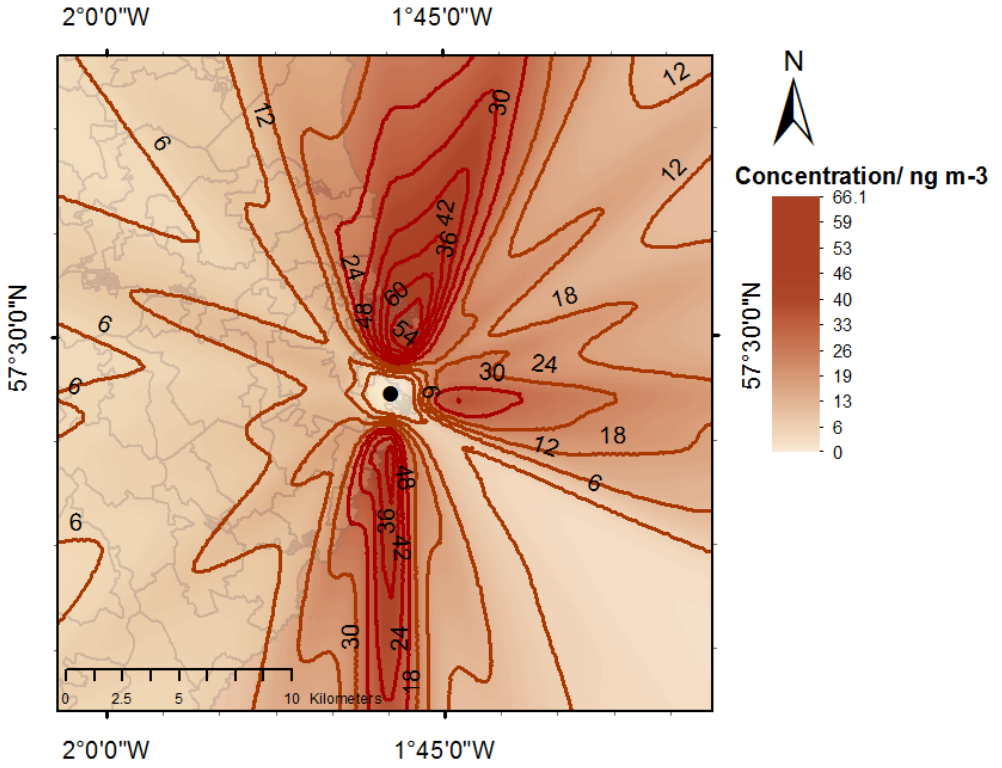


(d)

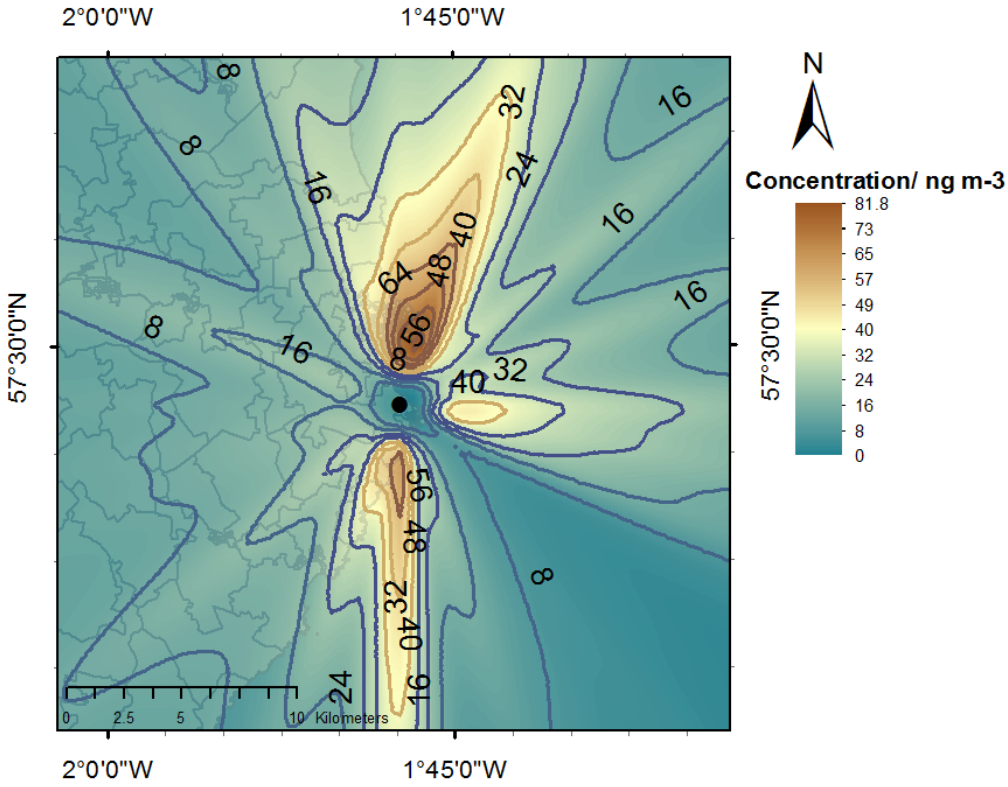
Figure 6.5: Contoured distributions of maximum annual concentration of amines in air for the worst case scenario in 2012: (a) MA (b) DMA (c) MEA and (d) the total NS and NA (ng/m^3) resulting from MA, DMA and MEA emissions for Ferrybridge.



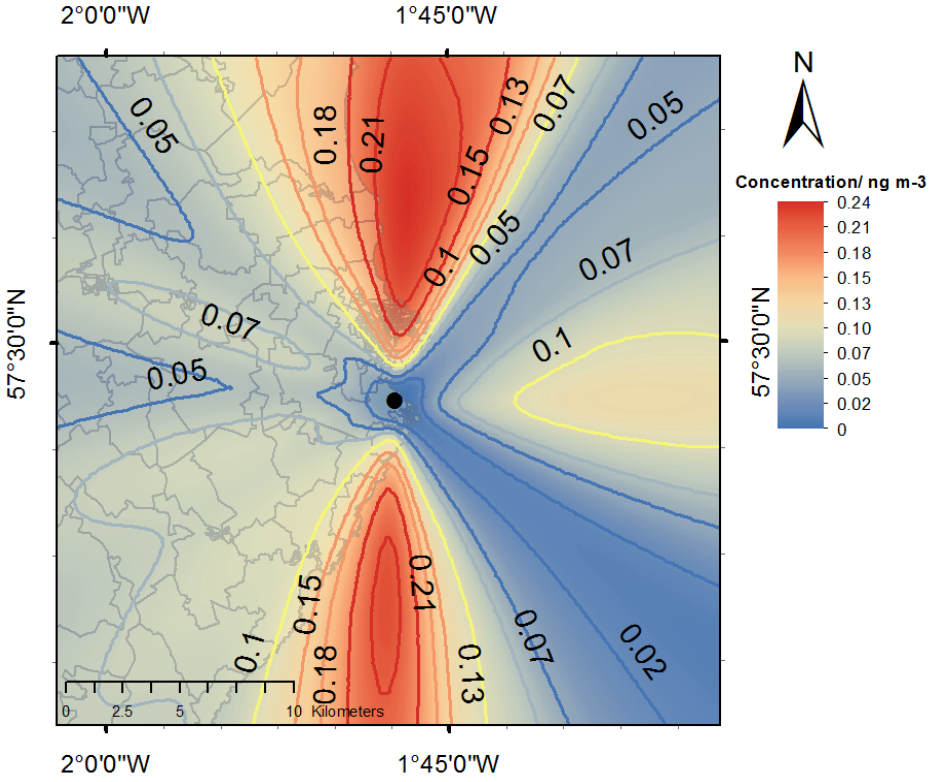
(a)


2°0'0"W
1°45'0"W
57°30'0"N
N
Concentration/ ng m-3
66.1
59
53
46
40
33
26
19
13
6
0
0
2.5
5
10 Kilometers

(b)

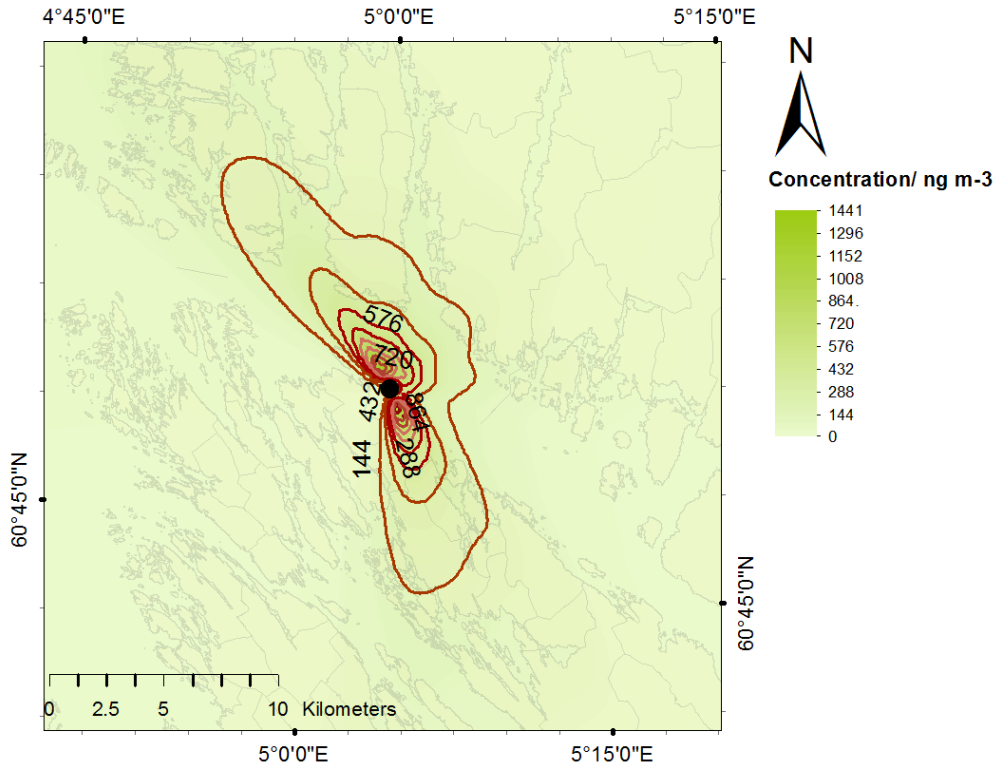

2°0'0"W
1°45'0"W
57°30'0"N
N
Concentration/ ng m-3
81.8
73
65
57
49
40
32
24
16
8
0
0
2.5
5
10 Kilometers

(c)

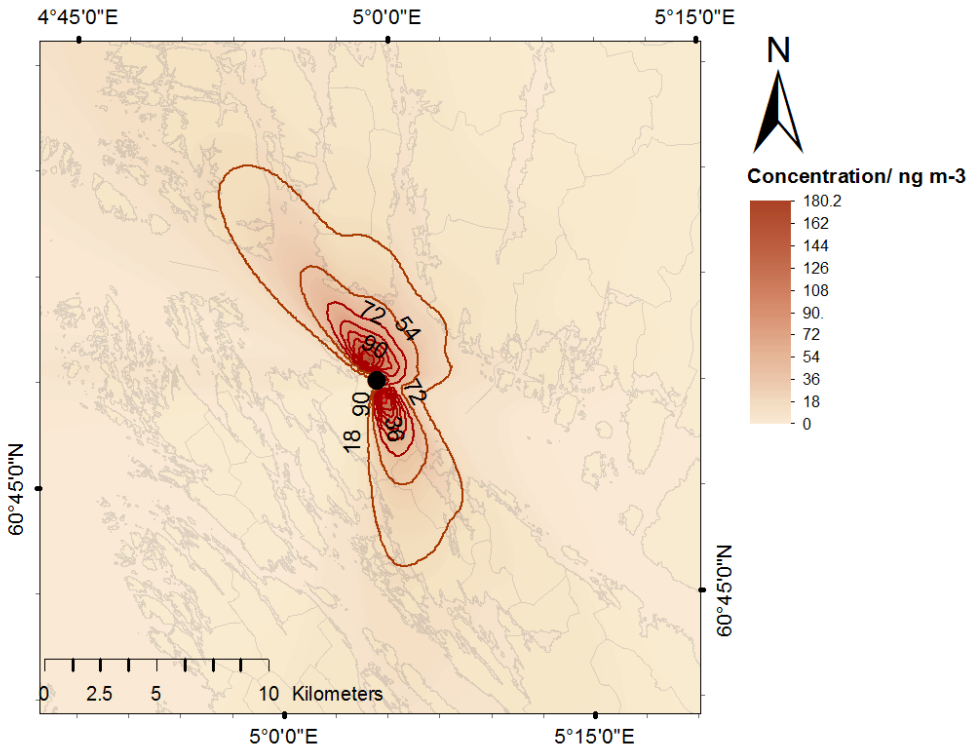


(d)

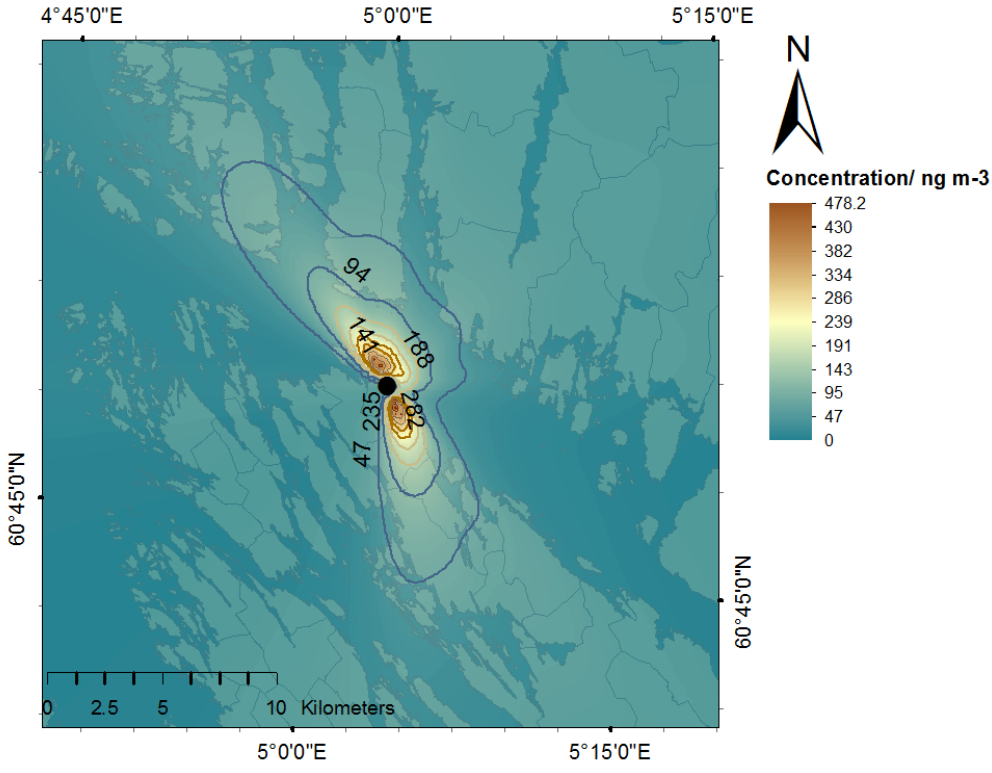
Figure 6.6: Contoured distributions of maximum annual concentration of amines in air for the worst case scenario in 2008: (a) MA (b) DMA (c) MEA and (d) the total NS and NA (ng/m^3) resulting from MA, DMA and MEA emissions for Peterhead.



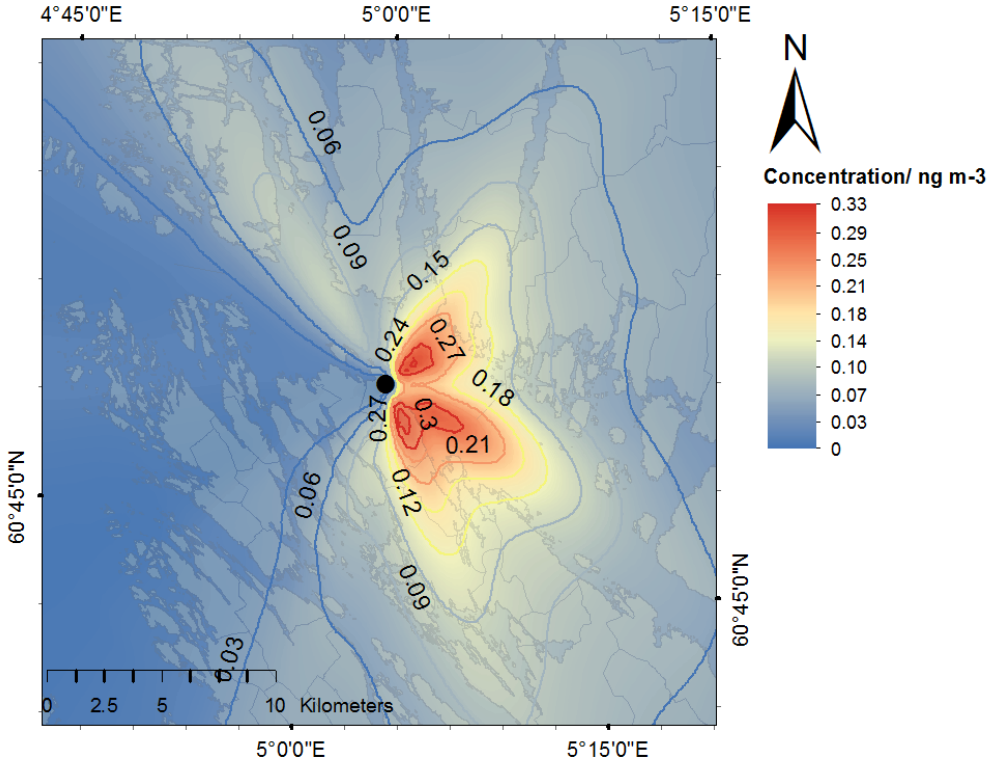
(a)


4°45'0"E
5°0'0"E
5°15'0"E
60°45'0"N
N
Concentration/ ng m-3
180.2
162
144
126
108
90.
72
54
36
18
0
72
54
90
72
90
18
0
2.5
5
10 Kilometers

(b)


4°45'0"E
5°0'0"E
5°15'0"E
60°45'0"N
N
Concentration/ ng m-3
478.2
430
382
334
286
239
191
143
95
47
0
94
141
188
47
235
282
0
2.5
5
10 Kilometers

(c)



(d)

Figure 6.7: Contoured distributions of maximum annual concentration of amines in air for the worst case scenario in 2012: (a) MA (b) DMA (c) MEA and (d) the total NS and NA (ng/m^3) resulting from MA, DMA and MEA emissions for Mongstad.

Percentage chemical transformation of amine to NS and NA

From Table 6.6, it can be realised that for Ferrybridge, the 0.29 ng m^{-3} of nitrosamines (NS) and nitramines (NA) constitutes of 11 % of NS and 89 % NA which are formed from the three parent amines that are MA, DMA and MEA (Figure 6.8). The 11% of NS comes from 29 % of MEA and 71 % DMA, whereas, the 89 % of NA is from 22 % of MEA, 40% of DMA and 37% of MA.

With respect to Peterhead, the 0.28 ng m^{-3} of NS and NA constitutes of 34 % of NS and 66 % NA formed from MA, DMA and MEA (Figure 6.9). The 34% NS comes from 31 % of MEA and 69 % DMA, whereas, the 66 % of NA comes from 35 % MEA, 30% of DMA and 35% of MA.

Finally for Mongstad, the 0.34 ng m^{-3} of NS and NA constitutes of 11 % of NS and 89 % NA formed from MA, DMA and MEA (Figure 6.10). The 11% NS is from 87 % of MEA and 13 % of DMA, whereas, the 89 % of NA comes from 44 % of MEA, 6 % of DMA and 49 % of MA.

Results show that most of the NS comes from MEA and DMA and not from MA since MA produces a primary NS which is unstable and undergoes dissociation to form its corresponding imine. It can also be seen that a much higher percentage formation exists for NA in comparison to NS. This is due to the fact that NS undergoes photolysis in the presence of sunlight; hence, it decreases in its concentration.

In contrast to NS which is photochemically-labile, NA is more stable as does not undergo photolysis in UV light but rather undergoes thermal decay to its corresponding imine. Therefore, NA exists in the atmosphere for longer in comparison to NS.

There is obviously a variation in the contribution from the parent amines to the formation of NS and NA for each emitting facility i.e. Ferrybridge, Peterhead and Mongstad. There are various factors that can play a role in influencing the production of NS and NA from the parent amines. These factors can range from different meteorological conditions considered to background NO_x and O_3 concentrations to terrain features to stack characteristics etc., considered for a particular modelling study and emitting facility.

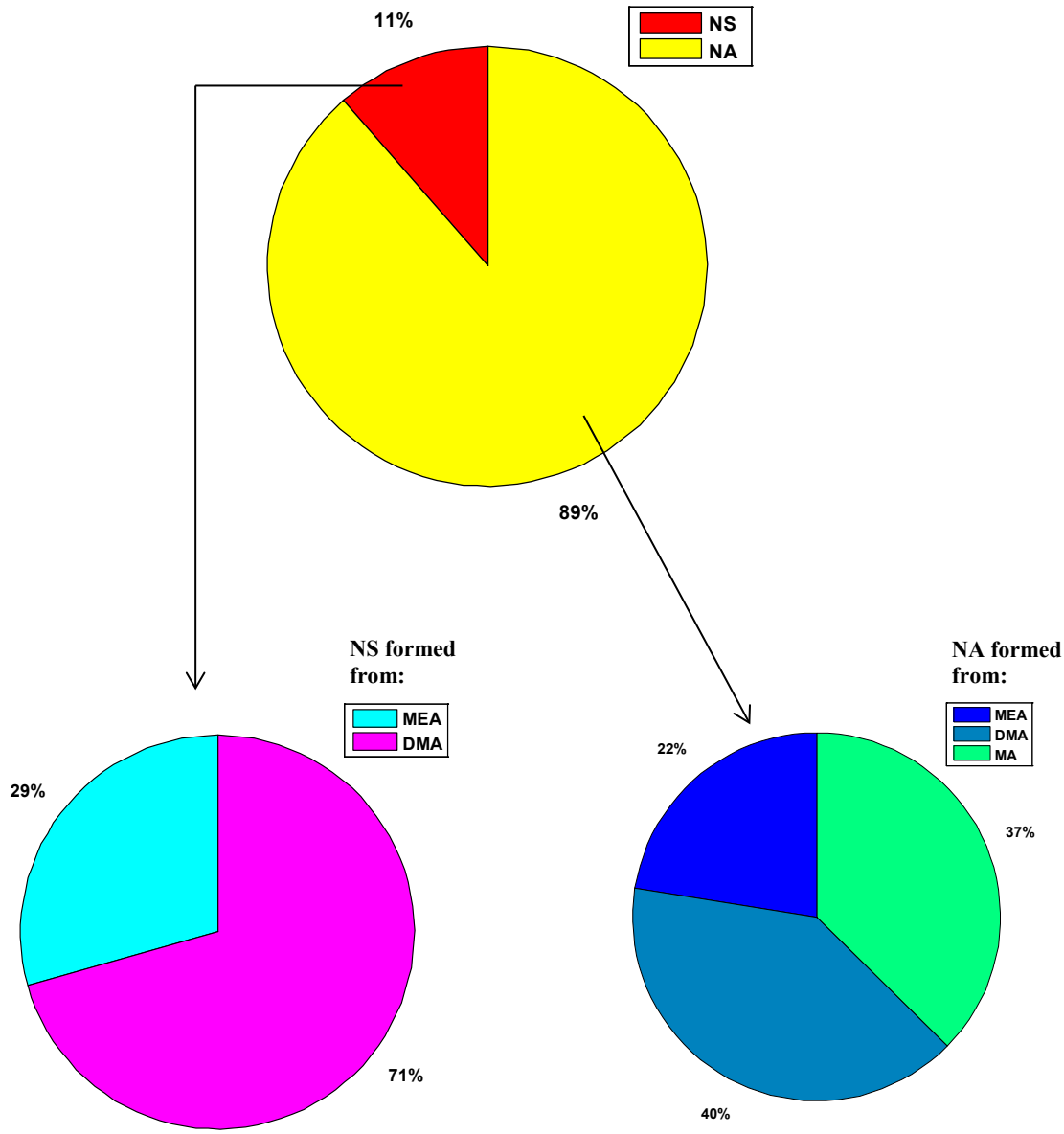


Figure 6.8: Pie charts showing the maximum contribution to NS and NA from the three amines MA, DMA and MEA for the worst case scenario modelled at Ferrybridge.

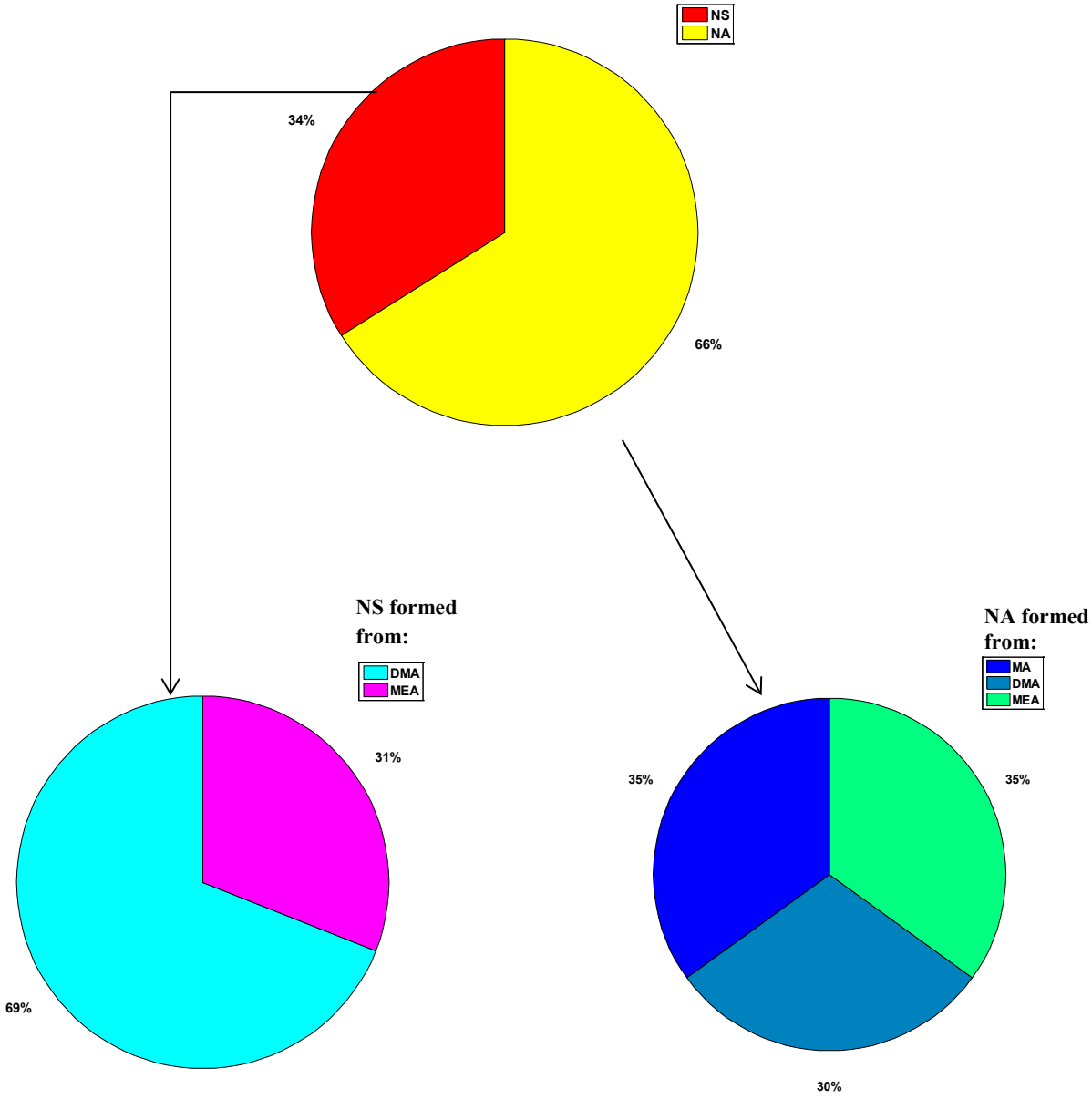


Figure 6.9: Pie charts showing the maximum contribution to NS and NA from the three amines MA, DMA and MEA for the worst case scenario modelled at Peterhead.

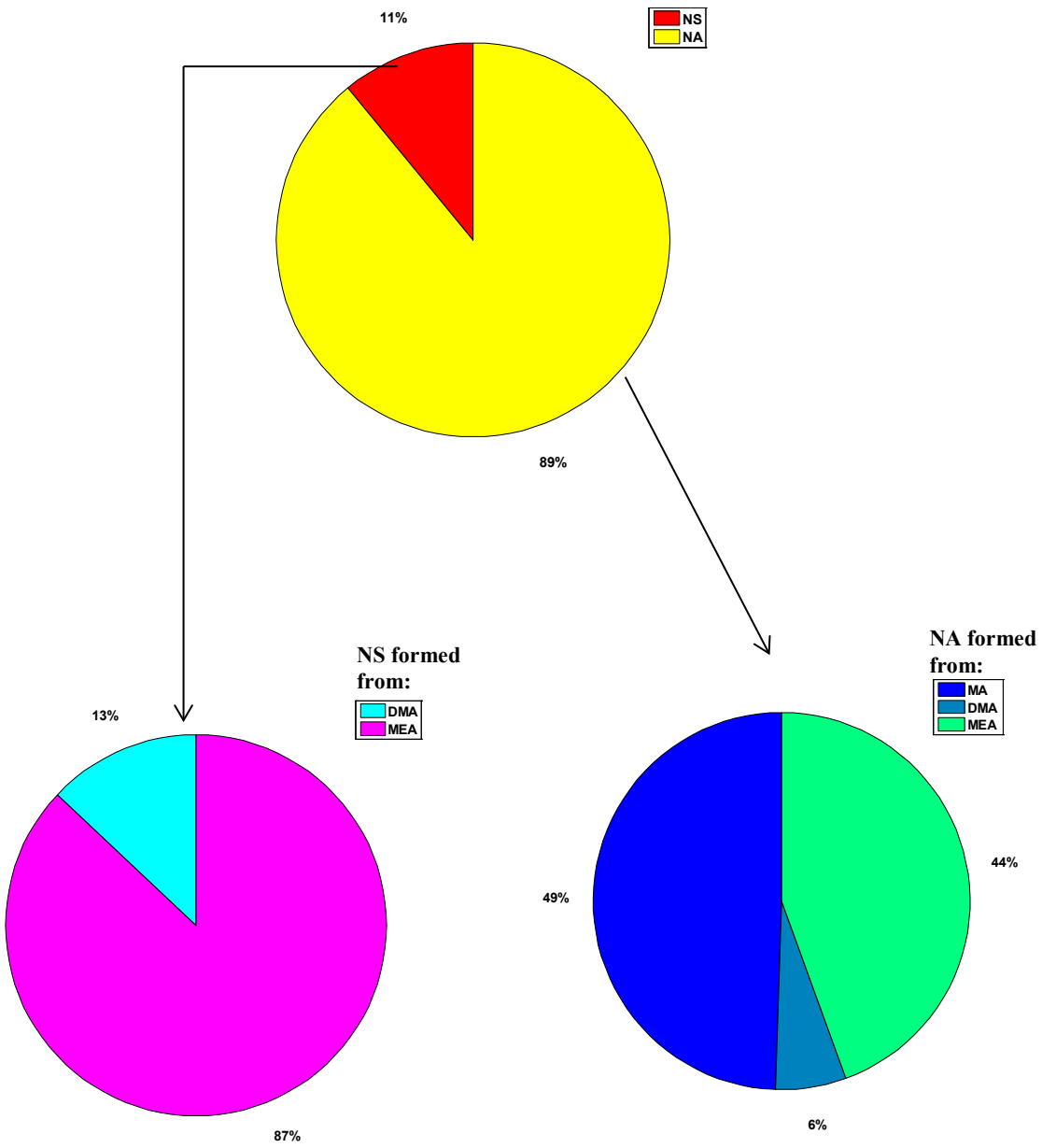


Figure 6.10: Pie charts showing the maximum contribution to NS and NA from the three amines MA, DMA and MEA for the worst case scenario modelled at Mongstad.

Comparison with IDM modelling

In contrast to the above results, amine concentrations from the inert dispersion model implementation in ADMS 5 were modelled to compare against the results from reactive dispersion for the influence of dispersion on chemistry (and vice versa) (Table 6.6). This is due to the IDM approach not considering chemistry which means the emitted amines are only dispersed. It was observed that for the worst case scenario on Ferrybridge, the resulting amine concentrations were 1, 4 and 5 % higher than when both chemistry and dispersion are modelled for MA, DMA and MEA. In the case of Peterhead, the resulting amine concentrations were 1, 1 and 5 % higher

whereas for Mongstad, the resulting amine concentrations were 2, 4 and 4 % higher than reactive dispersion estimates.

These values are still within the same order of magnitude. This strongly supports the phenomenon that dispersion processes reduce the concentrations of the reactive species a lot faster than the atmospheric chemical transformation processes. This is due to the dependency of the reaction coefficients on the parent amine concentration, influencing chemical transformation.

It is observed from the results that the IDM approach seems to always serve as a worst case upper boundary of expected concentration for the amines of interest. It only considers the amine emission without taking into account the detailed atmospheric chemisty. As a consequence, the estimated concentration of the resulting NS and NA, which pose a substantial health risk, are not evaluated acurately. It is indeed vital to obtain reliable concentrations of the resulting NS and NA within the area affected by the amine emissions around a facility to establish a realistic understanding of the human health risk they may pose.

IDM –FFY approach

An IDM-FFY approach was also implemented to predict the maximum ambient air concentration of NS and NA (using formation yields experimentally determined by Nielsen *et al.* (2011a)). Here for a worst case, a steady state of 1 % maximum NS formation from each of the three amines is considered. Additionally, for NA it is assumed that 0.4, 2.5 and 0.3 % of it is formed from MA, DMA and MEA (de Koeijer *et al.* 2013).

Resulting concentrations from employing this approach were seen to be a factor of 60 (Ferrybridge), 13 (Peterhead) and 94 (Mongstad) times higher than the estimates considering the chemical transport modelling as shown in Figure 6.11. The variation in the calculated factors between the different sites is influenced by many factors due to similar reasons as explained earlier. Thus, the chemical transport modelling preditcs lower NS and NA concentrations, although these are still within the same order of magnitude.

IDM-FFY has been one of the early methods employed for estimating NS and NA concentration using experimentally determined fixed formation yields (FFY) from the parent amine. However, when formation by chemistry is considered i.e. using

FFY, then the spatial distribution of the concentrations of the reaction products will have the same dispersion pattern as the parent amine. As a consequence, the highest impact of air concentrations will always be near the plant, which is not a realistic representation of the change in their concentration with increasing distance from the plant. Another limitation is that the IDM-FFY method depends on experimentally derived values which are sparse.

Therefore, the methodology developed in this work allows to combine the estimation of reliable reaction rates derived from quantum chemistry and kinetic modelling (as the theoretical values are within experimental accuracy as dicussed in chapter 5) with chemical transport modelling. This allows to consider the entire atmospheric fate of the involved amines including their growth and decay in a given study area. This results in more accurate estimation of amine and amine degradation product concentrations over time and space. The methodology can be applied to any amines used in CO_2 capture as it is independent from experimental parameters. It is expected that this approach can also provide a valuable input in studies assessing the environmental and human health risks associated with amine emissions from any PCCC facility irrespective of its geographic location and size.

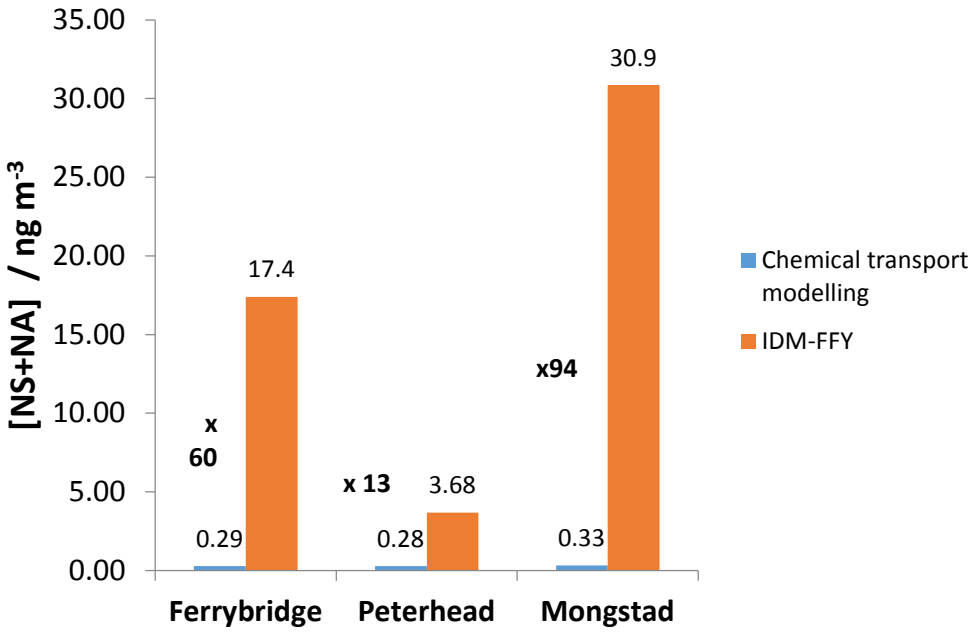
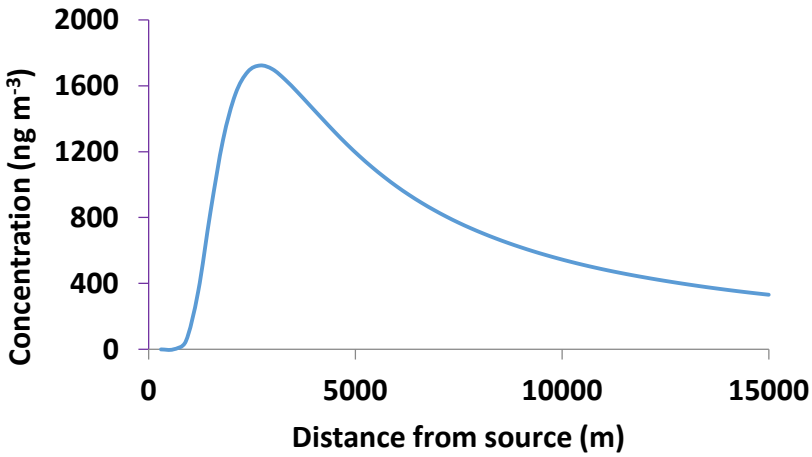


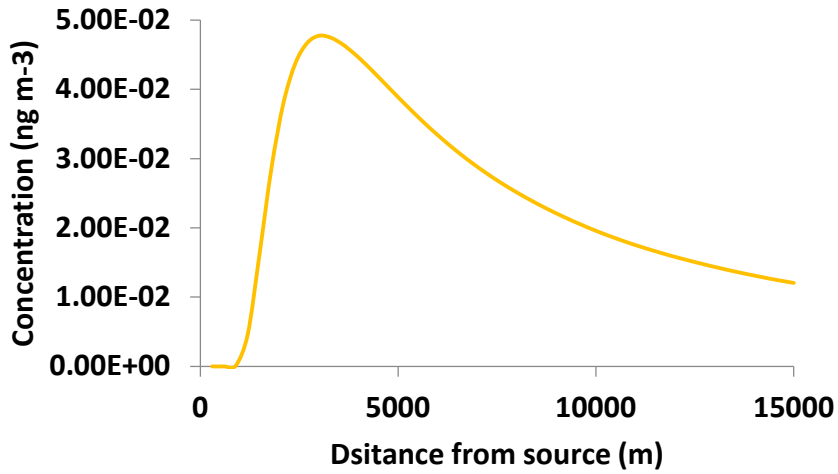
Figure 6.11: Bar chart showing the maximum annual concentration of NS and NA (ng/m^3) from all the three amines in air for the worst case scenario both from the chemical transport modelling and IDM-FFY approach for (a) Ferrybridge for 2012 (b) Peterhead for 2008 and (c) Mongstad for 2012.

6.6.1.2 Short term average MEA concentration for the worst-case scenario on Ferrybridge

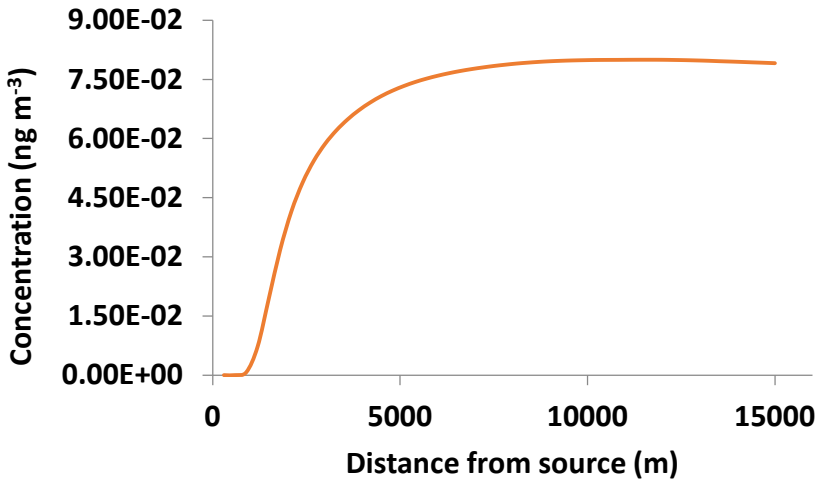
Since the long term simulations considered a period of a whole year, short term hourly average concentrations for MEA and its corresponding nitrosamines and nitramines were also calculated for the worst case scenario at Ferrybridge (for the first 24 hours of 2012 meteorological data). For illustrative purposes, results for the 15th hour on the 1st Jan 2012 are shown in Figure 6.12. The results suggest that the concentration of the gas phase amine rises initially but then reduces monotonically and exponentially, demonstrating that the loss-only process is influenced by the amine species. The concentration of nitrosamine grows sufficiently as the amine concentration increases, but then it decreases owing to the dominance of the photo-degradation reaction. Nitramine shows a monotonic growth, though with a decreasing gradient in comparison to the nitrosamine. As the rate constant of the nitrosamine is lower than that of the nitramine, its monotonic growth is comparatively slower.



(a)



(b)



(c)

Figure 6.12: Short term average concentrations (ng/m^3) against distance from source (m) for (a) MEA (b) resulting Nitrosamine (c) Nitramine, for MEA in year 2012 at Ferrybridge.

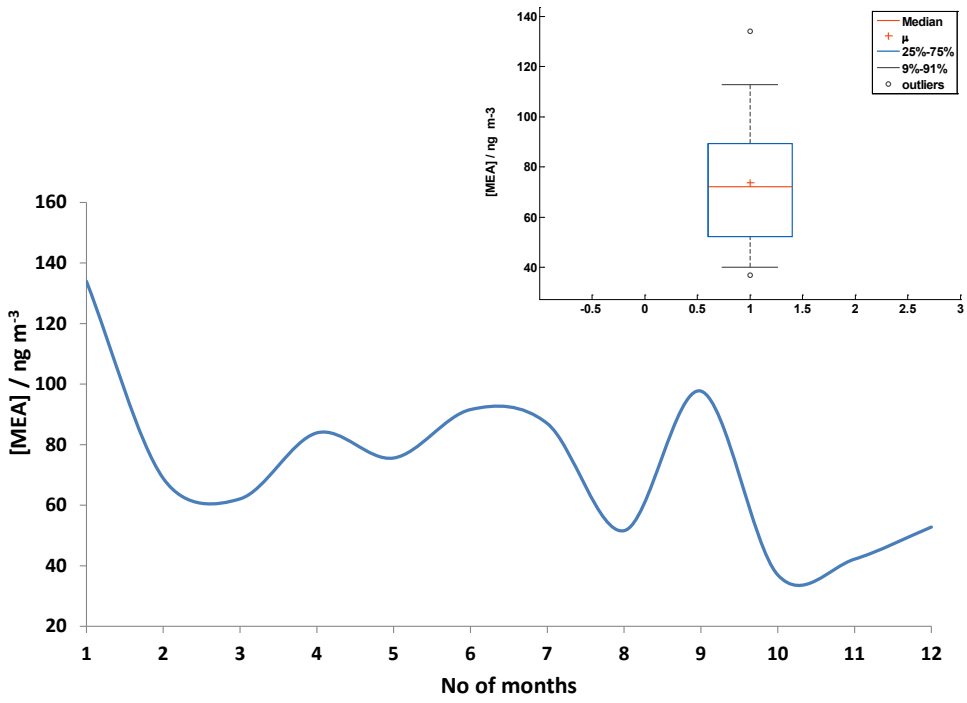
6.6.1.3 Monthly MEA concentration for the worst-case on Ferrybridge

Additionally, monthly MEA concentrations were also modelled for every month of the 2012 meteorological year at the maximum tolerable emission rate of 20.8 g/s. There are safety limits established in the literature for the monthly average concentrations of MEA to be below 10 µg/m^3 (Låg *et al.* 2009). Therefore, maximum monthly concentrations of MEA and its corresponding NS and NA, for the worst case scenario for each month of the year were modelled to observe the change in concentrations over time and to determine whether the obtained values exceeded the safety limit. The results for MEA and the degradation products are shown in Table 6.7. Additionally, Figure 6.13a-b, shows the graphical representation of the

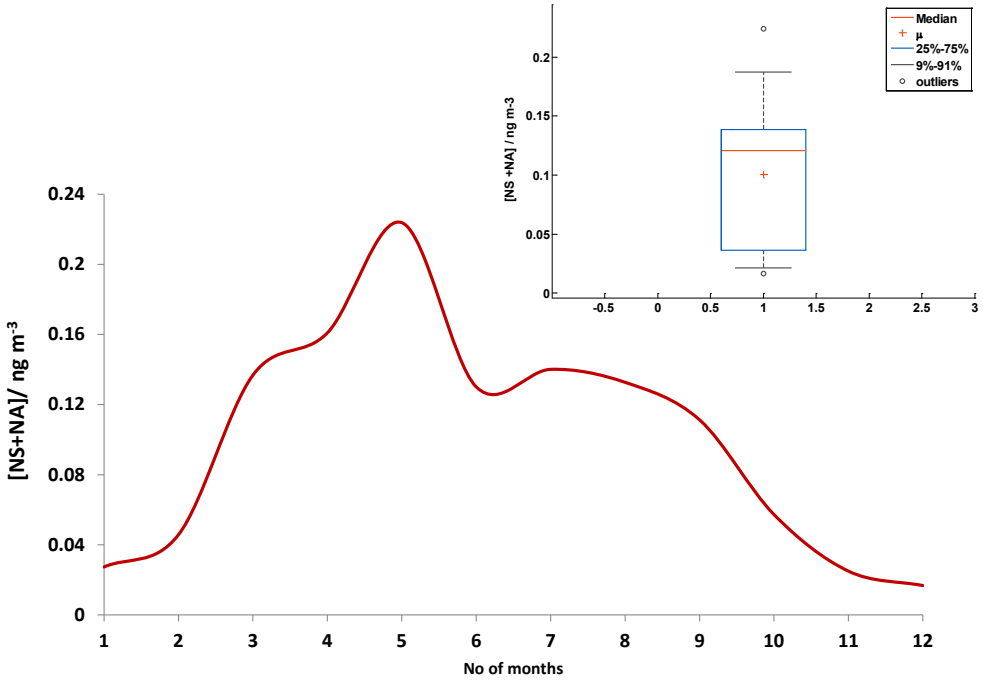
monthly variation in the MEA and the NS and NA concentrations along with their respective box and whisker plots outlining their respective lowest, lowest quartile, median, upper quartile and highest concentration values

Table 6.7: Monthly maximum long term average concentrations of MEA, NS and NA (ng/m^3) for the worst case emissions scenario for the meteorological year 2012.

Month	Monthly [MEA] / ng m^{-3}	Monthly [NS] / ng m^{-3}	Monthly [NA] / ng m^{-3}	[NS+NA] / ng m^{-3}
Jan	134	8.26×10^{-3}	1.91×10^{-2}	2.74×10^{-2}
Feb	68.9	5.63×10^{-3}	4.01×10^{-2}	4.57×10^{-2}
March	62.1	1.28×10^{-2}	1.24×10^{-1}	1.37×10^{-1}
April	83.9	1.49×10^{-2}	1.46×10^{-1}	1.61×10^{-1}
May	75.6	2.48×10^{-2}	1.99×10^{-1}	2.24×10^{-1}
June	91.6	2.01×10^{-2}	1.10×10^{-1}	1.30×10^{-1}
July	87.0	2.71×10^{-2}	1.13×10^{-1}	1.40×10^{-1}
August	51.6	1.67×10^{-2}	1.16×10^{-1}	1.33×10^{-1}
September	97.7	2.62×10^{-2}	8.51×10^{-2}	1.11×10^{-1}
October	37.0	7.06×10^{-3}	5.02×10^{-2}	5.73×10^{-2}
November	42.2	4.06×10^{-3}	2.09×10^{-2}	2.50×10^{-2}
December	52.8	4.23×10^{-3}	1.25×10^{-2}	1.67×10^{-2}



(a)



(b)

Figure 6.13: Monthly maximum average concentrations (ng/m^3) against months for (a) MEA and a box and whiskers plot showing the (a) lowest (37 ng/m^3), lower quartile (52.2 ng/m^3), median (72.3 ng/m^3), upper quartile (89.3 ng/m^3) and highest value (134 ng/m^3) of the MEA concentration for every month of the year 2012 and (b) resulting NS and NA, in year 2012, with their respective box and whisker plot showing lowest (0.02ng/m^3), lower quartile (0.04 ng/m^3), median (0.12 ng/m^3), upper quartile (0.14 ng/m^3) and highest value (0.22 ng/m^3) of the sum of NS and NA concentrations resulting from MEA for the sensitivity testing on the worst case scenario on Ferrybridge. The outlier for MEA concentration is 134 ng/m^3, whereas, 0.22 ng/m^3 for NS and NA.

From Figure 6.13a, it is observed that the monthly concentration for MEA ranges from 37 - 134 ng /m^3 with the maximum occurring in January. The maximum MEA concentration is then observed to decrease from January onwards only to increase in September and decrease afterwards. As par the box and whisker plot for MEA monthly concentration, the lowest (37 ng/m^3), the lowest quartile (52.2 ng/m^3), median (72.3 ng/m^3), upper quartile (89.3 ng/m^3) and highest (134 ng/m^3) values, respectively, are observed. An interquartile range of 37.1 ng/m^3 is calculated which shows the spread of the values, with the highest value of 134 ng/m^3 laying outside the box and whisker plot is considered to be an outlier.

The monthly concentrations for NS and NA resulting from MEA range from 0.02 – 0.22 ng /m^3, with the maximum monthly concentrations occurring in May (Figure 6.13b). As par the box and whisker plot for their monthly concentration, the lowest

(0.02 ng/m^3), the lowest quartile (0.04 ng/m^3), median (0.12 ng/m^3), upper quartile (0.14 ng/m^3) and highest (0.22 ng/m^3) values, respectively, are observed. An interquartile range of 0.10 ng/m^3 is calculated and the highest value of 0.22 ng/m^3 is considered as an outlier.

In January, when the MEA concentration is highest (134 ng/m^3), it does not form the degradation products; therefore, they have their lowest concentration (0.02 ng/m^3) during this time. Conversely, as the MEA concentration decreases until August, an increase in NS and NA concentration is observed during this time. This is in cognisant with the fact that the parent amine determines the fate of its products. The maximum concentration of 134 ng/m^3 which is 0.134 µg/m^3 for MEA, is 75 times lower than the safety limit of 10 µg/m^3. Hence, no risk is posed to the environment or humans during any of the months of the meteorological year 2012, at Ferrybridge with respect to MEA at maximum tolerable emission rate of 20.8 g/s.

The obtained maximum NS and NA concentration of 0.22 ng/m^3 does not exceed the 0.3 ng/m^3 annual average safety limit for which the worst case scenario is designed. However, if this maximum value of 0.22 ng/m^3 is compared to the monthly threshold concentrations for NS and NA which is of 0.02 ng/m^3 as defined in literature (USEPA). It certainly exceeds it by up to a factor of 11. For this reason, to have acceptable risk associated with respect to monthly threshold concentrations for NS and NA, the maximum tolerable emissions of MEA can be recalculated to re-design a new worst case.

6.6.2 Deposition to soil and water

Amine, nitrosamines and nitramines in the atmosphere are also subject to dry and wet deposition to soil and water. From the reactive dispersion modelling of the amines, total NS and total NA, long term hourly averaged wet (F_{wet}) and dry deposition fluxes (F_{dry}) are estimated by the model, which are listed in Table 6.8 for each of the emitting facility. There are no reported established thresholds for dry deposition of NS and NA to use for comparison with the obtained results. Nevertheless, there are environmental impacts associated with the amines when they undergo deposition to the soil, where they are subject to natural processes, such as biodegradation into nitrogen components, essential for plant growth. If increased amine deposition occurs then there is an increase in nitrogen content in the soil and

water which leads to eutrophication. Consequently, enhancing biomass production and reducing plant biodiversity. It is perceived that the all the dry deposition values are a factor of 1, 4 and 2 lower than the wet deposition for Ferrybridge, Peterhead and Mongstad respectively.

Table 6.8: The wet and dry deposition flux calculated for the amines, total nitrosamines and total nitramines for the worst case scenario modelled for each site.

µg/m^2/s	Ferrybridge		Peterhead		Mongstad	
	F_{wet}	F_{dry}	F_{wet}	F_{dry}	F_{wet}	F_{dry}
MA	1.57×10^{-3}	1.45×10^{-3}	3.04×10^{-4}	7.22×10^{-5}	1.94×10^{-3}	9.58×10^{-4}
DMA	1.58×10^{-3}	1.44×10^{-3}	1.16×10^{-3}	2.78×10^{-4}	2.22×10^{-4}	1.10×10^{-4}
MEA	2.24×10^{-4}	2.03×10^{-4}	1.33×10^{-3}	3.10×10^{-4}	5.99×10^{-4}	2.96×10^{-4}
Total NS	8.44×10^{-8}	7.77×10^{-8}	1.63×10^{-6}	3.83×10^{-7}	2.71×10^{-8}	1.44×10^{-8}
Total NA	2.51×10^{-6}	2.55×10^{-6}	4.00×10^{-6}	1.14×10^{-6}	2.43×10^{-3}	7.84×10^{-7}

The wet deposition fluxes values for each of the chemical species of interest are then used in determining the respective concentrations in water as per the mentioned relationship by Karl *et al.* (2011) presented in E.q 6.14. Subsequently, a comparison to safety limits in drinking water and aquatic life for the amines and the total NS and total NA is made as shown in Table 6.9.

Table 6.9: The concentrations of amines, nitrosamines and nitramines for the worst case scenario modelled for each site in water estimated from wet deposition fluxes and compared against safety limits.

Water		Total	
ng/L	MEA	NS	NA
Ferrybridge	8719	40	97
Peterhead	6011	32	79
Mongstad	9490	0.43	38
Safety limits (ng/L)			
aquatic	7500[a]	25[a]	200[a]
Drinking water	-	7[b],4[c,d]	1000[e]

[a] Brooks and Wright (2008); [b] Richardson *et al.* (2007); [c]Cal-EPA (2006), [d](Låg *et al.* 2011),[e] Wollin and Dieter (2005).

It is observed that the calculated concentration of MEA in water is below the threshold of 7500 ng/L (Brooks and Wright 2008) for Peterhead but it exceeds by 1.16 and 1.26 times for Ferrybridge and Mongstad, respectively. The aquatic life such as bacteria and algae will consequently be subject to chronic impacts from long term exposure of MEA in the environment from these two sites.

For the total nitrosamines from all the three amines, it can be seen that with respect to drinking water the values for Mongstad are below the safety limit of 4 ng/L (Låg *et al.* 2011). However, for Ferrybridge and Peterhead sites the calculated values exceed the safety limit of 4 ng/L (Låg *et al.* 2011) by a factor of 10 and 3. These sites also exceed the 7 ng/L safety limit (Richardson *et al.* 2007) by a factor of 6 and 5. In both instances, there is a concern to the human health. With respect to the aquatic environment, again only for Mongstad the calculated value is below the safety limit of 25 ng/L (Brooks and Wright 2008). While, for the Ferrybridge and Peterhead the calculated values exceed the safety limit by a factor of 2 and 1.

For the total nitramines from all the three amines, it was seen that with respect to drinking water the estimated values for each of the site were below 1000 ng/L (Wollin and Dieter 2005). Therefore, nitramines do not pose a risk to human health from exposure to drinking water. Additionally, with respect to the aquatic environment, the calculated values are below the safety limit of 200 ng/L (Brooks and Wright 2008) for all the site. Therefore, there is no risk to the aquatic environment either.

On the other hand, if the safety guideline of 4 ng/L (Låg *et al.* 2011) for the maximum sum of nitrosamines and nitramines for Norway is considered, then for Mongstad the calculated total nitrosamines and nitramines certainly exceeds it by almost a 100%. As a consequence of this, there is risk to the human health as well as the aquatic life from exposure to high concentrations of these chemical pollutants in water.

It is obvious that the maximum tolerable emissions estimated for each of the studied site exceed the safety limits established for MEA, nitrosamines and nitramines in water even when photochemical degradation was taken into account. However, it must be noted that the worst case scenario is specifically designed to estimate

maximum tolerable amine emissions such that the resulting total NS and NA do not exceed the safety limit of 0.3 ng/m^3 in air.

It is therefore, suggested that for the deposition calculations that the maximum tolerable amine emissions, E_{max}, be estimated from the using the maximum concentration output, $C_{max,out}$, at unity emissions which should be scaled until the critical concentration, C_{crit}, of the amine in water (and not air) is reached. This then used for the determination of the E_{max} (as par Karl *et al.* (2011)). By doing so, the obtained E_{max} calculated might be different to the E_{max} calculated using C_{crit}, of the amine in air, since these are two different environmental compartments and the safety limits vary for each of these

6.7 Parametric sensitivity analysis on worst-case scenario for Ferrybridge

In the modelling studies conducted various parameters are considered which are associated with unquantifiable uncertainties. This leads to an overall degree of uncertainty in the obtained modelled results. Quantifying the overall uncertainty as accurately as possible is challenging due to the large number of uncertain parameters considered. Nevertheless, an attempt is made to account for this uncertainty by performing sensitivity analysis to observe the influence of each individual parameter uncertainty on the results. The worst case scenario for Ferrybridge during 2012 for the three amines is considered as the base line case study for comparison to the sensitivity studies carried out. The knowledge gained from the sensitivity testing on the base line case study can be generalised to the other two sites, Peterhead and Mongstad as well.

The sensitivity study performed investigates how the concentration of the resulting NS and NA from the three amines is influenced by changing the rate constants describing the chemistry, the emission source parameters such as stack height, stack diameter, stack exit velocity and stack exit gas temperature. The effect of changing other parameters such as terrain, meteorological year, background pollutant emissions (NO_x and O_3) and NO_x/NO_2 ratio as well as background concentrations of OH radical are also investigated.

Each parameter is increased and decreased by a factor of 2 of its true value as listed in Table 6.10. The considered ranges are assumed to be considerably larger in comparison to the uncertainty ranges associated with the uncertain parameters. For instance, the experimentally determined value for k_{OH} for MA is 2.20 $\pm$ 0.22 x10^{-11} cm^3 $molecule^{-1}$ s^{-1} (Atkinson *et al.* 1977). Here the uncertainty range is $\pm$ 0.22 x10^{-11} cm^3 $molecule^{-1}$ s^{-1}. In this work, the calculated value of k_{OH} is 2.18x10^{-11} cm^3 $molecule^{-1}$ s^{-1} and therefore the maximum value for k_{OH} considered for sensitivity analyses was 4.36x10^{-11} cm^3 $molecule^{-1}$ s^{-1}, whereas, the minimum value 1.09x10^{-11} cm^3 $molecule^{-1}$ s^{-1}. Thus, the variation in the value certainly covers the uncertainty ranges associated with this parameter. The same holds true for the rest of the parameters considered.

The total maximum NS and NA concentrations from all the three amines for the baseline case is a value of 0.29 ng m^{-3} which is shown along with the results from the sensitivity tests are in Table 6.11. A box and whisper plot along with a graphical plot illustrated in Figure 6.14 outlines the lowest (0.1 ng/m^3), lower quartile (0.23 ng/m^3), median (0.29 ng/m^3), upper quartile (0.31 ng/m^3) and highest value (0.77 ng/m^3) of the sum of NS and NA concentrations resulting from the three amines for the sensitivity testing on the worst case scenario on Ferrybridge. Six outliers were also obtained at values 0.10, 0.46, 0.52, 0.53 and 0.77 ng/m^3.

Table 6.10: The values of the uncertain model parameters increased and decreased by a factor of 2 of its true value for consideration in sensitivity analysis conducted on the baseline worst-case scenario on Ferrybridge.

	MA			DMA			MEA		
	Halved	**Baseline**	**Doubled**	**Halved**	**Baseline**	**Doubled**	**Halved**	**Baseline**	**Doubled**
k_{OH} / cm^3 molecule^{-1} s^{-1}	1.09×10^{-11}	2.18×10^{-11}	4.36×10^{-11}	3.13×10^{-11}	6.26×10^{-11}	1.25×10^{-10}	4.60×10^{-11}	9.20×10^{-11}	1.84×10^{-10}
k_2	1.82×10^{-18}	3.64×10^{-18}	7.28×10^{-18}	1.82×10^{-18}	3.64×10^{-18}	7.28×10^{-18}	1.25×10^{-16}	2.49×10^{-16}	4.98×10^{-16}
k_3	8.50×10^{-13}	1.70×10^{-12}	3.40×10^{-12}	4.19×10^{-14}	8.37×10^{-14}	1.67×10^{-13}	2.81×10^{-14}	5.62×10^{-14}	1.12×10^{-13}
k_{4a}	4.85×10^{-13}	9.70×10^{-13}	1.94×10^{-12}	1.58×10^{-13}	3.15×10^{-13}	6.30×10^{-13}	4.20×10^{-15}	8.40×10^{-15}	1.68×10^{-14}
k_{4b}	1.01×10^{-13}	2.02×10^{-13}	4.04×10^{-13}	5.50×10^{-15}	1.10×10^{-14}	2.20×10^{-14}	2.07×10^{-15}	4.14×10^{-15}	8.28×10^{-15}
Branching ratio	0.175	0.35	0.70	0.19	0.38	0.76	0.025	0.05	0.1
$J / J(NO_2)$	0.265	0.53	1.06	0.62	1.24	2.48	0.29	0.58	1.16
Stack height / m	99	198	396						
Stack diameter / m	4.87	9.74	19.48						
Velocity / m s^{-1}	25	50	100						
Temperature / °C	45	90	180						
O_3 / µg m^{-3}	32.5	65	130						
NO_x	12.55	25.1	50.2						
NO_x/NO_2	0.245	0.49	0.98						
NO_x emissions / µg m^{-3}	8.1	16.2	32.4						
c for OH	1.19×10^{-3}	2.38×10^{-3}	4.75×10^{-3}						

Table 6.11: Sensitivity analysis for different model parameters: maximum long term average concentrations of the total NS and NA from the three amines at the maximum tolerable emissions from Ferrybridge.

NS+NA ($ng\ m^{-3}$)	This study (baseline)	k_{OH} doubled	k_{OH} halved	Branching ratio doubled	Branching ratio halved
	0.29	0.52	0.16	0.39	0.15
k_2 doubled	k_2 halved	k_3 doubled	k_3 halved	k_{4a} halved	k_{4b} doubled
0.16	0.53	0.31	0.28	0.16	0.28
J / J (NO_2) doubled	J / J (NO_2) halved	NO_x/NO_2 doubled	NO_x/NO_2 halved	NO_x emissions doubled	NO_x emissions halved
0.28	0.30	0.30	0.29	0.26	0.31
Stack exit temperature doubled	Stack exit temperature halved	Stack exit velocity doubled	Stack exit velocity halved	Stack height doubled	Stack height halved
0.19	0.30	0.23	0.38	0.17	0.46
Stack diameter doubled	Stack diameter halved	O_3 doubled	O_3 halved	Background NO_x doubled	No terrain
0.16	0.44	0.77	0.12	0.26	0.32
Domain doubled	Domain halved	Met 04	Met 05	Met 07	Met 08
0.30	0.28	0.37	0.29	0.28	0.27
Met 09	Met 10	Met 11	Met 13	[OH] doubled	[OH] halved
0.26	0.31	0.30	0.27	0.31	0.10

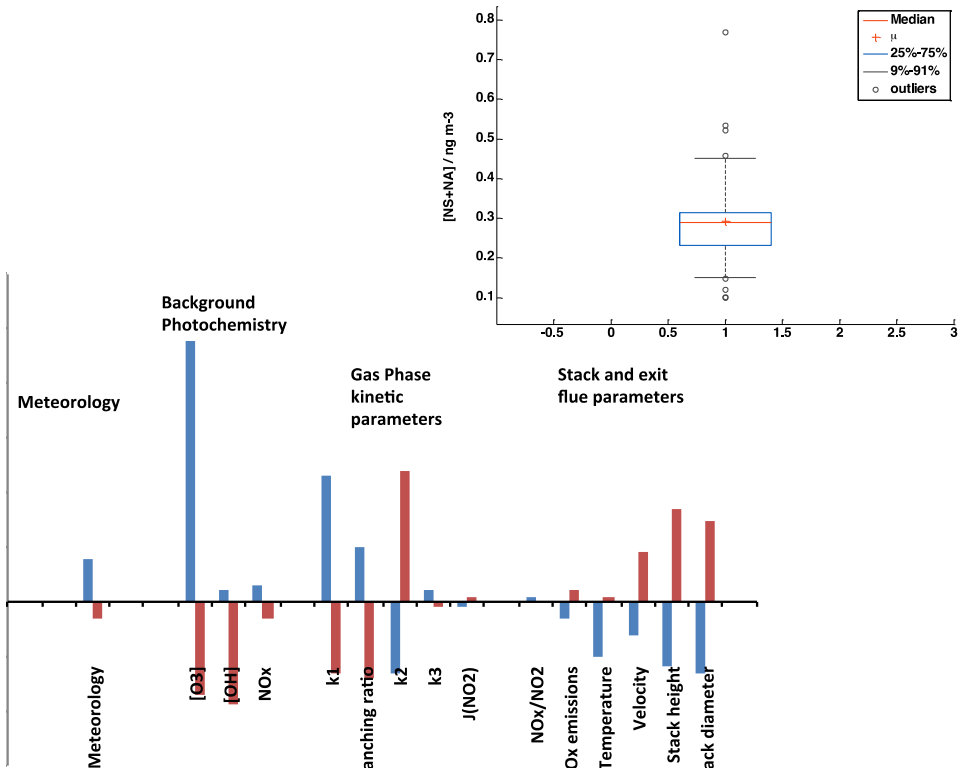


Figure 6.14: A graphical representation of the sensitivity analysis on the most uncertain parameters with a box and whiskers plot showing the lowest (0.1 ng/m^3), lower quartile (0.23 ng/m^3), median (0.29 ng/m^3), upper quartile (0.31 ng/m^3) and highest value (0.77 ng/m^3) of the sum of NS and NA concentrations resulting from the three amines for the sensitivity testing on the worst case scenario on Ferrybridge. Six outliers were also obtained at values 0.10, 0.46, 0.52, 0.53 and 0.77 ng/m^3.

6.7.1 Rate constants describing the atmospheric chemistry

Rate constants describing the chemistry and parameters directly related to the chemistry were varied up to highly improbable ranges to study how these particular parameters influence the fate of the total NS and NA formation from the three parent amines.

Rate constant, k_{OH} determines the rate of the reaction of the amine with OH radical to form the amino radical and water. Therefore, doubling the rate of this reaction causes the amine concentration to decrease as it gets used up to form the amino radical. The amino radical which is higher in concentration then reacts with NO and NO_2 to form the nitrosamine and nitramine, resulting in an increase in their concentration which exceeds the baseline value of 0.29 ng/m^3 by 80 %. Halving k_{OH}

has the opposite effect and reduces the concentration by up to 45 % of the baseline value.

Rate constant, k_2 determines the rate of the reaction of the alkyl amino radical with O_2 to form imine. This reaction competes with those that form the nitrosamines and nitramines. Therefore, doubling k_2 results in a decrease in the concentrations of nitrosamines and nitramines by up to 45 %, as it causes an increase in the imine concentration. The concentration of the amine is unaffected by this, therefore, it stays the same as the baseline amine concentration. Halving k_2 has the opposite effect and the concentration of the NS and NA exceeds the baseline value by 84 %.

Rate constant, k_3 determines the rate of the reaction of the alkyl amino radical with NO to form the nitrosamine. Therefore, doubling k_3 increases the formation of the nitrosamines i.e. its concentration. The concentrations of the amine and nitramine remain unaffected. The overall concentration nevertheless exceeds the baseline value by 8 %. Halving k_3 has the opposite effect, resulting reduction of 2 % of the baseline value

Rate constant, k_4 determines the rate of the reaction of the alkyl amino radical with NO_2 to form the nitramine. Therefore, doubling k_4 increases the formation of the nitramines i.e. its concentration doubles. The concentrations of the amine and nitrosamine are unaffected by this. Halving k_4 has the opposite effect. However, in both the cases the total NS and NA concentrations remain much below baseline value i.e. by 43 and 5 %.

J/J (NO_2) determines the rate of photolysis of the nitrosamine. Therefore, doubling it increases this rate and results in a decrease in the concentration of the nitrosamine. The concentrations of the amine and nitramine remain unaffected. The total NS and NA concentration is 2 % lower than the baseline value. Halving J/J (NO_2) has the opposite effect, resulting in an increase of 5 % of the baseline.

Doubling the branching ratio causes more of the amino radical to form in order to react with NO and NO_2, resulting in the production of nitrosamine and nitramine exceeding the baseline value by 36 %. Halving the branching ratio has the opposite effect and the resulting concentration is 49 % lower than the baseline value.

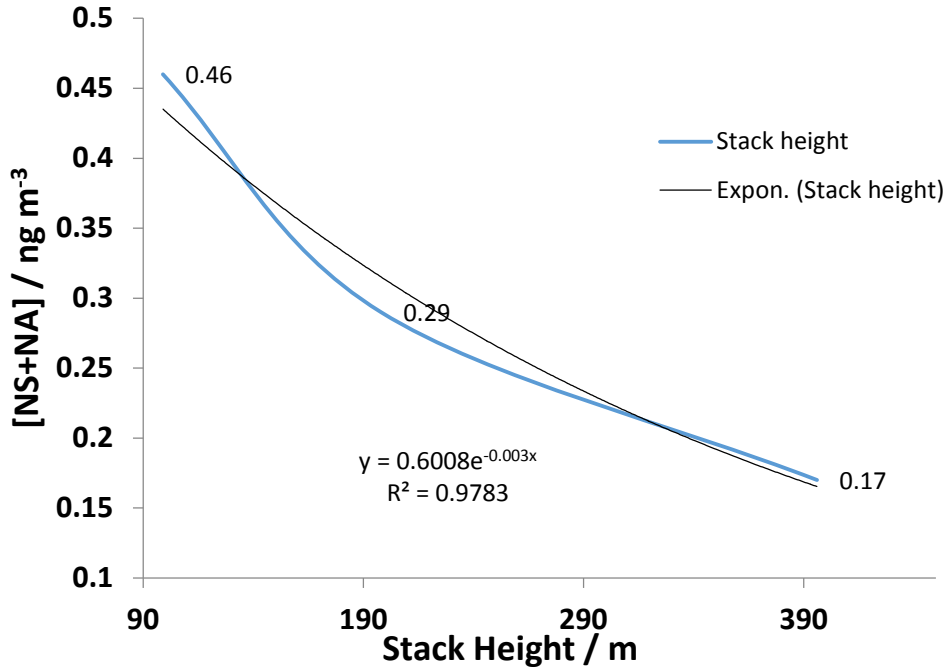
Hence, it is observed that increasing k_{OH}, k_3, k_4 and branching ratio values, whereas, reducing k_2 and $J/J(NO_2)$ values, overall leads to an increase in the NS and NA concentrations. Yet, the most influential parameters in determining the fate of the NS and NA are k_{OH}, branching ratio and k_2, which affected the concentration total NS and NA by up to 80, 84 and 49 %, respectively.

6.7.2 Stack and exit flue parameters

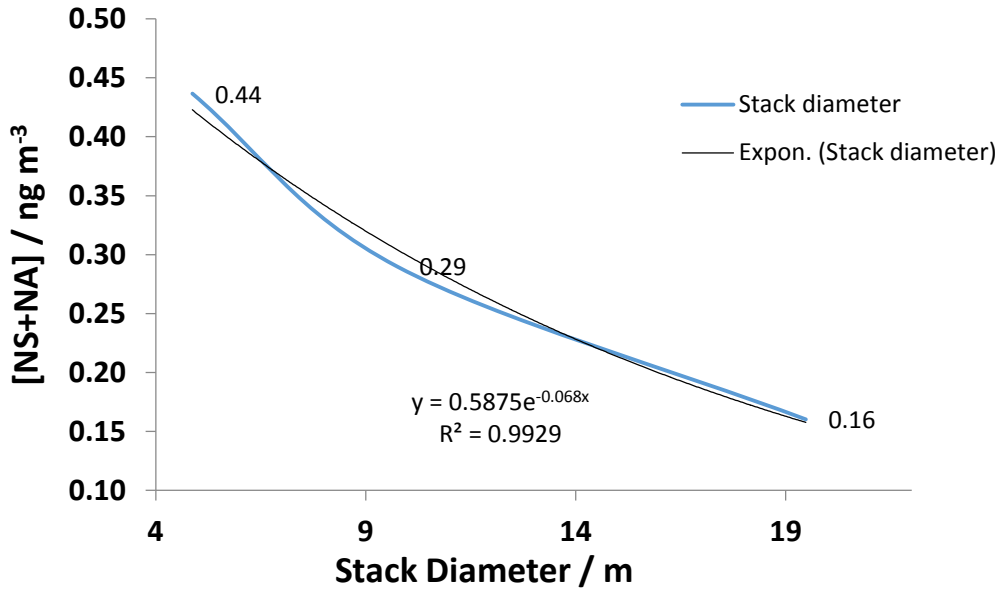
Parameters indirectly associated to amine chemistry were also varied for the purposes of sensitivity testing. With an increase in temperature, the density of the gases is decreased which causes them to go to upper layers of the atmospheric boundary layer and this consequently reduces the ground level concentrations. Additionally, the involved chemical reactions are exothermic reactions and therefore doubling the temperature (from base line temperature), shifts the reaction to the reactants, decreasing the concentration of the nitrosamines and nitramines by 35 % of the baseline value. Halving the temperature, results in an increase of 4 % of the NS and NA concentration in comparison to the baseline value.

Doubling the velocity of the exit flue gas results in a decrease of NS and NA concentration by 20 % of the baseline value, whereas, upon considering half the value of the velocity, the resulting concentrations rises by 32 %.

Doubling the stack height and diameter, results in a decrease in total NS and NA concentration by 42 and 45 % of the baseline value, respectively. Halving these parameters causes the concentrations to increase by 58 and 51%, respectively. From Figure 6.15a, it can be seen that there is an exponential dependency of the NS and NA concentration on the stack height. The same holds true for the NS and NA concentrations displaying an exponential dependency on the stack diameter (Figure 6.15b).



(a)



(b)

Figure 6.15: Plots showing an exponential dependency of the NS and NA concentrations with (a) Stack height and (b) Stack diameter.

Hence, from the sensitivity testing, it is deduced that increasing the stack height and diameter, stack exit velocity and stack exit gas temperature results in an increase in dispersion and consequently a decrease in the corresponding maximum year average concentrations of amines and the corresponding nitrosamine and nitramine. The decrease in concentrations suggests that the emissions can disperse farther from the

source and, therefore, have a reduced adverse effect on the environment. An increase in the concentration of these species is observed with decreasing the mentioned parameters; suggesting that the distance of dispersion of amine emissions is comparatively shorter. However, it is important to note that the most significant factor in determining dispersion is the stack height, exceeding the baseline value by 58 %.

6.7.3 Background gas concentrations

Doubling the NO_x/NO_2 ratio caused the baseline NS and NA concentration to increase by a 1% whereas halving it lead to an increase of 3 %. Therefore, it is deduced that varying this parameter has a negligible effect on the final output value.

Varying NO_x background concentration affected the nitrosamine and nitramine concentration by up to 11 %.

Changing the concentration of OH radical also affected the baseline NS and NA concentration. Doubling it, lead to an 8 % increase of the baseline value whereas, halving it brought about a 65 % reduction. OH is the precursor to the atmospheric chemistry of the amines and it will therefore influence the fate of the resulting degradation products.

NO_x emission at the stack comprises around 99.5 % of NO, which is a component of NO_x that leads to the formation of nitrosamine. Therefore, doubling the NO_x emissions results in an increase in the formation of the nitrosamine and subsequently a decrease in the nitramine concentration owing to the fact that there is more NO to compete with NO_2, for the amino radical. Overall it results in a decrease of the baseline value by 9 %. Halving NO_x decreases the concentration of the nitrosamine, causing the baseline value to increase by 8 %.

O_3 is a source of OH radicals; therefore, doubling O_3 background concentration increases the rate of amine and OH reaction, resulting in a decrease in the amine concentration. Subsequently, more of the amino radical is formed to react with NO and NO_2 to produce the corresponding nitrosamine and nitramine, exceeding the baseline value of the total NS and NA by 165 %. Halving O_3 concentration has the opposite effect, resulting in a 59 % reduction. From Figure 6.16, it can be seen that

the NS and NA concentration exhibit a linear dependency with O_3 background concentration.

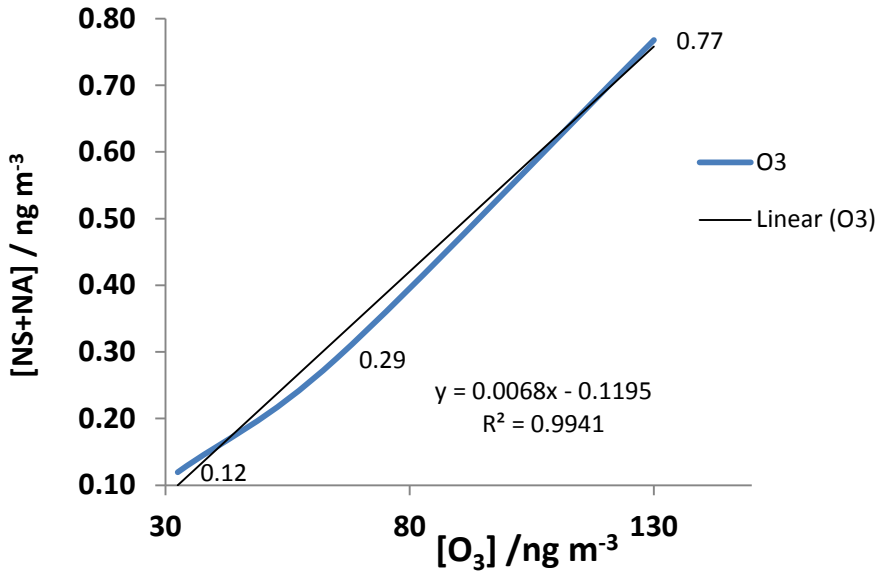


Figure 6.16: Plot showing a linear dependency of the NS and NA concentrations with $[O_3]$ / µg m^{-3}.

6.7.1 Different meteorological years

To investigate the effect of year-to-year variances on expected concentrations, model runs with meteorological years from 2004 to 2013 were executed for MA, DMA and MEA (Figure 6.17). The meteorological year that gives the maximum long term annual concentration of the sum of NS and NA is 2004, with a risk to the human health. In 2010, there is a risk to the human health as the concentration of the NS and NA exceed the baseline value of 0.29 ng m^{-3} by a 28 %. The baseline value is exceeded by 7 % and 3 % in the years 2010 and 2011.

For the meteorological year 2004, the maximum long term annual concentration of the total NS and NA (0.37 ng m^{-3}) is relatively higher than those determined for the rest of the years. This difference is due to the varying wind speed, wind direction, cloud cover, precipitation etc. between the two years. From the results (Table 6.12), the changes in the maximum concentrations and concentration patterns are apparent but the inter-annual variations are not that significant except from 2004 to 2005.

Table 6.12: Sensitivity analysis for different meteorological years: maximum long term average concentrations of the total NS and NA from the three amines at the maximum tolerable emissions and the percentage change (%Δ) from the baseline value of 0.29 ng m^{-3} in 2012.

Year	NS+NA (ng/m^3)	%Δ
2004	0.37	28
2005	0.29	0
2007	0.28	-3
2008	0.27	-7
2009	0.26	-10
2010	0.31	7
2011	0.30	3
2012	0.29	0
2013	0.27	-7

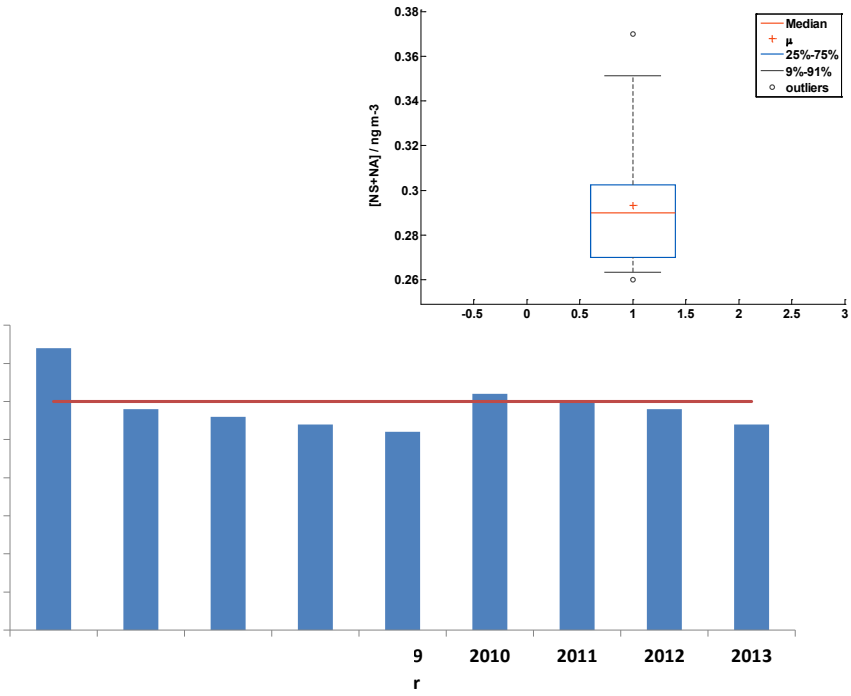


Figure 6.17: A graphical representation of the sensitivity analysis on the meteorological years from 2004 to 2013 with a box and whiskers plot showing the lowest (0.26 ng/m^3), lower quartile (0.27 ng/m^3), median (0.29 ng/m^3), upper quartile (0.30 ng/m^3) and highest value (0.37 ng/m^3) of the sum of NS and NA concentrations resulting from the three amines for the sensitivity testing on the worst case scenario on Ferrybridge. One outlier was also obtained at a value 0.37 ng/m^3 The red straight line corresponds to the safety limit of 0.3 ng m^{-3}.

6.7.2 With and without terrain

The effect of terrain on the modelled concentrations was also inspected since the topography of the area immediately surrounding Ferrybridge is moderately hilly. An increase in concentrations of the amine and nitrosamine was observed when no topography was considered. The baseline NS and NA value is exceeded by 10 %. In this scenario, the emissions could disperse further from the source without coming across any obstacles such as the hills in the region. This is due to the hills within the study domain being smaller than the stack height; therefore, the increase is not too significant. However, if the terrain features become more complex than obviously the baseline value will be more significantly affected.

6.7.3 Different emission scenario

An alternative emission based on the emissions data from CERC (2012c) and CERC (2012d) was also modelled to give an impression on the real case scenario (the same emissions shown in Table 6.4 were used for the Mongstad case study). Results are outlined in Table 6.13 where the sum of the nitrosamines and nitramines is calculated to be 0.01 ng/m^3. This value is less than the safety limit of 0.3 ng /m^3. For this reason, the concentrations of NS and NA are not harmful to the natural environment and human health.

Table 6.13: Maximum long term average concentrations of NS+NA (ng/m^3) for the alternate emissions scenario for the meteorological year 2012.

Dispersion model case	Guideline value	Maximum annual concentration of total NS and NA considering atmospheric chemistry
Air - likely case (ng/m^3)	0.3	0.01

6.8 Comparison to CERC results

6.8.1 Mongstad

For the purposes of comparison, the likely case using amine emissions reported in Table 6.4, were modelled for the site Mongstad using rate constants established in this work as well as the rate constants used in the studies performed by CERC (2012c) and CERC (2012d) as shown in Table 6.14.

Results from using the rates calculated in this work gave a sum of NS and NA from all the amines to be 0.06 ng/m^3. Whereas, a 17 % higher value of 0.07 ng/m^3 was calculated from using the rates considered by CERC (2012d). The mostly likely reason for the difference is mainly due to the use of less accurate rate constants considered by CERC (2012c) and CERC (2012d) from literature and assumed values for the unavailable rate constants. This was especially the case for MEA.

Therefore, this study provides more accurate results based on rate constants that were established computationally through a rigorous analysis using the same method for all the three amines. It is for this reason, that the uncertainty in the values is reduced.

6.8.2 Ferrybridge

On the other hand, the rates used by CERC (2012c) and CERC (2012d) were used in performing the worst case scenario on Ferrybridge to compare how different the total NS and NA is to the value of 0.29 ng/m^3 calculated in this work. It was seen that a value of 6.11ng/m^3 was calculated which is a factor of 21 times larger than the value of 0.29 ng/m^3. This difference is due to the difference in the order of magnitudes of the rate constant values considered which can significantly influence the amine atmospheric chemistry, consequently affecting the production of NS and NA.

Since there are experimental values available for the rate constants describing each pathway of the atmospheric chemistry scheme for DMA, a comparison was made to the values established in this work as well as those used by CERC (2012c) and CERC (2012d) for the worst case scenario modeled on Ferrybridge. The total NS and NA resulting from the rate values calculated in this work were of 0.13 ng/m^3 in concentration. This value was a factor of 4 lower than the experimental rate values and a factor of 44 lower than the CERC (2012c) and CERC (2012d) rate values. The difference again is due to the difference in the order of magnitudes of the rate constants used, which can significantly influence the fate of the resulting NS and NA.

Table 6.14: A summary of the rate constants (cm^3 molecule $^{-1}$ s^{-1}) describing the atmospheric chemistry scheme for each of the amines studied using quantum chemistry theoretical methods and kinetic modelling established in this work and those considered by CERC (2012c) and CERC (2012d) as well as those form experimental studies.

	MA **k/ cm^3 molcecule^{-1} s^{-1}**			**DMA** **k/ cm^3 molcecule^{-1} s^{-1}**			**MEA** **k/ cm^3 molcecule^{-1} s^{-1}**		
	This work	CERC (2012d)	Exp	This work	CERC (2012d)	Exp	This work	CERC (2012d)	Exp
k_{OH}	2.18×10^{-11}	1.73×10^{-11}	-	6.26×10^{-11}	6.50×10^{-11}	6.54×10^{-11}[a]	9.20×10^{-11}	3.10×10^{-11}	-
k_2	3.64×10^{-18}	6.36×10^{-19}	-	3.64×10^{-18}	9.54×10^{-20}	1.24×10^{-19}[b]	2.49×10^{-16}	9.54×10^{-20}	-
k_3	1.70×10^{-12}	2.39×10^{-13}	-	8.37×10^{-14}	2.39×10^{-13}	8.53×10^{-14}[c]	5.62×10^{-14}	2.39×10^{-13}	-
k_{4a}	9.70×10^{-13}	3.18×10^{-13}	-	3.15×10^{-13}	3.18×10^{-13}	3.18×10^{-14}[c]	8.40×10^{-15}	3.20×10^{-13}	-
k_{4b}	2.02×10^{-13}	1.27×10^{-12}	-	1.10×10^{-14}	3.20×10^{-14}	3.58×10^{-13}[b]	4.14×10^{-15}	3.20×10^{-14}	-
Branching ratio, k_1/ k_{OH}	0.35	0.75	-	0.38	0.42	0.37[b]	0.05	0.08	-
J / $J(NO_2)$	0.53,0.74	0	-	1.24,126	0.25	0.53[b]	0.58,0.59	0	

[a]Atkinson *et al.* (1978); [b]Lindley *et al.* (1979); [c]Lazarou *et al.* (1994)

6.1 Verification and Validation of modelled results

Due to lack of reliable published emission data from PCCC technology, therefore hypothetical worst case scenarios had to be modelled. As a consequence, fictive results are obtained for which no field measurements exist to compare with for the purposes of verification.

Generally, verification is very difficult due to the challenges confronted in measuring ambient concentrations of nitrosamines and nitramines at ng/m^3 detectable levels around an emitting facility. There have been very limited studies that have measured ambient air concentrations of MEA. Reported values of MEA collected weekly around Mongstad were below 0.01 ng m^{-3} (Tønnesen 2011). Poste *et al.* (2014) measured MEA concentrations of 0.2 – 1.86 µg L^{-1} in Norwegian lakes. When de Koeijer *et al.* (2013) compared their modelled concentrations for NA and NS with the field data collected eleven times over a period of four days at three different locations around the Mongstad, none of the chemicals could be detected above the chemical detection level. It was deduced from their results that their theory and methodology were still under development. Therefore, validation of the model by comparison to measurements would only be possible if at least the 'real' average amine emission rates were known. However, even then there would be a lot of uncertainty since meteorology and chemical processes on surfaces are not accounted for in the dispersion models.

One part of the model validation is the check of the mass balance consistency. That means that the total amount of losses through all processes (chemistry, deposition, advection and turbulent transport out of the study domain) is equal to the amount of emission (of the amine). Some dispersion models offer diagnostics to analyse the mass balance.

For the IDM approach where chemistry is not considered, it therefore then implies that the emitted amines are only dispersed. Considering such an method in dispersion models like AMDS 5, the models have then been validated with measurement data in tracer experiments by its developers (CERC). This indicates the dispersion of pollutants can be taken as validated.

The remaining uncertainty is then in the dry and wet deposition of amines and the other emitted compounds. There have been no experimental investigations of the

deposition rates. However, the uncertainty due to deposition can be quantified and it would still be possible to come up with a concentration range (lower and upper limit) which could in principle be compared to measurements. In the worst case scenario, yearly averages for the health impacts are mainly considered. Therefore, a measurement series covering one year or at least some parts of the year would be needed.

From modelling studies performed by Karl *et al.* (2015) and also in this work, it is deduced that chemistry does not affect the concentration of the emitted amine very much. This is due to the results from reactive dispersion (chemical transport modelling) and for passive dispersion (IDM) of the amine in being very similar. As first approximation, emitted amines are only dispersed and deposited. For nitrosamines and nitramines this is of course very different, and there is currently no chance to validate nitrosamine and nitramine concentration from the model output. Hence, when it is not possible to get real emission data and amine measurements, it is suggested to continue the modelling on a conceptual level i.e. worst case-scenario to establish maximum tolerable amine emissions, for the purposes of risk assessments.

6.2 Conclusions

Chemical transformation reactions of the amines were considered along with the dispersion and deposition processes in the atmosphere using an air dispersion model, ADMS 5. By doing so, it was possible to determine the fate of these amine emissions in time and space away from the emitting facility. The developed methodology assists with reliable estimations of the amines and their corresponding NS and NA concentrations in time and space from the source. Such an approach can be applied to any generic amine (as it does not rely on any experimentally determined FFYs) and to any PCCC plant irrespective of its geographic location and size. Since PCCC technology is yet to be widely implemented at a commercial scale in operation, the developed methodology in this work can ensure if a proposed facility complies with the safety regulatory limits which is essential for its chemical discharge permit. Additionally, the approach can establish maximum tolerable amine emissions for an emitting facility such that the risk is acceptable with regards to human health and the immediate environment. Therefore, the findings of this research are aimed at

delivering crucial and useful data to the CO_2 capture industry especially for industries to comply with air quality regulations.

To illustrate that the developed methodology is universal, its application on the three capture plants with different geographic locations was carried out. The resulting sum of NS and NA was compared with threshold limits for the worst case scenarios, to determine the risk these chemical discharges pose to the humans and environment.

Sensitivity studies were performed on the uncertain parameters considered in the Ferrybridge modelling study, to determine which of these significantly influenced the fate of the resulting NS and NA from the PCCC process. The parameters were varied by a factor of 2 of the true value to see if the atmospheric chemistry and dispersion processes behaved as expected. The considered ranges are assumed to be considerably larger in comparison to the uncertainty ranges associated with the uncertain parameters.

Fundamentally, from the sensitivity study it was deduced that the NS and NA concentrations exhibited an exponential dependency on stack height and stack diameter, whereas, there was a linear dependency with O_3 background concentration. Plume velocity, plume temperature, OH and NO_x concentrations also influence the fate of the total NS and NA from the three amines. However, the relationship between these parameters and the concentrations shows a more complex and non-linear dependence.

The knowledge gained from the sensitivity testing on the base line case study on Ferrybridge can be generalised to the other two sites, Peterhead and Mongstad as well. Results demonstrate that since Mongstad has the smallest stack height and diameter and the lowest plume velocity and temperature in comparison to the other two sites, its maximum total NS and NA calculated in air is larger. As a result, the emissions cannot disperse further from the source as well as go to the upper layers of the atmospheric boundary. Henceforth, it is important to take account of the most influential parameters during the design and consent phase of potential industrial applications. The developed method in this work can in fact be used to propose ideal plant parameters with respect to its design. An ideal geographical location for such an industrial application could also be recommended. Hence, useful information with regards to the impacts of amine-based PCCC technology could be provided to

decision makers. Over and above, if a PCCC plant is carefully planned, placed and operated, the CO_2 capture advantage of using amine solvents would outweigh the risk associated with solvent discharge issues.

Nevertheless, there is an immediate need to perform field experiments to measure the ambient concentrations of the products of interest such as amines, NS and NA in the study domain around the emitting facility. The experimental data can be used to validate the results from modelling studies. This will increase the confidence in using modelling results for drawing conclusions with regards to the maximum tolerable emissions of amines and the corresponding degradation products from PCCC plants.

Chapter 7 Risk assessment on human health and environment

7.1 Introduction

The human health risk assessment paradigm was explained in detail as par the USEPA approach in chapter 4. Safety limits established by various studies for MEA, NS and NA in air and drinking water were stated. Also, a detailed description with regards to the calculation performed by Lag *et al* (2011) of the DMEL for NDMA from inhalation and oral studies was given.

In this chapter, the cancer risk assessment is performed by following the USEPA (1998b) method (explained in detail in chapter 4 and briefly summarised here) which considers the atmospheric concentrations of NS and NA from ADMS. The risk assessment paradigm constitutes of four stages which are hazard identification and characterization, exposure assessment and risk characterisation. The impact that the chemical species can have on a receptor and the harm it can cause at varying exposure levels is recognised in hazard identification and characterization stages. The exposure assessment stage considers the concentration, time and frequency of human exposure to stressor levels in the contaminated environment and the precise amount of the stressor entering the receptor. Since the amine, nitrosamine and nitramines of interest are present in the air; therefore, the inhalation exposure pathway is taken into account. The final stage in risk assessment is the risk

characterisation which reviews and amalgamates the knowledge gathered from the previous stages so as to conclude concerning risk.

The deterministic risk analysis is taken a step further by taking in account the probability distribution of the uncertain parameters considered in the risk model. Therefore, a probabilistic risk estimation of human health risks caused by exposure to these chemical pollutant discharges is conducted to get an idea on the probability distribution of the estimated risk. By performing human health risk assessment the number of people (infants, children and adults) exposed to lethal concentrations of amine degradation products making them susceptible to developing cancer can be determined along with their spatial location.
In this work, DMEL was also calculated using the modified Ravnum *et al.* (2014) approach where the determined value was in close agreement to the values determined in literature.
Additionally, from the deposition studies the environmental risk associated with these chemical discharges is also evaluated with respect to drinking water and aquatic life.

In the next section the all the stages of the risk assessment are discussed.

7.2 Cancer risk assessment

7.2.1 Hazard identification and characterisation

Studies have revealed that nitrosamines such as NDMA cause liver damage in animals (Magee and Barnes 1956). It has been proposed that nitrosamines undergo DNA alkylation, causing permanent genetic mutations in the DNA of the cells, consequently, making them cancerous. On the other hand, experimental studies conducted in vivo and in vitro have revealed that nitramines promote tumour by undergoing deamination to form formaldehyde and ammonia. Nitramines such as dimethylnitramine (DMNA) and monoethanol nitramine (MEA-NO_2) have shown carcinogenic effects on laboratory animals but are less lethal than their corresponding nitrosamines (Selin 2011).

The types of tumours caused by exposure to these harmful chemicals consist of lung, skin, stomach, skin, kidney, nasal cavities, liver, brain, oesophagus, oral cavity, pancreases, hematopoietic system, gut, urinary bladder, nervous system etc. (Olajos

and Coulston 1978, Verna *et al.* 1996). From experimental investigations, it has been established that the covalent binding of these carcinogenic compounds show a linear dose-response relationship in the low dose region. As a consequence of this there is no threshold dose for the genotoxic effect on humans. So despite having scant data on these substances, there is enough evidence to infer that these classes of compounds pose risk to the humans even at the lowest exposure. Hence, it is crucial to estimate the tolerable carcinogenic risk levels in humans.

7.2.2 Derived Minimal Effect Level (DMEL)

USEPA (1990), WHO (2008), Låg *et al.* (2011) have all established tolerable risk levels for life time exposure to be kept below either 10 or 1 in a million people i.e. 10^{-5} or 10^{-6}. The exposure concentrations calculated from the atmospheric chemistry and dispersion modelling are compared against the tolerant nitrosamine and nitramine concentration in air, known as the derived minimal effect level (DMEL) for a deterministic human health risk analysis.

For the TCM, the Norwegian Climate and Pollution Agency had issued a discharge permit of having DMEL not exceeding 0.3 ng/m^3 for total NS and NA released in the flue gas in the air during its operation (Låg *et al.* 2011). However, in the UK or EU in general there are no environmental assessment levels or environmental quality standards set for the NS and NA. Therefore, the thresholds for TCM are considered instead as useful benchmarks since they have been calculated with regards to the methods used under the EU regulations on registration, evaluation, authorisation and restriction of chemicals (REACH).

Nonetheless, an attempt was made to calculate DMEL in this study is obtained using cancer oral slope factor and extrapolation modelling techniques from high-dose animal exposures conducted on rats (using raw data from Peto *et al.* (1991b)) to low-dose human exposures. This value is then used in calculating the risk for developing cancer through inhalation.

7.2.2.1 T25 dose descriptor estimation

In order to evaluate DMEL, the chronic dose rate resulting in 25% of animals in developing tumours at a certain tissue location within its lifetime known as T25 needs to be determined (Goodall and Kennedy 1976, Peto *et al.* 1991a). Assuming a

linear dose relationship, T25 (mg/kg bw/d) for NDMA is calculated using both male and female original raw rat data from Peto *et al.* (1991b) and derived according to the following relationship as defined by Ravnum *et al.* (2014) and Dybing *et al.* (1997):

$$T25 = f^2 \; x \; dose \tag{7.1}$$

where f = duration of exposure at which 25% tumours occur and is determined as shown:

$$f^2 = \frac{exposure\ duration}{animal\ lifeime} x \frac{observation\ duration}{animal\ lifetime} \tag{7.2}$$

and dose =dose $_{human}$ at which 25% tumour incidence and is determined as shown:

$$dose_{human} = dose_{rat} \; x \; (\frac{0.25\ kg\ rat}{70\ kg_{human}})^{1/4} \quad \text{according to WHO (2008)} \tag{7.3}$$

For Eq 7.1, % tumour incidence is calculated as follows:

$$\%\ tumour\ incidence = \left(\left(\frac{A}{B}\right) - \left(\frac{C}{D}\right)\right) x\ 100 \tag{7.4}$$

where, A = no of rats with tumours; B = total number of rats in the group (60); C = no of rats in control group with tumours (10) and D = total no of rats in the control group (240). The obtained % tumour value is then adjusted for background tumour incidence, carried out as the following:

$$Adjusted\ \%\ tumour = \left(\frac{\left(\frac{A}{B}\right) - (\frac{C}{D})}{1 - (\frac{C}{D})}\right) x\ 100 \tag{7.5}$$

7.2.2.2 DMEL estimation via extrapolation from high to low dose

Due to a linear-dose relationship expected for the dose descriptor T25 (Dybing *et al.* 1997), a linearised approach according to REACH (ECHA/REACH 2012) guidelines is considered for the extrapolation from high to low dose for the calculation of DMEL for a risk of 10^{-6} as shown:

$$DMEL\ (mg/kg\ bw/day)\ = T25\ x\ \left(\frac{10^{-6}}{25/100}\right) \tag{7.6}$$

7.2.2.3 Adjustment of DMEL for route to route extrapolation

A default sequence of extrapolation (ECHA/REACH 2012) is employed for the adjustment of the DMEL for the route of exposure, to extrapolate from oral exposure in rats to inhalation exposure in humans as shown:

$$DMEL\left(\frac{mg}{m^3}\right) in\ human =\ DMEL\ (mg/kg\ bw/day)\ in\ rat\ \boldsymbol{x}\frac{1}{1.15\ m^3/kg\ bw/day} \tag{7.7}$$

7.2.3 Exposure pathway

To calculate the intake of the NS and NA through inhalation, the following USEPA (1998b) approach (Eq.7.8) is used:

$$E_i = \frac{[X_j]\ .\ A.\ \ DBR\ .EF.ED}{AT\ .\ BW} \tag{7.8}$$

Where E_i = the daily intake through inhalation (mg/kg/d); $[X_j]$ = environmental concentrations of NS and NA (mg m^{-3}); EF = Exposure frequency (days/ year); ED = Exposure duration (years); BW = Body weight (kg); AT = Averaging time (days); A = Inhalation absorption factor (1/ unit less); DBR = Daily breathing factor (m^3/day).

It is important to note is that before using the maximum sum of NS +NA concentration obtained from dispersion modelling in E.q 7.8, the modeled concentrations have to be converted to the respective environmental NS + NA concentrations (X_j) within census areas around the PCCC plant. For this reason, Census Output Areas (COAs) with an average population of 300 were obtained from UK Small Area Health Statistics Unit (SAHSU) for 2011, originally supplied by the Office for National Statistics (ONS). For Mongstad the COAs were obtained from Statistics Norway. An area-weighting approach for the human exposure assessment for all the COAs that overlaps with the 30 km by 30 km study domain using the following relationship was used:

$$X_j = \sum_{S=1}^{S}([NS + NA])\frac{A_{sj}}{A_j} \quad (7.9)$$

Where X_j = is the concentration in COA *j*; [NS +NA] is the modelled pollutant concentration in grid cell s, *Asj* is the area of grid cell *s* lying in COA *j*, and *Aj* is the area of COA *j*.

7.2.4 Carcinogenic Risk characterisation

Carcinogenic risk is evaluated using the USEPA method (Eq.3). There are concerns when the risk value exceeds more than 1 in a million:

$$Risk_i = E_i.\,\mathrm{CSF}.\,\mathrm{ADAF}_i \quad (7.10)$$

Where

$$CSF = \frac{10^{-6}}{RfD} \quad (7.11)$$

Where E_i = the daily intake through inhalation (mg/kg/d) evaluated earlier, CSF = Cancer slope factor for NS and NA in this case $(mg/kg/d)^{-1}$; ADAF = Age-dependent adjustment factor for age bin I (1 / unit less) (USEPA 2015) and RfD is Risk Specific Dose (mg/kg-day) for the carcinogenic compound of interest. It is calculated from the reference concentration, RfC, which is the DMEL of 0.3 ng/m^3 i.e. 3 x 10^{-4} µg /m^3, as shown:

$$RfD = RfC\ x\ DBR\ x \frac{1}{BW} x\ \frac{mg}{10^3\ \mu g} \quad (7.12)$$

Using these equations gives a value for CSF $(mg/kg\text{-}d)^{-1}$ for as a function of age for the target receptor grouped as infants (0-4 years old), children (5-15 years old) and adults (16+ years old), respectively, as shown in Table 7.1, which is then used for the evaluation of the carcinogenic risk.

Table 7.1: Summary of parameters defined in the risk model for the different age groups of the population (USEPA 1998b).

Age (yr)	Exposure factors	EF (d/yr)	ED (yr)	BW (kg)	AT (d)	A	DBR (m^3/day)	ADAF	CSF $(mg/kg\text{-}d)^{-1}$

0 - 4	Infant	350	6	15	25550	1	10	10	5
5 - 15	Child	350	10	36	25550	1	20	3	6
16–90	Adult	350	30	70	25550	1	20	1	11.7

7.2.5 Uncertainty analysis

To account for uncertainties in the parameters used in the risk model and to predict the cancer incident probability from exposure to these amine and amine degradation products, a Monte-Carlo modelling approach was considered for infants, children and adults. Probability distribution functions based on the uncertainty of the parameters was defined in the risk model according to Table 7.2. The risk model was self-programmed in the symbolic mathematics engine, MATLAB. 1000, 000 iterations of this Monte-Carlo simulation were performed to achieve a stable and converged numerical output. This was done to determine the cancer risk probability for the population living within the studied domain.

Table 7.2: Probability distribution functions for the uncertain parameters defined in the risk model (TR = triangular [min, mode, max], LN= lognormal [geometric mean, geometric standard deviation]).

Parameters	Units	Infants	Children	Adult
Age	Year	0 - 4	5 - 15	16+
Body weight (BW) [a]	Kg	LN (6.79, 1.27)	LN (36.24, 1.05)	LN (59.78, 1.07)
Daily breathing rate [a]	m^3 /day	LN (5.69, 1.49)	LN (24.87, 1.38)	LN (32.74, 1.14)
Exposure duration [b] (ED)	Year	6	10	30
ADAF [b]	unit less	10	3	1
Inhalation absorption rate (A) [c]	unit less	1	1	1
[NS+NA] [d]	ng/m^3	LN (0.38, 0.13)	LN (0.38, 0.13)	LN (0.38, 0.13)
Exposure frequency (EF) [e]	day / year	Triangular [min, mode, max]; [180, 345, 365]	Triangular [min, mode, max]; [180, 345, 365]	Triangular [min, mode, max]; [180, 345,

				365]
Averaging Time (AT)[f]	Days	25550	25550	25550

N.B. CSF $(mg/kg/d)^{-1}$ is calculated from Eq 7.11 and Eq 7.12 considering the probability distribution functions defined for BW.

[a] Liao and Chiang (2006); [b]USEPA (2005); [c] CalEPA (2003);[d] This work (worst case O_3 scenario); [e](Smith 1994); [f](USEPA 1998b).

7.3 Results and discussion

7.3.1 Determination of DMEL

The evaluated DMEL using raw data from Peto *et al.* (1991b) for female rats ranged from 0 to 3.1 ng/m^3 whereas for male, the range was from 0 – 0.38 ng/m^3. Results demonstrated that the male rats were the most sensitive sex to the exposure. A small section of the calculations employing raw data from male rats is highlighted in Table 7.3. It can be seen that there are three doses that give (adjusted) tumour incidences closer to 25%. Therefore, the DMEL for each of these doses is evaluated and then an average of the evaluated DMELs is considered for the purposes of a worst case scenario.

Table 7.3: Estimation of DMEL for NDMA using the obtained T25 from raw data collected by Peto *et al.* (1991b) for bile duct tumours in male rats.

$dose_{rat}$ (mg/kg bw/d)	$dose_{human}$ (mg/kg bw/d)	Exposure and Observation time (months)	No. of male rats with tumours	Adjusted tumour incidence (%)	T25 (m/kg bw/d)	DMEL (ng/m^3) for 10^{-6} risk
0.109	0.027	30.48	13	18.26	0.059	0.205
0.131	0.032	28.44	14	20.00	0.056	0.196
0.174	0.043	25.44	19	28.70	0.042	0.145

The estimated DMEL value of 0.2 ng/m^3 was determined using oral data from rat. Additionally, inhalation data collected by Klein *et al.* (1991) was also used to evaluate DMEL. The same approach as Låg *et al.* (2011) was used to calculate DMEL (details of the calculation were explained in chapter 4). A value of 0.4 ng/m^3

was evaluated which was in agreement to that estimated by Låg *et al.* (2011). An average of the DMEL evaluated using the two different approaches is then considered which is 0.3 ng/m^3.

The obtained DMEL value is deduced to be the safest concentration with respect to cancer risk estimations for genotoxic substance such as NS and NA from the PCCC process. It is in very good agreement to the ones established by other regulatory authorities and researchers such as Låg *et al.* (2011) which suggest a values of 0.30 ng/m^3 using oral exposure data from Peto *et al.* (1991a) and Peto *et al.* (1991b) as well as inhalation exposure data from rat studies by Klein *et al.* (1991).

Others have set their own standards such as WHO (2008) suggesting a DMEL value of 0.31ng/m^3, HealthCanada (2011) of 0.31 ng/m^3 and Cal-EPA (2006) of 0.28 ng/m^3. USEPA (1986) suggests a lower DMEL value of 0.07 ng/m^3, whereas Ravnum *et al.* (2014) suggests a value of 0.86 ng/m^3 for NDMA of using raw data by Peto *et al.* (1991a) and Peto *et al.* (1991b) raw data to calculate an average value for T25 from three doses as opposed to using that the calculated T25 by Dybing *et al.* (2008) which was considered in the study by Låg *et al.* (2011). Ravnum *et al.* (2014) also used a linearised approach as opposed to a large assessment factor resulting in a higher calculated value.

In chapter 4, detailed description of calculations performed by Låg *et al.* (2011) for the DMEL of NDMA derived from inhalation and oral studies was given. In this work, the DMEL is calculated following a modified Ravnum *et al.* (2014) approach. Here the oral rat exposure data is extrapolated to human inhalation exposure with T25 calculated according to e.q 7.1 following Ravnum *et al.* (2014). However, Ravnum *et al.* (2014) did not adjust the dose in rats to the dose in human, whereas, this extrapolation was taken into account according WHO (2008). Also, the % tumour incidence for consideration in e.q 7.1 was calculated and adjusted according WHO (2008) in this work. Therefore, the obtained DMEL value of 0.3 ng/m^3 is comparable to those obtained by other government bodies and researchers. Thus, it is assumed that the type of extrapolation method employed is of minimal significance.

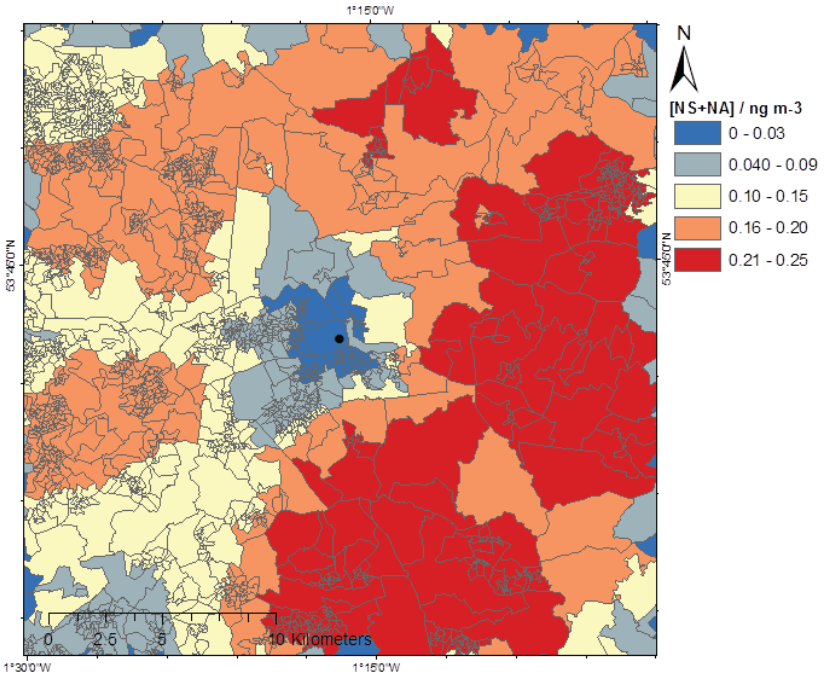
Since there is lack of data in literature on nitramines (expect for only Fjellsbø *et al.* (2013)), the estimated DMEL for nitrosamines can also be applied to the nitramines. This is due to the pronounced potency of nitrosamines in comparison to nitramines.

7.3.2 Exposure assessment

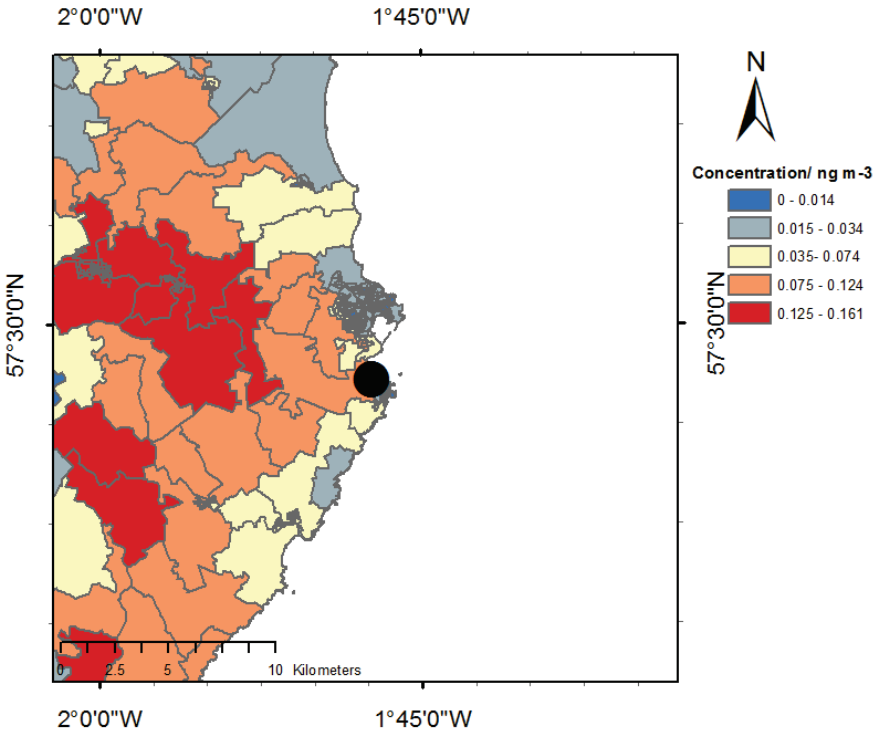
The calculated maximum emission rates for MEA, DMA and MA for each of the emitting plant along with their corresponding maximum long term-average concentration of the total nitrosamine and nitramines are shown in Table 7.4. It can be seen that for Ferrybridge and Peterhead their maximum long term-average concentration of the total nitrosamine and nitramines of 0.29 and 0.28 ng m^{-3} whereas for Mongstad it is 0.34 ng m^{-3}. However, the concentrations form the atmospheric dispersion modelling need to be adjusted for environmental concentrations of these chemicals of interest within census areas around each of the PCCC plant using an area-weighting approach as shown in Figure 7.1a-c. It is observed that the resulting concentrations are reduced with the maximum value now being 0.25, 0.16 and 0.17 ng m^{-3} for Ferrybridge, Peterhead and Mongstad. Therefore, from the exposure assessment it is seen that no human population exposed to concentration above the established DMEL value of 0.30 ng m^3 to adversely affect the human health.

Table 7.4: Maximum amine emission rates, total NS and NA concentratrions calcuated for Ferrybridge, Peterhead and Mongstad for the worst case scenario.

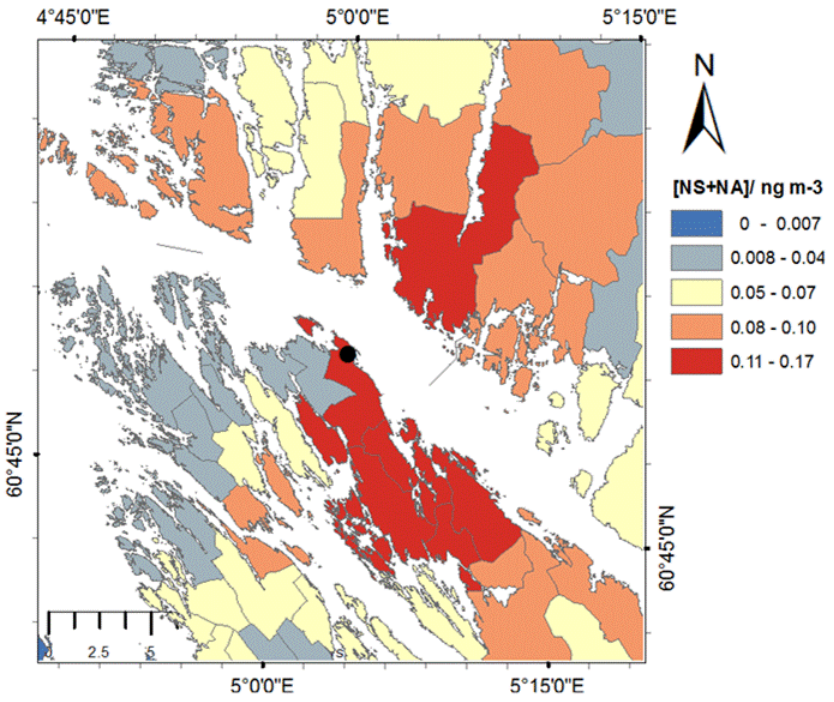
	Maximum emission rates (g/s)	Maximum long term-average [NS+NA] / ng m^{-3}	Readjusted Maximum long term-average [NS+NA] / ng m^{-3}
Ferrybridge	MEA 20.8 DMA 138 MA 125	0.29	0.25
Peterhead	MEA 26.8 DMA 20.5 MA 5.39	0.28	0.16
Mongstad	MEA 7.59 DMA 0.87 MA 22.5	0.34	0.17


1°15'0"W
N
[NS+NA] / ng m-3
0 - 0.03
0.040 - 0.09
0.10 - 0.15
0.16 - 0.20
0.21 - 0.25
53°45'0"N
53°45'0"N
0
2.5
5
10 Kilometers
1°30'0"W
1°15'0"W

(a)


2°0'0"W
1°45'0"W
N
Concentration/ ng m-3
0 - 0.014
0.015 - 0.034
0.035- 0.074
0.075 - 0.124
0.125 - 0.161
57°30'0"N
57°30'0"N
0
2.5
5
10 Kilometers
2°0'0"W
1°45'0"W

(b)



(c)

Figure 7.1: Rescaled annual average concentration of [NS+NA] ng m^{-3} to Census Output Areas for exposure assessment for the worst case estimates from the three amines over a 30 km by 30 km domain centered on (a) Ferrybridge for the meteorological year of 2012 (b) Peterhead for 2008 and (c) Mongstad for 2012.

7.3.3 Human health risk assessment

The number of infants, children and adults living in the census boundary covering a domain of 30 km by 30 km centred on Ferrybridge and Peterhead, respectively, are shown in Table 7.5. Due to confidentiality reasons Statistics Norway could not provide detailed information on the number of infants, children and adults constituting of the total population living around Mongstad.

Table 7.5: The number of infants, children and adults living around Ferrybridge, Peterhead and Mongstad as par their respective census data.

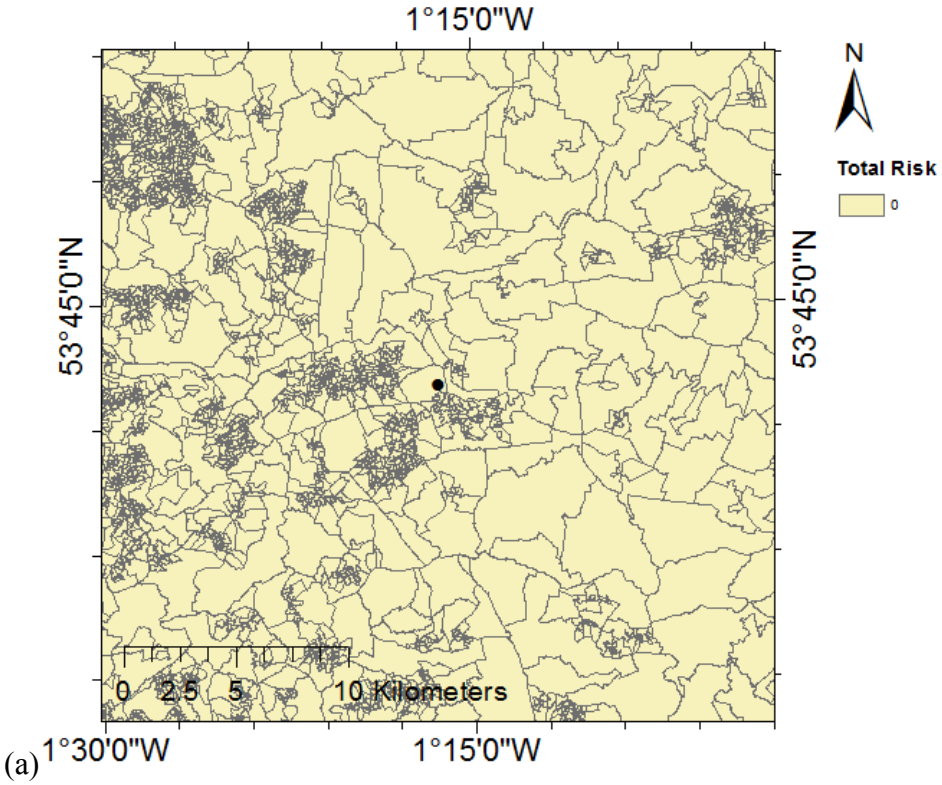
	Age 0-4 years	Age 5-15 years	Age 16-90+ years
Ferrybridge	36,379	74,447	466, 447
Peterhead	2024	4203	28996
Mongstad		107852	

Cancer risk determinations have been conducted at each grid point of the study domain for each site using E.q 7.10. Results show that there is no risk to the adults,

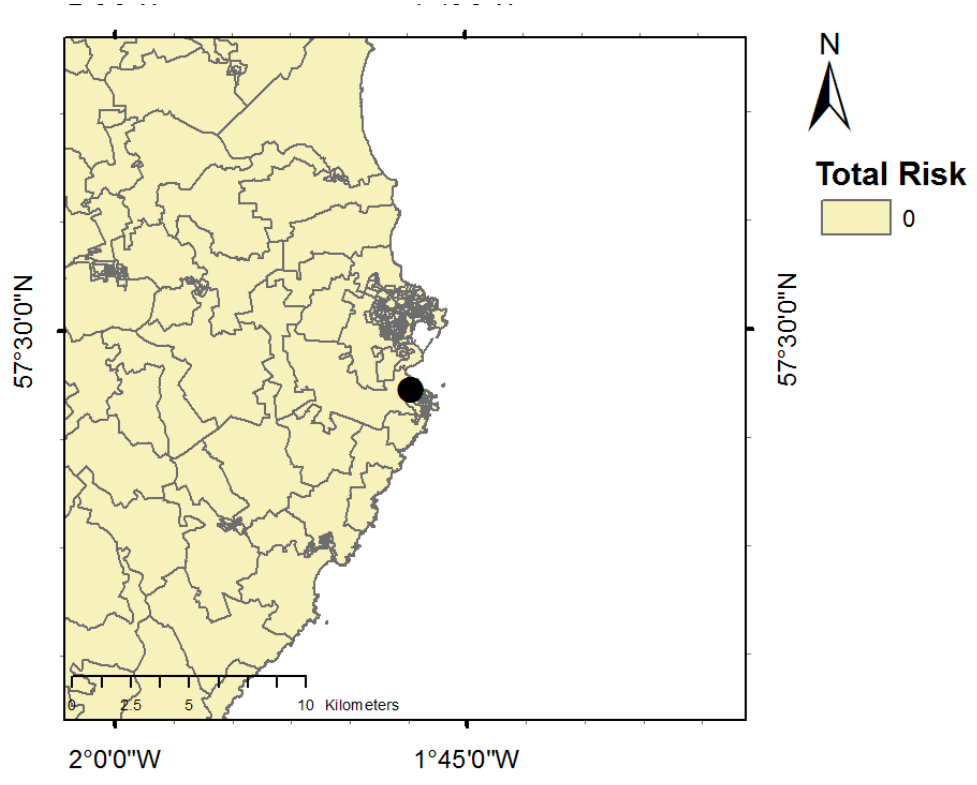
children and neither to the infants for developing cancer from long term exposure to the NS and NA that form from the amine emissions from Ferrybridge and Peterhead, respectively (Figure 7.2a-b).

For Mongstad, despite not knowing the exact number of infants, children and adults that constitute of the total population, cancer risk determinations have nevertheless been conducted at each grid point of the study domain. At first the risk is calculated assuming all of the resident people are adults, the results show that there is no risk of developing cancer. However, if it is assumed that all the people were either all children or infants, then again no child or infant was observed to developing cancer from long term exposure to the NS and NA that form from the amine emissions from this site (Figure 7.2c).

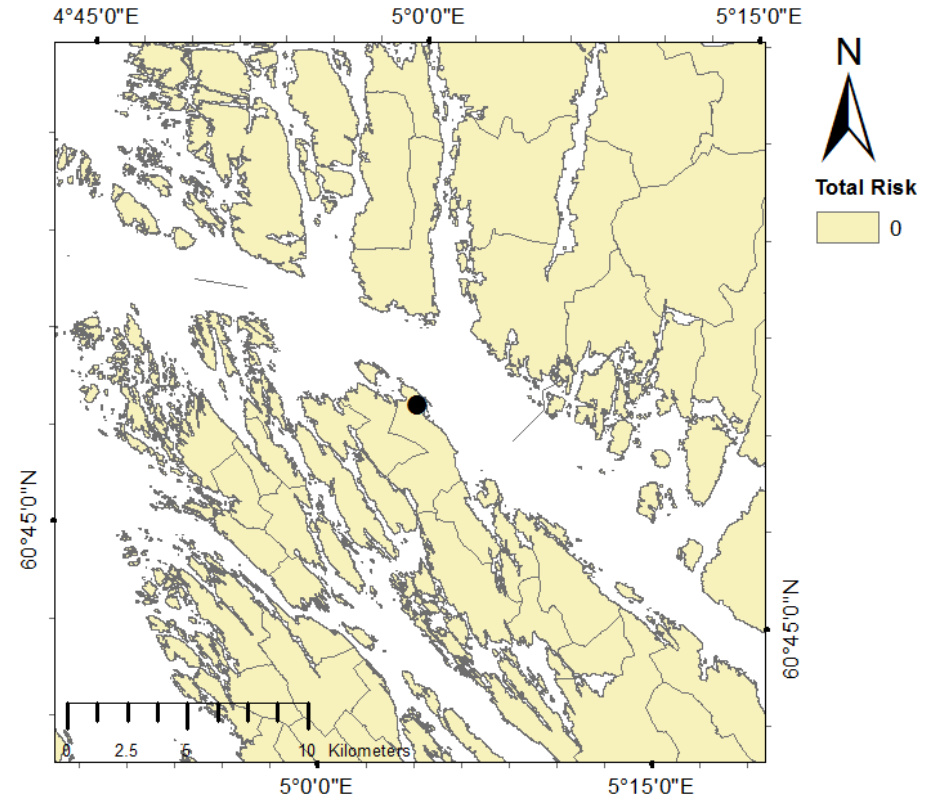
Overall, for all the three emitting facilities, it is observed that the maximum risk value for the worst case scenario does not exceed the threshold value of $1.0x10^{-6}$ where action is required. For this reason, there is no risk to the people living near the plant.



(a)



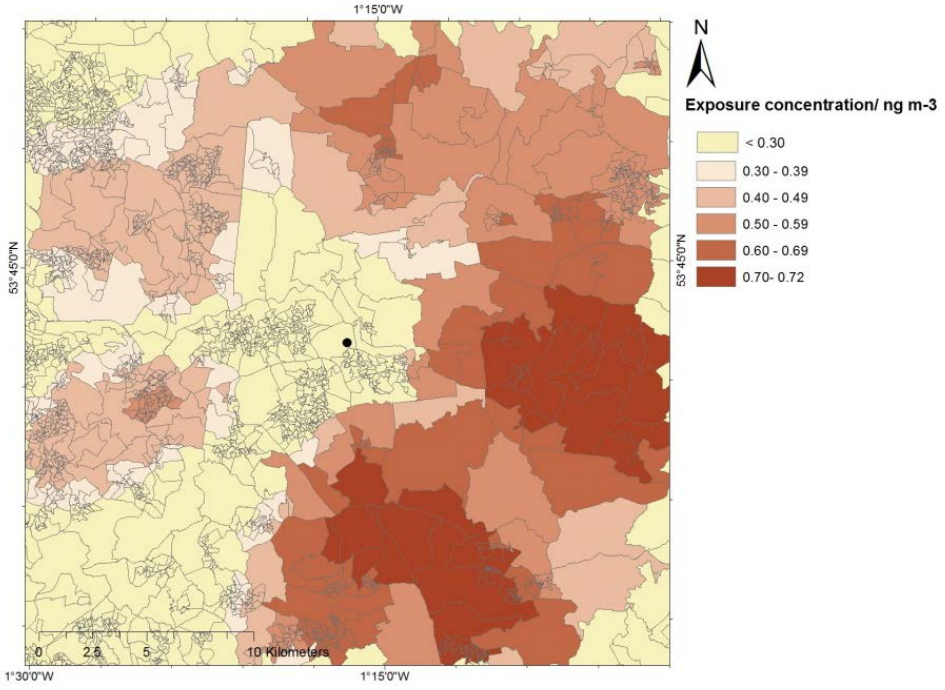
(b)



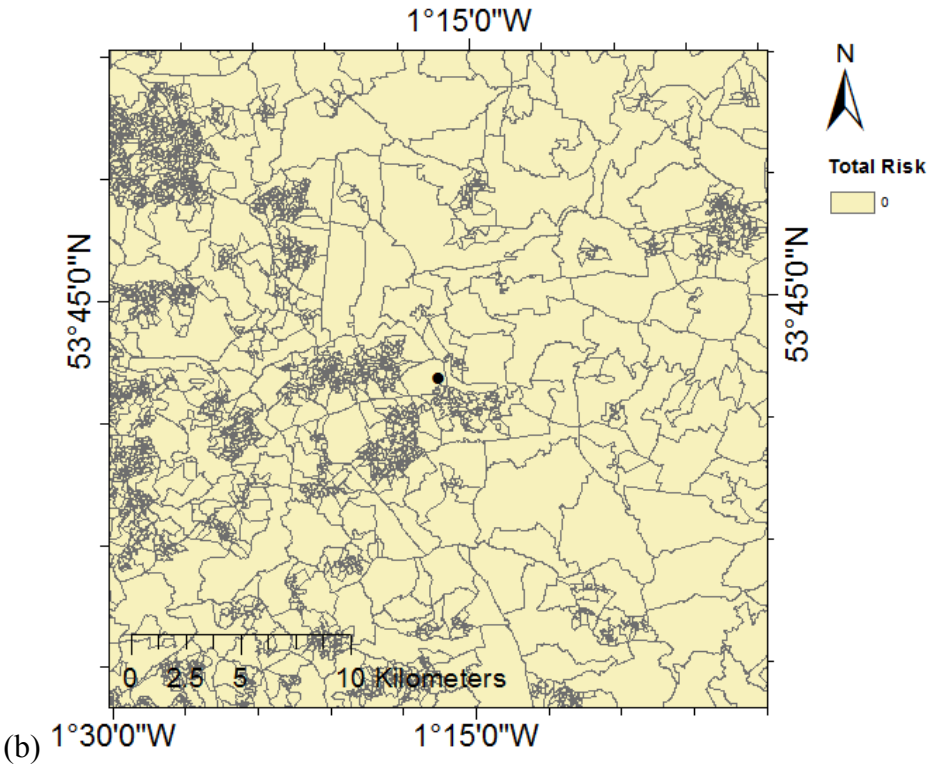
(c)

Figure 7.2: Census area output showing the total (adult + child + infant) carcinogenic risk to the population in the study domain centered on (a) Ferrybridge (b) Peterhead and (c) Mongstad.

However, when exposure assessments were performed on the sensitivity output of the most uncertain parameter, O_3, for Ferrybridge as shown in Figure 7.3a, it was seen that about 16545 infants, 34699 children and 223103 adults were exposed to concentrations above 0.30 ng/m^3. Cancer risk determinations showed that none of the population was susceptible to developing cancer from long term exposure to the NS and NA that form from the amine emissions from the power plant (Figure 7.3b). The total maximum risk for this scenario is 4.57x10^{-7}, which is below the threshold value. It should be noted that this a highly improbable case, as this is the most unfavorable scenario which gives fictive risk estimates. So even though such a scenario would be highly unlikely to happen under real plant operating conditions, it would still be recommended to ensure that the general population is not exposed to concentrations of NS and NA higher than 0.3 ng/m^3 to keep the risk as negligible.



(a)

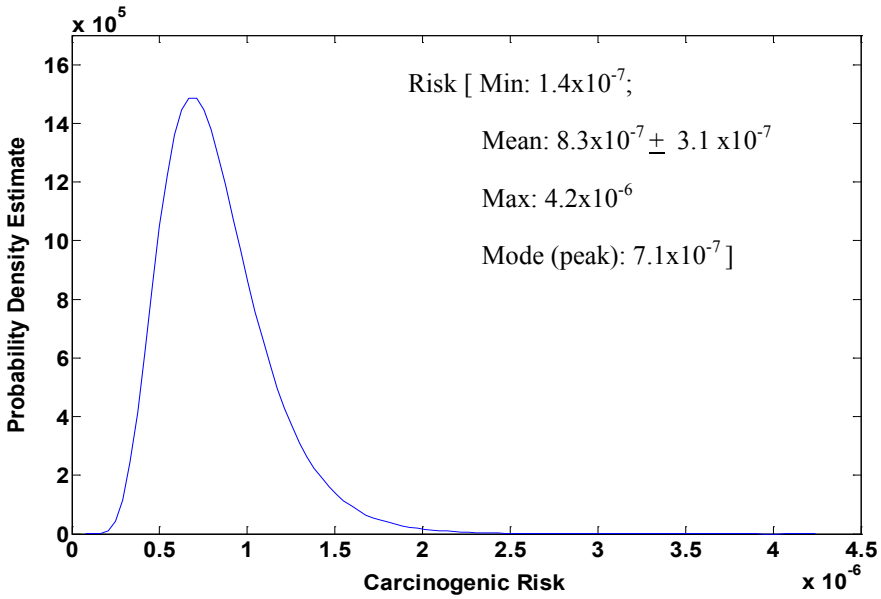


(b)

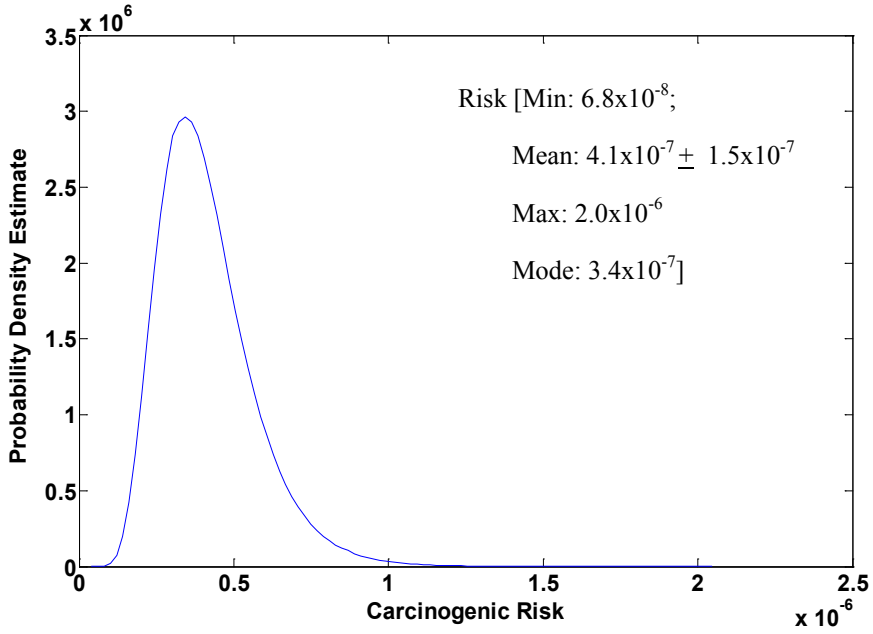
Figure 7.3: (a) Highlighted census area exposed to concentrations above 0.3 ng/ m^3 (b) total cancer risk for Ferrybridge for the sensitivity scenario of maximum concentration of O_3.

7.3.4 Probabilistic risk assessment

For the probabilistic health risk assessment, a probability density function of Monte Carlo Simulation results for infant, child and adult as well as the corresponding cumulative probability is shown in Figure 7.4a-d. A distribution of the risk is observed in each case with maximum risk calculated as $4x10^{-6}$, $2x10^{-6}$and $2x10^{-6}$ for infant, child and adult. These values are 2 and 4 times higher than that defined by USEPA of 1 in a million ($1x10^{-6}$), suggesting a potential cancer risk to 4 out of a million infants, 2 out of a million children and 2 out of a million adults. However, the corresponding probability density estimate for the maximum risk for each of the receptor is well below 1, therefore these estimates are unlikely to occur. Additionally, the mode of the risk is found to be between $7.1x10^{-7}$ for infants and $3.4x10^{-7}$ for children and adults and these are well below the $1x10^{-6}$ threshold.

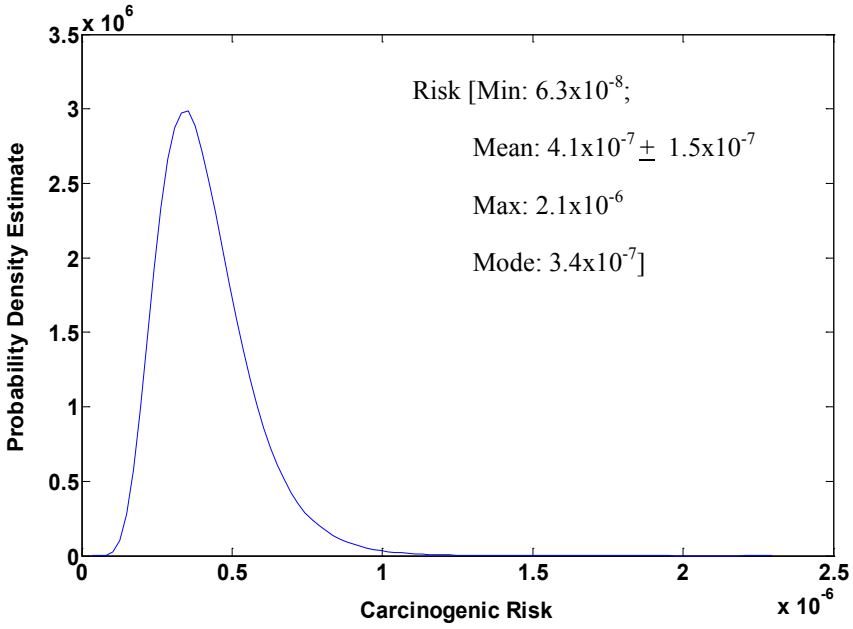

x 10^5
16
14
12
10
8
6
4
2
0
Probability Density Estimate
Risk [Min: 1.4x10^-7;
Mean: 8.3x10^-7 ± 3.1 x10^-7
Max: 4.2x10^-6
Mode (peak): 7.1x10^-7]
0
0.5
1
1.5
2
2.5
3
3.5
4
4.5
Carcinogenic Risk
x 10^-6

(a)


x 10^6
3.5
3
2.5
2
1.5
1
0.5
0
Probability Density Estimate
Risk [Min: 6.8x10^-8;
Mean: 4.1x10^-7 ± 1.5x10^-7
Max: 2.0x10^-6
Mode: 3.4x10^-7]
0
0.5
1
1.5
2
2.5
Carcinogenic Risk
x 10^-6

(b)

(c)



(d)

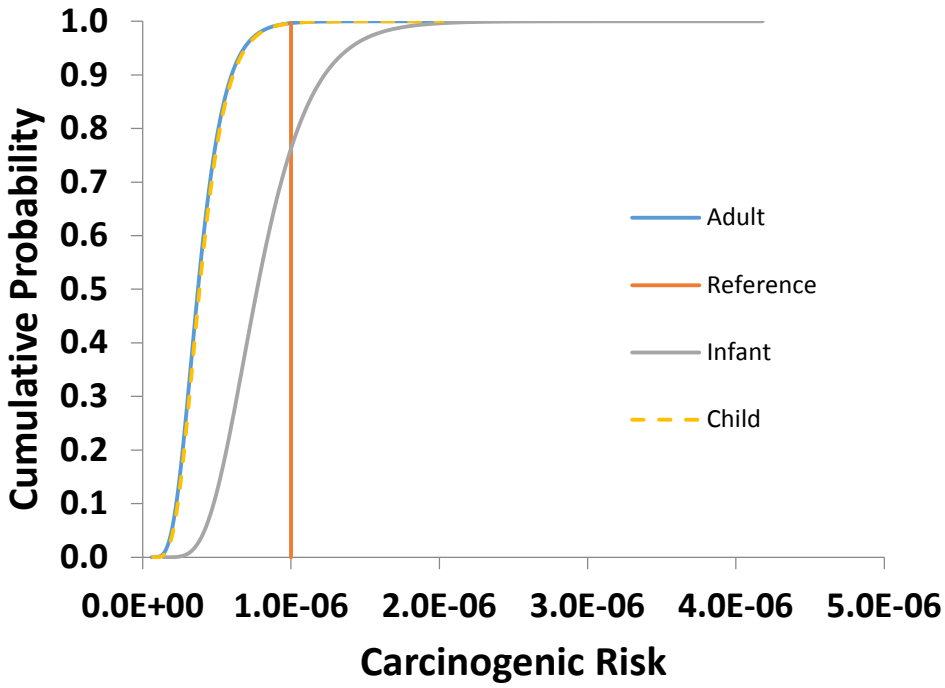


Figure 7.4: Probability density function of Monte Carlo simulations result for the (a) infant health risk (b) child health risk (c) adult health risk and (d) comparison of the distributions for infant, child and adult with the reference risk level of 10^{-6}.

7.4 Environmental risk analysis

In this study, the total nitrosamine and the total nitramine from the three amines deposited to water was calculated each of the capture plant, which is the PEC value. The established PNEC values in literature are stated in Table 7.6. The ratio of PEC/PNEC gives the environmental risk value which if less than 1 suggests that there is no risk from the chemical discharges to the environment.

Accordingly, as seen from Table 7.6, the environmental risk for Ferrybridge and Mongstad with respect to MEA is greater than 1 which can affect aquatic life, where for Peterhead the risk is below 1.

With respect to nitrosamine in aquatic life and drinking water only for Mongstad the risk is below 1 but not for the other two sites.

For nitramine, there is no risk from drinking water with respect to all the capture plants. There is also no risk to the aquatic environment.

If the threshold of 4 ng/L for the total NS and NA established for Mongstad, is applied then it is obvious that none of the capture facility meets the safety regulatory limit with respect to drinking water.

Overall, it is concluded that for all the capture sites, there is some risk attributable to the environment from the chemical discharges in the atmosphere which get deposited to the aquatic environments such as lakes. Conversely, it should be noted that these results are for a fictive worst case studies designed with respect to safety limits of the NS and NA in air. Since the safety limits are different for the two different environmental compartments, the results are only suitable for comparison with the respective environmental medium. It is best to re-design each of the worst case studies with respect to critical amine concentration in water as opposed to air, if the risk is to be kept a minimum.

Table 7.6: Environmental risk analysis for each of the capture plant with their corresponding PEC/PNEC values.

Water ng/L	MEA	NS	NA	PEC/PNEC MEA	NS		NA	
					aquatic	drinking	aquatic	drinking
Ferrybridge	8719	40	97	>1	2	6	0	0
Peterhead	6011	32	79	<1	>1	5	0	0
Mongstad	9490	0.43	38	>1	0	0	0	0
Safety limits (ng/L) aquatic	7500	25	200					
Drinking water	-	7	1000					

7.5 Conclusions

Risk estimations of cancer risk caused by exposure to the chemical pollutant discharges were performed following the USEPA (1998b) method which considers the atmospheric concentrations of NS and NA obtained from atmospheric chemistry and dispersion modelling. The maximum cancer risk for humans is within acceptable limits for the scenarios considered for each of the plants.

To account for uncertainties in the parameters used in the risk model and to predict the cancer incident probability from exposure to these amine and amine degradation products, a Monte-Carlo modelling approach was considered. A probability distribution function based on the uncertainty for some of the parameter was defined in the developed risk model. 1000, 000 iterations of the Monte-Carlo simulation were performed to achieve a stable and converged numerical output. This was done to determine the cancer risk probability for the people living within the studied domain. Results show a distribution of the risk with the maximum risk calculated as $4x10^{-6}$, $2x10^{-6}$and $2x10^{-6}$ for infant, child and adult. This suggests a potential human health risk to 4 out of a million infants, 2 out of a million children and 2 out of a million adults. However, the corresponding probability estimate density for the maximum risk for each of the receptor is well below 1, therefore unlikely to occur. Additionally, the mode of the risk is found to be between $7.1x10^{-7}$ for infants and

$3.4x10^{-7}$ for children and adults, which are well below the $1x10^{-6}$ threshold. Hence, there is no risk to the human health.

The risk from exposure of these chemicals in drinking water was also estimated along with the risk to the aquatic environment. It was predicted that there was some risk attributable to the environment from the MEA and the total NS except for the total NA for the worst case scenario modelled on each of the plants. Therefore, it would be suggested to risk managers and decision makers to keep the amine emissions lower than the maximum tolerable emissions rates estimated to have negligible risk with respect to the aquatic life and drinking water.

On the whole, the obtained finding from this work strongly support that the developed methodology is reliable in assessing the fate of the amine emissions which remains a key area to address for the large scale carbon capture and storage implementation. The method is new as it conjoins theoretical quantum chemistry and kinetic modelling to atmospheric dispersion modelling to cancer and environmental risk assessments. It makes it possible to account for the atmospheric chemistry, dispersion, deposition of amine and its degradation products from the plant both temporally and spatially. Useful information can be provided to risk managers in terms of the number of people who might be at a risk of developing cancer from an emitting facility or even a proposed one. By doing so, the fate of the released pollutants from amine-based post combustion CO_2 capture technology can be assessed as completely as possible.

Nevertheless, there is still a need to perform toxicology studies and extensive field experiments to assist with the in-depth understanding of the impacts of amine based PCCC technology on the environment (Karl *et al.* 2011) a lot more realistically.

Chapter 8 Conclusions and Recommendations for Future Research

8.1 Achievements and conclusions from the research

Amine-based solvent PCCC technology results in the production of malevolent compounds such as nitrosamines and nitramines. It is, therefore, a pre-requisite to gain a sound understanding of the atmospheric processes that govern the fate of these chemical discharges. The assessment of atmospheric fate of these amine emissions in the atmosphere is acquired by studying their atmospheric chemistry, their expected dispersion and transport pathways away from the source and deposition to the soil and water. By doing so, the concentrations of the amines and amine degradation products from the plant both temporally and spatially are assessed as fully as possible. Subsequently, the risk posed to human health and the natural environment is estimated.

In this work, the reactions of the amines of interest (MEA, DMA and MA) with OH radicals and of the resulting alkyl amino radicals with NO, NO_2 and O_2 were investigated using a combination of quantum chemical methods and kinetic modelling. An insight into relevant reaction mechanisms describing the entire amine atmospheric chemistry was acquired. Reaction coefficients for every reaction defining the amine atmospheric chemistry scheme were evaluated. It was observed that the calculated rate constants for DMA were within the same order of magnitude to those determined experimentally. Hence, a very good agreement between the

calculated and the experimental rate constants was achieved. For this reason, it was presumed that, in the absence of experimentally reported rate constants, the method used for evaluating the kinetics describing the atmospheric chemistry of DMA was appropriate for MA and MEA. As the calculated rates were independent of any experimental parameters, therefore, the established method is applicable to any generic amine used in the PCCC process.

Results also showed that the reaction of the amines with OH radical was the fastest, whereas, the reaction of the amino radical with O_2 was the slowest step in the scheme. Imines were as a result found to be more stable and expected to prevail in the atmosphere.

Due to the role of the amines and its carcinogenic products such as, nitrosamines and nitramines in the atmosphere, it is imperative to determine their lifetimes. The outcome of this study shows that MA has a longer lifetime than MEA. Subsequently, primary amines form primary nitrosamines that are highly unstable with very short lifetimes in comparison to stable nitrosamines formed from secondary amines. Though nitrosamines undergo photolysis, nitramines are comparatively stable and can undergo dissociation to form their corresponding imines. Imines such as methylene imine have been discovered in interstellar cloud dust (Godfrey *et al.* 1973, Dickens *et al.* 1997).

The fundamental value of the developed technique is that one theoretical method is capable of investigating the reactions mechanisms and evaluating reaction kinetics of any generic amine with atmospheric OH radicals and of the resulting alkyl amino radicals with NO, NO_2 and O_2, therefore, making it universal. Since the method is independent of experimental data, it is possible to study amines that have not been experimentally investigated as yet.

The method is further developed by adjoining quantum chemistry theoretical methods and kinetic modelling to dispersion and deposition calculation. It is achieved by using the calculated rate constants to serve as input variables for advection-diffusion-reaction equations to be solved by an air dispersion model, ADMS 5. This can assist in the the determination of accurate environmental concentrations of the amine, nitrosamines and nitramines in time and space away from the emitting source.

To illustrate the implementation of the approach, case studies on three significant capture plants at different geographic locations were conducted. Maximum tolerable emissions of the amine emissions were proposed for each of the site such that the resulting nitrosamines and nitramines are within the proposed safety limits. Hence, worst case scenarios were created from modelling experience such that the risk from these chemical discharges for each of the emitting source was acceptable to the human health and the immediate environment.

To account for uncertainties in the parameters considered in the study, parametric sensitivity analysis was performed on a base line case which was the Ferrybridge plant. Due to this, the parameters that most influenced the fate of the resulting nitrosamines and nitramines from PCCC process were determined. The study revealed that the nitrosamines and nitramines concentrations displayed an exponential dependency on stack height and stack diameter, respectively. A linear dependency with O_3 background concentration was also observed. Other parameters such as plume velocity, plume temperature, OH and NO_x concentrations also influenced the fate of the nitrosamines and nitramines. However, the relationship between these parameters and the concentrations showed a more complex and non-linear dependence. Overall, the sensitivity study uncovered the factors which should be considered in keeping the amount of the amine degradation products as small as possible.

The understanding grown from sensitivity analysis on Ferrybridge can be generalised to Peterhead and Mongstad. It is perceived that the reason Mongstad has the largest nitrosamines and nitramines concentrations in air for the worst case study is due to its stack height and diameter, plume velocity and temperature being lowest in comparison to the other two plants. The emissions therefore do not disperse further from the Mongstad stack as well as reach to the upper layers of the atmospheric boundary layers. Hence, it is crucial for risk managers and decision makers to consider such substantial parameters during the design and consent phase of potential industrial applications.

Again, the method is developed even further by conjoining it to cancer risk estimations from exposure to these chemical discharges using the USEPA (1998b) method. Deterministic risk estimations with respect to nitrosamines and nitramines

show that the maximum cancer risk for humans is within acceptable limits for the scenarios modelled on each of the plants.

Additionally, to account for the uncertainties in the parameters, their respective probability distribution function was considered in a risk model. The cancer incident probability from exposure to these amine and amine degradation products was predicted using a Monte-Carlo modelling approach. Results depicted a normal distribution of the risk, with a maximum risk lower than that defined by USEPA of 1 in a million. Hence, no risk to the human health was predicted. Risk from exposure to MEA, total nitrosamines and nitramines in drinking water as well as to the aquatic environment was also estimated. The studies conducted on each of the plants, showed that there was some risk was associated with MEA and nitrosamines but not to nitramines.

Hence, the developed methodology is novel as it combines theoretical quantum chemistry and kinetic modelling with dispersion and deposition calculations to cancer and environmental risk assessments. The established approach makes it possible to assess the fate of any generic amine both temporally and spatially from any amine-based PCCC plant irrespective of its size and geographic location. Useful information with regards to the impacts of amine-based PCCC technology can be provided to decision makers and risk managers in terms of the number of people who might be at a risk of developing cancer from an emitting facility or even a proposed one.

Commercial scale implementation of the PCCC technology using amine solvents is not as extensive because is in its early stages. The world's first commercial scale PCCC the installation has been to a current Boundary Dam power station in Canada, which began operation in October 2014. A pictorial representation of some of the operational or under construction PCCC plants worldwide is given in Figure 8.1. It is essential to make sure that the PCCC process is associated with an overall positive human health and environmental impact. Therefore, with the established procedure it can be made sure if a proposed facility complies with the safety regulatory limits, essential for its chemical discharge permit. The approach can also establish maximum tolerable amine emissions for an emitting facility which should not be exceeded to keep the risk to human health and the immediate environment tolerable.

The technique can in fact be used to propose ideal plant design parameters and an ideal geographical location for a proposed industrial application. Hence, if a PCCC plant is carefully planned, placed and operated, the advantage of employing amines for reducing the enormous CO_2 emissions would most likely outweigh the risk associated with solvent discharge issues.

In conclusion, the outcome from this work strongly supports that the developed methodology is reliable in assessing the fate of the amine emissions which remains a key area to address for the large scale carbon capture and storage implementation. Therefore, the findings of this research are aimed at delivering crucial and useful data to the CO_2 capture industry especially for compliance with air quality regulations.



Figure 8.1: A pictorial representation of some of the operational or under construction PCCC plants worldwide.

8.2 Limitations and unanswered questions

For a complete environmental risk assessment, detailed and reliable emission data for PCCC plants is essential. Such data is the basis for developing accurate risk assessment as it provides the necessary atmospheric input concentrations which can then be assessed for the environmental fate processes described. The absence of this vital input data due to lack of measurements as well as confidentiality reasons, prevented the atmospheric and environmental fate of these amine emissions from being utilised in a full and relevant risk assessment. Therefore, worst case scenarios

were created from experience which gave estimated results which overestimate all values. If there was experimental data of the ambient concentrations of the products of interest such as, amines, NS and NA in the study domain around the emitting facility, it could have been used to validate the modelling study results. This could have increased the confidence in using modelling results for drawing conclusions with regards to the maximum tolerable emissions of amines and the corresponding degradation products from PCCC plants. However, experimental studies have yet not been able to detect nitrosamine and nitramines as they are below detection levels.

The amine chemistry considered is not very detailed, but very simple and is only restricted to gaseous phase. The chemistry scheme can be extended to incorporate much more detail when information from experimental studies becomes available. The scheme can also be extended to account for aqueous phase chemistry as well as particulate formation from amines.

Future work into the development for accurate quantitative estimations for environmental fate and toxicity assessment of nitrosamines and nitramines would be beneficial. This would offer a modelling tool based on experimental data for the future assessment of other nitrosamine and nitramine compounds as degradation products from MEA or other amine solvents used in PCCC.

8.3 Recommendation for Future Research

On the whole, this study enhanced the existing understanding with respect to amines and their impact on the human health and the natural environment. However, there is sparse toxicity data on nitrosamine and nitramines. Therefore, the study has had to rely on using previous and/or related literature data.

There are still a number of key knowledge gaps which need to be addressed before amines can be employed for CO_2 capture at a full-scale plant. Some of the recommendations are explained below.

- One of the limitations in this work was the lack of detailed emission data; therefore, in future direct emissions data would be best to be used in carrying out future risk assessments for full scale PCCC plants. Such full scale plants should conduct exhaustive emission programs so as to obtain reliable emission data. By doing so the main remaining concerns with respect to PCCC emissions would be addressed.

-There is a need to perform atmospheric experiments which could involve using real samples from the emissions to completely characterise these chemical discharges using analytical techniques. This would assist in addressing the uncertainty associated with the formation, accumulation and lifetimes of NS and NA in the atmosphere. The atmospheric chemistry scheme can then be extended to account for the mechanisms for the newly identified products.

-There is also an immediate need to perform field experiments to measure the ambient concentrations of the products of interest such as amines, NS and NA in the study domain around the emitting facility. The experimental data can be used to validate the results from the modelling studies. This will increase the confidence in using modelling results for drawing conclusions with regards to the maximum tolerable emissions of amines and the corresponding degradation products from PCCC plants.

-If a dispersion model can account for a very detailed chemistry of the amines and could solve the dispersion and chemistry simultaneously, the accuracy in the results can be increased.

-Additionally, due to the carcinogenic nature of these chemical discharges, there is a need to perform vigorous sensitivity studies to assist with the development of the regulatory limits for PCCC and their consideration for full-scale plants.

-Toxicity and ecotoxicity studies are also required to assist with the understanding of the impacts of amine-based solvent PCCC technology on humans and the environment (Karl *et al.* 2011) a lot more realistically. For this the toxicity exposure limits would require further improvement to develop the current regulatory limits. Both experimental and laboratory approaches are needed to study the impact of amines, NS and NA on humans and the environment such as terrestrial and aquatic ecology.

In due course when more detailed information is available with respect to newly identified toxic products from amine-based CO_2 capture technology, then this developed methodology can be extended to account for them.

References

. "Computational Chemistry Comparison and Benchmark Database." 2015, from http://cccbdb.nist.gov/exp1x.asp.

Aas, N., et al. (2010). Emission measurements at Dong's pilot plant for CO2 capture in Esbjerg. in Environmental Impacts of Amine Emission During Post Combustion Capture, Oslo, Norway.

Andersen, A., et al. (2008). "First-principles-derived kinetics of the reactions involved in low-temperature dimethyl ether oxidation." Molecular Physics **106**(2-4): 367-396.

Anderson, L. G., et al. (1988). "Kinetics of the reaction of hydroxyl radicals with 2-(dimethylamino)ethanol from 234–364 K." International Journal of Chemical Kinetics **20**(2): 103-110.

Angove, D., et al. (2013). Deliverable 4.2: Determination of the fate of PCC emissions into the atmosphere. Prepared for: ANLEC R&D, CSIRO, Australia.

Atkinson, R., et al. (1977). "Rate constants for the reaction of the hydroxyl radical with methanethiol and methylamine over the temperature range 299-426 DegK." J. Phys. Chem **66**: 1578-1581.

Atkinson, R., et al. (1978). "Rate constants for the reactions of the OH radical with (CH3)2NH, (CH3)3N, and C2H5NH2 over the temperature range 298–426 °K." The Journal of Chemical Physics **68**(4): 1850-1853.

Azzi, M., et al. (2014). Assessing Atmospheric Emissions from Amine based CO2 PCC Process and their Impacts on the Environment A Case Study. Volume 2: Atmospheric chemistry of MEA and 3D air quality modelling of emissions from the Loy Yang PCC plant, CSIRO, Australia.

Barker, J. R., et al. (2003). "Master equation analysis of pressure-dependent atmospheric reactions." Chem. Rev. **103**(12): 4577-4592.

Batchelor, G. K. (2000). An Introduction to Fluid Dynamics, Cambridge University Press.

Becke, A. D. (1988). "Density-functional exchange-energy approximation with correct asymptotic behavior." Phys. Rev.A **38**(6): 3098-3100.

Becke, A. D. (1993). "Density ‐ functional thermochemistry. III. The role of exact exchange." The Journal of chemical physics **98**(7): 5648-5652.

Bedell, S. A. (2009). "Oxidative degradation mechanisms for amines in flue gas capture." Energy Procedia **1**(1): 771-778.

Bello, A., et al. (2005). "Pathways for the Formation of Products of the Oxidative Degradation of CO2-Loaded Concentrated Aqueous Monoethanolamine Solutions during CO2 Absorption from Flue Gases." Industrial & Engineering Chemistry Research **44**(4): 945-969.

Beychok, M. (2005). Fundamentals Of Stack Gas Dispersion. Irvine, CA, 92612, United States, Milton R. Beychok.

Bluett, J., et al. (2004). "Good Practice Guide for Atmospheric Dispersion Modelling." Ref. ME522, Ministry of the Environment, Wellington, New Zealand.

Booth, A., et al. (2012a). Environmental impacts of amines and their degradation products: Current status and knowledge gaps. 1st Post Combustion Capture Conference. Norway, SINTEF Materials and Chemistry.

Booth, A., et al. (2012b). Emissions from post-combustion CO2 capture plants Norway, SINTEF Materials and Chemistry**:** 5.

Borduas, N., et al. (2013). "Gas Phase Oxidation of Monoethanolamine (MEA) with OH Radical and Ozone: Kinetics, Products, and Particles." Environmental Science & Technology **47**(12): 6377-6383.

Bosanquet, C. H., et al. (1936). "The spread of smoke and gases from chimneys." Transactions of the Faraday Society **32**(0): 1249-1263.

Brakstad, O. G., et al. (2010). Support on input to environmantl discharges - Evaluation of degradation components, SINTEF.

Brantom, P. G. (1983). Dose-response relationships in nitrosamine carcinogenesis, University of Surrey.

Bråten, H. B., et al. (2009). Final Report on aTheoretical Study on the Atmospheric Degradation of Selected amines, NILU**:** 94.

Brooks, S., et al. (2008). "The toxicity of selected primary amines and secondary products aquatic organisms: A review."

Brown, J. L. (1999). "N-Nitrosamines." Occup Med **14**(4): 839-848.

Cal-EPA (2006). Public health goal for N-Nitrosodimethylamine in drinking water, NNitrosodimethylamine. California Environmental Protection Agency.

CalEPA (2003). "Air Toxics Hot Spots Program Guidance Manual for Preparation of Helath Risk Assessment."

Carl, S. A., et al. (1998). "Sequential two (blue) photon absorption by NO_2 in the presence of H_2 as a source of OH in pulsed photolysis kinetic studies: rate constants

for reaction of OH with CH_3NH_2, $(CH_3)_2NH$, $(CH_3)_3N$, and $C_2H_5NH_2$ at 295 K." J. Phys.Chem. A **102**(42): 8131-8141.

CERC. "http://www.cerc.co.uk/environmental-software/ADMS-model/options.html."

CERC. "http://www.cerc.co.uk/environmental-software/model-validation.html " Retrieved 8/7/15, from (http://www.cerc.co.uk/environmental-software/model-validation.html). .

CERC (2010). Modelling Atmospheric Dispersion for Components from Post-Combustion Amine-based CO_2 Capture in: Price, C.,Stocker, J, Carruthers, D, Strickland, S, McHugh, C. (Ed.), Contract number 257,430,113: Final report prepared for CO_2 Capture Mongstad Project, Gassnova SF

CERC (2012a). ADMS 5 Amine Chemistry Supplement.

CERC (2012b). ADMS 5 Atmospheric Dispersion Modelling System, User Guide version 5. Cambridge. **2013**.

CERC (2012c). Atmospheric Chemistry Modelling -Acitivity 1: Gaseous Phase Chemistry Modelling (inititaed by hydroxyl radical) - Executive Summary, in: Price, C., Strickland, S., Carruthers, D . (Eds.), Contract number 257,430,174: Atmospheric Chemistry Modelling. prepared for CO_2 Capture Mongstad Project, Statiol Petroluem SF**:** 25.

CERC (2012d). Atmospheric Chemistry Modelling Activity 1: Gaseous Phase Chemistry Modelling (initiated by hydroxyl radical), in: Price, C., Strickland, S. (Ed.), Contract number 257,430,174: Atmospheric Chemistry Modelling. prepared for CO_2 Capture Mongstad Project, Gassnova SF**:** 120.

CERC (2012e). NOx Chemistry model.

Chakma, A., et al. (1988). "Identification of methyl diethanolamine degradation products by gas chromatography and gas chromatography-mass spectrometry." Journal of Chromatography A **457**(0): 287-297.

Chakma, A., et al. (1997). "Methyl-diethanolamine degradation — Mechanism and kinetics." The Canadian Journal of Chemical Engineering **75**(5): 861-871.

CHEMESSEN, I. "Mol-Instincts." Mol-Instincts Chemical Property Database, from http://search.molinstincts.com/search/searchTextForm.ce.

Chi, S., et al. (2002). "Oxidative Degradation of Monoethanolamine." Industrial & Engineering Chemistry Research **41**(17): 4178-4186.

CICADS. (2002). "http://www.inchem.org/documents/cicads/cicads/cicad38.htm."

Climate, N. (2011). Pollution Agency: Permit for Activities Pursuant to the Pollution Control Act for CO2 Technology Centre Mongstad DA.

Crawford-Brown, D. J. (1999). Risk-Based Envrionmnetal Decisions Methods and Culture, Kluwer Academic Publishers, Norwell, MA.

da Silva, E. F., et al. (2012). "Understanding 2-Ethanolamine Degradation in Postcombustion CO2 Capture." Industrial & Engineering Chemistry Research **51**(41): 13329-13338.

Dacunto, P., et al. (2007). A Better Way to Illustrate Atmospheric Dispersion in the Classroom. American Society of Engineering Educators, Mid-Atlantic Section Spring 2007 Conference Proceedings, Newark, NJ.

Davis, J., et al. (2009). "Thermal degradation of monoethanolamine at stripper conditions." Energy Procedia **1**(1): 327-333.

de Koeijer, G., et al. (2009). "European CO2 test centre mongstad–Testing, verification and demonstration of post-combustion technologies." Energy Procedia **1**(1): 1321-1326.

de Koeijer, G., et al. (2013). "Health risk analysis for emissions to air from CO2 Technology Centre Mongstad." Int. J. Greenhouse Gas Control **18**(0): 200-207.

De Stefani, E., et al. (1996). "Dietary nitrosodimethylamine and the risk of lung cancer: a case-control study from Uruguay." Cancer Epidemiol Biomarkers Prev **5**(9): 679-682.

DEFRA. "http://laqm.defra.gov.uk/review-and-assessment/tools/background-maps.html."

Dickens, J. E., et al. (1997). "Hydrogenation of interstellar molecules: a survey for methylenimine (CH2NH)." Astrophys J **479**(1 Pt 1): 307-312.

Dunning, T. H. (1989). "Gaussian basis sets for use in correlated molecular calculations. I. The atoms boron through neon and hydrogen." The Journal of Chemical Physics **90**(2): 1007-1023.

Dybing, E., et al. (2008). "Risk assessment of dietary exposures to compounds that are genotoxic and carcinogenic--an overview." Toxicol Lett **180**(2): 110-117.

Dybing, E., et al. (1997). "T25: a simplified carcinogenic potency index: description of the system and study of correlations between carcinogenic potency and species/site specificity and mutagenicity." Pharmacol Toxicol **80**(6): 272-279.

ECHA/REACH (2012). Guidance on information requirements and chemical safety assessment,Chapter R.8: Characterisation of dose [concentration]-response for human health.

Eide-Haugmo, I., et al. (2009). "Environmental impact of amines." Energy Procedia **1**(1): 1297-1304.

eKlima. "www.sharki.oso.dmni.no."

Emmerson, K., et al. (2013). 3D Dispersion Modelling of Monoethanolamine (MEA) from a Hypothetical Power Station; Deliverable 4.3: Determination of the fate of PCC emissions into the atmosphere, CSIRO.

EPA. (2015). "Human Health Risk Assessment, United States Environmnetal Protection Agency." Retrieved 05/0615, 2015, from http://www.epa.gov/risk_assessment/health-risk.htm.

Eurostat. "http://ec.europa.eu/eurostat."

Eyring, H. (1935). "The activated complex and the absolute rate of chemical reactions." Chem. Rev. **17**(1): 65-77.

Fatehifar, E., et al. (2006). "A MATLAB ‐ based modeling and simulation program for dispersion of multipollutants from an industrial stack for educational use in a

course on air pollution control." Computer Applications in Engineering Education **14**(4): 300-312.

Fazil, A. M. (2005). A primer on risk assessment modelling: focus on seafood products. Food and Agriculture Organisation of United Fisheries technical Paper. Rome.

Fernandez-Ramos, A., et al. (2006). "Modeling the kinetics of bimolecular reactions." Chem. Rev. **106**: 4518-4584.

Finlayson-Pitts, B. J., et al. (1999). Chemistry of the upper and lower atmosphere: theory, experiments, and applications, Academic press.

Fitzgerald, F. D., et al. (2014). "Ferrybridge CCPilot100+ Operating Experience and Final Test Results." Energy Procedia **63**: 6239-6251.

Fjellsbø, L. M., et al. (2013). "Screening for potential hazard effects from four nitramines on human eye and skin." Toxicology in Vitro **27**(4): 1205-1210.

Fowler, T., et al. (2012). Atmospheric Chemistry Modelling of Components from Post-Combustion Amine-Based CO2 Capture 1-27.

Frisch, M. J., et al. (2009). "Gaussian 09, Revision D.01."

Fritz, W. (1975). "P. Bogovski, R. Preussmann, E. A. Walker und W. Davis (Ed.): N-Nitroso Compounds Analysis and Formation. Proceedings of a Working Conference held at the Deutsches Krebsforschungsinstitut Heidelberg, 13.–15. October 1971, IARC Scientific Publications Nr. 3, Lyon: WHO International Agency for Research on Cancer 1972, 140 Seiten mit zahlreichen Abb. und Tab. Preis: 25 SFr." Food / Nahrung **19**(3): 293-293.

Fussgaenger, R. D., et al. (1980). "Lethal exitus of a patient with N-nitrosodimethylamine poisoning, 2.5 years following the first ingestion and signs of intoxication." Oncology **37**(4): 273-277.

Galano, A., et al. (2008). "Branching ratios of aliphatic amines + OH gas-phase reactions: a variational transition-state theory study." J. Chem.Theory and Comput. **4**(2): 322-327.

Galano, A., et al. (2006). "Computational quantum chemistry: a reliable tool in the understanding of gas-phase reactions." J.Chem.Edu. **83**(3): 481.

Geiger, G., et al. (1981). "Photolysis of dimethylnitrosamine in the gas phase." Helv.Chim. Acta. **64**(4): 989-995.

Godfrey, R. D. J., et al. (1973). "Discovery of interstellar methanimine (formaldimine)." Journal Name: Astrophys. Lett. 13: No. 2, 119-121(Feb 1973).; Other Information: Orig. Receipt Date: 30-JUN-73: Medium: X.

Goff, G. S., et al. (2004). "Monoethanolamine Degradation: O2 Mass Transfer Effects under CO2 Capture Conditions." Industrial & Engineering Chemistry Research **43**(20): 6400-6408.

Gonzalez, C. A., et al. (1994). "Nutritional factors and gastric cancer in Spain." Am J Epidemiol **139**(5): 466-473.

Goodall, C. M., et al. (1976). "Carcinogenicity of dimethylnitramine in NZR rats in NZO mice." Cancer Lett **1**(5): 295-298.

Goodman, M. T., et al. (1992). "High-fat foods and the risk of lung cancer." Epidemiology **3**(4): 288-299.

Goodsite, M. M., et al. (2011). Advances in Quantum Chemistry: Applications of Theoretical Methods to Atmospheric Science, Academic Press.

GORSE, R. A., et al. (1977). "Hydroxyl Radical Reactivity with Diethylhydroxylamine." Science **197**(4311): 1365-1367.

Gouedard, C., et al. (2012). "Amine degradation in CO2 capture. I. A review." International Journal of Greenhouse Gas Control **10**(0): 244-270.

Graff, O. F. (2010). Emission measurement and analysis from Mobile Carbon Capture Test Facility. in Environmental Impacts of Amine Emission During Post Combustion Capture, Oslo, Norway.

Gurvich, L. V., et al. (1991). Thermodynamic Properties of Individual Substances. New York, Hemisphere Publishing Corp.

Haggerty, H. G., et al. (1990). "Role of metabolism in dimethylnitrosamine-induced immunosuppression: a review." Toxicology **63**(1): 1-23.

Harris, G. W., et al. (1983). "Notes. Rates of reaction of hydroxyl radicals with 2-(dimethylamino)ethanol and 2-amino-2-methyl-1-propanol in the gas phase at 300 .+-. 2 K." Environ. Sci & Technol **17**(1): 50-51.

HealthCanada (2005). Quantitative risk assessment of NDMA in drinking water. Ottawa, Ontario, Health Canada, Healthy Environments and Consumer Safety Branch, Biostatistics Unit.

HealthCanada (2011). N-Nitrosodimethylamine (NDMA) in Drinking Water.

Hsu, C. S., et al. (1985). "Diethanolamine (DEA) degradation under gas-treating conditions." Industrial & Engineering Chemistry Product Research and Development **24**(4): 630-635.

Hurley, P. J., et al. (2005). "TAPM: a practical approach to prognostic meteorological and air pollution modelling." Environmental Modelling & Software **20**(6): 737-752.

IEA (2004). Organisation for Economic Cooperation and Development, Prospects for CO_2 Capture and Storage. Paris, France, IEA Publishing.

IHCP (2003). Institute for Health and Consumer Protection.Technical Guidance Document on Risk Assessment in support of Commission Directive 93/67/EEC on Risk Assessment for new notified substances;Commission Regulation (EC) No 1488/94 on Risk Assessment for existing substances; Directive 98/8/EC of the European Parliament and of the Council concerning the placing of biocidal products on the market.

IPCC (2007a). Climate Change 2007,Synthesis report; Intergovernmental Panel on Climate Change IPCC Secretariat, Geneva, Switzerland.

IPCC (2007b) "Intergovernmental Panel on Climate Change (IPCC) Climate Change , Working Group II report: Impacts, Adaption and Vulnerability."

IPSC. (2002). "N-nitrosodimethyl. International Programme on Chemical Safety." Retrieved 5th June, 2015, from http://www.inchem.org/documents/ehc/ehc/ehc005.htm.

Jackson, P., et al. (2010). Theoretical study of the atmospheric fate of 2-aminoethanol (MEA), CSIRO Report, available at: ht tp://www. gassnova. no/frontend/files/CONTENT/Rapporter/AtmosphericFormation CSIRO. pdf.

Jordal, K., et al. (2004). Oxyfuel combustion for coal-fired power generation with CO2 capture–opportunities and challenges. 7 th International Conference on Greenhouse Gas Technologies, Vancouver, Canada.

Karl, M., et al. (2008). Amine Worst Case Studies. Worst case studies on amine emissions from CO2 capture plants (Task 6). Norway**:** 14-26.

Karl, M., et al. (2014). "Uncertainties in assessing the environmental impact of amine emissions from a CO2 capture plant." Atmos. Chem. Phys.(14): 8633-8693.

Karl, M., et al. (2012). "Study of OH-initiated degradation of 2-aminoethanol." Atmos. Chem. Phys. **12**(4): 1881-1901.

Karl, M., et al. (2015). "Modelling atmospheric oxidation of 2-aminoethanol (MEA) emitted from post-combustion capture using WRF-Chem." Sci Total Environ **527-528**: 185-202.

Karl, M., et al. (2011). "Worst case scenario study to assess the environmental impact of amine emissions from a CO2 capture plant." Int. J. Greenhouse Gas Control **5**(3): 439-447.

Kennard, M. L., et al. (1983). "Gas chromatographic technique for analysing partially degraded diethanolamine solutions." Journal of Chromatography A **267**(0): 373-380.

Kennard, M. L., et al. (1985). "Mechanisms and kinetics of diethanolamine degradation." Industrial & Engineering Chemistry Fundamentals **24**(2): 129-140.

Klein, R. G., et al. (1991). "Effects of long-term inhalation of N-nitrosodimethylamine in rats." IARC Sci Publ(105): 322-328.

Klippenstein, S. J. (1992). "Variational optimizations in the Rice–Ramsperger–Kassel–Marcus theory calculations for unimolecular dissociations with no reverse barrier." The Journal of Chemical Physics **96**(1): 367-371.

Klippenstein, S. J., et al. (1999). VariFlex, Version 1.0. Argonne National Laboratory. Argonne, IL, .

Knudsen, S., et al. (2009). NILU Technical Report, TR 04/2009, Kjeller, Norway.

Koch, R., et al. (1996). "Rate constants for the gas-phase reaction of OH with amines: tert-butyl amine, 2,2,2-trifluoroethyl amine, and 1,4-diazabicyclo[2.2.2] octane." Int. J. Chem. Kinet. **28**(11): 807-815.

Kohl, A. L., et al. (1997). Chapter 5 - Alkaline Salt Solutions for Acid Gas Removal. Gas Purification (Fifth Edition). A. L. Kohl and R. B. Nielsen. Houston, Gulf Professional Publishing**:** 330-414.

Kolderup, H., et al (2012). Emission studies at the Maasvlakte CO2 capture pilot plant, University of Texas Conference on CO2 capture and storage.

Kootstra, F., et al. (2000). "Efficient real-space approach to time-dependent density functional theory for the dielectric response of nonmetallic crystals." J. Chem. Phys **112**(15): 6517-6531.

Korsunskii, B., et al. (1967). "Thermochemical and kinetic investigation of N, N-dimethylnitrosoamine." Bulletin of the Academy of Sciences of the USSR, Division of chemical science **16**(3): 509-511.

La Vecchia, C., et al. (1995). "Nitrosamine intake and gastric cancer risk." Eur J Cancer Prev **4**(6): 469-474.

Låg, M., et al. (2009). Health effects of different amines and possible degradation products relevant for CO2 capture. **/:** 3.

Låg, M., et al. (2011). Health effects of amines and derivatives associated with CO_2 capture. Oslo, Norway, The Norwegian Institute of Public Health**:** 45.

Lamb, H. (1932). Hydrodynamics. Cambridge, Cambridge University Press.

Lazarou, Y. G., et al. (1994). "Gas-phase reactions of $(CH_3)_2N$ Radicals with NO and NO_2." J. Phys. Chem. **98**(8): 2110-2115.

Lee, C., et al. (1988). "Development of the Colle-Salvetti correlation-energy formula into a functional of the electron density." Physical review B **37**(2): 785.

Lee, V. M., et al. (1996). "An evaluation of the roles of metabolic denitrosation and alpha-hydroxylation in the hepatotoxicity of N-Nitrosodimethylamine." Chem Res Toxicol **9**(8): 1319-1324.

Lepaumier, H., et al. (2011). "Comparison of MEA degradation in pilot-scale with lab-scale experiments." Energy Procedia **4**: 1652-1659.

Lepaumier, H., et al. (2009). "New Amines for CO2 Capture. I. Mechanisms of Amine Degradation in the Presence of CO2." Industrial & Engineering Chemistry Research **48**(20): 9061-9067.

Lessmann, H., et al. (2009). "Skin sensitizing properties of the ethanolamines mono-, di-, and triethanolamine. Data analysis of a multicentre surveillance network (IVDK) and review of the literature." Contact Dermatitis **60**(5): 243-255.

Liao, C. M., et al. (2006). "Probabilistic risk assessment for personal exposure to carcinogenic polycyclic aromatic hydrocarbons in Taiwanese temples." Chemosphere **63**(9): 1610-1619.

Lindley, C. R. C., et al. (1979). "Rate studies of the reactions of the $(CH_3)_2N$ radical with O_2, NO, and NO_2." Chem. Phys. Lett. **67**(1): 57-62.

Linstrom, P. J., et al. (1998). NIST chemistry webbook, NIST Standard Reference Database Number 69, National Institute of Standards and Technology Gaithersburg, MD.

Lu, D.-h., et al. (1992). "POLYRATE 4: A new version of a computer program for the calculation of chemical reaction rates for polyatomics." Computer Physics Communications **71**(3): 235-262.

Magee, P., et al. (1956). "The production of malignant primary hepatic tumours in the rat by feeding dimethylnitrosamine." Br. J. Cancer **10**(1): 114.

Martin, S., et al. (2012). "New Amines for CO2 Capture. IV. Degradation, Corrosion, and Quantitative Structure Property Relationship Model." Industrial & Engineering Chemistry Research **51**(18): 6283-6289.

McMillen, D. F., et al. (1982). "Hydrocarbon bond dissociation energies." Annual Review of Physical Chemistry **33**(1): 493-532.

McNaught, A. D., et al. (1997). IUPAC. Compendium of Chemical Terminology

Oxford, Blackwell Scientific Publications.

Meisen, A., et al. (1982). "DEA degradation mechanism." Hydrocarbon Process.;(United States) **61**(10).

Meloni, G., et al. (2006). "Energy-Resolved Photoionization of Alkylperoxy Radicals and the Stability of Their Cations." Journal of the American Chemical Society **128**(41): 13559-13567.

Mirvish, S. S., et al. (1976). "Air—Water and Ether—Water Distribution of N—Nitroso Compounds: Implications for Laboratory Safety, Analytic Methodology, and Carcinogenicity for the Rat Esophagus, Nose, and Liver." Journal of the National Cancer Institute **56**(6): 1125-1129.

Mokrushin, V., et al. (2011). "ChemRate, version 1.5.8; ." from http://kinetics.nist.gov/chemrate/.

Møller, C., et al. (1934). "Note on an approximation treatment for many-electron systems." Physical Review **46**(7): 618.

Nielsen, C., et al. (2011a). Summary Report: Photo-oxidation of Methylamine, Dimethylamine and Trimethylamine. Climit project no. 201604 NILU OR 2/2011, ISBN 978-82-425-2357-0, NILU.

Nielsen, C. J., et al. (2011b). "Atmospheric chemistry of 2-aminoethanol (MEA)." Energy Procedia **4**(0): 2245-2252.

Nielsen, C. J., et al. (2012). "Atmospheric chemistry and environmental impact of the use of amines in carbon capture and storage (CCS)." Chem. Soc. Rev. **41**(19): 6684-6704.

Nielsen, C. J., et al. (2010). Theoretical evaluation of the fate of harmful compounds post emission. Tel-Tek

OECD (2003). Organisation of Economic Co-operation and Development. Descriptors of selected key generic terms used in chemical hazard/risk assessment. .

Olajos, E. J., et al. (1978). "Comparative toxicology of N-nitroso compounds and their carcinogenic potential to man." Ecotoxicol Environ Saf **2**(3-4): 317-367.

Onel, L., et al. (2012). "Direct determination of the rate coefficient for the reaction of OH radicals with monoethanol amine (MEA) from 296 to 510 K." J. Phys. Chem. Lett. **3**(7): 853-856.

Onel, L., et al. (2013). "Gas-Phase Reactions of OH with Methyl Amines in the Presence or Absence of Molecular Oxygen. An Experimental and Theoretical Study." The Journal of Physical Chemistry A **117**(41): 10736-10745.

Pedal, I., et al. (1982). "Fatal nitrosamine poisoning." Arch Toxicol **50**(2): 101-112.

Peng, C., et al. (1996). "Using redundant internal coordinates to optimize equilibrium geometries and transition states." J. Comput. Chem. **17**(1): 49-56.

Peng, C., et al. (1993). "Combining synchronous transit and quasi‐newton methods to find transition ttates." Is. J. Chem. **33**(4): 449-454.

Peto, R., et al. (1991a). "Dose and time relationships for tumor induction in the liver and esophagus of 4080 inbred rats by chronic ingestion of N-nitrosodiethylamine or N-nitrosodimethylamine." Cancer Res **51**(23 Pt 2): 6452-6469.

Peto, R., et al. (1991b). "Effects on 4080 rats of chronic ingestion of N-nitrosodiethylamine or N-nitrosodimethylamine: a detailed dose-response study." Cancer Res **51**(23 Pt 2): 6415-6451.

Pitts, J. N., et al. (1978). "Photooxidation of aliphatic amines under simulated atmospheric conditions: formation of nitrosamines, nitramines, amides, and photochemical oxidant." Environmental Science & Technology **12**(8): 946-953.

Pobel, D., et al. (1995). "Nitrosamine, nitrate and nitrite in relation to gastric cancer: a case-control study in Marseille, France." Eur J Epidemiol **11**(1): 67-73.

Polderman, L., et al. (1955). "Why Monoethanolamine Solutions Breaks Down in Gas-Treating Service." Oil Gas J **54**((No. 2)): 180-183.

Pople, J. A., et al. (1987). "Quadratic configuration interaction - a general technique for determining electron correlation energies." J. Chem. Phys **87**: 5968-5975.

Poste, A. E., et al. (2014). "Amines and amine-related compounds in surface waters: A review of sources, concentrations and aquatic toxicity." Science of The Total Environment **481**(0): 274-279.

Raghavachari, K., et al. (1989). "A fifth-order perturbation comparison of electron correlation theories." Chemical Physics Letters **157**(6): 479-483.

Ravnum, S., et al. (2014). "Human health risk assessment of nitrosamines and nitramines for potential application in CO2 capture." Regul Toxicol Pharmacol **69**(2): 250-255.

REACH (2010). Characterisation of dose [concentration]-response for human health. In: Guidance on information requirements and chemicals safety assessment,Chapter R8.

Reh, B. D., et al. (2000). "O6-methylguanine DNA adducts associated with occupational nitrosamine exposure." Carcinogenesis **21**(1): 29-33.

Richardson, S. D., et al. (2007). "Occurrence, genotoxicity, and carcinogenicity of regulated and emerging disinfection by-products in drinking water: a review and roadmap for research." Mutat Res **636**(1-3): 178-242.

Risch, H. A., et al. (1985). "Dietary factors and the incidence of cancer of the stomach." Am J Epidemiol **122**(6): 947-959.

Robinson, R. K., et al. (2013). "A comparative ab initio study of hydrogen abstraction from n-propyl benzene." Combustion and Flame **160**(12): 2642-2653.

Rogers, M. A., et al. (1995). "Consumption of nitrate, nitrite, and nitrosodimethylamine and the risk of upper aerodigestive tract cancer." Cancer Epidemiol Biomarkers Prev **4**(1): 29-36.

Romaniello, P., et al. (2005). "Time-dependent current-density-functional theory for the metallic response of solids." Phys. Rew. B. **71**(15): 155108.

Rovira, J., et al. (2013). A Revision of Current Models for Environmental and Human Health Impact and Risk Assessment for Application to Emerging Chemicals.

Global Risk-Based Management of Chemical Additives II. B. Bilitewski, R. M. Darbra and D. Barceló, Springer Berlin Heidelberg. **23:** 91-108.

Scire, J. S., et al. (2000). "A user's guide for the CALPUFF dispersion model." Earth Tech, Inc: 521.

Seinfeld, J. H., et al. (2006). Atmospheric chemistry and physics: from air pollution to climate change, John Wiley & Sons.

Selin, N. E. (2011). Environmental Guidelines and Regulations for Nitramines: A Policy Summary (Revision 2), Massachusetts Institute of Technology (MIT)**:** 21.

Shao, R., et al. (2009). Amines used in CO2 Capture- Health and Environmental Impacts**:** 3-26.

Shell. (2015). "Peterhead CCS Project ", from (http://www.shell.co.uk/energy-and-innovation/the-energy-future/peterhead-ccs-project.html).

Silva-Junior, M. R., et al. (2008). "Benchmarks for electronically excited states: time-dependent density functional theory and density functional theory based multireference configuration interaction." J. Chem. Phys. **129**(10): 104103.

Škraba, A., et al. (2012). Integrating Air-Pollution Dispersion Simulation Models and GIS for Urban Air-Pollution Emergency Management. Proceedings of International Conference, MATHMOD.

Smith, R. L. (1994). "Use of Monte Carlo simulation for human exposure assessment at a superfund site." Risk Anal **14**(4): 433-439.

So, S., et al. (2014). "Atmospheric Chemistry of Enols: A Theoretical Study of the Vinyl Alcohol + OH + O2 Reaction Mechanism." Environmental Science & Technology **48**(12): 6694-6701.

Stephens, P. J., et al. (1994). "Ab Initio calculation of vibrational absorption and circular dichroism spectra using density functional force fields." J. Phys. Chem. **98**(45): 11623-11627.

Stern, N. (2006). Stern Review: The economics of Climate Change.

Stohl, A., et al. (2005). "Technical note: The Lagrangian particle dispersion model FLEXPART version 6.2." Atmos. Chem. Phys. **5**(9): 2461-2474.

Strazisar, B. R., et al. "Degradation of Monoethanolamine Used in Carbon Dioxide Capture from Flue Gas of a Coal-fired Electric Power Generating Station."

Strazisar, B. R., et al. (2003). "Degradation Pathways for Monoethanolamine in a CO2 Capture Facility." Energy & Fuels **17**(4): 1034-1039.

Suciu, N., et al. (2013). Environmental Fate Models. Global Risk-Based Management of Chemical Additives II. B. Bilitewski, R. M. Darbra and D. Barceló, Springer Berlin Heidelberg. **23:** 47-71.

TAMP (2010). URL:http://www.cmar.csiro.au/research/tapm.

Tang, Y., et al. (2012). "A systematic theoretical study of imines formation from the atmospheric reactions of $R_nNH_2{-}n$ with O_2 and NO_2 (R = CH_3 and CH_3CH_2 ; n = 1 and 2)." Atmos. Environ. **55**(0): 185-189.

TCM (2012). In: Stokset, V. (Ed). CO_2 Technology Center Mongstad DA., Avialable at: http://www.tcmda.com/no.

Thermopedia.

Thielen, H., et al. (2007). "Advanced Atmospheric Dispersion Modelling and Probabilistic Consequence Analysis for Radiation Protection Purposes."

Tian, W., et al. (2009). "Direct dynamics study on the mechanism and the kinetics of the reaction of CH3NH2 with OH." J. Quantum. Chem. **109**(7): 1566-1575.

Tønnesen, D. (2011). "Update and Improvement of Dispersion Calculations for Emissions to Air from TCM's Amine Plant." NILU OR **52**.

Truhlar, D. G., et al. (1984). "Variational transition state theory." Annual Review of Physical Chemistry **35**(1): 159-189.

Tuazon, E. C., et al. (1994). "Kinetics and products of the gas-phase reactions of O_3 with amines and related compounds." Res. Chem. Intermed. **20**(3-5): 303-320.

Tuazon, E. C., et al. (1984). "Atmospheric reactions of n-nitrosodimethylamine and dimethylnitramine." Environ. Sci. Technol. **18**(1): 49-54.

USEPA Long-term limit value for N-nitrosodiethylamine (DEN) corresponding to a 10−6 lifetime cancer risk, US Environmental Protection Agency, IRIS database:http://www.epa.gov/IRIS/subst/0042.htm.

USEPA (1986). Quality Criteria for Water

USEPA (1990). The Clean Air Act, 42 USC 7412(f).

USEPA (1998a). Guidelines for Ecological Risk Assessment. Washington, DC.

USEPA (1998b). Human Health Risk Assessment Protocol For Hazardous Waste Combustion Facilities. EPA530-D-98-001A.

USEPA (1999). Human Health and Ecological Risk Assessment Support to the Development of Technical Standards for Emissions from Combustion Units Burning Hazardous Wastes: Background Document. Washington, DC.

USEPA (2005). Guidelines for Carcinogen Risk Assessment Washington, DC

USEPA. (2015). "Cancer Risk Calculations. Handbook for Implementing the Supplemental Cancer Guidance at Waste and Cleanup Sites." from http://www.epa.gov/oswer/riskassessment/sghandbook/riskcalcs.htm.

USETox™. "Human effects modelling in USETox™." 2015, from http://www.usetox.org/sites/default/files/support-tutorials/effects_1.pdf.

Verna, L., et al. (1996). "N-nitrosodiethylamine mechanistic data and risk assessment: bioactivation, DNA-adduct formation, mutagenicity, and tumor initiation." Pharmacol Ther **71**(1-2): 57-81.

Whitten, G., et al. (1963). "Accurate and Facile Approximation for Vibrational Energy - Level Sums." The Journal of Chemical Physics **38**(10): 2466-2473.

WHO (2008). N-Nitrosodimethylamine in Drinking-water. Background document for development of WHO Guidelines for Drinking-water Quality.

Wigner, E. (1932). "On the quantum correction for thermodynamic equilibrium." Phys. Rev. **40**(5): 749.

Wiliams, M. (2002). Climate Change Information Kit, UNEP and UNFCCC.

Wollin, K., et al. (2005). "Toxicological guidelines for monocyclic nitro-, amino- and aminonitroaromatics, nitramines, and nitrate esters in drinking water." Arch Environ Contam Toxicol **49**(1): 18-26.

Wu, Y., et al. (2014). "Using Computer Modelling to Simulate Atmospheric Movement and Potential Risk of Pollutants from Post-combustion Carbon Capture Projects." Energy Procedia **63**(0): 976-985.

Xiao, R., et al. (2014). "Thermodynamic and kinetic study of ibuprofen with hydroxyl radical: A density functional theory approach." International Journal of Quantum Chemistry **114**(1): 74-83.

Xie, H.-B., et al. (2014). "Atmospheric chemical reactions of monoethanolamine initiated by OH radical: mechanistic and kinetic study." Environ. Sci. Technol. **48**(3): 1700-1706.

Zhao, Y., et al. (2005). "Benchmark database of barrier heights for heavy atom transfer, nucleophilic substitution, association, and unimolecular reactions and its use to test theoretical methods." The Journal of Physical Chemistry A **109**(9): 2012-2018.

Zhao, Y., et al. (2008). "Density functionals with broad applicability in chemistry." Acc. Chem. Res. **41**(2): 157-167.

Zheng, J., et al. (2009). "The DBH24/08 database and its use to assess electronic structure model chemistries for chemical reaction barrier heights." J. Chem. Theory. Comput. **5**(4): 808-821.

Zhou, J., et al. (2011). "Quantum Chemical Investigation on the Mechanism and Kinetics of PBDE Photooxidation by ·OH: A Case Study for BDE-15." Environmental Science & Technology **45**(11): 4839-4845.